THE COMPRESSIVE STRENGTH OF FLY ASH CONCRETE AND ITS MINERALOGY

by

Volker R. Gogol

A thesis submitted for the degree of Master of Science in Applied Science to the Faculty of Engineering at the University of Cape Town.

Department of Civil Engineering
University of Cape Town

February 1994

THE COMPRESSIVE STRENGTH OF FLY ASH CONCRETE AND ITS MINERALOGY

by Volker R.Gogol

The use of fly ash as a cement extender in portland cement concrete is well established. Strict requirements are set for the fly ash on its physical properties and chemical composition to ensure its successful application as a partial replacement material for cement.

An investigation was undertaken into the effectiveness and properties of a high carbon clinker ash when used as a cement extender at a 30% direct mass to mass substitution for portland cement. The clinker ash came from the Van Eck power station in Windhoek, Namibia and was milled to pass a 63micron sieve. For comparison fly ashes from the Escom power stations of Lethabo, Duvha and Matla were used. Both concrete and pure paste specimens were prepared for the evaluations.

The compressive strengths of the concretes were tested at different time intervals on cubes cured for up to 28 days. Samples from the paste cubes were prepared by crushing and freeze-drying, to be used in differential thermal analysis (DTA) and thermogravimetric analysis (TGA), which gave information on the mineralogy and hydration progress respectively. Ultimately, the results from the paste analyses were related to the strength development of the concretes. A good correlation was found between the total amount of bound water in the pastes and the compressive strength of the concretes.

The study showed that, even with the milled clinker ash containing >30% carbon, it could successfully be used as a cement extender in concrete. In addition to pozzolanic reactivity of the ash, it also had some inherent cementicious character. The long-term effects, that is to say at times after 28 days of curing, have still to be investigated to determine the effect, if any, on the durability of concrete containing the high carbon milled clinker ash.

INDEX

1. INTRODUCTION

The use of Fly Ash as a mineral additive to Portland Cement Concrete has been known since early this century, however extensive research during the past two to three decades is responsible for the present knowledge about the topic. Being a waste product of thermal power stations and available in huge quantities, fly ash as a cement extender presents itself as a very attractive application in terms of economic considerations. In addition to the benefits gained by lowering of building costs (due to a reduction in cement consumption), the incorporation of fly ash into concrete yields many more desirable benefits in the field of general concrete properties in the fresh as well as hardened state. Further aspects like improved durability and increased resistance to degradation (chemical and physical) enhance -the offset against the disadvantages involved with the blending of cement with fly ash.

The main drawback arising from fly ash being added to or partially substituted for the cementitious content of a concrete mix, is the retarded strength development during early age relative to the mix with only cement as binder material. This drawback can be bypassed with appropriate adjustment of the particular mix design by increasing the cement/water ratio, thus increasing the cement content. In other words a higher target strength may be aimed for in the design of the concrete mix to ensure comparative strength values. However this would adversely affect the improved cost factor and hence point back to using a straight cement component in the mix design on the basis of economic considerations.

The use of fly ash as a cement extender is not a trivial matter and requires careful consideration and planning, taking into account all the participating factors in preparing the mix design.

In the presented work, an investigation was undertaken into the relationships between the properties of fly ash (chemical, mineralogical and physical) and strength development of the fly ash concrete up to 28 days of age. Compressive strength was chosen as the comparative parameter, as this is generally still the concrete property on which the largest emphasis is placed in determining quality of the material.

The following four coal ashes were compared in their performance as cement extenders in concrete:

- fly ash from the Lethabo power station,
- fly ash from the Duvha power station,
- fly ash from the Matla power station and
- a milled clinker ash from the Van Eck power station in Windhoek, Namibia.

Samples of the ashes and the cement used were characterized according to their chemical composition, mineralogy and fineness. For each type of ash, a concrete mix was prepared and the compressive strength of cubes tested at the time intervals of 3, 7, 14, 21 and 28 days after casting. In parallel, pastes were made up with the same ratio of cement to ash. The paste cubes were cured under the same conditions as the concrete cubes. At the particular time intervals, these were used to carry out differential thermal analyses as well as thermogravimetric analyses.

2. LITERATURE SURVEY

2.1 FLY ASH - THE MATERIAL

The residue of the coal burning process in modern thermal power stations is referred to as pulverized fuel ash (pfa) of which fly ash is the portion of fine material. Fly ash is classified as a pozzolanic material. Pozzolans are defined as "siliceous or siliceous and aluminous materials which in themselves possess little or no cementitious value but will, in finely divided from and in the presence of moisture, chemically react with calcium hydroxide at ordinary temperatures to form compounds possessing cementitious properties" (ASTM-618-89, 1988).

Generally one can differentiate between two classes of fly ash: either 'low-lime fly ash' with truly pozzolanic characteristics or 'high-lime fly ash' showing some cementitious properties in addition to the pozzolanic reactivity. This classification is mainly determined by the type of coal that is burnt to produce the ash. The low-lime fly ash ($CaO < 10\%$) results from the burning of anthracite and bituminous coals, whereas the high-lime fly ash ($CaO > 10\%$) is produced from sub-bituminous and lignite coals. Under the additional condition that the sum of the oxides ($SiO_2 + Al_2O_3 + Fe_2O_3$) has a minimum of 70%, the low-lime fly ash corresponds to the ASTM-618 specification for type F-fly ash, whereas in the case that the sum of the three oxides has a minimum of 50%, the high-lime fly ash complies with the ASTM-618 type C-fly ash. Truly pozzolanic ashes are referred to as type-F (ASTM), whereas ashes displaying some hydraulic properties are classified as type-C (ASTM).

The situation with South African fly ashes is clear-cut in terms of the above definitions and terminology: All the ashes comply with the definition of type-F fly ash. The composition of different fly ashes is given in Table 2.1.

Fly ash is a product of the combustion process of finely ground coal at thermal power stations. In the furnace, which operates at a temperature of about 1500°C, the carbonaceous content of the coal is burnt very rapidly. The remaining material, consisting of mainly silica, alumina and iron oxide, melts while still being suspended in the injection gas stream. The very rapid cooling of the flue gases results in the solidification of the melt droplets into fine spherical hollow particles of fly ash. Such rapid cooling yields incomplete crystallization and hence a partly amorphous material is formed. It is this glassy phase which is responsible for the pozzolanic activity of the fly ash.

The glassy phase is a typical silica-alumina glass, whereas mullite ($3Al_2O_3 \cdot 2SiO_2$) is the main constituent of the crystalline phase. In addition, the crystalline iron oxides of haematite (Fe_2O_3) and magnetite (Fe_3O_4) are found as separate particles, as is quartz. Types of fly ash with high alkaline earth contents often contain spinel ($MgO \cdot Al_2O_3$) and wollastonite ($CaO \cdot SiO_2$). Any carbon that may still be present, is in the form of char particles.

Initial mechanical means, followed by electrostatic precipitators, collect the ash according to particle size, the largest ash particles being collected first. The coal characteristics, the burning profile at the power station and the collection setup are all important variables influencing the properties and consistency of the fly ash. The issue of characterizing the fly ash is not a simple task, as a wide range of properties needs to be taken into consideration.

The pozzolanic activity of fly ash in concrete is largely dependent on the fineness (particle size and particle size distribution) of the ash. The smaller the ash particles, the bigger is the surface area for a given mass of material and hence more reaction sites are present for the hydration process to initiate. However, a lower limit to particle size also exists from a practical point of view, for example, the finer the ash, the more difficult its the handling and storing becomes.

The compatibility of portland cement and fly ash arises from the mineralogical and chemical composition of the two materials. To produce portland cement a finely ground mixture of calcareous materials (commonly limestone or chalk) and argillaceous materials (commonly clay or shales) and/or other silica, alumina or iron oxide bearing materials is burned at a temperature of above 1400°C to produce clinker. The clinker is then cooled, ground and intermixed with a small proportion of gypsum (to delay setting time) and possibly some other inorganic additives for specialized applications (Mantel, 1992).

As is shown in Table 2.1 below, both portland cement and fly ash consist essentially of silica, alumina, calcium and iron (all in oxide form), but in varying proportions. The exact chemical composition, as well as physical properties, differentiate cement and fly ash into the groups of a hydraulic binder and pozzolan respectively. Portland cement (ordinary and rapid-hardening) are covered by the specification SABS 471, whereas fly ash to be used as cement extender has to comply with the specification SABS 1491-2.

Table 2.1 : Chemical Analysis of Portland Cement and Fly Ash.

[a] after Mantel, 1992

[b] Lethabo fly ash (Grieve, 1991)

[c] CANMET data for ASTM class F fly ash (Malhotra and Painter, 1988)

[d] ASTM class F fly ash (Galeota *et al.*, 1992)

Oxide	Portland Cement[a]	Fly Ash		
		South Africa[b]	Canada[c]	Italy[d]
SiO_2	22.9%	52.55%	47.1%	45.8%
Al_2O_3	4.2	29.75	23.0	31.2
Fe_2O_3	3.8	3.95	20.4	3.96
CaO	65.0	5.45	1.21	6.90
MgO	3.3	1.35	1.17	1.79
SO_3	0.2	2.10	0.67	1.00
Na_2O	0.1	0.20	0.54	0.24
K_2O	0.6	0.50	3.16	0.84

2.2 FLY ASH IN CONCRETE

The use of fly ash as a cement extender in concrete affects both the fresh and hardened properties of the material. In general, the early-age strength development of fly ash concrete is retarded in relation to a mix without any fly ash added, even though its long-term strength may be comparable. Much too often however, the early-age compressive strength of concrete is considered the sole and absolute indicator of quality, and this aspect is the reason for much criticism of fly ash concrete. Another aspect is that the benefits gained from correct curing are often not recognized and instead higher costs are incurred by increasing the cement content of a mix in order to meet specifications. If the above attitude about concrete strength can be changed, much can be achieved in the fields of economics and concrete quality by only changing the methodology and practice of concreting.

2.2.1 FLY ASH AND PORTLAND CEMENT

There are two basic methods of fly ash inclusion in concrete: (1) to use a composite cement containing fly ash produced either by blending or intergrinding, and (2) to introduce the fly ash as a direct admixture during mixing. The main benefit of the second method is that the mix design may be proportioned to meet the exact requirements of the specific application, without being limited by the fixed cement-to-fly ash ratios set by the supplier of blended cement. There are two approaches. Using the 'replacement method', the cement is simply replaced on a mass-to-mass basis, which results in an increase in the binder volume due to the lower density of fly ash in relation to cement. Hence an adjustment in the aggregate content is required to incorporate this volume change. The second approach, referred to as the

'design method', is based on the underlying principle that there exists an optimum amount of fly ash for a specific concrete mix, which is a function of its water-portland cement ratio (Dhir, 1986). Swamy (1990) presents some guidelines on fly ash concrete mix proportioning and concludes that, for given conditions of curing and age of testing, the properties developed by the material are greatly influenced by the particular method used to determine the mix design. In Appendix D different methods of mix design incorporating fly ash into concrete are presented.

In the following text where the chemistry of cement hydration and cement-fly ash hydration is discussed, the practice of using cement chemistry notation is followd. The accepted abbreviations used are as follows.

Table 2.2 : Cement chemistry notation as in Fulton (Addis, 1986).

Oxide	Abbreviation
CaO	C
Al_2O_3	A
SiO_2	S
Fe_2O_3	F
MgO	M
Na_2O	N
K_2O	K
H_2O	H
SO_3	S"

The detailed interaction of fly ash and portland cement during the hydration and hardening process is not yet fully understood. It has been established however that the pozzolanic reaction of fly ash may be summarized as the reaction of the free lime or portlandite ($Ca(OH)_2$), produced in the cement hydration, with the glassy phase of the fly ash to produce calcium silicate- and

aluminate hydrates. However, the cement hydration and the pozzolanic reaction of the fly ash do not proceed independently and hence mutually influence one another. Reaction profiles (rates, surface reactions, nucleation and crystallization) and reaction products formed cannot be considered individually as they are interdependent, adding to the complexity of the system.

Research by Bijen (1992) on the pozzolanic reaction of fly ash in concrete has been reported by the Dutch Concrete Society. Under ambient conditions, the reaction of fly ash with portland cement does not start immediately when the mixing water is added. During this period of passivity, the fly ash acts mainly as precipitation sites for lime and calcium-silicate-hydrate-gel (CSH) resulting from the cement hydration. After this dormant period, the pozzolanic activity starts, which is a slow process in terms of reaction rate. This delayed fly ash reaction is the basis for the different behavior in the fresh state of concrete which incorporates fly ash. As the fly ash initially behaves more or less as inert material, it essentially produces a higher water-to-cement ratio (W/C). Hence the concrete will initially be less strong and have a higher permeability.

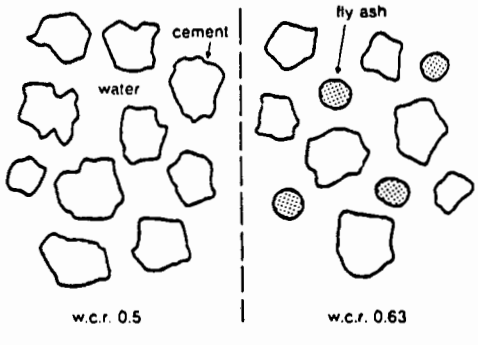

Figure 2.1 : Illustration of the effectively higher W/C ratio due to the presence of 'inert' fly ash during the dormant period (Bijen, 1992).

Once the pozzolanic reaction is initiated, the negative effects due to the higher W/C ratio are reduced in the sense that the fly ash contributes to the

development of strength. The extent of reaction is a function of the composition and physical properties of the ash, with fineness and surface area being of particular importance. The start of the pozzolanic reaction is associated with the decomposition of the glass phase of the ash. Because the glassy phase is the active component in the material, the ratio of glass to crystalline phases is of prime importance. The pozzolanic activity of fly ash in concrete is greatly determined by the alkalinity of the pore water. Generally speaking, a pH of greater than 13 has to be attained before effective dissolution of the glassy phase takes place. The hydration reaction of the cement increases the pH by releasing $Ca(OH)_2$ into the pore water, hence the rate of the cement hydration reaction plays an important part in determining the length of the dormant period of the fly ash.

The following factors influence the development of alkalinity and thus ultimately the pozzolanic activity (Bijen, 1992):

- The type of fly ash and type of cement used will have a particular alkaline content in terms of their chemical composition.
- The fineness of cement used. The finer the cement, the higher the rate of hydration, thus the faster the increase of the pH of the pore water.
- For a higher W/C ratio, the alkalinity of the pore water will be lower and hence the pozzolanic reaction retarded.
- A higher temperature will result in an increased rate of development of alkalinity and hence faster reaction of the glassy phase of the fly ash.
- The effect of curing, especially during the dormant period, is very pronounced for fly ash concrete in the sense that a deficiency in water will terminate any pozzolanic reaction.

The dissolution of the fly ash in the pore water results in the reduction of the free lime concentration of the water. The effect of reducing the free lime content and actually transforming it into a cementitious binder material and thus aiding in the strength development of the concrete, is one of the most beneficial consequences derived from using fly ash. The pozzolanic reaction would be terminated, if the free lime content were to be exhausted. However in practice such a situation will not be reached with portland cements as the latter will, in the presence of moisture, continue to hydrate for many years. As long as lime is made available from the cement hydration, the fly ash-lime reaction will result in a gain in strength. Nevertheless the hydration of the cement and as a consequence the pozzolanic reaction, will slow down with time. The decrease in permeability, which may be visualized as less space being available for the pozzolanic reaction products to form, as well as a reduction in the alkalinity with time, are two factors which limit the pozzolanic reaction in concrete with progressing time.

The calcium silicate hydrate gel formed in the pozzolanic reaction is not of uniform composition, nor does it show consistency in its degree of crystallinity. Two types of CSH are distinguished: 'Type One', being poorly crystalline with a molar ratio CaO to SiO_2 between 0.8 and 1.5, whereas type 'Type Two' shows a higher degree of crystallinity with ratios between 1.5 and 2.0.

The hydration of portland cement is a complex process where numerous chemical reactions take place, which form a variety of products (Mantel, 1992, Heckroodt, 1990 and Bye, 1983). On the addition of water, the first compound to react is tri-calcium aluminate (C_3A). The reaction would proceed virtually instantaneously in the absence of gypsum ($CaSO_4 \cdot 2H_2O$), leading to the phenomenon of 'flash-set' where the concrete sets in seconds. The gypsum,

which is introduced during the clinker milling stage of cement production, dissolves in the water and reacts with the reaction products of C_3A to form ettringite ($C_3A{\cdot}3CS"{\cdot}H_{32}$), which is an insoluble calcium sulphoaluminate hydrate. The ettringite forms a framework for subsequent hydration reactions. The next compound to react with water and calcium hydroxide is tetra-calcium alumino ferrite (C_4AF) to produce mainly hydrogarnet (C_6AFH_{12}). Subsequently tri-calcium silicate (C_3S) and then di-calcium silicate (C_2S) undergo hydration to form $C_3S_2H_3$ (and $Ca(OH)_2$), with the calcium- silicate hydrate further strengthening the framework of hydration products. The structure of the hydrated cement paste is made up of precipitated solid material, which consists mainly of porous calcium silicate hydrate gel (tobermorite gel), well-crystallized calcium hydroxide and ettringite.

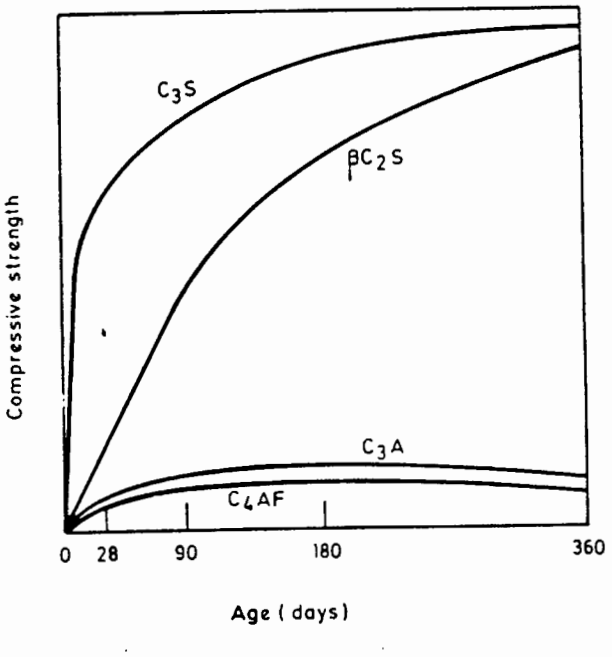

Figure 2.2: Relative rates of strength development for the clinker compounds of portland cement (Addis, 1986).

The contributions which the above clinker compounds offer to the actual strength development of portland cement show markedly different trends. C_3S and C_3S are responsible for the development of strength with C_3A and C_4AF playing a rather insignificant role. These trends are depicted graphically in Figure 2.2 .

Helmuth (1987), Jawed et al.(1991) and Krüger (1990) have reported on the effect of fly ash on the process of hydration of portland cement, specifically on the hydration of C_3S and C_3A.

2.2.2 FLY ASH AND THE HYDRATION OF C_3S

The hydration of tri-calcium silicate (C_3S) in the presence of fly ash is initially retarded, then after this induction period of about 24 hours, the rate accelerates. The retardation is illustrated in Figure 2.3 which shows that the main heat evolution peak due to the hydration of C_3S is delayed to a later time. The reasoning for this behaviour is as follows. The process of chemisorption of Ca^{2+}-ions onto the surface of fly ash particles results in a decrease in the calcium ion concentration in the pore water. As a result, the homogeneous nucleation of $Ca(OH)_2$ (formed as hydration by-product) is retarded. However, if the reaction mechanism proceeds via heterogeneous nucleation, the chemisorption would accelerate the nucleation of the calcium hydroxide. Furthermore, the 'poisoning effect' of soluble silicate, aluminate and especially organic species which oppose the nucleation and growth mechanisms of calcium hydroxide and calcium silicate hydrates, retard the reaction of C_3S.

In addition to the chemical effects, there is the physical effect of fine fly ash particles adhering to the surface of cement grains, thereby hindering the

interaction of the cement with water. The fly ash particles thus effectively create space between individual cement particles thereby providing additional volume for the deposition of hydrates formed by the cement particles. This deflocculation process is another example in which the fineness of the fly ash used is the determining factor for efficiency.

A further consequence of the availability of space is the fact that, once a hydrate structure is formed, the presence of the fly ash enhances the continued growth of the hydration products as it provides the space needed for further hydrates to form.

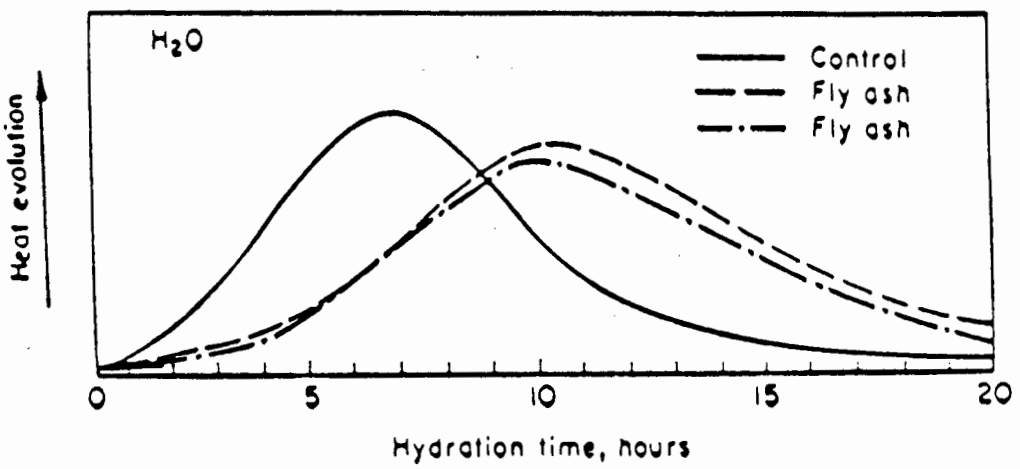

Figure 2.3 : Heat evolution profiles for C_3S systems hydrated in water (Helmuth 1987).

The following schematic diagram (Figure 2.4) depicts the hydration mechanism for the C_3S-fly ash system. The pozzolanic reaction is simplified, but it shows the following important steps.

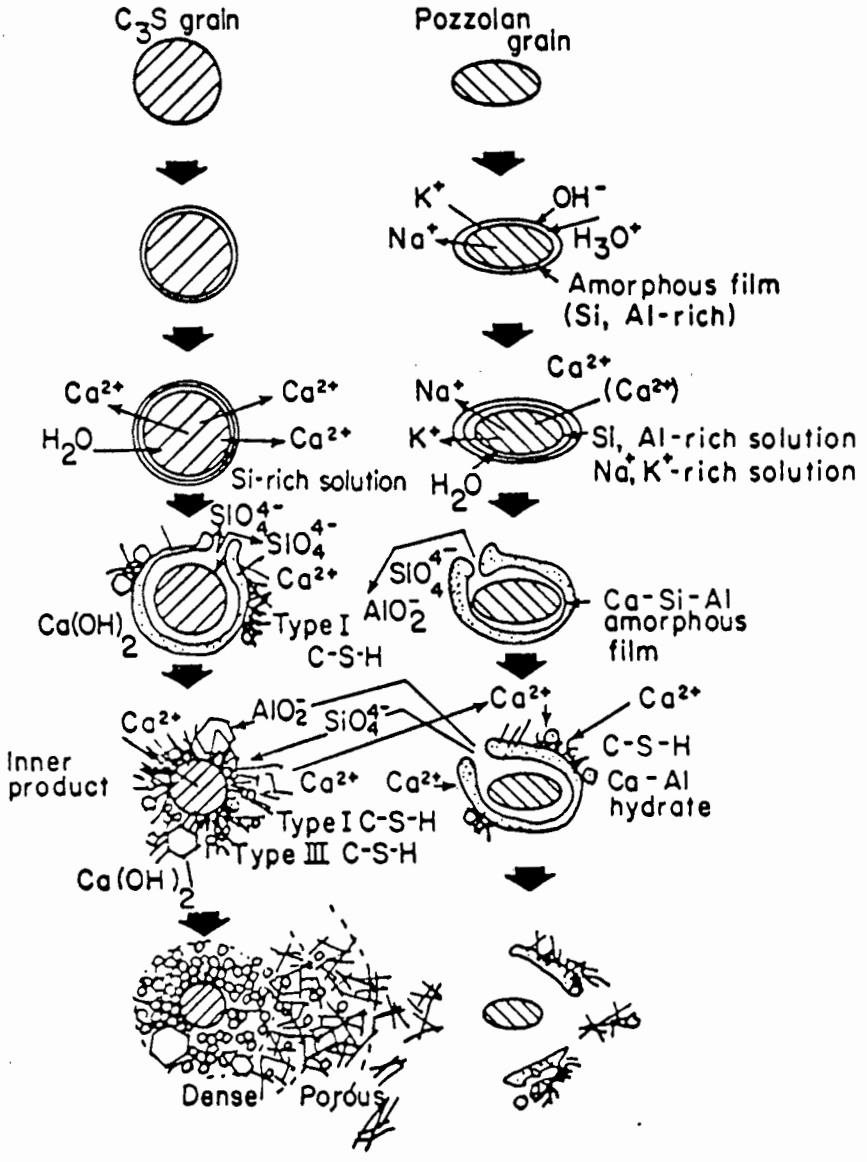

Figure 2.4 : Schematic representation of the hydration mechanism for the C_3S-fly ash system (Helmuth 1987).

The C_3S surfaces release calcium ions into the liquid phase thereby saturating it. A proportion of these ions is adsorbed onto the pozzolan particle (fly ash) surface. The surfaces of the C_3S particles, in contact with water, are hydrated

to form calcium silicate hydrate. Surface reactions on the fly ash particles result in the precipitation of porous hydrate structures with low Ca-to-Si ratio on these surfaces. Sodium and potassium ions are removed from the pozzolan surface by the action of the surrounding water, leaving behind a Si-rich and Al-rich amorphous surface layer. The dissolving Na^+ and K^+ ions increase the hydroxyl concentration in the liquid phase and thereby enhance the dissolution of $(SiO_4)^{4-}$ and $(AlO_2)^-$, which readily combine with Ca^{2+} from the liquid phase to build up the hydrate layer on the fly ash particle

The action of osmotic pressure brings about a swelling of the hydrate layer and a void is formed between the layer and the pozzolan particle. If the pressure in the void further increases, the film of the void ruptures and $(SiO_4)^{4-}$, $(AlO_2)^-$, Na^+ and K^+ ions are released into the solution (which is still at a high calcium ion concentration). Combination of $(SiO_4)^{4-}$ and $(AlO_2)^-$ with Ca^{2+} results in more calcium silicate and aluminate hydrates being formed. The presence of alkalis opposes the precipitation of hydrates. The glassy phase of fly ash tends to have a high sulphur and alkali content concentrated in the surface of the particle, which often leads to void space in the form of a complete shell around individual particles where very little activity occurs.

2.2.3 FLY ASH AND THE HYDRATION OF C_3A

Helmuth (1987) reports that the pozzolanic action of the fly ash again results in a retardation of the hydration during the very early stages which changes to an acceleration with time.

In the schematic diagram (Figure 2.5), the mechanism for the hydration of the pozzolan-C_3A system in the presence of calcium hydroxide as well as ettringite

is presented. The mechanism depicted explains the accelerating action of the fly ash on the C_3A hydration. The pozzolan adsorbs calcium ions from the liquid phase and provides precipitation sites for ettringite and other hydrates. In this way the fly ash promotes the formation of ettringite as well as the consequent transformation of the latter to mono-sulphoaluminate hydrate. The pozzolanic reaction follows a similar reaction profile as in the hydration of C_3S described above. In addition to ettringite and mono-sulphoaluminate, calcium aluminate hydrate and calcium silicate hydrate precipitate on the surface film outside the pozzolan particles and on the hydrate layer of the C_3A particles, depending on the concentration of the calcium- and sulphate ions in solution. The sulphate concentration is thus very important in so far as influencing the precipitation site: Calcium aluminate hydrate is found preferentially at a surface of low sulphate concentration.

It becomes evident how important the knowledge of the particular fly ash composition is if a homogeneous microstructure in the final concrete is aimed for. For example a high sulphate concentration of the fly ash, which will be concentrated in the surface of individual particles, will determine the hydrate structure forming around it.

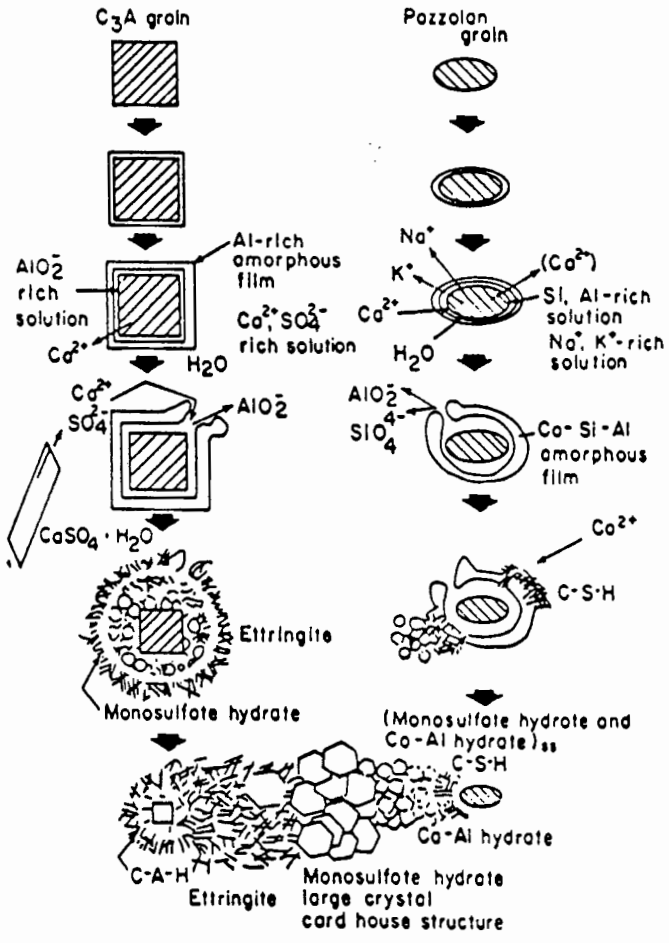

Figure 2.5 : Schematic representation of the hydration mechanism for the C_3A-fly ash system (Helmuth 1987).

2.2.4 FLY ASH AND THE HYDRATION OF PORTLAND CEMENT

The overall hydration of portland cement under the influence of fly ash, is expected to follow similar reaction paths and mechanisms as described for the individual clinker minerals. However, the fact that the reactions take place simultaneously and consecutively, will certainly influence the kinetics and characteristics of individual reactions. The role which water-soluble components of the ash play, is extremely complex and cannot be generalized, as it depends on the particular fly ash used. It can be concluded though, that

the pozzolanic reaction decreases the free lime content and is responsible for the lowering of the Ca-to-Si ratio of the calcium silicate hydrate in the cement/fly ash concrete mix.

2.3 THE PERFORMANCE OF FLY ASH CONCRETE

The aim of a great deal of research on fly ash concrete is to attain the ability to accurately predict the early-age as well as long-term characteristics of the concrete from the measurable properties of the fly ash to be used. However, as pointed out in previous discussions, the complexity of the component interactions in the mix is the biggest stumbling block in achieving this aim. If the processes of the chemical and physical interactions of the systems on the addition of water could be fully understood, the variability in properties of a particular fly ash could be incorporated in the mix design. Until such time as our understanding grows considerably, each fly ash-concrete system has to be treated as a separate entity, allowing for unforeseen effects which will hopefully show up during the preparation and evaluation of trial mixes for the particular mix design. The status of fly ash is lifted more and more from the misconception of a useless waste material to a beneficial cementitious binder material. This change in attitude will certainly continue, even if the material is only judged by the most conservative critics in terms of the economic savings achieved.

2.3.1 WORKABILITY OF FLY ASH CONCRETE

The workability of a concrete mix is a broad term covering numerous aspects of the performance of the material in the fresh state. Terminology like 'plasticity', 'mobility' and 'consistency' is often used synonymously for the concept of workability. Such loose definitions lead to confusion. In Fulton (Addis, 1986) workability is related to the ease of transporting, placing and compacting concrete in such a way as to minimize segregation or separation of individual constituents. According to this view, workability is merely a characteristic of

the particular mix which gives an indication of the flow properties. It is not at all an absolute figure that allows comparisons of concretes containing different materials or produced under different conditions. A suitably workable mix for mass concreting of a dam wall will certainly be unsuitable to be placed and compacted in a heavily reinforced structure.

Further difficulties arise from the methods of assessing the workability. Different tests have been formulated, for example, flow test, ball penetration test, compacting factor test, K-slump test, slump test and the Vebe consistometer. Results cannot be interpreted interchangeably between different test methods, nor will the results of tests carried out by different operators necessarily be consistent. For example, it may well be that two mixes give a zero slump value but at the same time may be differentiated very clearly on grounds of their Vebe time values. It is not surprising that in practice workability judgment based on experience is often considered of more value than, for example, a figure obtained from the slump test.

Factors influencing the workability of concrete include particle interference (interlock) and specific surface area, in so far as any increase in either of these will reduce the workability (Addis, 1986). The concrete mix design, the texture and shape of the coarse aggregate, the fineness of the fine aggregate as well as the interaction of individual concrete components all influence its workability and are all aspects contributing to the behaviour of the concrete in the fresh state.

The introduction of fly ash as a cement replacement will further govern the flow characteristics of the paste. It is generally accepted that fly ash improves the workability of concrete (Krüger and Van Dijk, 1985). For example, an

under-sanded mix will benefit from fly ash replacement for part of the portland cement on a mass-to-mass basis. This is due to the lower density fly ash which results in an increase in the volume of the paste, as well as the so called lubricating effect of the fine ash.

Dartsch and Herten (1992), in their study of using fly ash in concrete and precast concrete applications, contrasted the 'filler effect' against the 'lubrication effect' of fly ash in concrete. Figure 2.6 gives a schematic representation of the two concepts. It must be noted however that this approach is a very simplistic one based on numerous assumptions and is merely used to illustrate the concepts graphically.

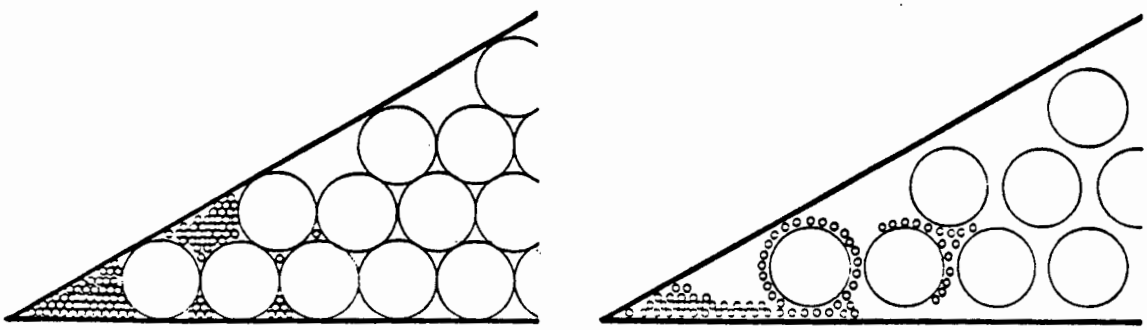

Figure 2.6 : Filler effect in relation to lubrication effect (Dartsch and Herten 1992).

The first illustration shows the filler effect for spheres of diameter d and d/10 packing in such a way as to give the densest filling, where the d/10 spheres resemble the fine fly ash. In the second diagram, the lubrication effect of fly ash is visualized. The spheres are arranged according to the 'planetary system'

with the larger spheres being encircled by a large number of spheres of the smaller size. In this case the relationship between individual sizes is more important than the absolute size of the particle. The second diagram is applicable to the improved workability accounted to the 'ball-bearing effect', recognizing the fact that actual fly ash particles are spherical in shape.

Both the filler and lubrication effects are present when fly ash is added to concrete and both of these effects contribute to the reduced water requirement of the concrete. The filler effect improves the particle packing by filling interstices and contributes to a more compact final material. Another important consequence of the filler effect is the reduction of air entrapment and hence a decrease in total porosity. The compacting and homogenizing action of the fine fly ash particles is very beneficial in decreasing permeability, but it is even more advantageous in the interfacial zone between the aggregate and matrix. Filling this space solves many problems of non-uniformity on a microscale. The generally improved particle packing reduces the amount of non-surface adsorbed water in the concrete, hence the observation that fly ash addition to concrete reduces the amount of bleeding. It must be remembered that the above diagrammatic representation deals merely with the physical size relationships, ignoring any adhesive, cohesive or chemical interactions.

Hansen and Hedegaard (1992) investigated the effect of the amount of fly ash in a concrete mix with special reference to the plasticizing ability of such an addition. Their work showed that Lyse's Rule (which states that 'for given materials, the consistency of fresh portland cement concrete is determined exclusively by the free water content of the concrete mix'), also applies to fly ash concretes, although in a slightly modified form. The enhanced

$$\frac{W}{c + F\left(dc/df\right)} = \alpha$$

where α is a constant and is equal to the minimum modified water-to-(cement plus fly ash) ratio (by equivalent volumes) at which it is possible to mix, cast and compact fresh concrete to maximum density by traditional means. The value of α ranges between 0.35 and 0.38 when no superplasticizers are used and will be lower if the latter are correctly employed in the mix design. The other symbols used in the equation above are :

W = free water content (kg per m^3)

c = portland cement content (kg per m^3)

F = fly ash content (kg per m^3)

dc and df represent the particle density of the cement and fly ash respectively (kg per m^3).

2.3.2 STRENGTH DEVELOPMENT OF FLY ASH CONCRETE

The following discussion concentrates on the development of compressive strength of fly ash concrete. The compressive strength is indeed a very important parameter of the material which is reflected in the habit of concrete users to rationalize general quality of the concrete by the universal indicator of compressive strength.

The intricate details of the interactions between cement, mineral admixture (fly ash), aggregate and water have not yet been resolved. However the progress made in research on this topic reveals more and more information which leads to a better understanding of the general topic of concrete technology.

Figure 2.7 below is taken from work published by Dhir (1986). This graphical representation of strength development patterns serves as a good starting point to compare the strengths of OPC and fly ash concretes. Both concretes have been designed for the same workability and 28-day wet-cured characteristic compressive strength. The philosophy of mix design is the first factor influencing early-age and long-term strength. Design criteria according to specifications have to be aimed for in a very specific way. The two basic principles governing the achievement of set requirements are the quantity of cement (cementitious material) to be used and the water to total cementitious material ratio.

For the two concretes designed to the same 28 day specifications, no significant difference in the strength development before the age of 28 days is observed.

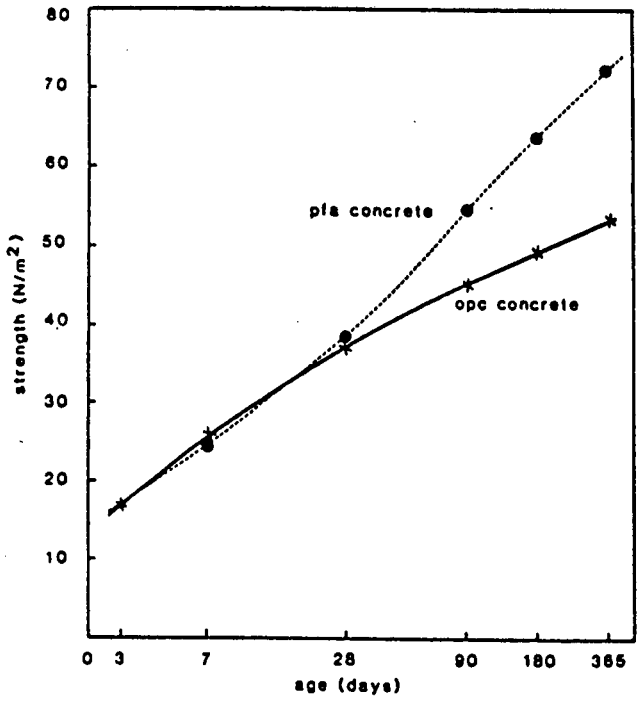

Figure 2.7: Strength development as a function of time for concretes cured at 20°C (Dhir, 1986).

However, after 28 days the fly ash concrete shows a gradual increase in strength over the OPC mix and it is this effect of fly ash which makes it a beneficial concrete ingredient in situations where high ultimate strengths are to be achieved. The strength-age factor (the ratio of compressive strength at any age to the strength value at 28 days) which relates the gain in strength to the 28-day strength, shows the same trend for OPC as well as fly ash mixes: With increasing design strength, the strength-age factor decreases. This factor is specific to the materials used for a particular mix.

Berry and Malhotra (1987), in addition to the selection of mix proportions, listed the following variables influencing the strength development of fly ash concretes:

- the properties of the fly ash
- chemical composition
- particle size
- reactivity
- temperature and other curing conditions.

Dhir (1986) referred to the availability of moisture and the prevailing temperature as being two factors of utmost importance to the development of strength.

The particle size influence is twofold. Firstly, the fineness of the fly ash particles determines its efficiency in dispersing the cement clusters, which improves the hydration process and hence enhances strength development. Secondly, the finer the ash, the more surface area is available. Generally, cementing activity takes place on the surface of the solid phases, through various heterogeneous processes of diffusion, dissolution and precipitation of reaction products. Thus surface area plays an important role in determining the kinetics of such processes in that a fine ash renders a large number of precipitation sites during the hydration of the cement. Feldman (1989) pointed to the controlling factors for cement hydration as being the availability of water and the availability of space for the hydration products to form. The author characterized the fly ash in the early periods of hydration as inert material hence the high effective water to cement ratio will allow a greater degree of hydration of the cement. The author concluded from his work that blending of cement pastes with fly ash resulted in a homogeneous hydrate product with a low C/S ratio CSH gel which gave a stronger body.

Fly ash reactivity refers to the pozzolanic activity of the material. The rate of this process, as described earlier, is slow to start with, but increases with time

and eventually, after 28 days, the steady increase in strength can be ascribed to the contribution of the pozzolanic reaction. This strength contribution is a function of the availability of moisture, the absence of which will limit the continued long-term strengthening of the concrete (hence the influence of curing). In fact, fly ash incorporation as a mineral admixture makes the concrete more sensitive to proper curing than an equivalent OPC mix. This is due to the fact that as far as the strength development is concerned, the pozzolanic contribution is relied upon to make up for the reduced portland cement content.

The effect of temperature on the strength development clearly distinguishes the fly ash concrete from a OPC mix. On heating, fly ash concretes exhibit a gain in strength as is depicted in Figure 2.8 below.

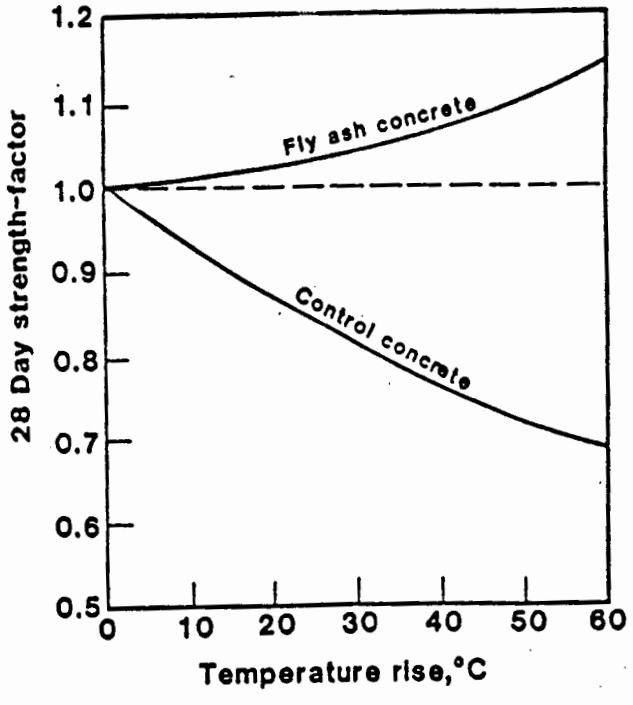

Figure 2.8: Effect of temperature rise during curing on the development of compressive strength (Berry and Malhotra, 1987).

The explanation given for strength gain of fly ash concretes on heating is that the heat initiates the pozzolanic reaction The pozzolanic strengthening continues even if the initiating external heating is discontinued. On the other hand, Alis et al. (1992) showed that low temperature curing (10°C) severely retards the development of compressive strength of fly ash concrete at early ages and at least up to 90 days (as measured in his work).

Hedegaard and Hansen (1992) attempted to explain the mechanism behind the compressive strength development of fly ash concretes. Their work was based on the principle that the portland cement and the fly ash may be considered as contributing independently to the development of concrete strength. This principle was also used by Popovics (1991), in proposing a model based on the 'Breakdown Method' to mathematically identify the fly ash contribution to measured strength. The former authors visualized a superposition of two independent mechanical pore-filling mechanisms being active in the cement-fly ash paste: the one mechanism due to pore-filling stemming from the cement hydration and the other derived from the reaction of the fly ash. Reasoning for such a proposal is given by the fact that the CSH gel formed during the cement hydration is similar in structure and properties to the gel formed by the (pozzolanic) reaction of fly ash combining with $Ca(OH)_2$. Hence the hydration reaction of the portland cement as well as the pozzolanic reaction of the fly ash lead to very much the same reaction product.

If the assumption holds, that the fly ash concrete strength development may be described in these simple terms, then it should be possible to express the process in terms of a modified Bolomey equation. The original Bolomey equation is given by Hedegaard and Hansen (1992) as $\mathbf{S = A(C/W) + E}$ where

S = strength of concrete (MPa), C = cement content (kgm^{-3}), W = free water content (kgm^{-3}), and A and E = constants for given materials, age and curing conditions of the concrete. The equation was suggested by Bolomey in 1927 on a purely empirical basis.

The modified equation as proposed by the authors is as follows:

$$S_f = A\left(\frac{C}{W}\right) + B\left(\frac{F}{W}\right) + E$$

where S_f = strength of fly ash concrete (MPa)

C = cement content (kg per m^3)

F = Fly ash content (kg per m^3)

W = Water content (kg per m^3)

A, B, E, = constants for given materials, age and curing conditions of the concrete

The above equation may be rewritten in the following way:

$$S_f = A\left(\frac{C + (k_s)F}{W}\right) + E$$

where k_S = cementing efficiency index of the fly ash

= (B/A)

k_S relates the reactivity of fly ash in relation to the reactivity of cement on the basis of strength. (For example if k_S = 0.2, for a specific amount of cement to be replaced by fly ash while maintaining the strength of the concrete, it would take five times by mass the amount of fly ash.) The value of k_S is specific to a concrete in terms of materials, age and curing regime and has to be determined. A value for k_S = 0.20 is generally taken as a first estimate.

Hedegaard and Hansen (1992) further postulated that the traditional water/cement ratio for normal portland cement concretes also applies in a modified form to the fly ash concrete situation:

> "For given materials, age and curing conditions, the strength of hardened concrete is determined exclusively by the ratio between the content of free water and portland cement in the concrete, jointly with the ratio between the content of free water and fly ash. Thus, the strength of fly ash concrete is independent of the absolute content of free water, portland cement and fly ash in the concrete."

2.3.3 DURABILITY AND PROPERTIES OF FLY ASH CONCRETE

In Fulton (Addis, 1986) the concept of durability of concrete is defined as "the ability of concrete to retain its strength, impermeability, dimensional stability and appearance over a prolonged period of service under the conditions for which it was designed".

The durability of concrete depends to a very large extent on its permeability. Ballim (1993) defines permeability as a transport concept which relates to the ease of fluid (gases and liquids) passage through the material. Permeability indicates the degree of interconnection of the pore structure of the concrete. This terminology contrasts the definition of porosity which is a bulk concept, referring to the non-solid component of the material. It is important to differentiate between these two concepts for the sake of investigating durability aspects of concrete. There is no doubt that with advance in adequate and reliable test procedures for permeability, this property of concrete will gain more and more importance and validity as a measure of short-term and long-term performance of the material.

The permeability of the concrete determines to a large extent its durability in that it controls the ingress and permeation of (aggressive) agents. Chemical deterioration processes are a function of the availability of the reacting species, which is governed by permeability, as well as the reaction conditions prevailing in the concrete environment, which is the pore structure in this case. For example, the particular mechanism of fluid transfer is a function of the relative humidity in the pore structure. The actual movement of molecules is either by:

- Adsorption, with bonding either van der Waal type or of chemical nature.
- Diffusion, driven by a concentration gradient.
- Mass flow under the influence of a pressure gradient.

The change of movement of water from adsorption to diffusion to mass flow is a function of the increase in the relative humidity in the pore structure.

Many destructive forces act on concrete in service which set up internal and external stresses. These forces, which are either material-related or environmental, may lead to premature deterioration of the concrete and result in a reduction in service life or unexpected failure of the structural member.

Mechanisms of deterioration caused be chemical reactions (Ballim, 1993) include:

- Dissolution of products of cement hydration.
- Exchange reactions between acids and the alkaline components of the hardened cement paste.
- Conversion of the products of hydration by external agents, with associated expansive forces causing deterioration.
- Internal processes of deterioration, which are due to incompatibilities between individual concrete constituents and can lead to alkali-silica reaction or delayed ettringite formation for example.
- Steel corrosion in reinforced concrete caused by de-passivation of the steel.

In the context of the presented topic, the effect of fly ash addition on the durability of concrete is to be emphasized. Ellis (1992) pointed out that for durable concrete, fly ash does not replace portland cement in the true meaning of the word, but due to its presence and influence rather contributes as an

additional factor to improve durability. The author lists five ways by which fly ash in concrete improves the durability of the material:

- Reduction in permeability.
- Improving the sulphate resistance.
- Lowering the potential of alkali-silica reaction.
- Increasing the resistance to freezing and thawing.
- Enhancing the resistance to corrosion in aggressive environments like marine conditions.

A high degree of impermeability is an important prerequisite for achieving durable concrete. Fly ash densifies the microstructure of concrete in two ways. The presence of the ash as a fine powder improves the physical particle packing by filling voids and interstices. However, a different mechanism of densification is even more important, namely the pozzolanic reaction of the fly ash which provides additional calcium silicate gel which further fills the available pore space. The deposition of the extra hydration products creates a more discontinuous pore structure and clogs pore channels. The result is that fluid transport is slowed down dramatically and hence the ingress of aggressive chemicals is limited (see Figure 2.9 below).

If sulphates enter the pore structure of set concrete, they chemically react with calcium hydroxide to form gypsum compounds and with hydrated calcium aluminate to form ettringite. The formation of both of these reaction products results in an increase in the solid volume of the cement matrix and the resultant expansive forces could lead to disruption. Fly ash enhances the resistance to sulfate attack by a threefold mechanism:

- The pozzolanic reaction of fly ash reduces the amount of $Ca(OH)_2$ present by consuming it.
- Fly ash as a cement replacement reduces the amount of portland cement, which lowers the absolute calcium aluminate content and then decreases ettringite formation.
- By reducing the permeability, the fly ash limits the penetration of sulphates into the material.

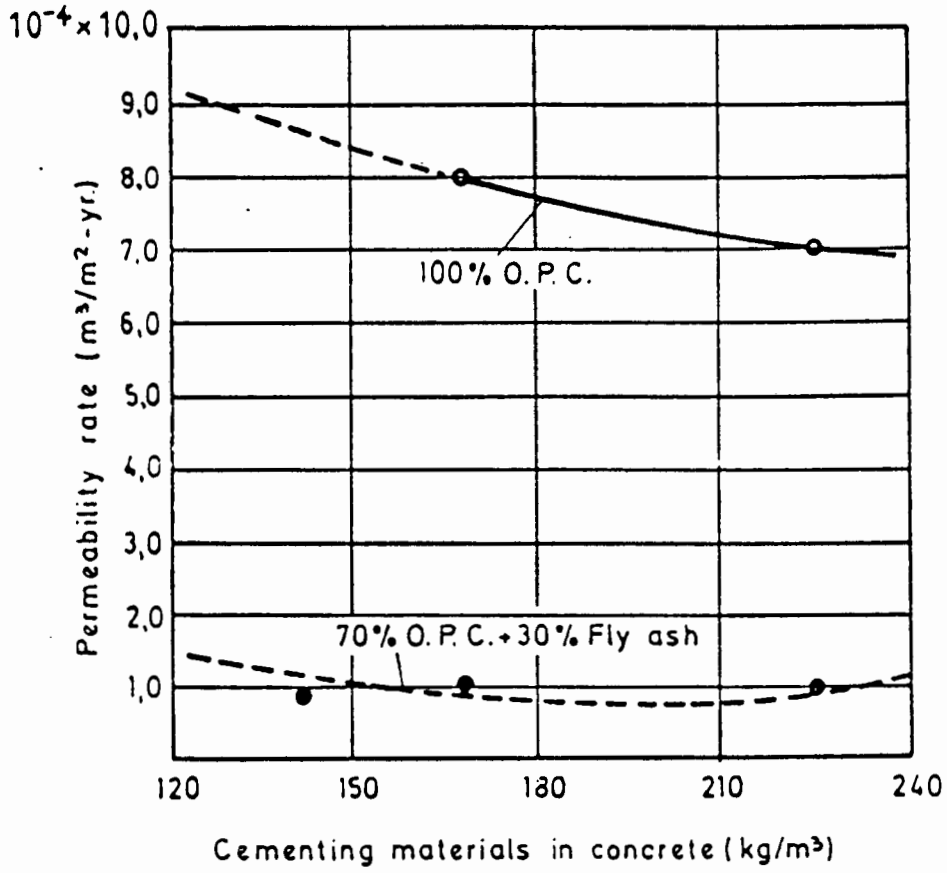

Figure 2.9: Permeability of fly ash concrete (Elfert, 1987).

Another deterioration process which limits the durability of concrete in service, is that of alkali-aggregate reactions (AAR). Under certain conditions, the

aggregates are not chemically inert and undergo reaction with alkalies present in the concrete to form expansive reaction products. It is a slow process, often taking years, but can lead to the disruptive expansion and failure of the concrete. Three conditions have to be met for AAR to take place (Davies and Coull, 1991):

- The aggregate must contain reactive constituents.
- The alkali content of the concrete itself must be sufficiently high to initiate and feed the reaction.
- A favorable environment of temperature and moisture must exist.

If the addition of fly ash to concrete restricts any of these necessary conditions, it will effectively oppose alkali-aggregate deterioration.

Three types of alkali-aggregate reaction are can occur (Ballim, 1993):

- Alkali-silicate reaction, where alkalies present in the pore water of the concrete react with silicates in the aggregate.
- Alkali-silica reaction, where the reaction is between alkalies in the pore water and amorphous or crypto-crystalline silica in the aggregate.
- Alkali-carbonite reaction which is found in concretes containing carbonate rock aggregates.

Fly ash is particularly effective in limiting AAR in the case of the alkali-silica reaction. In general, the contribution of fly ash to the total alkalinity is not significant, compared to portland cement. The total alkali content of the concrete is a function of the cement content (which is the largest source of soluble alkalis), the quantity of $Ca(OH)_2$ produced during hydration, as well as the amount of sodium and potassium hydroxide formed as by-products during the cement hydration. The mere presence of fly ash thus lowers the alkali concentration in the gel/pore structure of the concrete, because of the lower cement content. Furthermore, during the pozzolanic reaction of fly ash,

$Ca(OH)_2$ is consumed and alkali metals are combined into the calcium silicate matrix (Ellis, 1992). The second condition for AAR described above is counter-acted by the fly ash, in that it lowers the alkalis present, which would be necessary to support the alkali-silica reaction.

The resistance of fly ash concrete to cycles of freezing and thawing is another bonus derived from the improved impermeability of the material. Saturation is a prerequisite for damage by freezing and thawing, and hence the mechanism of enhancing the resistance is by limiting the ingress of water into the structure. Fulton (Addis, 1986) referred to the action of fly ash as enhancing the "watertightness" of the concrete. Nasser and Lai (1992) found that the resistance of fly ash concretes to freeze-thaw damage could weaken on continued cycling and proposed that it was due to a mechanism of slow displacement of microcrystalline $Ca(OH)_2$ and fibrous ettringite hydrates from the dense CSH zones to air voids in the structure.

The corrosion of reinforced steel in concrete is a major source of deterioration of structural members, especially in aggressive environments like marine conditions. The densification of the microstructure due to fly ash in the concrete is again the important parameter, this time limiting the chloride diffusion and preventing oxygen from entering the concrete. As the pH decreases due to the ingress of chlorides, a point is reached where the passivation layer of the steel is destroyed and corrosion is initiated. To achieve improved corrosion resistance of the reinforcing steel, the use of fly ash is more and more frequently exploited. The research of Ellis (1992) has shown that this philosophy is indeed a valid one. The corrosion resistance of the steel improved as the fly ash content increased as a fraction of the total cementitious material, even though the 28-day strength decreased as the cement was

replaced. Maslehuddin et al. (1989) investigated the steel corrosion characteristics of fly ash concretes and concluded that the steel corrosion resistance was even better when, at a constant cement level, the sand content of the mix was adjusted on a mass-to-mass replacement basis with fly ash.

The above characteristics of fly ash concrete proving it to be a high quality, durable material, have been found to apply in various investigations of high-volume fly ash concretes (substitution up to > 50% used) carried out by Malhotra (1989 and 1992) and Sivasundaram (1989). Because fly ash concretes show a lower temperature rise during initial hydration, a very useful structural application is that of mass concreting, for example in mat foundations, large retaining walls and dams. Botha (1990) investigated the heat development of fly ash concrete during building of two dams in Venda and Botswana. It was concluded that the concrete performed well in terms of keeping the heat of hydration low while maintaining good strength development which made shutter stripping possible after 48 hours.

2.4 CONCLUSION

There is no doubt that the correct use of fly ash as a mineral admixture in concrete offers many advantages. The benefits range from cost savings to enhanced material quality of the concrete. With special emphasis on the long-term durability aspects of fly ash concrete, the possibility of incorporating fly ash points in new directions that can be followed in mix design philosophy. A challenge certainly lies in optimizing the amount of fly ash used in concrete for a particular application as this will greatly influence the effectiveness of the material.

With continued research finding new and enhanced applications, the topic of fly ash concrete will continue to gain importance and acceptance. The correct utilization of fly ash in concrete ensures a prolonged densification of the microstructure due to the pozzolanic reaction. The improved impermeability achieved in this way may well become a significant factor in guarding concrete structures in urban environments against the aggressive chemicals of pollution.

The importance of curing of fly ash concrete must be stressed. Without effective curing of the concrete, the presence of the fly ash as a replacement for portland cement may possibly cause adverse effects leading to a less stable microstructure with subsequent accelerated deterioration.

Whichever criticism is raised against fly ash as a cement extender, the fact remains that, using a waste material available in large amounts to achieve improved quality concrete is a very attractive venture.

3. EXPERIMENTAL APPROACH

3.1 MATERIALS

3.1.1 CEMENT

The cement used in all the concretes and pastes was the ordinary portland cement (OPC) from the Ulco factory of Anglo Alpha.

The compositional analysis of the cement, carried out by the Blue Circle Cement (Pty) Ltd Laboratories, is given in Table 3.1. The fineness measurements, as determined on a Malvern 2600 HSD laser diffraction spectrometer in the Physics Department of the University of Cape Town, are tabulated in Table 3.2 (with complete data of the fineness measurements provided in Appendix A). The Malvern spectrometer was supported by the Malvern version B software package. Two sets of data were collected, one using a 300mm focal lens and the other a 63mm focal lens.

3.1.2 CEMENT EXTENDERS

The cement extenders introduced into the concretes and pastes as partial substitution for the cement were fly ash from the Lethabo, Duvha and Matla power stations as well as a milled clinker ash from the Van Eck power station in Windhoek, Namibia. The Van Eck ash has been classified as a clinker ash according to the definitions given by Kruger (1990). At the Van Eck power station, the coal is introduced in pellet form of size about 2cm to 4cm and the produced ash is a combination of the coarser bottom ash and fine fly ash.

All the coal ashes were analyzed for their chemical composition by the Blue Circle Cement (Pty) Ltd Laboratories (Table 3.1). The fineness was determined with the

Malvern laser diffraction spectrometer (Physics Department of the University of Cape Town). Some important results from the fineness measurements are listed in Table 3.2, with complete data sheets attached in Appendix A. Figure 3.1 and 3.2 show the histograms of frequencies of particle size distributions obtained from the laser diffraction experiments (300mm lens) on the Van Eck material as collected and the commercially available Lethabo fly ash. It is clear how coarse the clinker ash is in comparison to the fly ash.

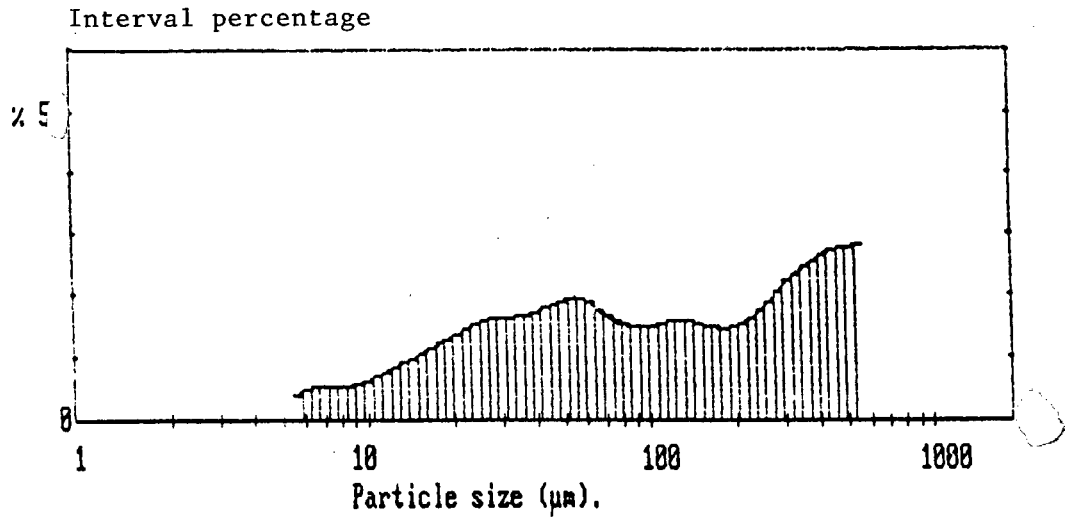

Figure 3.1: Particle size distribution for the collected Van Eck clinker ash.

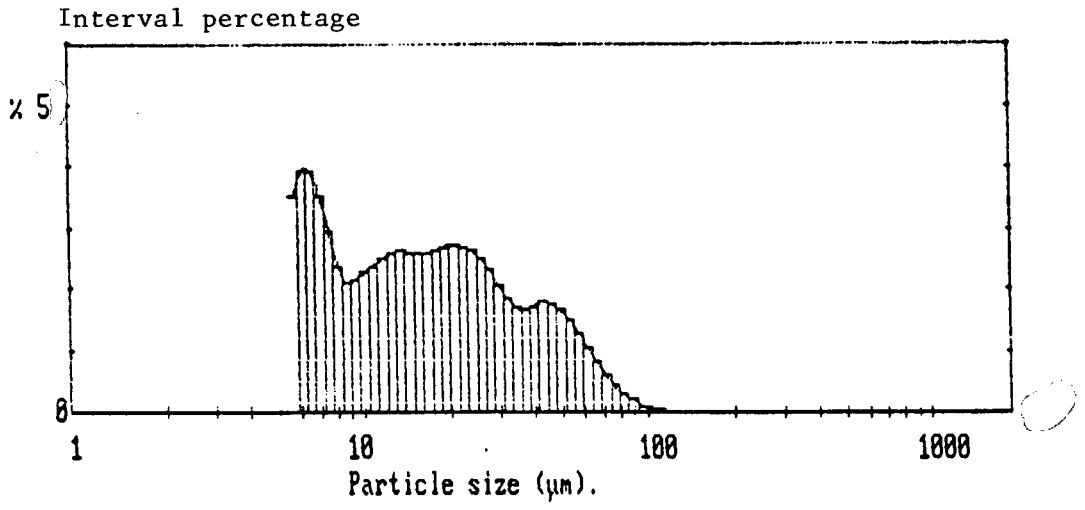

Figure 3.2: Particle size distribution for commercially available Lethabo fly ash.

The American standard, ASTM C618-89 differentiates fly ashes on the basis of the sum of the percentages of SiO_2, Al_2O_3 and Fe_2O_3 into Type F or Type C. The fly ashes of Lethabo, Duvha and Matla all comply with the Type F specification, with the sum being greater than or equal to 70%. For the clinker ash from the Van Eck power station the quantities of the three compounds add up to 59.55% and under the above classification the ash would fall under the category of Type C.

However, because the Van Eck material is not a true fly ash and contains carbon in excess of 30% by mass, it is suggested that the above classification should not be accepted as absolute. This proposition is further emphasized when looking at the calculated chemical composition of the Van Eck material based on 0% carbon (also given in Table 3.1). If thus only the non-volatile constituents are considered, the chemical composition of the Van Eck clinker ash is remarkably similar to that of the fly ashes and the sum of the oxides, SiO_2, Al_2O_3 and Fe_2O_3, is greater than 70%. The only noticeable difference is that the lime content of the Matla fly ash is about double that of the other ashes. However, the carbon content, as determined by loss on ignition at 950°C, is 35.38% for the Van Eck material which, according to the ASTM C618-89 standard (which allows a maximum carbon content of 12% for Type F and 6% for Type C), renders it totally unsuitable for use as a cement extender in concrete.

Table 3.1: Chemical composition of the cementicious materials used.

	Ulco OPC	Lethabo Fly Ash	Duvha Fly Ash	Van Eck Clinker Ash	Van Eck Clinker Ash*	Matla Fly Ash
CaO (%)	65.61	4.69	4.47	2.76	4.27	9.30
SiO_2 (%)	21.51	54.07	53.11	35.89	55.54	47.84
Fe_2O_3 (%)	2.68	3.30	5.71	3.78	5.85	3.78
Al_2O_3 (%)	4.50	32.85	30.76	19.88	30.76	30.18
MgO (%)	2.28	1.27	0.97	0.64		2.46
TiO_2 (%)	0.28	1.66	1.64	0.97		1.58
Mn_2O_3 (%)	1.06	0.04	0.06	0.03		0.06
K_2O (%)	0.57	0.55	0.63	0.34		0.72
Na_2O (%)	n.a.	0.55	n.a.	0.16		0.55
SO_3 (%)	n.a.	0.35	n.a.	0.01		0.36
LOI, 950°C (%)	n.a.	0.50	n.a.	35.38		3.00

Van Eck Clinker Ash* = Calculated composition of Van Eck ash based on 0.0 LOI
n.a. = not analysed for.

To standardize the influence of particle size on the concrete properties and the reactivity, the ashes were passed through a 63μm sieve and only the fraction passing was used in the concretes and pastes. In Table 3.2, the designation Lethabo(-63) thus refers to fly ash from the Lethabo power station which has been passed through a 63μm sieve. For the Van Eck ash, the sample designated as 'collected' represents the form of the material as being collected at the power station prior to milling. The milling of the ash was carried out by Scientific Services Namibia (Pty) Ltd Laboratory in Windhoek.

Samples of the four ashes, before sieving, were sent to the Division of Building Technology, CSIR, Pretoria. The samples were analyzed by X-ray diffraction to obtain a comparative estimate of the amount of glassy phase present. The four diffractogrammes are provided in Appendix A. A visual inspection of these

diagrams gave the following ranking of the ashes as a function of decreasing glass content:

Van Eck > Lethabo > Matla > Duvha.

The above sequence was supported by Kruger (1993). It must, however, be mentioned that, on visual inspection, the diagrams of Lethabo and Matla are very similar. Bosch and Willis (1990) found the ranking of the glass content for fly ashes collected during 1987 and 1988 to be as follows:

Matla > Lethabo > Duvha.

The important conclusion that may be drawn from both sequences is that Duvha fly ash has the least amount of glass, Lethabo and Matla have similar amounts and Van Eck contains the highest percentage of glassy phase.

To be able to comment on the repeatability of the fineness results, three determinations for the Van Eck(-63) material were carried out using the 63mm focal lens. The three results for the specific surface area in m^2/cc were 1.0206, 1.1117 and 1.0901. Based on these values, the 95% confidence interval was calculated to be 1.0741 ± 0.118 m^2/cc. by the statistical equation (Skoog *et al.*, 1988):

$$\text{Confidence limits for } \mu = \bar{x} \pm {ts}/{\sqrt{N}}$$

where μ = population mean

$\bar{x}$ = sample mean

t = statistical parameter

s = standard deviation

N = number of replicate measurements

The three values for specific surface area used in the calculation do fall into the calculated interval and thus, assuming the sample is representative, it may be concluded that the results tabulated comply with a 95% confidence level.

Table 3.2: Results from the fineness measurements carried out on the Malvern laser diffraction spectrometer.

	Span*		Specific Surface Area, m^2/cc**	
Focal Length	63mm	300mm	63mm	300mm
Ulco OPC	2.21	2.14	0.5819	0.6128
Lethabo	2.60	3.09	0.7712	0.7472
Lethabo(-63)	2.35	2.37	0.7722	0.9393
Duvha	2.82	2.19	0.6393	0.7529
Duvha(-63)	2.20	2.33	0.6607	0.7201
Van Eck, collected	2.29	4.08	0.2838	0.1627
Van Eck, milled (not sieved)	1.83	2.26	1.2492	1.1354
Van Eck(-63)	2.12	1.99	1.1117	1.1510
Matla	2.56	2.17	0.7626	0.7694
Matla(-63)	2.15	1.98	0.8388	0.7732

Span* = measure of the range of particle sizes
Specific Surface Area** = calculated value based on the laser diffraction pattern

3.1.3 AGGREGATES

The 19mm Malmesbury Greywacke stone served as coarse aggregate whereas the Klipheuwel pit sand (FM = 1.83) made up the fine aggregate in the concrete mixes.

3.1.4 MIXING WATER

The mixing water used for the concrete mixes and pastes was Cape Town tap water as supplied to the Civil Engineering Concrete Laboratory. A sample of the

water was analyzed by J.Muller Laboratories in Cape Town. The results reported for the parameters of significance to concrete are tabulated in Table 3.3.

Table 3.3: Important parameters of the chemical composition of concrete and paste mixing water.

pH	8.47
Total Dissolved Solids 180°C (Calc)	103 mg/l
Chloride	29 mg/l
Total Alkalinity ($CaCO_3$)	35 mg/l
Sulphate (SO_4)	< 5 mg/l

3.2 MIX DESIGN AND SAMPLE PREPARATION

The calculations of mix proportions for the concretes were based on the mix design method as suggested in Fulton (Addis, 1986). The mixes were designed with a W/(C+FA) ratio (water-to-cement-plus-fly-ash-ratio) of 0.56. The same ratio was used for the clinker ash. Table 3.4 summarizes the mix proportions of the concrete mixes.

Table 3.4: Concrete Mix Proportions.

Material	Mass per m^3
Cement	227
Fly Ash	97
Water	180
Stone	1150
Sand	770

A constant water to total cementitious material ratio of 0.56 as design criterion means constant mix proportions for all the concretes prepared. The fly ashes and clinker ash were introduced at a 30% straight mass to mass substitution for portland cement. Thus the type of cement extender is the only entity changing between different concretes (and pastes) - no adjustments in water or aggregate content were made to incorporate differences in the characteristics of the ashes. The control mix was designed for a workability of between 60mm and 70mm slump. The slump measurements obtained for the fly ash concretes and clinker ash concrete would be a reflection of the influence of the particular cement extender on the water requirement of the mix as well as its plasticizing abilities.

Six concrete mixes were prepared, which are designated as follows:

Designation	Description	
M1		Control mix, no fly ash added
M2	Extender:	Lethabo (-63μm) fly ash
M3	Extender:	Commercially available Lethabo fly ash
M4	Extender:	Duvha (-63μm) fly ash
M5	Extender:	Van Eck (-63μm) milled clinker ash
M6	Extender:	Matla (-63μm) fly ash

The concrete designated M3 in comparison to M2 would show any effect which the sieving procedure had on the concrete properties. For every mix, 20 concrete cubes of size 100mm were cast and compacted for 30 seconds on a vibrating table. After 24 hours in the humid room the cubes were demoulded and standard cured in water (22-25°C). At time intervals of 3, 7, 14, 21 and 28 days respectively, the density of four cubes was calculated (from the saturated mass and saturated volume) and the compressive strength determined with an Amstler compression tester (loading rate = about 15MPa/min).

In parallel, pastes were prepared from cement plus extender (at a W/(C+FA) ratio of about 0.4), without any aggregate additions. Because no microstructural investigation was going to be carried out on the paste samples, the exact amount of mixing water added was not a significant factor. Five cubes of size 70mm were cast for each blend, compacted for a few seconds on a vibrating table, stored in the humid room for a day, demoulded and then wet cured with the concrete cubes. At each particular time interval (as above) of the sample, a cube was crushed, material removed from the center of the cube (to minimize the effect of carbonation) and milled by mortar and pestle to pass a 106μm sieve. This paste sample was then immediately frozen at -74°C to terminate the hydration reaction

and the ice removed by sublimation under vacuum overnight. (The freeze-drying facility of the Department of Biochemistry at the University of Cape Town was used.) The dried sample was milled again by motar and pestle to pass a 63μm sieve. In this form, the samples were studied by differential thermal analysis (DTA) and thermogravimetric analysis (TGA) techniques.

The thermal properties of the samples prepared from the pastes were studied with a TGDTA Stanton Redcroft 780 Thermal Analyzer at the Chemical Engineering Department of the University of Cape Town. The apparatus records simultaneously the differential thermal changes as well as the change in mass for a sample. Alumina (25mg) served as reference material. A constant heating rate of 10°C/min from ambient temperature to 600°C under controlled atmospheres was set. All the samples were analyzed in dry nitrogen, introduced at a flow rate of 30ml/min. Material from the pastes containing the Van Eck ash were also analyzed in normal air atmosphere (also at a flow rate of 30ml/min). From the thermogravimetric traces, the derivative thermogravimetric plots were generated by manipulating the data with the aid of computer spreadsheet functions.

The DTA, TGA and DTG (derivative of TGA) plots for the different pastes are given in Appendix C.

4. RESULTS AND DISCUSSION - CONCRETE PROPERTIES

4.1 THE FRESH STATE

To quantify the workability of the fresh concretes, the standard slump test was carried out. The results are quoted in Table 4.1.

Table 4.1: Workability of concretes.

Concrete Mix	Extender	Slump (mm)
M1	None	65
M2	Lethabo(-63)	170
M3	Lethabo	160
M4	Duvha(-63)	80
M5	Van Eck(-63)	70
M6	Matla(-63)	125

The workability of a concrete is directly related to the water requirement of the mix, that is, the more water added to the mix, the greater the slump. The partial substitution of fly ash for cement increases the fraction of fines, thus increasing the total surface area. The larger surface area requires more water to wet all the surfaces during the mixing process and there should thus be an inverse correlation between the slump and the surface area of the mix components if the water content is kept constant. Plotting the values from Table 4.1 against the specific surface areas given in Table 3.2, yields the graphical representation given in Figure 4.1.

As far as the fly ash concretes are concerned, it appears that, for constant water content of the concrete, the increase in surface area due to the fly ash addition actually increases the slump. This finding contradicts the expected trend. The reason is that the increase in workability (which is due to the larger plasticizing effect of the finer ash and which results in a larger slump), overrides the increase

in water requirement (which is due to the larger surface area to be wetted and which results in a smaller slump).

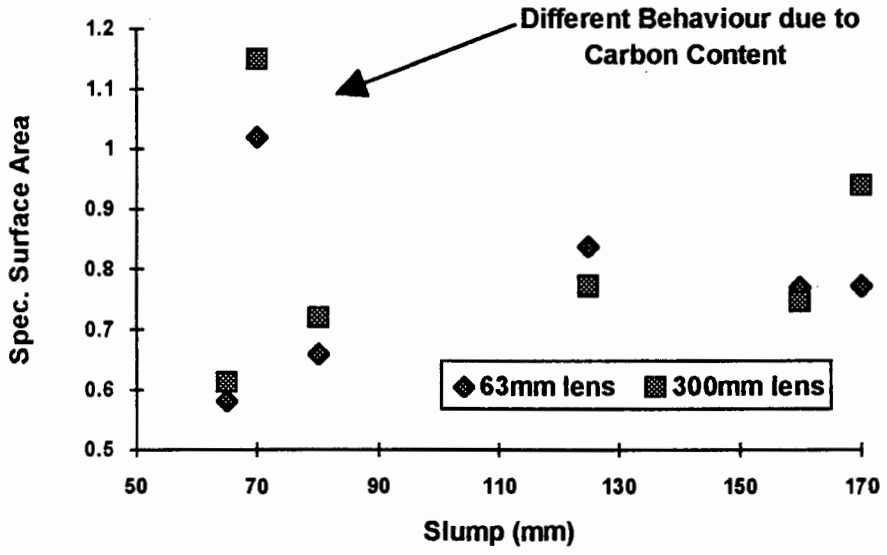

Figure 4.1: Relationship between the specific surface area of the ash and the workability of the test mix.

The Van Eck material does not follow this trend, probably because the exceptionally high carbon content of the ash dominates its behaviour. Although the ash has the highest surface area, it is thought that the porous carbon absorbs a large amount of water, with the result that the slump is decreased.

Comparing the slump values for mixes M1 and M2, it can be concluded that the absence of ash particles greater than 63μm did not influence the workability of the two concretes significantly. The difference of 10mm recorded by the slump test does not differentiate the two concrete mixes meaningfully.

4.2 THE HARDENED STATE

For each concrete cube the saturated mass and saturated volume was determined prior to compression testing, in order to calculate the density. The complete set of data, including the saturated volume, saturated mass and density together with standard deviations is given in Appendix B.

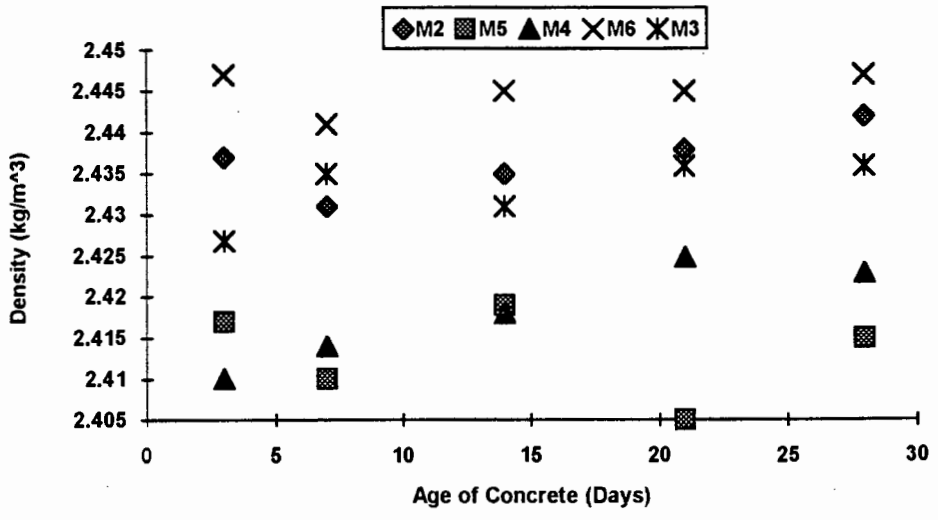

Figure 4.2: Graphical representation of the concrete densities.

As can be seen from Figure 4.2, the densities of the various concretes fall within a narrow range and remain relatively constant over the curing period. The concrete containing the Van Eck material, though tending towards the lower range of calculated densities, is not significantly different from the other concretes. Thus the influence of the high carbon content on the density of the concrete is minimal.

The compressive strength of the concretes was tested at the different time intervals after casting. Table 4.2 lists the average results for the six concrete mixes together with the calculated strength of a control mix with only 70% of the cement content used in the present mix design. If the 70% strength value of the control

mix is used for comparison, any inherently cementicious character of the ashes should be easier to detect.

Table 4.2: Compressive strength of concretes.

		Average Compressive Strength of Concrete Cubes (MPa)				
Mix	Extender	3 Days	7 Days	14 Days	21 Days	28 Days
M1	None	17.8	26.1	33.2	36.8	39.0
70% M1	None	12.5	18.3	23.2	25.8	27.3
M2	Lethabo(-63)	11.3	17.9	21.8	26.3	28.3
M3	Lethabo	10.0	15.8	21.0	25.1	26.8
M4	Duvha(-63)	11.0	16.7	22.1	25.7	28.4
M5	Van Eck(-63)	12.8	20.1	25.0	28.3	30.7
M6	Matla(-63)	10.7	18.0	22.6	25.5	28.1

Compared to the fly ash concretes, the Van Eck concrete recorded higher values of compressive strength at all test dates, particularly after three and seven days of curing, when the differences in strengths were most noticeable.

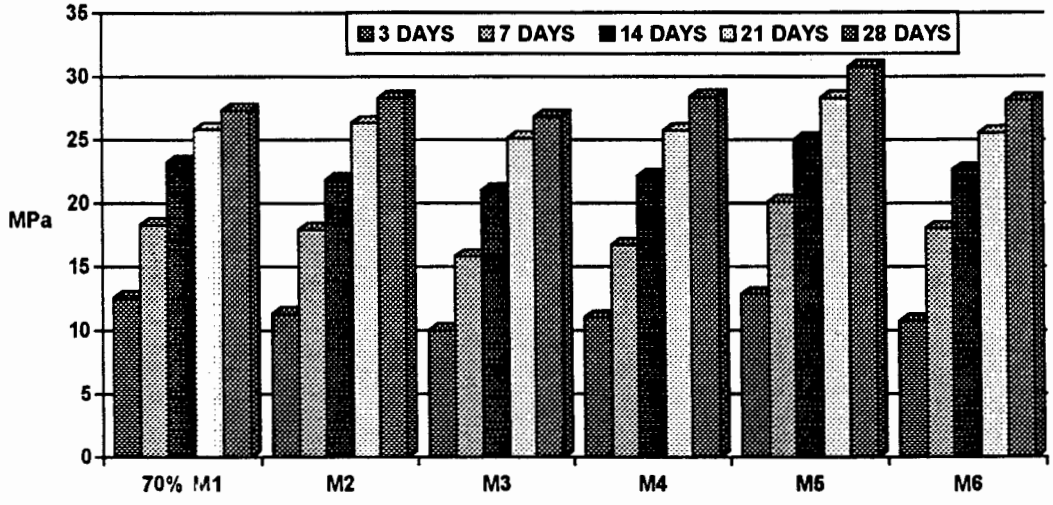

Figure 4.3: Compressive strengths of concretes.

If a fly ash is a truly pozzolanic material, it will initially merely resemble a filler material which aids the dispersion of cement particles and renders additional sites for hydration products to form. In other words, until the pozzolanic reaction starts, the strength of the concrete containing the fly ash should be about 30% less than that of the control mix. However, this is a very simplistic approach which does not take into account possible enhancing effects, such as improved packing, or more important, the influence of the resulting change of actual (W/C) ratio.

In Table 4.3 the compressive strengths of the different concretes are compared with the calculated 70% strength of the control mix. A plus and minus sign show higher or lower values respectively. In Figure 4.4, the data is presented in graphical format with the zero line indicating the position of the 70% control reference strength.

Table 4.3: Comparison between strengths of test concretes and the calculated 70% strength of the control mix.

	3 Days	7 Days	14 Days	21 Days	28 Days
M2 - Lethabo(-63)	-	-	-	+	+
M3 - Lethabo	-	-	-	-	-
M4 - Duvha(-63)	-	-	-	-	+
M5 - Van Eck(-63)	+	+	+	+	+
M6 - Matla(-63)	-	-	-	-	+

The concrete with the milled (and sieved) Van Eck clinker ash distinguishes itself clearly from the concretes containing the fly ashes. Right from the start the Van Eck mix developed a higher compressive strength than the calculated 70% strength value of the of the control mix cured for the same period. The milled clinker ash thus contributed significantly to the strength development of the concrete over the

time span tested, particularly during the first seven days of curing. The fly ash concrete, on the other hand, had initially lower strengths than that expected from the simple dilution model, but after about seven days of curing, their strengths increased at a faster rate than that of the control mix, eventually exceeding the calculated 70% strength values after about 21 days of curing.

Taking into account the degree of reproducibility of strength determinations, the results indicate that the four fly ashes seem not to possess any significant cementicious character of their own. The reason for the relatively low initial strengths of the fly ash concretes are not clear, but it is probably the combined result of changes in specific surface areas, packing efficiencies and actual (W/C) ratios. The pozzolanic activity of the fly ashes becomes noticeable after about seven days of curing.

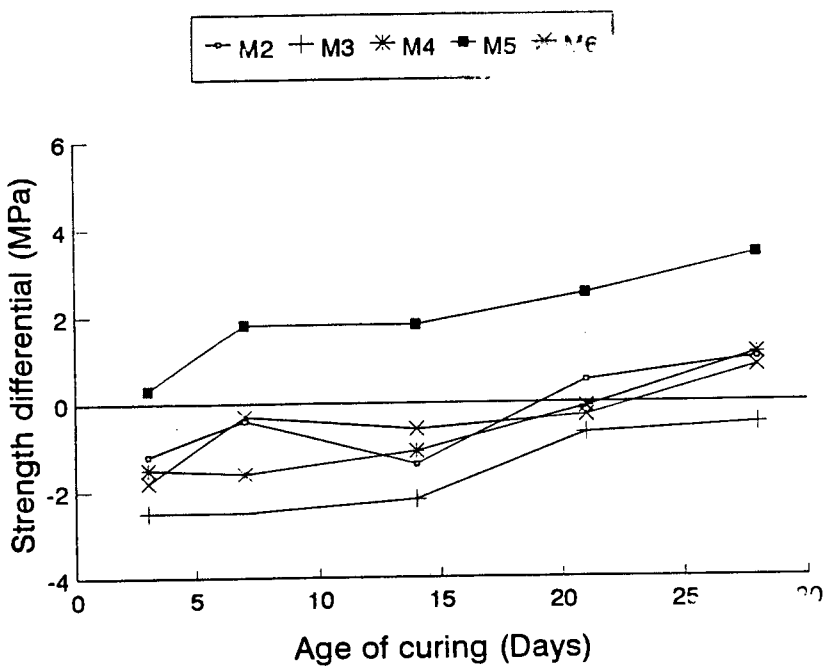

Figure 4.4: Strength differentials between test mixes and calculated 70% strength of the control mix.

In contrast, the milled clinker ash appears to have a definite cementicious character of its own, which is mainly active during the first seven days of curing, with the result that the compressive strength of its mix is consistently higher than that of the fly ash mixes. The reasons why this material shows cementicious behaviour do not lie in its chemistry (it has practically the same chemical composition as the fly ashes), but it could be the result of its higher glassy phase content and the higher specific surface area, compared to the fly ashes. On the other hand, the pozzolanic reactivity of the milled clinker ash is very similar to that of the fly ashes, as shown by the similarity of the slopes of the curves after 14 days of curing.

To use fly ash effectively as a cement extender in concrete, it is important to understand the pozzolanicity of the material. In order to quantify this aspect, various test methods have been developed (Wesche, 1991). One of these is to calculate the pozzolanic activity index (PAI) relative to portland cement which is given by PAI = A/B · 100 where A is the average compressive strength of test mix cubes and B is the average compressive strength of control mix cubes. The pozzolanic activity index is generally quoted at 28 days, although calculated at any time interval (Table 4.4).

Table 4.4: Pozzolanic activity indices.

Days	M2	M3	M4	M5	M6
3	63.5	56.2	61.8	71.9	60.1
7	68.6	60.5	64.0	77.0	69.0
14	65.7	63.3	66.6	75.3	68.1
21	71.5	68.2	69.8	76.9	69.3
28	72.6	68.7	72.8	78.7	72.1
Average	68.4	63.4	67.0	76.0	67.7

The PAI values are the highest for the Van Eck concrete. It must however be remembered that the higher strength for the Van Eck mix does not result only from pozzolanic strengthening, but is aided by the additional binding capacity of the material. According to Wesche (1991), pozzolanic activity of fly ash commences after 14 days and thus calculated PAI values for three and seven days resemble more a strength index than a measure of pozzolanicity.

The presence of the high percentage of carbon in the Van Eck material dominates the colour of the concrete prepared with the ash. On the photograph (Figure 4.5) the colour difference between a 100mm cube of concrete containing the black Van Eck(-63) material and Lethabo(-63) fly ash is shown.

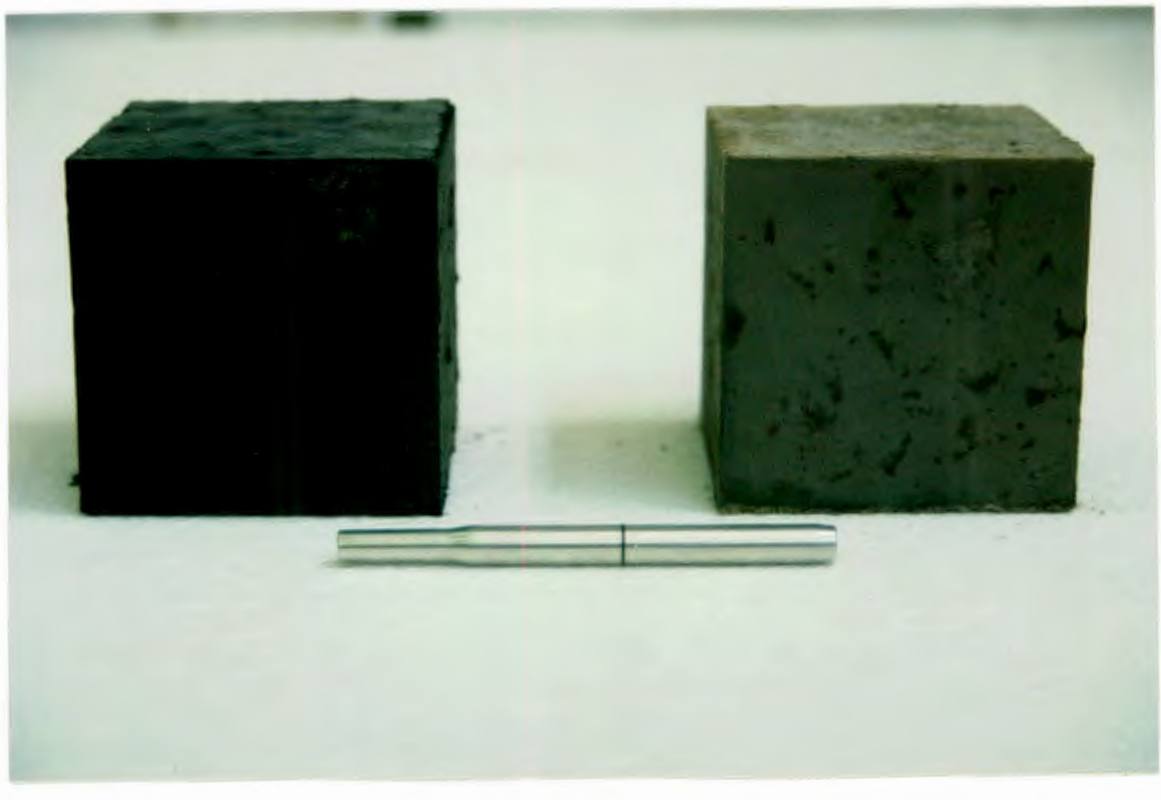

Figure 4.5 : Photograph showing a cube of concrete with Van Eck(-63) milled clinker ash (left) and one with Lethabo(-63) fly ash (right), both at a 30% direct substitution level of the cement extender.

5. RESULTS AND DISCUSSION - PASTES

The study of the thermal decomposition behaviour of cements and cement blends is of a complex nature. Differential thermal analysis (DTA) and thermogravimetric analysis (TGA) are two dynamic thermal methods complementing each other and if used together can lead to successful interpretations and findings which would be difficult to achieve with other experimental tools. Both methods however are very sensitive to procedure details and instrumental factors like heating rate and furnace atmosphere, as well as sample details such as particle size and packing density.

Soomro (1988) summarizes the method of differential thermal analysis as follows. It involves measuring the heat changes associated with chemical and physical transformations taking place on gradual heating of a test sample. Transformations such as dehydration, crystalline transition, lattice destruction, oxidation and decomposition are generally accompanied by thermal changes which can be detected by DTA . In order to relate a peak in a DTA plot to a specific phase or phase change in the material, its temperature, endothermal or exothermal character, intensity and other general characteristics (like peak shape) need to be determined. The application of DTA as an experimental tool shows limitations in cases where overlap of thermal reactions occurs, as this leads to difficulties in resolution of the peaks. Other important factors influencing the success of DTA as an analysis tool, include equipment parameters like heating rate, sample characteristics such as size and packing as well as the stoichiometry and crystallography of the phase or compound.

A comprehensive guide to differential thermal analysis is given by MacKenzie (1957). With the use of figure 5.1, which shows an idealized peak, the significance of the peak characteristics may be explained as follows. Along the line AB, no reaction is taking place, as the temperature difference remains zero. At B an endothermic reaction starts giving rise to the peak BCD. At C, the minimum of the peak, the rate of heat absorption by the reaction, equals the difference between the rate of heat supply to the test sample and to the reference material. It is important to note that point C does not correspond to the temperature where the reaction rate is at maximum or the temperature where the reaction is completed. The temperature of the reaction rate maximum is given by the inflection point of the curve between points B and C, while the reaction is terminated at the inflection point between C and D.

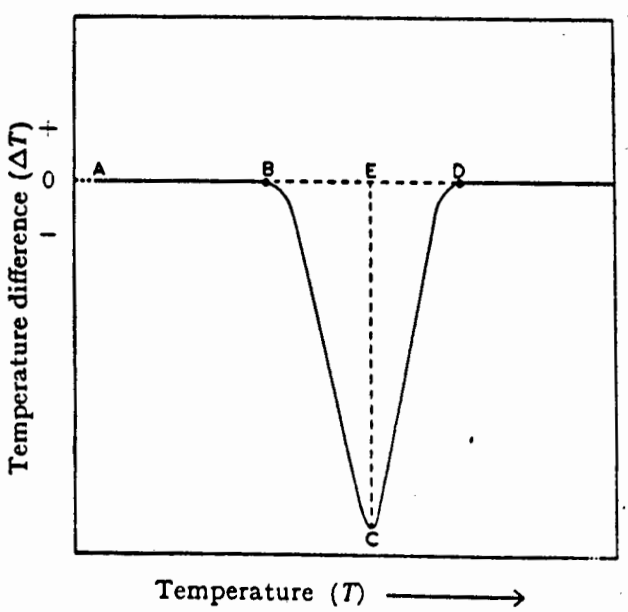

Figure 5.1: Idealized endothermic peak on a differential thermal curve (MacKenzie, 1957).

From point D onwards the temperature difference between the sample and the reference material is zero again until another transformation occurs. The temperature at point C is referred to as the peak temperature and is taken by convention as a characteristic of the phase or compound present. The peak area (area BCD) is proportional to the amount of reactant. BD is termed the peak width whereas the distance EC is known as the peak height.

The qualitative aspect of differential thermal analysis involves the identification of peaks obtained. From literature it is evident that no characteristic values for peak temperatures apply for the same minerals. For example, Marchese and Sersale (1986) quote the peak temperature for ettringite (calcium aluminate trisulphate hydrate) as 150°C , Bye (1983) quotes 132°C , whereas Soomro (1988) notes a temperature of 130°C. In the temperature range of 225°C to 400°C, the first peak for hydrogarnet (tricalcium aluminate hexahydrate) was reported by Marchese and Sersale (1986) as well as Taylor (1964). The latter lists 120°C as the DTA temperature characteristic for tobermorite gel. An endothermic peak at 200°C is evidence of either low-sulphate calcium sulpho-aluminate hydrate or of a solid solution of this compound with tetra-calcium aluminate hydrate (Soomro, 1988). Between 400°C and 600°C the thermal effect of portlandite in the form of a well defined endothermic peak has been reported by all the above authors.

Generally, the degree of overlap between the endotherms of ettringite and calcium silicate hydrate gel is extensive so that resolution of these is difficult, if not impossible. It is for this reason that Soomro (1988) summarizes the peaks on a DTA thermogram into three temperature regions showing the major decomposition reactions:

- The endotherms occurring between 105° and 440°C are related to the dehydration or water loss by calcium silicate hydrate. (The hydrogarnets and ettringite also fall in this temperature range.)
- The temperature range between 440° and 580°C holds the peak due to the dehydroxylation of calcium hydroxide, which was formed by the hydrolysis of the calcium silicates during the hydration reaction;
- Between 580° and 1000°C decarbonation of calcium carbonate formed during exposure to air occurs.

5.1.1 IDENTIFICATION OF PEAKS

With reference to Figure 5.2 and Figure 5.3 (as well as the thermograms attached in Appendix C), the following minerals are identified according to their characteristic peak temperatures.

a.) Evaporation: None

b.) Dehydration reactions:

- The ettringite ($C_3A{\cdot}3C\bar{S}{\cdot}31$-$32H$) and tobermorite (C-S-H) gel ($3CaO{\cdot}2SiO_2{\cdot}3H_2O$) endotherms occur between 105°C and 150°C. The ettringite thermal effect overlaps the tobermorite peak. It should be noted that, per molecule, ettringite contains 31 to 32 water molecules in contrast to the 3 water molecules of the gel. The combined peak of ettringite and tobermorite broadens towards higher temperatures as the hydration reaction proceeds with time (comparing the DTA thermogram after 3 days of curing, Figure 5.2, with that given in Figure 5.3 after 28 days of curing).
- The endotherm at 190°C is ascribed to low-sulphate calcium sulpho-aluminate hydrate ($3CaO{\cdot}Al_2O_3{\cdot}CaSO_4{\cdot}12H_2O$), possibly in solid solution with tetra-calcium aluminate hydrate ($4CaO{\cdot}Al_2O_3{\cdot}12H_2O$). This peak

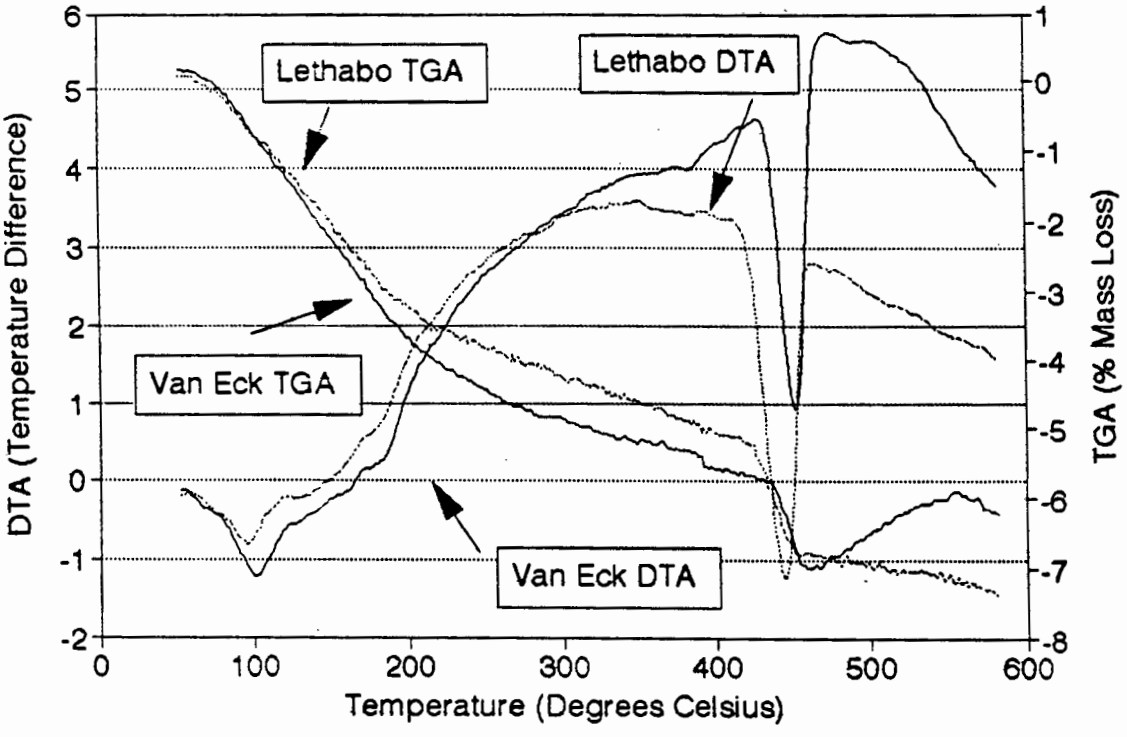

Figure 5.2: DTA and TGA plots (dry nitrogen atmosphere) for the pastes containing the Van Eck(-63) and Lethabo(-63) ashes after 3 days of curing

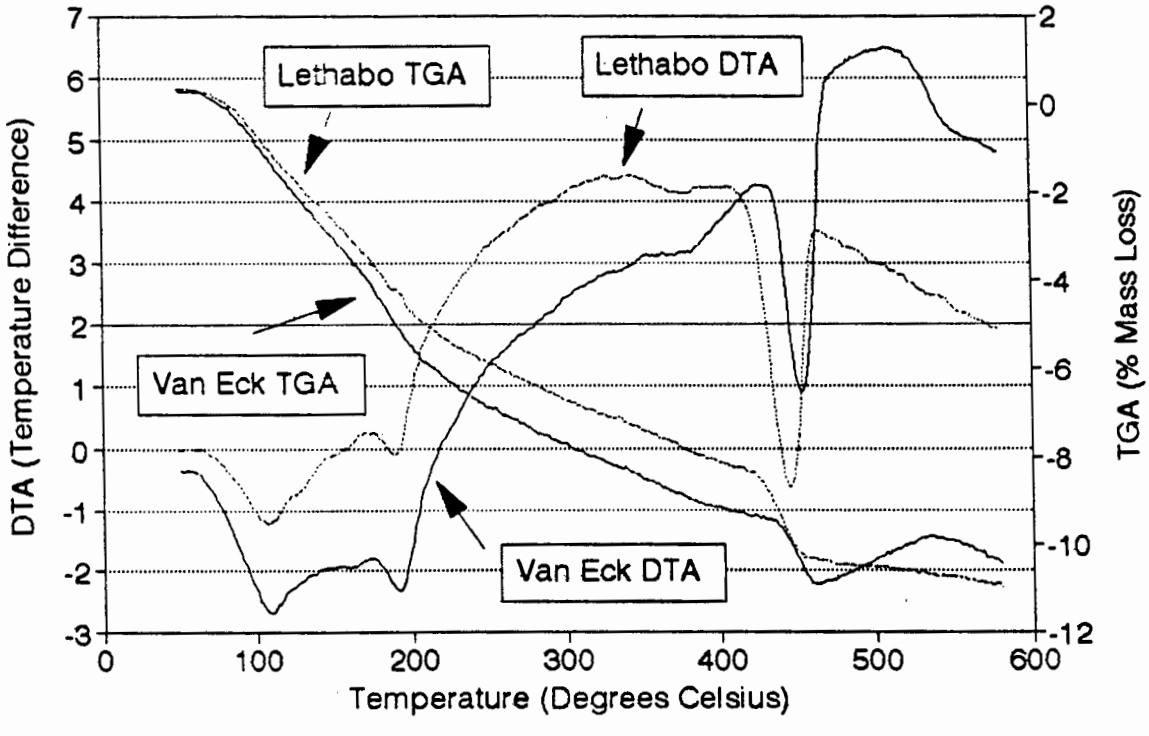

Figure 5.3: DTA and TGA plots (dry nitrogen atmosphere) for the pastes containing the Van Eck(-63) and Lethabo (-63) ashes after 28 days of curing

appears to be more pronounced for the pastes containing fly ash or the clinker ash than for the control mix (see Figure 5.4). The chemical compositions given in Table 3.1 show markedly higher values for alumina in the ashes than in the OPC, which could be the reason for the formation of larger amounts of the above-mentioned hydrates in the pastes containing the ashes.

- Hydrogarnet ($3CaO{\cdot}Al_2O_3{\cdot}6H_2O$) appears as a small endothermic peak at about 370°C.

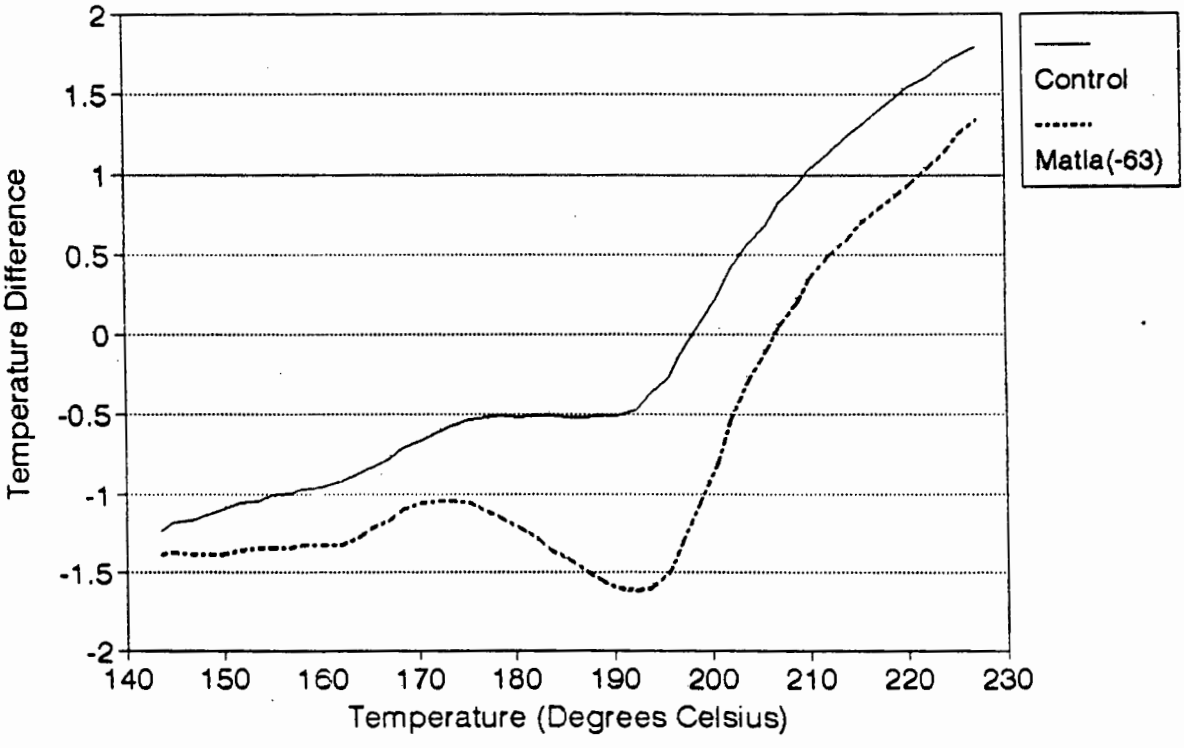

Figure 5.4: DTA thermogram showing the endothermic peak for low-sulphate calcium sulpho-aluminate hydrate for the OPC and Matla(-63) pastes (dry nitrogen atmospheres) after 28 days of curing

b.) Dehydroxylation reactions:

- The portlandite ($Ca(OH)_2$) endotherm is identified at 450°C. The portlandite peaks for all the pastes are very similar in shape. The peaks are strong and sharp with the maxima very close at 450°C. This peak shape does not change over the curing period. For the pastes containing the Van Eck(-63) material, the portlandite peak is displaced upward as well as to a slightly higher temperature. This shift is due to the superposition effect of a large exothermic effect following immediately on the dehydroxylation reaction.

In the temperature range between 350°C and 580°C the paste samples containing the Van Eck ash show a different thermal behaviour to the other materials. To explain this behaviour, reference is made to Figure 5.5 and Figure 5.6. The DTA thermograms show the Control, Lethabo(-63), Lethabo, Duvha(-63) and Matla(-63) paste samples heated in a dry nitrogen atmosphere and the Van Eck(-63) paste sample in air, all after 28 days of curing. The oxygen present in the air atmosphere allowed oxidation reactions to take place and hence differentiated the Van Eck material even more clearly from the other pastes.

The letter **A** (Figure 5.5) denotes the portlandite peak at 450°C for the fly ash pastes. For the Van Eck paste, three peaks are superimposed in this temperature region. Peak **C** is identified as the endothermic portlandite peak whereas it is suggested that **B** points to a exothermic peak resulting from the oxidation reaction of mainly maghemite, Fe_2O_3 (MacKenzie, 1957) as well as magnetite, Fe_3O_4. Overlapping these two peaks, a third peak **D** starts at about 370°C, and extends to temperatures beyond 580°C. This exothermic peak is ascribed to carbon burning off.

The above explanation is substantiated by the thermogravimetric data presented in Figure 5.6. After about 450°C the TGA curve for the Lethabo(-63) paste decreases, which indicates a mass loss.

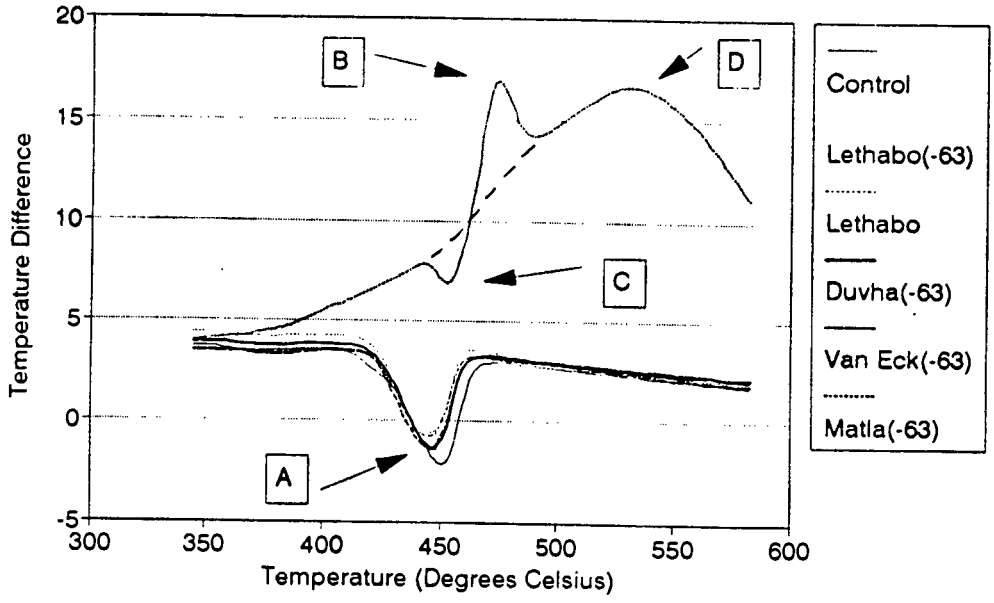

Figure 5.5: DTA Thermogram after 28 days of curing for the Van Eck (-63) paste in an air atmosphere and the other samples heated in a dry nitrogen atmosphere.

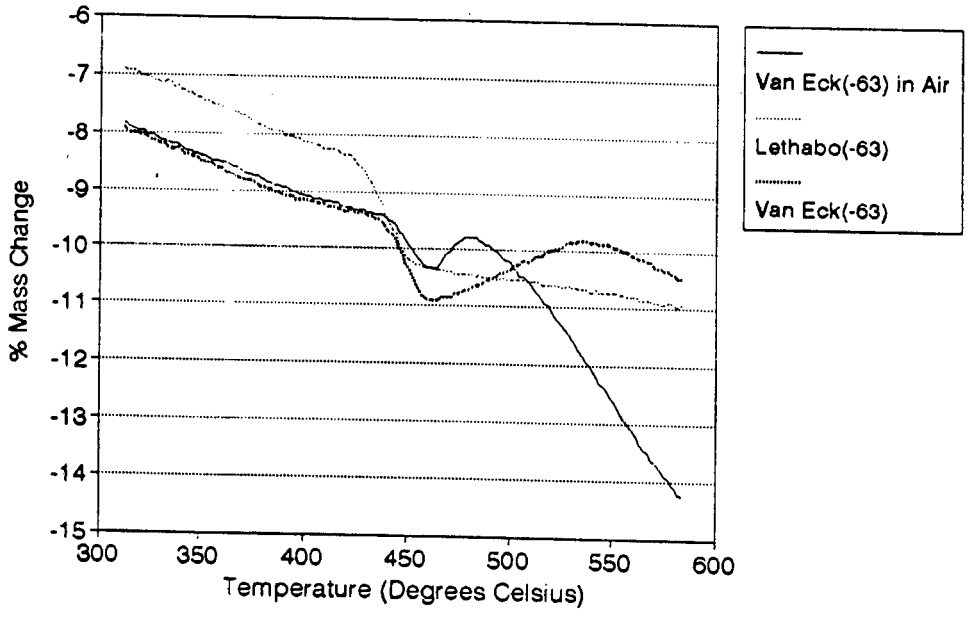

Figure 5.6: TGA plots for the Van Eck(-63) pastes in dry nitrogen and air as well as the plot for the Lethabo(-63) paste heated in dry nitrogen after 28 days of curing.

The Van Eck(-63) pastes however, show an initial mass gain after 450°C followed by a mass loss. This effect is more pronounced when the sample was heated in an air atmosphere where oxidation reactions took place. In relation to the fly ashes, the Van Eck material is in a much more reduced form because of the lower burning temperatures of the coal in the power station. Hence a large amount of volatile matter is still present in the clinker ash which starts to burn off beyond 400°C (Figure 5.5, curve D).

c.) Decarbonation reactions: These are not observed. Samples of the pastes were taken from the center of the cubes and exposure to air was very limited which practically excluded any carbonation from taking place.

5.2 THERMOGRAVIMETRIC ANALYSIS

Whereas differential thermal analysis (DTA) is based on energy changes, thermogravimetry (TGA) is based on mass changes. The decomposition reactions like dehydration or dehydroxylation are associated with a loss in mass (water in these cases). The mass change is measured against the inert reference material and expressed as a percentage of the test sample mass. All the TGA plots of percentage mass loss against temperature for the different ashes and the control paste are given in Appendix C.

In addition to the thermogravimetric plots, the data was further manipulated and the derivative of the thermogravimetric plots calculated, which gives the rate of mass change and can be plotted either against temperature or time. Such derivative thermogravimetric analysis (DTGA) curves are provided in Appendix C. The advantage of DTGA plots is that they help to establish temperatures where

thermal reactions start and end. Another advantage of DTGA is that reactions with overlapping peaks in DTA and TGA curves are often successfully separated. DTGA plots for the different ashes and the control mix are attached in Appendix C.

5.2.1 QUANTITATIVE ANALYSIS - THE AMOUNT OF BOUND WATER

The total amount of bound water present in the hydrated phases of the pastes was estimated as follows. The limiting temperatures of the thermal decomposition reactions were established from the DTGA curves in that maxima (turning points) on these traces corresponded to maximum rates of mass change. The vertical lines marked x and y (see Figure 5.7) depict how the limiting temperatures were obtained.

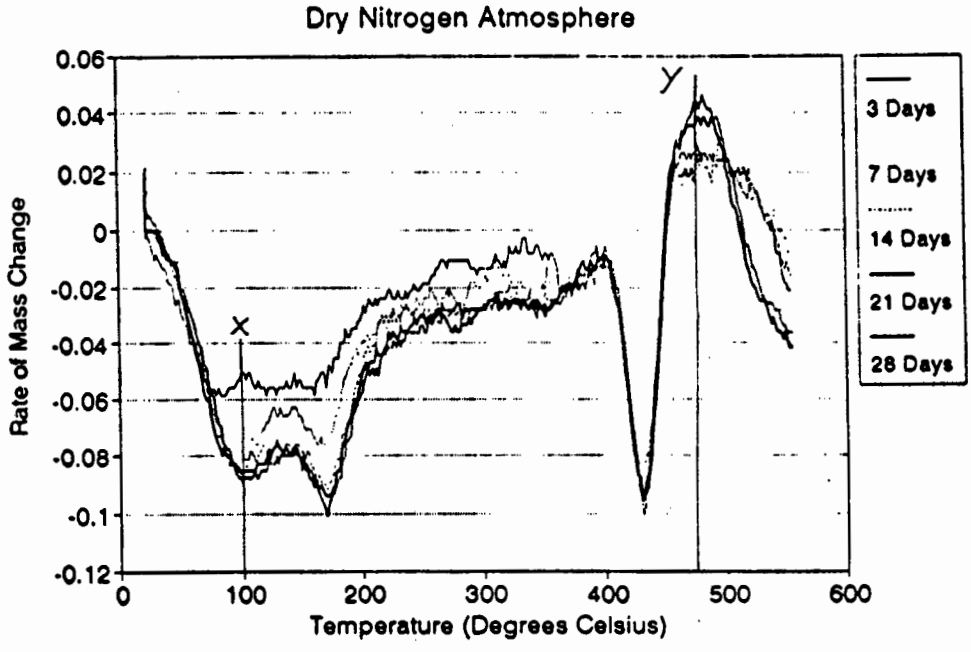

Figure 5.7: DTGA plot for the Van Eck(-63) paste samples over the total curing period.

The thermal decomposition reactions between 100°C and 600°C resulting in water loss were divided into two groups. The first group included the temperature range of 100°C to 400°C over which the mass loss due to dehydration (DH) was obtained, whereas the second group ranged from 400°C to 470°C to account for the mass loss as a result of the process of dehydroxylation (DX) of portlandite formed by the hydrolysis of calcium silicates. Figure 5.7 was used as the basis to choose the maximum temperature of the dehydroxylation reaction. The choice of 470°C was made in order to exclude the effects due to mass gain for the Van Eck (-63) material at temperatures higher than 470°C.

As shown in Figure 5.8, the amount of water and hydroxyl lost was estimated by reading off the corresponding mass changes as percentages between the specified temperatures and calculating the absolute value of the incremental weight change.

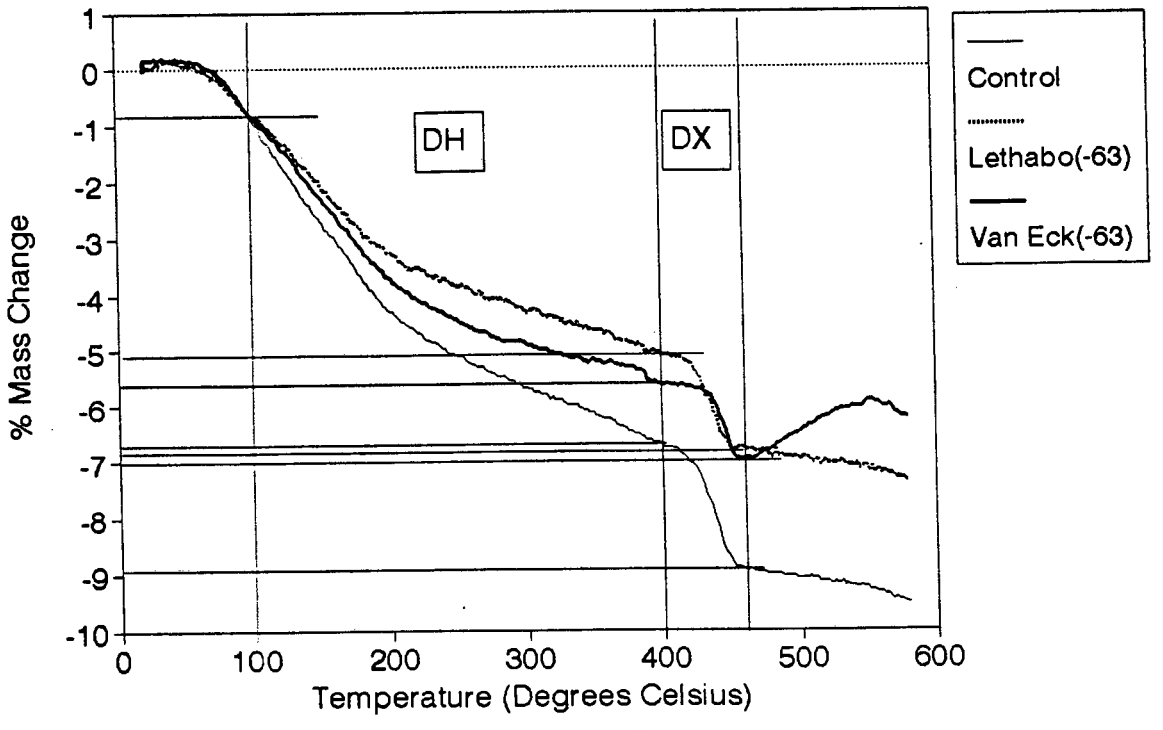

Figure 5.8: Determination of mass loss.

The percentage mass losses due to dehydration and dehydroxylation for the different pastes at the various curing times are tabulated in Table 5.1.

Table 5.1: Percentage mass loss due to dehydration and dehydroxylation, as well as total amount of bound water.

	Curing Time (Days)				
	3	7	14	21	28
	Control				
% DH	5.9	6.7	8.0	8.1	8.2
% DX	2.2	2.5	2.6	2.7	3.3
DH + DX	8.1	9.2	10.6	10.8	11.5
	Lethabo(-63)				
% DH	4.3	5.8	6.6	7.5	7.7
% DX	1.7	2.3	2.3	2.4	2.5
DH + DX	6.0	8.1	8.9	9.9	10.2
	Lethabo				
% DH	4.3	6.2	6.7	7.5	7.6
% DX	1.8	2.4	2.3	2.4	2.4
DH + DX	6.1	8.6	9.0	9.9	10.0
	Duvha(-63)				
% DH	4.3	6.2	6.6	7.5	8.1
% DX	2.0	2.3	2.8	2.6	2.3
DH + DX	6.3	8.5	9.4	10.1	10.4
	Van Eck(-63)				
% DH	4.8	6.7	8.1	8.4	8.6
% DX	1.3	1.8	1.6	1.7	1.8
DH + DX	6.1	8.5	9.7	10.1	10.4
	Matla(-63)				
% DH	4.5	5.6	6.6	7.5	7.8
% DX	1.7	2.1	2.2	2.6	2.7
DH + DX	6.2	7.7	8.8	10.1	10.5

In Figure 5.9, the compressive strength of the concrete mixes is plotted as a function of the total amount of bound water determined in the corresponding pastes. A good correlation is found. As the amount of bound water in the paste increases, so does the compressive strength of the concrete. The total amount of bound water as determined from the TGA plots relates to the amount of hydrates formed during the hydration and can be used as an indication of the strength development. Assuming that the extrapolated curve starts at the point (0,0), it can be concluded that the rate of hydration increases (the slope increases). This conclusion is valid only up to 28 days after casting as this is the curing period over which the samples were tested.

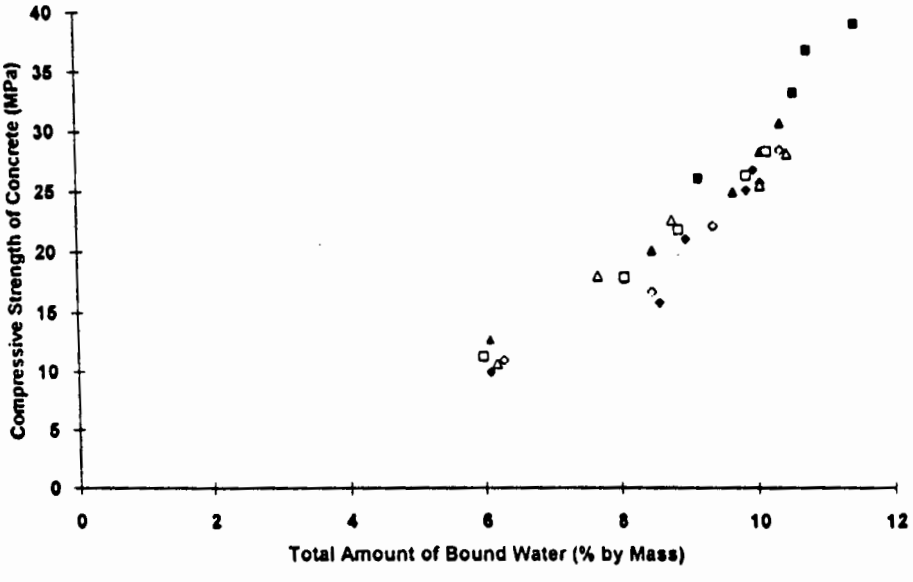

Figure 5.9: Compressive strength of concrete as a function of the total amount of bound water in the corresponding pastes.

Figure 5.10 gives the compressive strength of the concretes as a function of the amount of water lost due to dehydration reactions in the pastes, whereas Figure 5.11 relates the compressive strength of the concretes to the amount of water lost

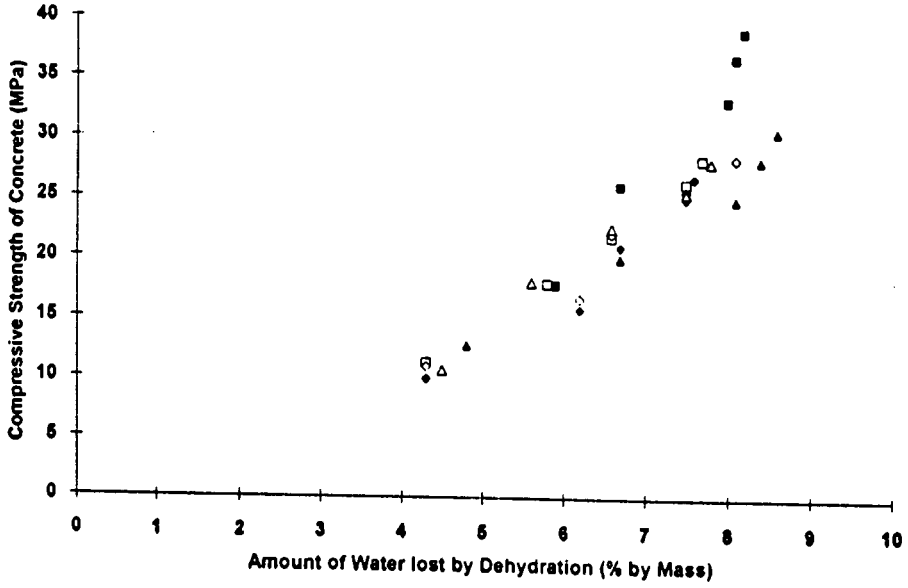

Figure 5.10: Compressive strength of concrete as a function of the amount of water lost due to dehydration reactions in the corresponding pastes.

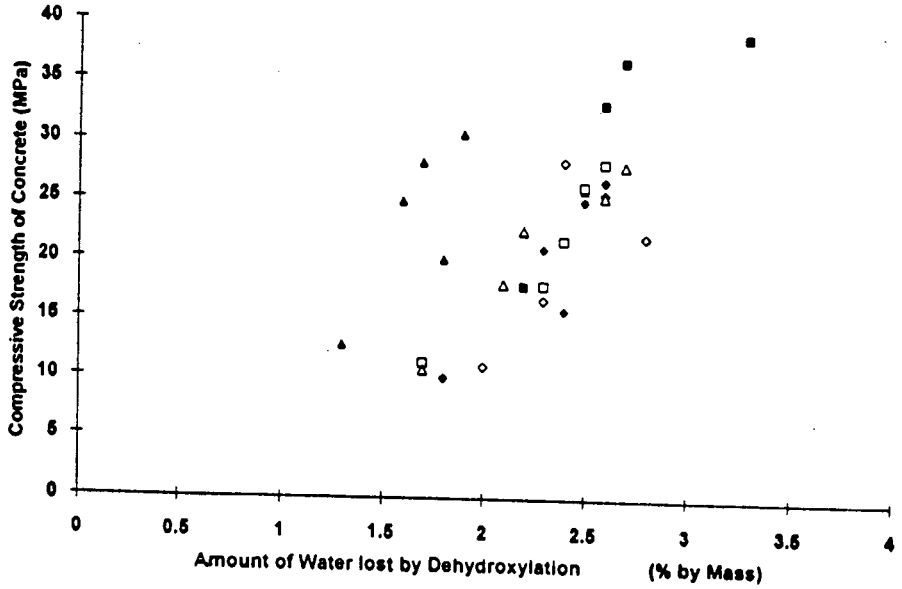

Figure 5.11: Compressive strength of concrete as a function of the amount of water lost due to dehydroxylation reactions in the corresponding pastes.

by dehydroxylation reactions in the pastes. The degree of scatter for the dehydroxylation plot is much greater than that of the dehydration plot. This is to be expected from the fact that the amount of portlandite (which is given by the percentage water lost by dehydroxylation), makes no direct contribution to the strength development of the paste (and hence the concrete). Nevertheless the trend of increasing concrete strength for increasing amount of water lost is still observed.

6. SUMMARY AND DISCUSSION

The effectiveness and properties of a clinker ash from the Van Eck power station in Windhoek (Namibia) if used as cement extender in concrete were investigated. The milled clinker ash was compared to three fly ashes (Lethabo, Duvha and Matla) on the basis of the effect on strength development of concrete prepared with the ashes introduced as a 30% direct mass to mass substitution for cement. The concrete with the Van Eck milled clinker ash unexpectedly yielded the highest values of compressive strength over the curing period tested.

The approach used for the investigation into the effect of the different ashes on compressive strength was to keep all the parameters in the concrete mix design constant and only change the type of ash to be used as cement extender. By only substituting the type of extender, the effect that the ashes have on the mixing water requirement was not adjusted for. In other words, by using constant proportions of water, cement and aggregates, the consistency or workability of the mixes was not kept constant.

The effect which the different ashes had on the workabilities of the concretes were quite different and the slump values show a large variation. The Van Eck mix, with a slump of 70mm, was very similar to the control mix (containing only OPC and no extender) in the fresh state, whereas the Lethabo(-63) mix, with a slump of 170mm, showed very different flow characteristics. Because of the fact that virtually no change (5mm difference in slump) in the flow properties occurred when partially substituting milled Van Eck ash for the cement, it must be concluded that the clinker ash has no influence on the water requirement of the concrete mix. Although the milled clinker ash had the largest surface area, as

determined by laser diffraction spectrometry, the water requirement of the concrete was not reduced. It is thus concluded that the presence of >30% carbon in the Van Eck material is responsible for the fact that no water reduction has been achieved. In Fulton (Addis, 1986), the porosity of carbon, leading to additional water absorption, is mentioned as being the factor responsible for the adverse effect of the material on the workability of a concrete. However, keeping in mind that a maximum of 12% carbon in fly ash is specified in ASTM 618-89 (1988), the Van Eck ash performed well.

Due to the water reducing capabilities of the Lethabo fly ash, less mixing water would have been needed in the concrete to obtain a specific slump value if compared to the Van Eck ash. The Lethabo mix, in contrast to the Van Eck mix, is thus essentially at a higher water to cementitious material ratio if the mix design of constant mix proportions is followed. Because the W/C ratio of concrete is inversely proportional to the compressive strength of a concrete, the lower strengths tested for the fly ash concretes in relation to the clinker ash concrete must be interpreted in the context explained above. It should thus not be concluded, by judging on the criterion of compressive strength up to 28 days, that the Van Eck ash necessarily outperforms, for example, the high quality fly ash from the Lethabo power station. The performance of a concrete with or without an extender is primarily influenced by the mix design. An aspect that is still to be investigated is thus the strength development of concretes containing the ashes used in this study, but with the concretes designed to yield a constant slump.

The pozzolanic reactivity of the Van Eck material is very similar to that of the fly ashes. This important parameter (obtained from comparing the slopes on the plot of strength differentials versus curing period in Figure 4.4 as well as calculating

the pozzolanic activity indices in Table 4.4) seems to be unaffected by the carbon present in the clinker ash. In addition to a similar pozzolanic reactivity as the fly ashes, the milled clinker ash possesses some inherent cementicious character which is clearly noticeable in the time period before the pozzolanic reaction starts. This behaviour is normally found only with Type C fly ashes. But the fact that, on correcting the chemical composition for the carbon, the criterion set in the ASTM Standard 618-89 (1988) for the sum of the oxides of SiO_2, Al_2O_3 and Fe_2O_3 having a minimum of 50% is not met any longer, the classification of the ash as being similar to a Type C fly ash is not correct. It is suggested that the milled Van Eck material be classified as a clinker ash resembling a Type F fly ash (based on the corrected chemical composition) which possesses some cementicious character in addition to the pozzolanic reactivity.

The densities of the concretes with cement extenders compare well. Again, the effect of a large amount of porous carbon present in the Van Eck mix is insignificant in changing the density of the concrete.

In conclusion, the exceptionally high carbon content of the Van Eck material (35.38%) showed a surprisingly small influence on the properties of the concrete containing the ash. Contrary to general belief, the research proved that, up to 28 days after casting the concrete, the high carbon clinker ash is a very effective cement extender. However, the fact that concrete prepared with the Van Eck material as cement extender is dark gray or black, as depicted on the photomicrograph in Chapter Four, must be taken into consideration in those applications of the material where the aesthetics are of importance.

Differential thermal analysis as a qualitative method could successfully be used to identify various phases at different stages in the hydration reactions of the pastes. Pastes of OPC plus 30% of fly ashes of Lethabo(-63), Lethabo, Duvha(-63) and Matla(-63) show a very similar thermal behaviour up 600°C. On the other hand, for the Van Eck(-63) material on the other hand additional peaks as well as different peak characteristics are observed. Peaks for ettringite, tobermorite, low-sulphate calcium sulpho-aluminate hydrate and tetra-calcium aluminate hydrate, hydrogarnet and portlandite are identified for all the pastes. The analysis of the paste containing the Van Eck material, shows additional peaks for the iron oxides of maghemite and magnetite as well as for the carbon burning off.

Thermogravimetric analysis of the paste samples clearly distinguishes between the fly ash pastes from the clinker ash paste at temperatures higher than 470°C. For the Van Eck paste, an initial mass gain is observed after 470°C which is accentuated when the samples were heated in air rather than a dry nitrogen atmosphere. The oxidation of maghemite and magnetite which shows as a exothermal peak results in this mass gain.

The quantitative analysis of the amount of water lost by dehydration and dehydroxylation could successfully be determined from the TGA plots. The important result however, is that these figures, obtained from the paste samples, could be related to the strength development of the respective concrete. The correlation between the compressive strength of concrete and the amount of water lost by dehydration was better than that between the compressive strength of the concrete and the dehydroxylation losses. This finding is consistent with the fact that it is mainly the hydrates dehydrating in the temperature range between 100°

and 470°C that contribute significantly to strength development, whereas the portlandite is ineffective in this respect.

More work needs to be done to fully evaluate the effectiveness of the Van Eck material, for example a comparison of concretes containing the ashes which are designed to constant slump, as well as a study on the durability of Van Eck concrete. However, the fact that a milled clinker ash containing over 30% carbon has successfully been used as a cement extender may be of benefit to some of the older type power stations still in use today. In most of these power stations, the ash is collected as clinker ash which includes coarse bottom ash and the fly ash. It is indeed a positive prospect that these ashes, which generally have high carbon contents, can nevertheless be used as portland cement extenders in concrete.

7. REFERENCES

Addis, B.J. (Editor) (1986) *Fulton's Concrete Technology*, Sixth Revised Edition, Portland Cement Institute, Midrand, South Africa.

Alis, J.C. et al. (1992) Mechanical Properties of Fly Ash Concrete Cured under different Temperatures and Humidity Conditions, *Fly Ash, Silica Fume, Slag and Natural Pozzolans in Concrete*, Proceedings Fourth International CANMET/ACI Conference, Instanbul, Turkey, Supplementary Papers, pp.1023-40.

American Society for Testing and Materials, ASTM (C618-89) (1988) Standard Specification for Fly Ash and Raw or Calcined Natural Pozzolan for Use as a Mineral Admixture in Portland Cement Concrete, Philadelphia.

Ballim, Y. Chemical deterioration processes, Personal Notes, presented at the University of Cape Town, February 1993.

Ballim. Y. Permeability of Concrete, Personal Notes, presented at the University of Cape Town, February 1993.

Berry, E.E. and Malhotra, V.M. (1987) Fly Ash in Concrete, *Supplementary Cementing Materials for Concrete*, edited by Malhotra, V.M., Energy, Mines and resources Canada, Minister of Supply and Services Canada, CANMET.

Bijen, J.M.J.M.et al. (1992) *Fly Ash as Addition to Concrete*, A.A.Balkema Publishers (for CUR), Centre for Civil Engineering Research and Codes.

Bosch, G.L and Willis, J.P. (1990) The Chemical and Mineralogical Compostions, and Particle Size Distribution, of Fly Ash form three South African Power Stations, *First National Symposium*, CSIR Conference Centre, Pretoria.

Botha, J. and Amtsbüchler, R. (1990) Heat Development in FA Concrete, *First National Symposium*, CSIR Conference Centre, Pretoria.

Bye, G.C. (1983) *Portland Cement: Composition, Production and Properties*, Pergamon Press.

Dartsch, B. and Herten, D.L. (1992) Einsatz von Steinkohlenflugasche im Beton- und Fertigteilwerk, *Concrete Precasting Plant and Technology*, **1**.

Davis, D.E. and Coull, W.A. (1991) Alkali-Aggregate Reaction, Choosing the right Aggregate and Cement for Concrete, *A Hippo Quarries Technical Publication*, Second Edition.

Dhir, R.K. (1986) Pulverized Fuel Ash: Concrete Technology and Design, *Cement Replacement Materials*, Volume 3, edited by Swamy, R.N., pp.197-255, Blackie & Son Ltd.

Elfert, R.J. (March 1987) Bureau of Reclamation Experiences with Fly ash and other pozzolans in Concrete, *Proceedings Third International Ash*

Utilization Symposium, Pittsburgh, Pa, US Bureau of Mines Information Circular IC 8640, pp.80-93.

Ellis, W.E. (1992) For Durable Concrete, Fly ash does not "replace" Cement, *Concrete International*, July, pp.47-51.

Feldman, R.N. (1989) Studies on Mechanism of Development of Physical and Mechanical Properties of High Volume Fly Ash-Cement Pastes, *Third CANMET/ACI International Conference on Fly Ash, Silica Fume, Slag and Natural Pozzolans in Concrete*, Supplementary Papers, Trondheim, Norway.

Galeota, D. et al. (May 1992) Mechanical Properties of Concretes containing Fly Ash, *Fly Ash, Silica Fume, Slag and Natural Pozzolans in Concrete*, Proceedings Fourth International CANMET/ACI Conference, Instanbul, Turkey, Supplementary Papers.

Grieve, G.R.H. (1991) The Influence of two South African Fly Ashes on the Engineering Properties of Concrete, Ph.D. Thesis, University of the Witwatersrand, Johannesburg.

Hansen, T.C. and Hedegaard, S.E. (1992) Modified Rule of Constant Water Content for Constant Consistency of fresh Fly Ash Concrete Mixes, *Materials and Structures*, **25**, pp.347-354.

Hansen, S.E. and Hedegaard, T.C. (1992) Modified Water/Cement Ratio Law for Compressive Strength of Fly Ash Concretes, *Materials and Structures*, **25**, pp.273-283.

Helmuth, R. (1987) Fly Ash in Cement and Concrete, Portland Cement association, Illinois, U.S.A..

Heckroodt, R. (1990) The Hydration of Portland Cement, Personal Notes.

Jawed, I. *et al.* (1991) Hardened Mortar and Concrete with Fly ash, RILEM Report 7: *Fly Ash in Concrete - Properties and Performance*, edited by Wesche, K., Chapman & Hall.

Krüger, J.E. and Van Djik, J. (1985) Fly Ash Concrete, Personal Notes, Inorganic Materials Division, National Building Research Institute, CSIR.

Kruger, R.A. (1990) The Chemistry of Fly Ash and the Pozzolanic Reaction, *ChemSA*, November 1990, pp.301.

Kruger, R.A. (1990) Ten Years of Research into Ash Utilisation, *First National Symposium*, CSIR Conference Centre, Pretoria.

Kruger, R.A. (1993) Personal Communication.

MacKenzie, R.C. (Editor) (1957) The Differential Thermal Investigation of Clays, The Central Press, Aberdeen.

Malhotra, V.M. and Painter, K.E. (1988) Early-age Strength Properties and Freezing and Thawing Resistance of Concrete incorporating High Volumes of ASTM class F Fly Ash, *Int. J. Cement Composites and Lightweight Concrete*, 11, no.1, pp.37-46.

Mantel, D.G. (1992) *The Manufacture, Properties and Applications of Portland Cements, Cement Additives and Blended Cements*, Pretoria Portland Cement 64pp.

Malhotra, V.M. (June 1989) Durability of Concrete incorporating high-volume of low-calcium (ASTM F) Fly Ash, *Durability of Concrete, Aspects of Admixtures and Industrial By-Products*, Second International, pp.93-104.

Malhotra. V.M. (May 1992) CANMET Investigation dealing with high-volume Fly ash Concrete, Advances in Concrete Technology, *Proceedings of International Conference*, Athens, Greece, pp.433.470.

Marchese, B. and Sersale, R. (1968) Stability of Hydrogarnet Series Terms to Sulphate Attack, Supplementary Paper 2-6, *Proceedings of the Fifth International Symposium on the Chemistry of Cement*, Tokyo, pp.133-137.

Maslehuddin, M. et al. (1987) Effect of Fly ash addition on the Corrosion Resisting Characteristics of Concrete, *ACI Materials Journal*, Jan-Feb, pp.42-50.

Nasser, K.W. and Lai, P.S.H. (1992) Resistance of Fly Ash Concrete to freezing and thawing, *Fly ash, Silica Fume, Slag and Natural Pozzolans in Concrete*, Proceedings Fourth International CANMET/ACI Conference, Instanbul, Turkey, **1**, pp.205-26.

National Building Research Institute (1985) Final Report on the Development of a Mix Design Method for FA Concrete, Pretoria, R.S.A..

Popovics, S. (1991) A Model for Estimation of the Contribution of Fly Ash to Concrete Strength, *Blended Cements in Construction*, Papers presented at the International Conference on Blended Cements in Construction, University of Sheffield.

Sivasundaram, V. (June 1989) Long-term Strength Development of high-volume Fly Ash Concrete, *Third International Conference on the Use of Fly ash, Silica Fume, Slag and Natural Pozzolans*, Trondheim, Norway.

Skoog, D.A. *et al.* (1988) Fundamentals of Analytical Chemsitry 5th Edition, Saunders College Publishing, U.S.A., 894pp.

Soomro, M.A. (1980) Thermal Analysis and its Applications in the Study of Cement, *Mehran University Research Journal of engineering and Technology*, **7**, no. 4, October 1988, pp. 17-22.

South African Bureau of Standards, The Structural Use of Concrete, Part 2: Materials and Execution of Work, SABS 0100-2:1992.

Swamy, R.N. (1990) The Role of Mineral Admixtures on enhancing the Quality of Concrete, *Properties of Fresh Concrete*, Proceedings of the RILEM Colloquium, Hanover, pp.125-133.

Swamy, R.N. (1990) Fly ash Concrete - Potential without Misuse, *Materials and Structures*, **23**, pp.397-411.

Wesche, K. (Editor) (1991) *Fly Ash in Concrete Properties and Performance*, Rilem Report 7, E & FN Spon (Chapman & Hall), London.

APPENDIX A

Sample: Ordinary portland cement from Ulco factory, Anglo Alpha.

Focal Length: 63mm

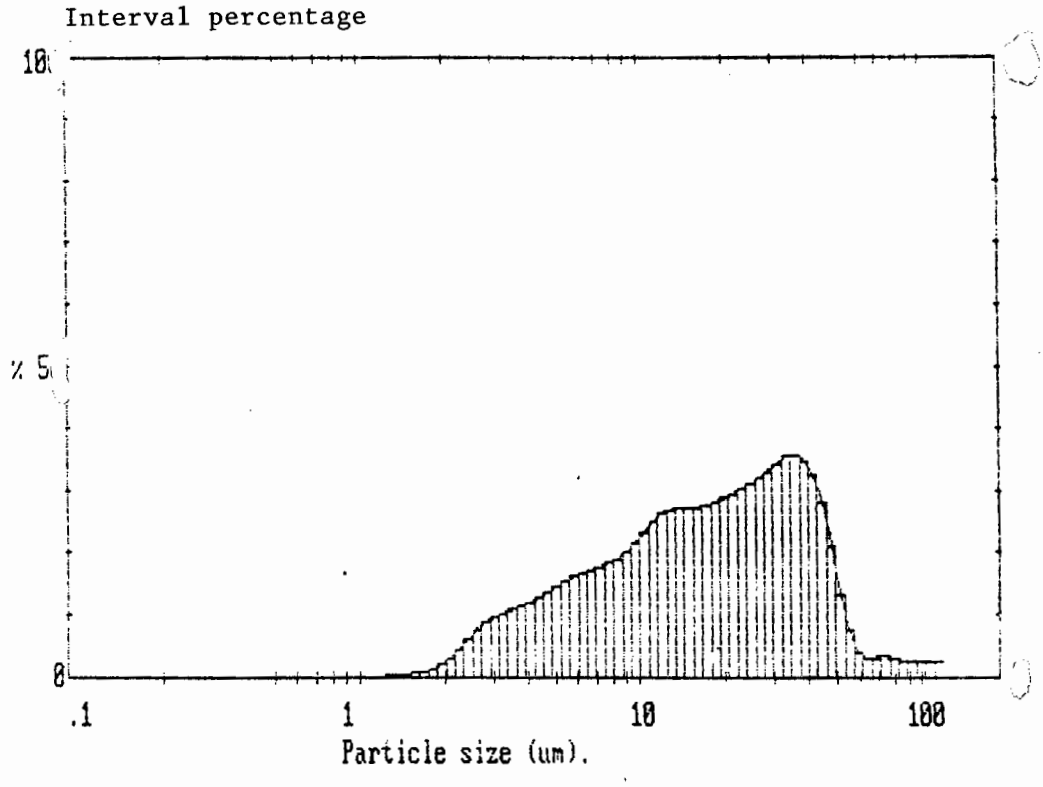

High Size	In %	High Size	In %	High Size	In %	High Size	In %	High Size	In %	High Size	In %	Span 2.21
118	0.3	57.3	1.3	24.0	3.1	10.8	2.4	4.84	1.4	2.18	0.3	D[4,3] 21.80um
110	0.3	49.5	2.1	22.3	3.0	10.0	2.2	4.50	1.3	2.03	0.2	
102	0.3	42.1	2.8	20.7	2.9	9.31	2.0	4.19	1.2	1.88	0.1	D[3,2] 10.31um
95.2	0.3	35.8	3.2	19.3	2.8	8.66	1.9	3.89	1.1	1.75	0.1	
88.4	0.3	30.2	3.5	17.9	2.8	8.05	1.9	3.62	1.1	1.63	0.1	
82.1	0.3	25.4	3.6	16.7	2.8	7.49	1.8	3.37	1.0	1.51	0.1	D[v,0.9] 12.94um
76.6	0.3	21.4	3.6	15.5	2.7	6.97	1.7	3.13	1.0	1.41	0.0	
71.2	0.3	18.0	3.5	14.4	2.7	6.48	1.7	2.91	0.9	1.31	0.0	
66.2	0.3	15.2	3.3	13.4	2.7	6.02	1.6	2.71	0.8	1.22	0.0	D[v,0.1] 4.38um
61.6	0.4	12.7	3.2	12.5	2.7	5.60	1.5	2.52	0.6			
57.3	0.7	10.8	3.1	11.6	2.5	5.21	1.5	2.34	0.4			

Source = :Sample	Beam length = 2.0 mm	Model indp	D[-,0.5] 1.48um
Focal length = 63 mm	Log. Diff. = 2.451		
Presentation = 21	Obscuration = 0.1940	Volume Conc. = 0.0371%	Shape OFF
	Volume distribution	Sp.S.A = 0.5819 m²/cc.	

UCT Physics Department

Sample: Lethabo fly ash as supplied.

Focal Length: 63mm

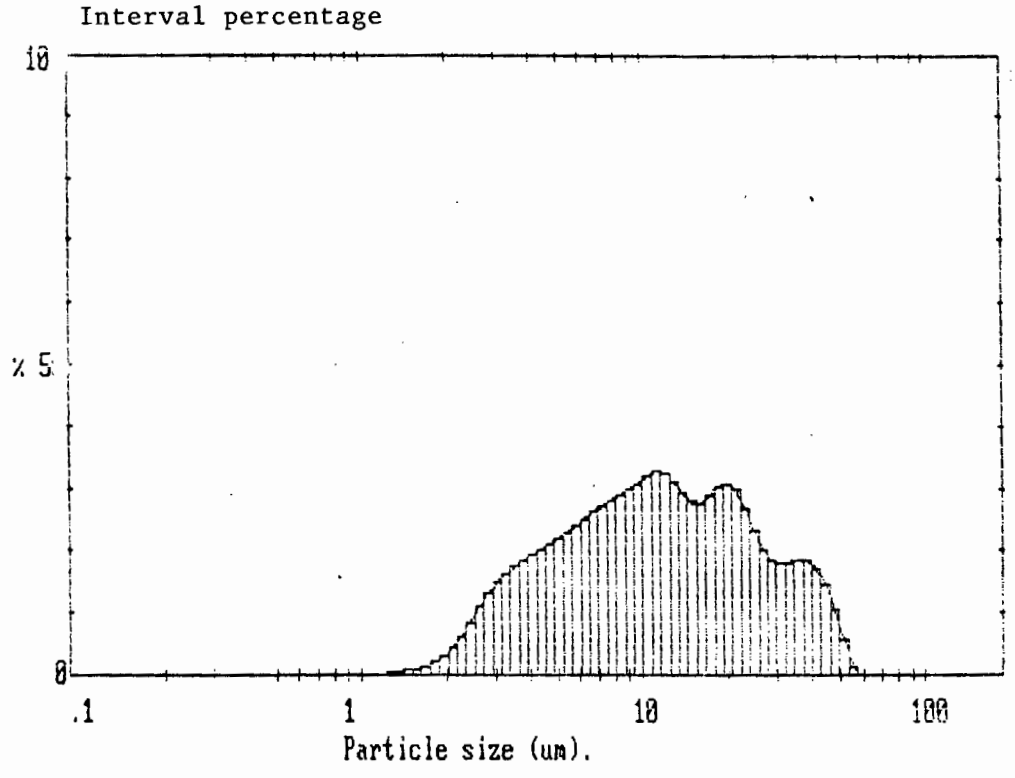

High Size	In %	High Size	In %	High Size	In %	High Size	In %	High Size	In %	High Size	In %	Span 2.60
118	0.0	37.3	0.6	24.0	2.7	10.8	3.2	4.84	2.1	2.18	0.4	D(4,3) 14.98um
110	0.0	35.5	1.0	22.3	3.0	10.0	3.1	4.50	2.0	2.03	0.3	
102	0.0	33.8	1.6	20.7	3.1	9.31	3.0	4.18	1.9	1.88	0.2	
95.1	0.0	32.1	1.7	19.3	3.1	8.68	2.9	3.89	1.8	1.75	0.1	D(3,2) 7.78um
88.6	0.0	30.5	1.8	17.9	2.9	8.06	2.8	3.62	1.7	1.63	0.1	
82.4	0.0	29.0	1.9	16.7	2.8	7.49	2.8	3.37	1.6	1.51	0.1	
76.6	0.0	27.4	1.8	15.5	2.8	6.97	2.6	3.13	1.5	1.41	0.1	D(v,0.5) 12.54um
71.3	0.0	26.0	1.8	14.4	3.0	6.48	2.5	2.91	1.3	1.31	0.0	
66.2	0.0	24.8	1.9	13.4	3.1	6.02	2.4	2.71	1.1	1.22	0.0	
61.6	0.0	23.7	2.0	12.5	3.3	5.60	2.3	2.50	0.9			D(v,0.1) 1.97um
57.3	0.1	22.8	2.3	11.6	3.3	5.21	2.2	2.34	0.8			

Source = Sample	Beam length = 2.0 mm	Model 1+2+	D(v,0.9) 31.17um
	Log. Diff. = 4.011		
Focal length = 63 mm	Obscuration = 0.1931	Volume Conc. = 0.0278%	
Presentation = 2nd	Volume distribution	Sp.S.A 0.7712 m²/cc.	Shape OFF

UCT Physics Department

Sample: Lethabo(-63) fly ash.

Focal Length: 63mm

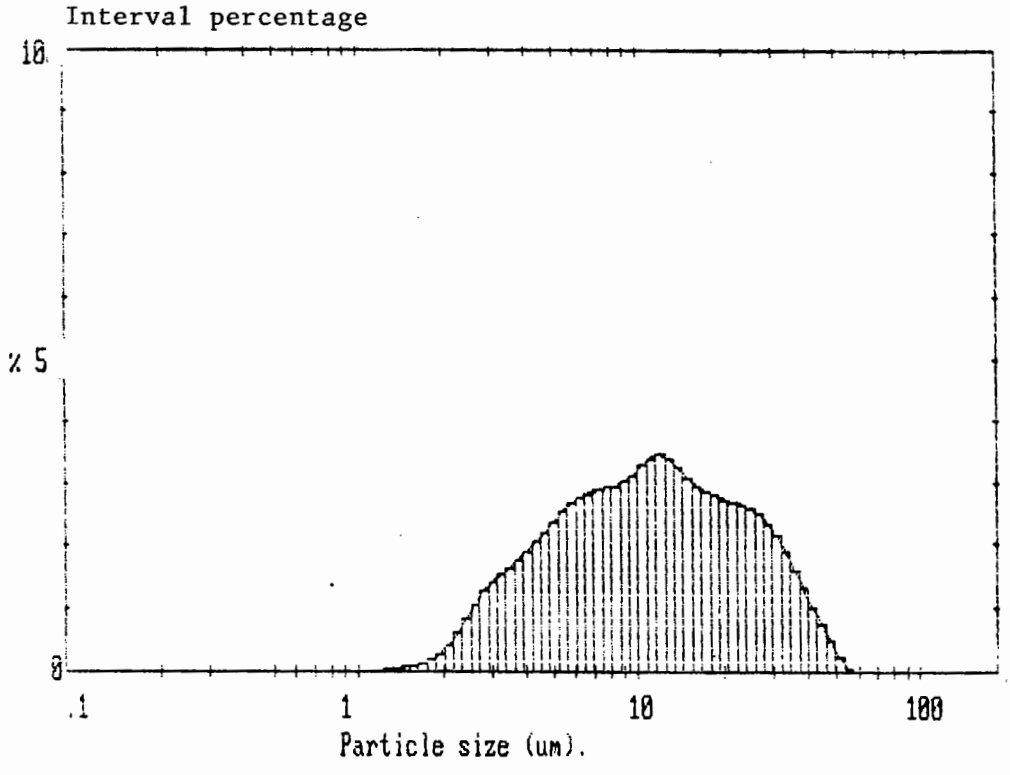

High Size	In %	High Size	In %	High Size	In %	High Size	In %	High Size	In %	High Size	In %	Span 2.35
118	0.0	53.3	0.2	24.0	2.7	10.8	3.3	4.84	2.2	2.18	0.4	D[4,3] 15.95µm
110	0.0	49.6	0.5	22.3	2.7	10.0	3.2	4.50	2.1	2.03	0.3	
102	0.0	46.1	0.8	20.7	2.8	9.31	3.0	4.19	1.9	1.88	0.2	
95.2	0.0	42.8	1.0	19.3	2.8	8.66	3.0	3.89	1.8	1.75	0.1	D[3,2] 7.77µm
88.6	0.0	39.8	1.3	17.9	2.9	8.05	3.0	3.62	1.7	1.63	0.1	
82.4	0.0	37.0	1.6	16.7	3.0	7.49	2.9	3.37	1.5	1.51	0.1	
76.6	0.0	34.4	1.9	15.5	3.1	6.97	2.9	3.13	1.4	1.41	0.1	D[v,0.9] 29.34µm
71.2	0.0	32.0	2.2	14.4	3.3	6.48	2.8	2.91	1.3	1.31	0.0	
66.2	0.0	29.8	2.4	13.4	3.4	6.02	2.7	2.71	1.1	1.22	0.0	
61.6	0.0	27.7	2.5	12.5	3.5	5.60	2.6	2.52	0.8			D[v,0.1] 3.66µm
57.3	0.1	25.8	2.6	11.6	3.4	5.21	2.4	2.34	0.6			

Source = :Sample	Beam length = 2.0 mm	Model indp	D[v,0.5] 10.91µm
	Log. Diff. = 3.762		
Focal lengtr = 63 mm	Obscuration = 0.1969	Volume Conc. = 0.0284%	Shape OFF
Presentation = pil	Volume distribution	Sp.S.A 0.7722 m²/cc.	

UCT Physics Department

Sample: Duvha fly ash as supplied.

Focal Length: 63mm

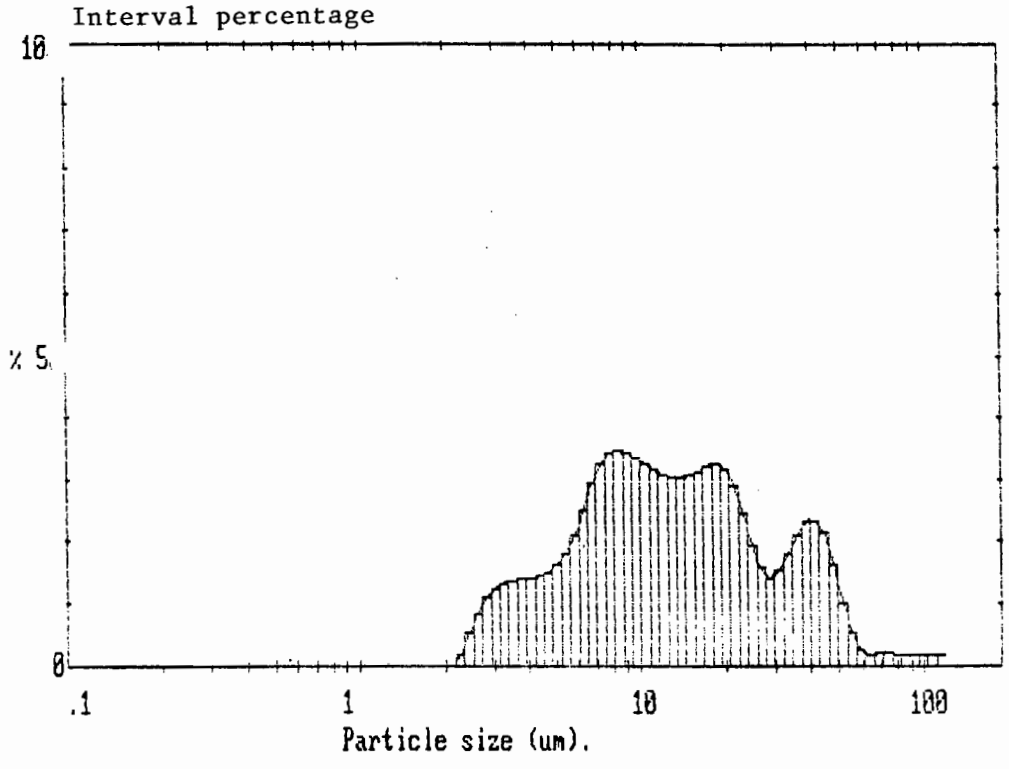

High Size	In %	High Size	In %	High Size	In %	High Size	In %	High Size	In %	Span 2.52
116	0.2	53.3	1.0	24.0	2.5	10.8	3.3	4.84	1.5	2.18	0.0	D(4,3) 17.56um
110	0.2	49.5	1.7	22.3	2.9	10.0	3.4	4.50	1.4	2.03	0.0	
102	0.2	46.1	2.2	20.7	3.2	9.31	3.4	4.19	1.4	1.88	0.0	D(3,2) 9.39um
95.2	0.2	42.8	2.4	19.3	3.3	8.66	3.5	3.89	1.4	1.75	0.0	
88.6	0.2	39.8	2.3	17.9	3.2	8.05	3.4	3.62	1.4	1.63	0.0	D(v,0.9) 39.38um
82.4	0.2	37.0	2.1	16.7	3.1	7.49	3.3	3.37	1.3	1.51	0.0	
76.6	0.2	34.4	1.8	15.5	3.1	6.97	3.0	3.13	1.2	1.41	0.0	
71.2	0.2	32.0	1.5	14.4	3.1	6.48	2.5	2.91	1.1	1.31	0.0	D(v,0.1) 4.30um
66.2	0.2	29.8	1.4	13.4	3.1	6.00	2.1	2.71	0.9	1.22	0.0	
61.6	0.3	27.7	1.6	12.5	3.1	5.60	1.9	2.52	0.5			D(v,0.5) 12.42um
57.3	0.6	25.8	1.9	11.6	3.2	5.21	1.6	2.34	0.2			

Source = :Sample	Beam length = 2.0 mm	Model indp
	Log. Diff. = 3.309	
Focal length = 63 mm	Obscuration = 0.1926	Volume Conc. = 0.0334%
Presentation = pil	Volume distribution	Sp.S.A 0.6393 m²/cc.

Erase Off

UCT Physics Department

Sample: Duvha(-63) fly ash.

Focal Length: 63mm

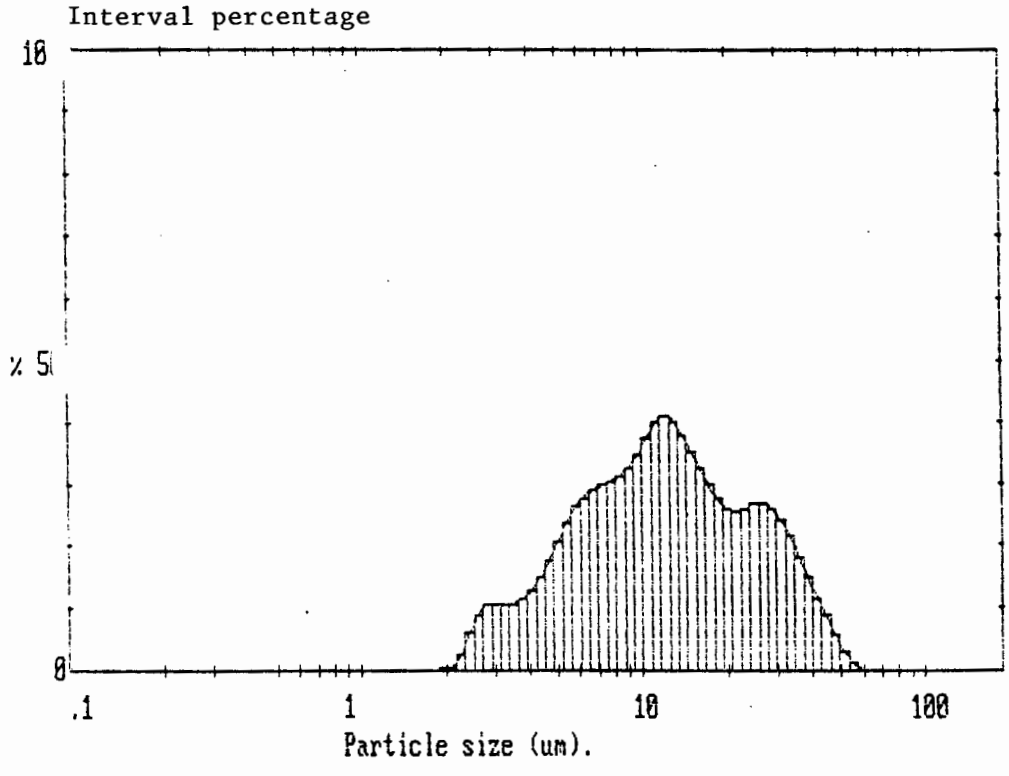

High Size	In %	High Size	In %	High Size	In %	High Size	In %	High Size	In %	Span 2.20
118	0.0	53.3	0.3	24.0	2.6	10.8	3.8	4.84	1.8	2.18	0.1	D[4,3] 14.31um
110	0.0	49.5	0.6	22.3	2.6	10.0	3.5	4.50	1.5	2.03	0.0	
102	0.0	46.1	0.9	20.7	2.6	9.31	3.3	4.19	1.3	1.88	0.0	D[3,2] 9.08um
95.1	0.0	43.0	1.2	19.3	2.9	8.66	3.2	3.89	1.2	1.75	0.0	
88.6	0.0	40.0	1.5	17.9	3.0	8.05	3.1	3.62	1.1	1.63	0.0	
82.4	0.0	37.0	1.8	16.7	3.3	7.49	3.0	3.37	1.1	1.51	0.0	D[v,0.9] 30.54um
76.6	0.0	34.4	2.1	15.5	3.6	6.97	2.9	3.13	1.1	1.41	0.0	
71.2	0.0	32.0	2.4	14.4	3.8	6.48	2.8	2.91	1.1	1.31	0.0	
66.2	0.0	29.8	2.6	13.4	4.0	6.02	2.7	2.71	0.7	1.22	0.0	D[v,0.1] 4.48um
61.6	0.0	27.7	2.7	12.5	4.1	5.60	2.4	2.52	0.6			
57.3	0.1	25.8	2.7	11.6	4.0	5.21	2.1	2.34	0.3			D[v,0.5] 11.87um

Source = :Sample	Beam length = 2.0 mm	Model indp	Shape OFF
	Log. Diff. = 3.792		
Focal length = 63 mm	Obscuration = 0.1965	Volume Conc. = 0.0331%	
Presentation = pil	Volume distribution	Sp.S.A 0.6607 m²/cc.	

UCT Physics Department

Sample: Van Eck clinker ash as collected.

Focal Length: 63mm

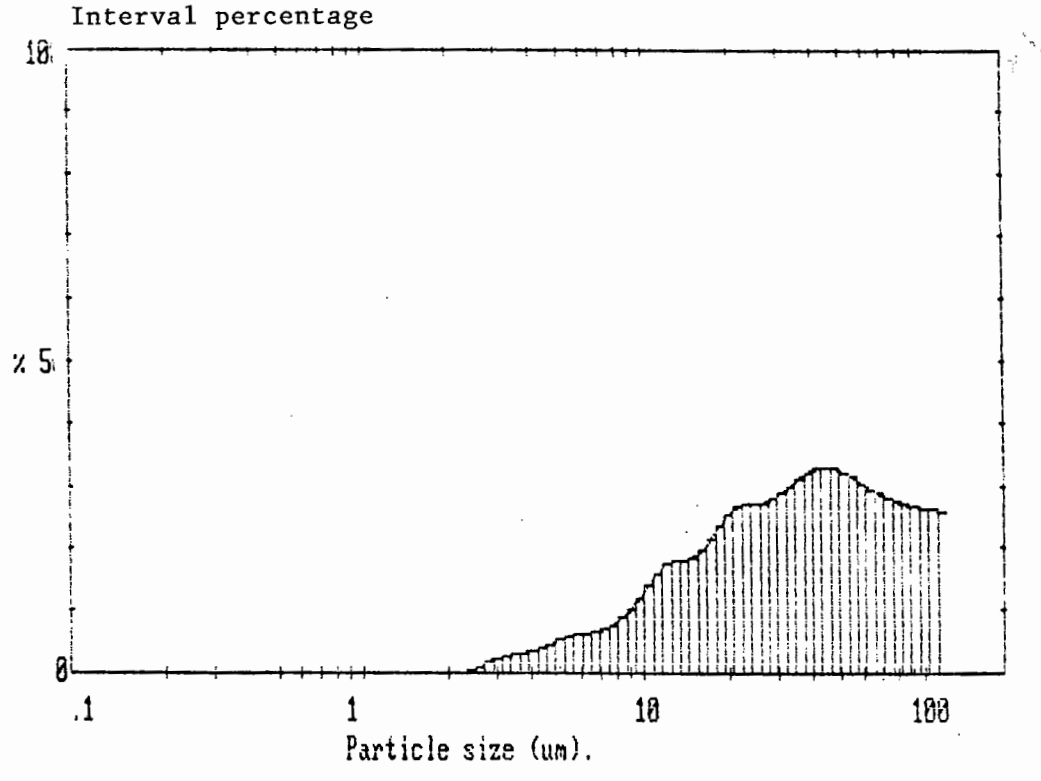

High Size	In %	High Size	In %	High Size	In %	High Size	In %	High Size	In %	Span 2.29
118	2.6	57.3	3.3	24.0	2.7	10.8	1.4	4.84	0.3	2.18	0.0	D(4,3) 42.43um
110	2.5	49.5	3.3	22.3	2.7	10.0	1.2	4.50	0.4	2.03	0.0	
102	2.7	43.1	3.3	20.7	2.6	9.31	1.2	4.19	0.4	1.88	0.0	
95.2	2.7	42.8	3.3	19.3	2.4	8.66	0.9	3.89	0.3	1.75	0.0	D(3,2) 31.14um
88.6	2.7	36.8	3.2	17.9	2.2	8.05	0.8	3.62	0.3	1.63	0.0	
82.4	2.8	37.0	3.1	16.7	2.0	7.49	0.7	3.37	0.3	1.51	0.0	
76.6	2.8	34.4	3.0	15.5	1.9	6.97	0.7	3.13	0.2	1.41	0.0	D(v,0.9) 90.07um
71.2	2.9	32.0	2.9	14.4	1.8	6.48	0.6	2.91	0.2	1.31	0.0	
66.2	3.0	29.8	2.8	13.4	1.8	6.02	0.6	2.71	0.1	1.22	0.0	
61.6	3.1	27.7	2.8	12.5	1.8	5.60	0.6	2.52	0.0			D(v,0.1) 9.38um
57.3	3.2	25.8	2.7	11.6	1.6	5.21	0.5	2.34	0.0			

Source = :Sample	Beam length = 2.0 mm Log. Diff. = 5.691	Model ind:	D(v,0.5) 35.01um
Focal length = 63 mm Presentation = pil	Obscuration = 0.1914 Volume distribution	Volume Conc. = 0.0750% Sp.S.A 0.2838 m²/cc.	Enabe OFF

UCT Physics Department

Sample: Van Eck milled clinker ash.

Focal Length: 63mm

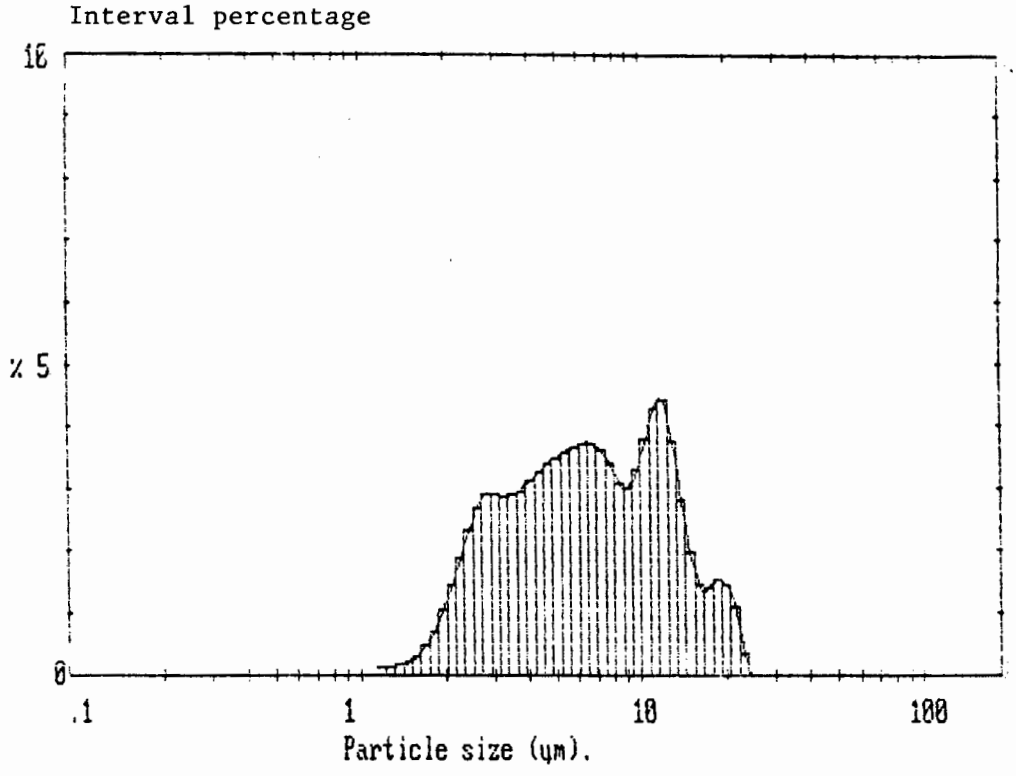

High Size	In %	High Size	In %	High Size	In %	High Size	In %	High Size	In %	High Size	In %	Span 1.83
119	0.0	53.3	0.0	24.0	0.4	10.8	3.8	4.94	3.4	2.18	1.4	D(4,3) 7.58µm
110	0.0	49.5	0.0	22.3	1.1	10.0	3.3	4.50	3.3	2.03	1.0	
102	0.0	46.1	0.0	20.7	1.5	9.31	3.0	4.19	3.1	1.88	0.7	D(3,2) 4.80µm
95.2	0.0	42.8	0.0	19.3	1.5	8.66	3.1	3.89	3.0	1.75	0.5	
88.6	0.0	39.8	0.0	17.9	1.4	8.05	3.4	3.62	2.9	1.63	0.3	
82.4	0.0	37.0	0.0	16.7	1.4	7.49	3.6	3.37	2.9	1.51	0.2	
76.6	0.0	34.4	0.0	15.5	2.0	6.97	3.7	3.13	2.9	1.41	0.2	D(v,0.9) 14.13µm
71.2	0.0	32.0	0.0	14.4	2.8	6.48	3.7	2.91	2.9	1.31	0.1	
66.2	0.0	29.8	0.0	13.4	3.8	6.02	3.7	2.71	2.7	1.22	0.1	
61.5	0.0	27.7	0.0	12.5	4.4	5.60	3.6	2.52	2.3			D(v,0.1) 2.56µm
57.3	0.0	25.8	0.0	11.6	4.3	5.21	3.5	2.34	1.9			

Source = :Sample	Beam length = 2.0 mm	Model indp	D(v,0.5) 6.31µm
Focal length = 63 mm	Log. Diff. = 3.982	Volume Conc. = 0.0170%	
Presentation = pil	Obscuration = 0.1914	Sp.S.A 1.2492 m²/cc.	Shape OFF
	Volume distribution		

UCT Physics Department

Sample: Van Eck(-63) milled clinker ash.

Focal Length: 63mm

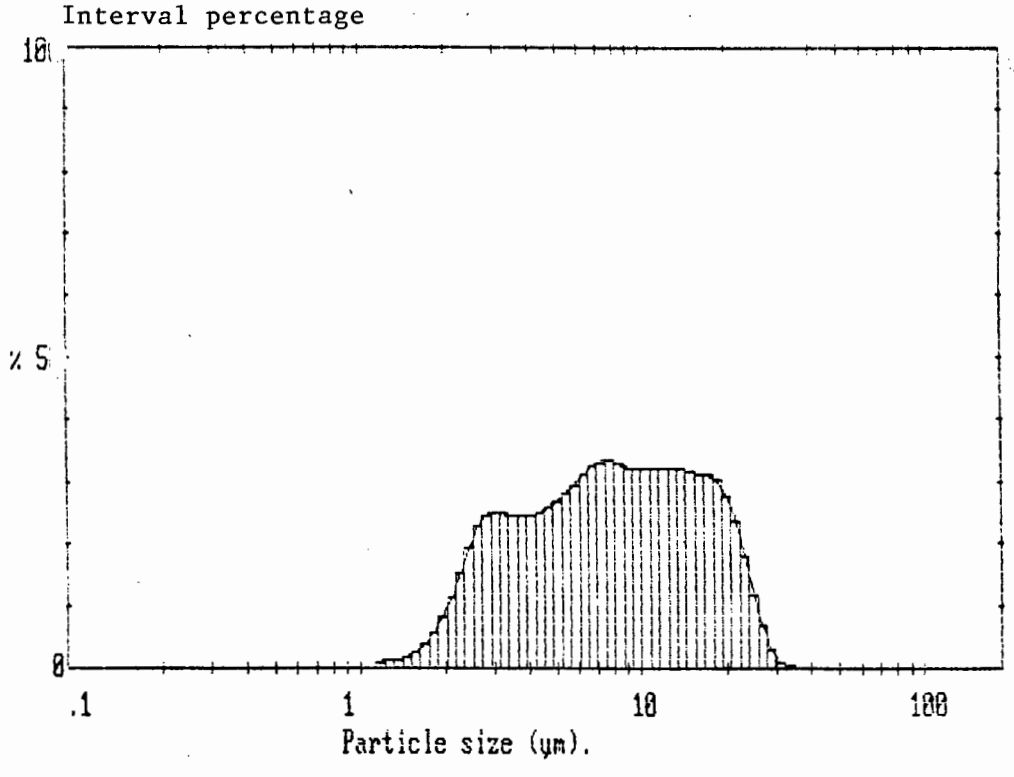

High Size	In %	High Size	In %	High Size	In %	High Size	In %	High Size	In %	High Size	In %	Span 2.12
113	0.0	53.3	0.0	24.0	1.8	10.8	3.2	4.84	2.6	2.18	1.1	D(4,3) 9.40µm
110	0.0	49.5	0.0	22.3	2.4	10.0	3.2	4.50	2.6	2.07	0.8	
106	0.0	46.1	0.0	20.7	2.8	9.31	3.3	4.19	2.5	1.98	0.5	
99.2	0.0	42.8	0.0	19.3	3.0	8.66	3.3	3.89	2.5	1.75	0.4	D(3,2) 6.70µm
88.6	0.0	39.8	0.0	17.9	3.1	8.05	3.4	3.62	2.5	1.63	0.3	
83.4	0.0	37.0	0.0	16.7	3.2	7.49	3.4	3.37	2.5	1.61	0.3	
78.0	0.0	34.4	0.0	15.5	3.2	6.97	3.3	3.13	2.5	1.41	0.1	D(v,0.9) 14.00µm
73.2	0.0	32.0	0.1	14.4	3.2	6.48	3.1	2.91	2.5	1.31	0.1	
68.2	0.0	29.8	0.3	13.4	3.2	6.02	3.0	2.71	2.5	1.22	0.1	
63.6	0.0	27.7	0.7	12.5	3.2	5.60	2.8	2.52	1.9			D(v,0.1) 3.52µm
59.3	0.0	25.8	1.2	11.6	3.2	5.21	2.7	2.34	1.6			

Source = :Sample	Beam length = 2.0 mm	Model incp		D(v,0.5) 7.70µm
Focal length = 63 mm	Log. Diff. = 4.579			
Presentation = pil	Obscuration = 0.194%	Volume Conc. = 0.0194%		
	Volume distribution	Sp.S.A 1.1117 m²/cc.		Shape OFF

UCT Physics Department

Sample: Van Eck(-63) milled clinker ash (repeat).

Focal Length: 63mm

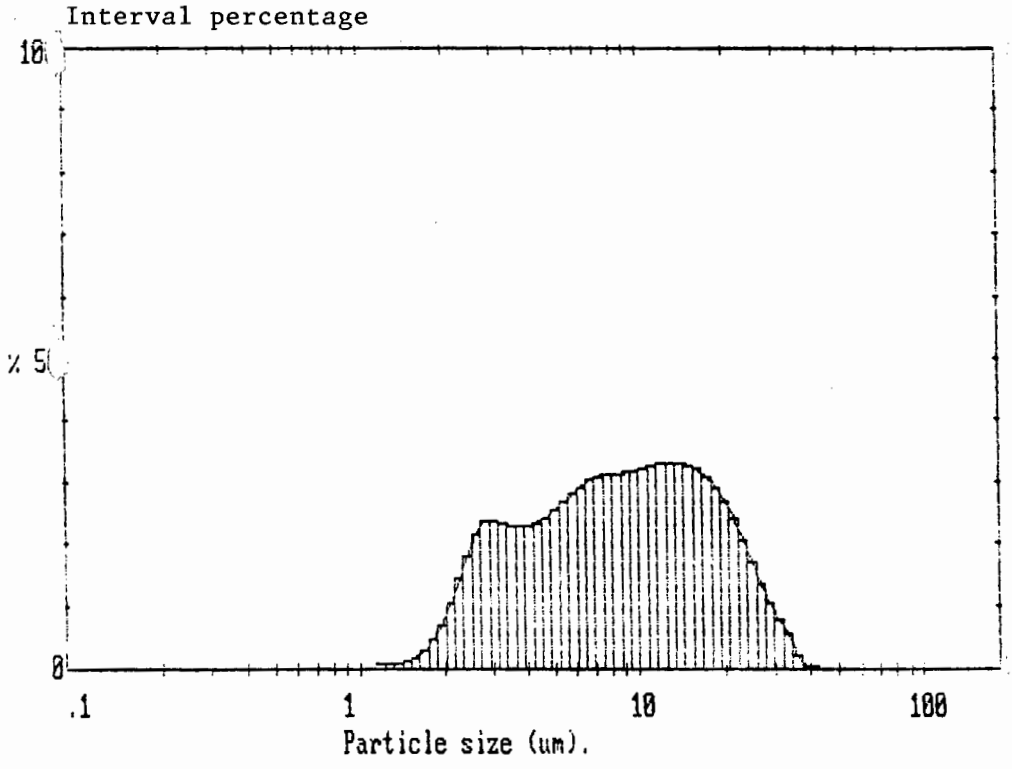

High Size	In %	High Size	In %	High Size	In %	High Size	In %	High Size	In %	High Size	In %	Span 2.17
118	0.0	53.3	0.0	24.0	2.1	10.8	3.2	4.84	2.5	2.18	1.0	D(4,3) 10.76um
110	0.0	49.5	0.0	22.3	2.4	10.0	3.1	4.50	2.4	2.03	0.7	
102	0.0	46.1	0.0	20.7	2.7	9.31	3.2	4.19	2.3	1.88	0.5	
95.2	0.0	42.9	0.0	19.3	2.9	8.66	3.2	3.89	2.3	1.75	0.3	D(3,2) 6.88um
88.6	0.0	39.9	0.1	17.9	3.1	8.05	3.1	3.62	2.3	1.63	0.2	
82.4	0.0	37.0	0.2	16.7	3.2	7.49	3.1	3.37	2.4	1.51	0.1	
76.6	0.0	34.4	0.6	15.5	3.3	6.97	3.0	3.13	2.4	1.41	0.1	D(v,0.9) 20.98um
71.2	0.0	32.0	0.8	14.4	3.3	6.49	2.9	2.91	2.4	1.31	0.1	
66.2	0.0	29.8	1.1	13.4	3.3	6.02	2.8	2.71	2.3	1.22	0.1	
61.6	0.0	27.7	1.4	12.5	3.3	5.60	2.7	2.52	1.8			D(v,0.1) 2.79um
57.3	0.0	25.8	1.7	11.6	3.3	5.21	2.6	2.34	1.4			

Source = :Sample	Beam length = 2.0 mm	Model indp	D(v,0.5) 8.39um
Focal length = 63 mm	Log. Diff. = 2.863		
Presentation = pil	Obscuration = 0.2012	Volume Conc. = 0.0220%	
	Volume distribution	Sp.S.A 1.0206 m²/cc.	Shape OFF

UCT Physics Department

Sample: Van Eck(-63) milled clinker ash (repeat).

Focal Length: 63mm

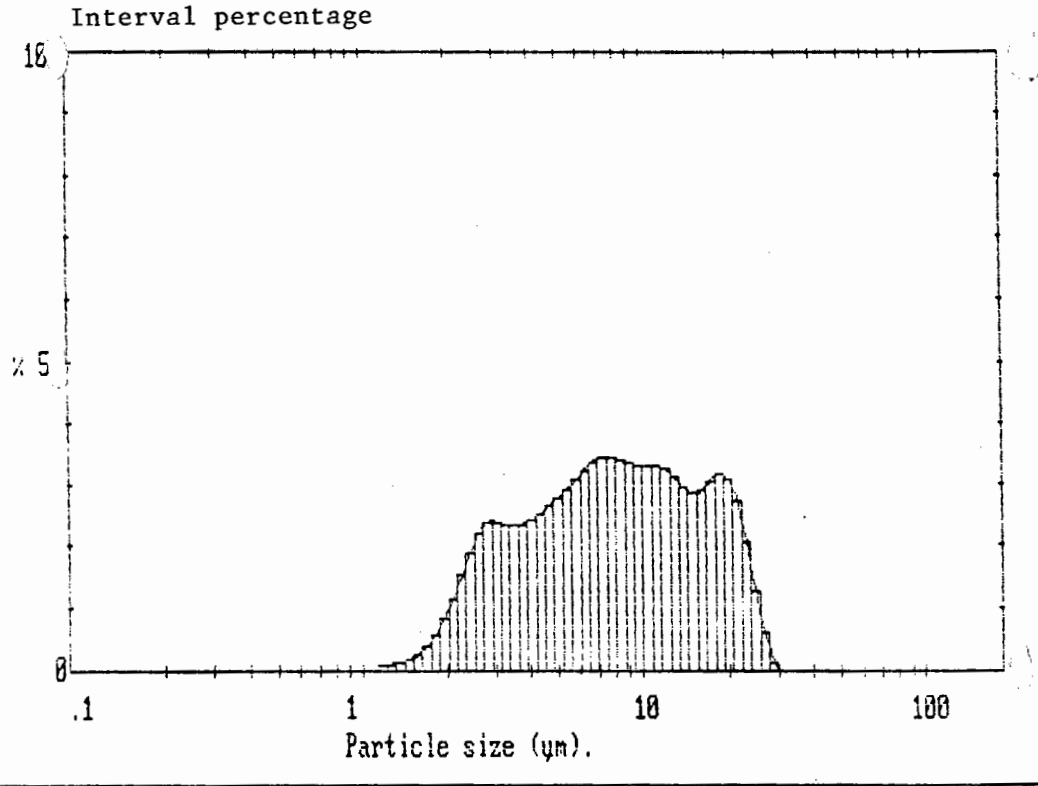

High Size	In %	High Size	In %	High Size	In %	High Size	In %	High Size	In %	High Size	In %	Scan 2.13
118	0.0	53.3	0.0	24.0	2.1	10.8	3.3	4.84	2.7	2.18	1.2	D(4,3) 9.45µm
110	0.0	49.5	0.0	22.3	2.7	10.0	3.3	4.50	2.5	2.03	0.8	
102	0.0	46.1	0.0	20.7	3.1	9.31	3.4	4.19	2.4	1.88	0.6	
95.2	0.0	42.8	0.0	19.3	3.2	8.66	3.4	3.89	2.4	1.75	0.4	D(3,2) 5.50µm
88.6	0.0	39.8	0.0	17.9	3.1	8.05	3.5	3.62	2.3	1.63	0.3	
82.4	0.0	37.0	0.0	16.7	2.9	7.49	3.5	3.37	2.2	1.51	0.2	
76.6	0.0	34.4	0.0	15.5	2.9	6.97	3.4	3.13	2.4	1.41	0.1	D(v,0.9) 19.24µm
71.2	0.0	32.0	0.0	14.4	3.0	6.48	3.2	2.91	2.4	1.31	0.1	
66.2	0.0	29.8	0.1	13.4	3.1	6.02	3.1	2.71	2.2	1.22	0.1	
61.6	0.0	27.7	0.6	12.5	3.3	5.60	2.9	2.52	1.9			D(v,0.1) 2.11µm
57.3	0.0	25.8	1.3	11.6	3.5	5.21	2.8	2.34	1.5			

Source =	Sample	Beam length = 2.0 mm	Model indp	D(v,0.5) 7.75µm
		Log. Diff. = 3.921		
Focal length = 63 mm		Obscuration = 0.1965	Volume Conc. = 0.0201%	Scale OFF
Presentation = pil		Volume distribution	Sp.S.A 1.0901 m²/cc.	

UCT Physics Department

Sample: Matla fly ash as supplied.

Focal Length: 63mm

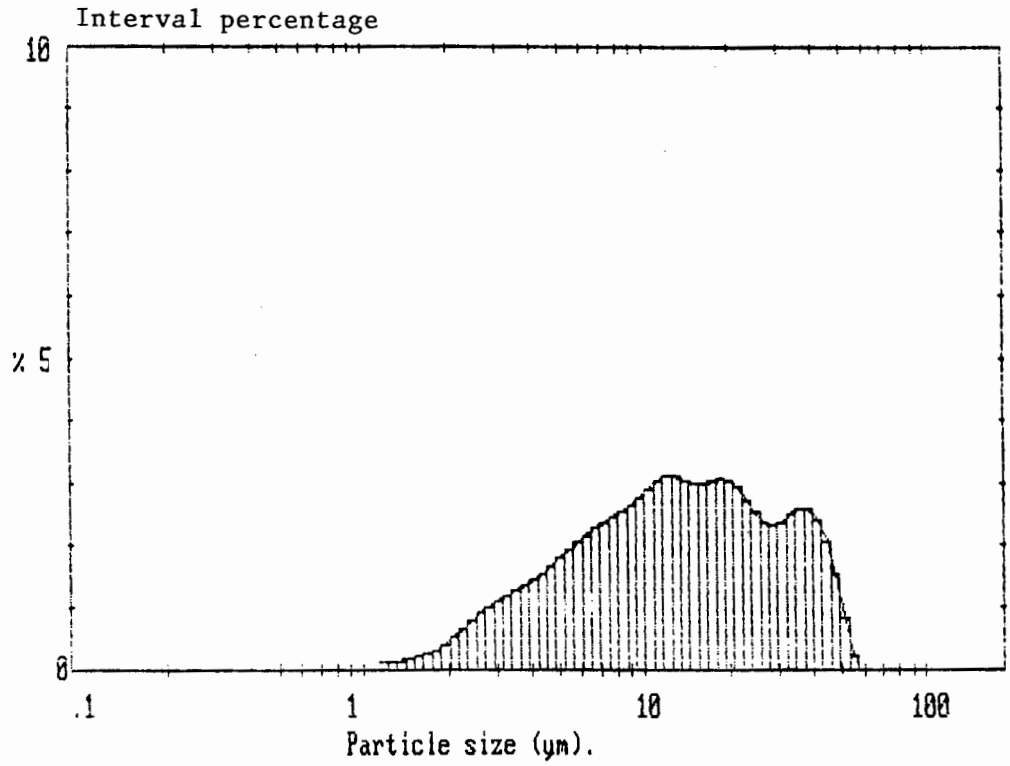

High Size	In %	High Size	In %	High Size	In %	High Size	In %	High Size	In %	High Size	In %	Span 2.56
118	0.0	53.3	0.9	24.0	2.9	10.8	2.9	4.84	1.7	2.18	0.5	D(4,3) 16.24µm
110	0.0	49.5	1.5	22.3	3.0	10.0	2.8	4.50	1.6	2.03	0.4	
102	0.0	46.1	2.1	20.7	3.1	9.31	2.7	4.19	1.4	1.88	0.3	D(3,2) 7.87µm
95.2	0.0	42.8	2.4	19.3	3.1	8.66	2.6	3.89	1.4	1.75	0.3	
88.6	0.0	39.8	2.6	17.9	3.0	8.06	2.5	3.62	1.3	1.63	0.2	
82.4	0.0	37.0	2.6	16.7	3.0	7.49	2.4	3.37	1.2	1.51	0.2	D(v,0.9) 36.82µm
76.6	0.0	34.4	2.5	15.5	3.0	6.97	2.3	3.13	1.1	1.41	0.2	
71.2	0.0	32.0	2.4	14.4	3.1	6.48	2.2	2.91	1.0	1.31	0.1	
66.2	0.0	29.8	2.3	13.4	3.1	6.02	2.1	2.71	0.9	1.22	0.1	D(v,0.1) 3.65µm
61.6	0.0	27.7	2.3	12.5	3.1	5.60	1.9	2.52	0.8			
57.3	0.2	25.8	2.6	11.6	3.1	5.21	1.8	2.34	0.7			

Source = :Sample	Beam length = 2.0 mm	Model indp	D[v,..5.. 12.97µm
	Log. Diff. = 3.450		
Focal length = 63 mm	Obscuration = 0.1981	Volume Conc. = 0.0290%	
Presentation = pil	Volume distribution	Sp.S.A 0.7626 m²/cc.	Shape OFF

UCT Physics Department

Sample: Matla(-63) fly ash.

Focal Length: 63mm

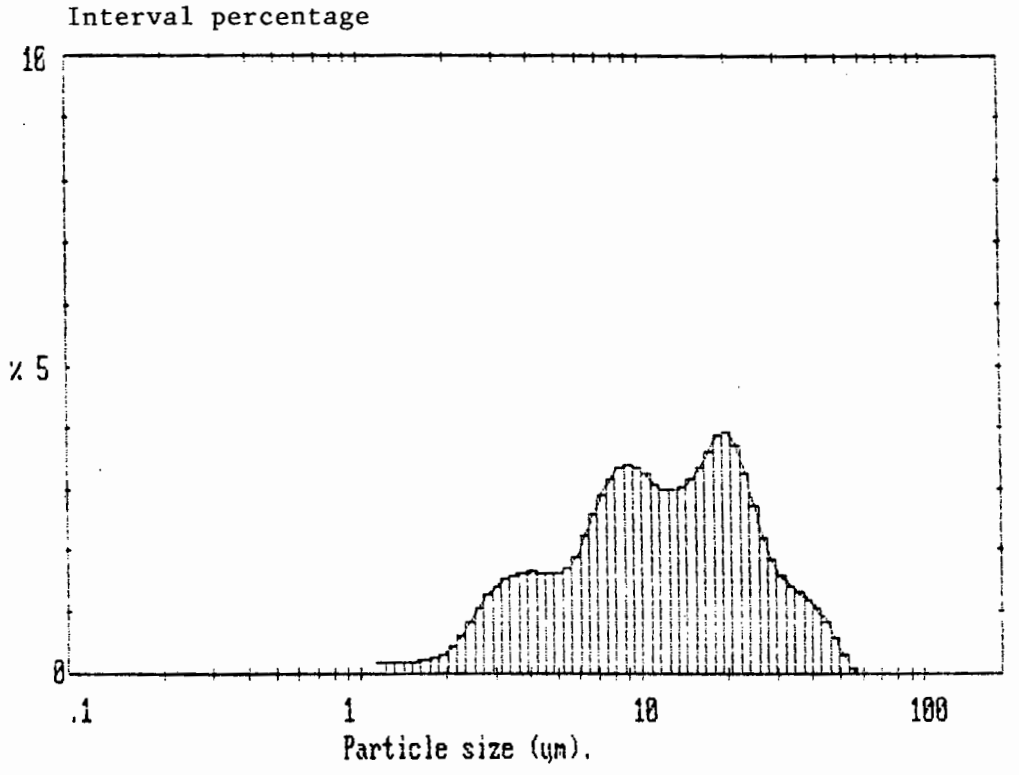

High Size	In %	High Size	In %	High Size	In %	High Size	In %	High Size	In %	Span 2.15
118	0.0	53.3	0.3	24.0	3.3	10.8	3.3	4.84	1.6	2.18	0.4	D[4,3] 14.13µm
110	0.0	49.5	0.6	22.3	3.7	10.0	3.4	4.50	1.7	2.03	0.3	
102	0.0	46.1	0.9	20.7	3.9	9.31	3.4	4.19	1.7	1.88	0.2	
95.2	0.0	42.8	1.1	19.3	3.9	8.66	3.4	3.89	1.6	1.75	0.2	D[3,2] 7.15µm
88.5	0.0	39.8	1.2	17.9	3.6	8.05	3.2	3.62	1.6	1.63	0.2	
82.4	0.0	37.0	1.3	16.7	3.4	7.49	2.9	3.37	1.5	1.51	0.2	
76.6	0.0	34.4	1.4	15.5	3.2	6.97	2.6	3.13	1.4	1.41	0.2	D[v,0.9] 27.93µm
71.3	0.0	32.0	1.6	14.4	3.1	6.48	2.2	2.91	1.3	1.31	0.2	
66.3	0.0	29.8	1.8	13.4	3.0	6.02	1.9	2.71	1.1	1.22	0.2	
61.7	0.0	27.7	2.0	12.5	3.0	5.60	1.7	2.52	0.8			D[v,0.1] 3.42µm
57.3	0.1	25.8	2.7	11.6	3.1	5.21	1.6	2.34	0.6			

Source = :Sample	Beam length = 2.0 mm	Model indp	D[v,0.5] 11.40µm
Focal length = 63 mm	Log. Diff. = 2.578		
Presentation = pil	Obscuration = 0.193%	Volume Conc. = 0.0256%	
	Volume distribution	Sp.S.A 0.8388 m²/cc.	Shape OFF

UCT Physics Department

Sample: Ordinary portland cement from Ulco factory, Anglo Alpha

Focal Length: 300mm

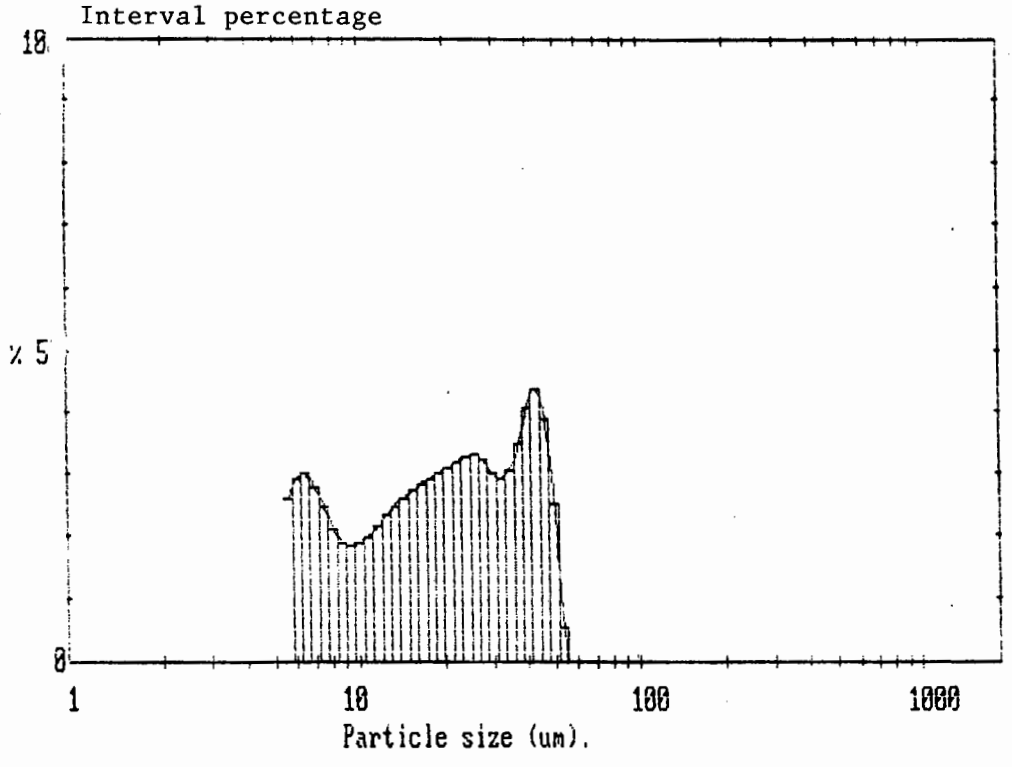

High Size	In %	High Size	In %	High Size	In %	High Size	In %	High Size	In %	High Size	In %	Span 2.14
564	0.0	254	0.0	114	0.0	51.3	2.5	23.1	3.2	10.4	1.9	D[4,3] 20.23µm
524	0.0	236	0.0	106	0.0	47.7	3.9	21.4	3.1	9.64	1.9	
489	0.0	219	0.0	98.6	0.0	44.4	4.4	19.9	3.0	8.97	1.9	
456	0.0	204	0.0	91.7	0.0	41.2	4.1	18.5	2.1	8.34	2.1	D[3,2] 9.79µm
425	0.0	190	0.0	85.3	0.0	38.4	3.5	17.2	2.8	7.76	2.5	
396	0.0	176	0.0	79.3	0.0	35.7	3.1	16.0	2.7	7.21	2.8	
369	0.0	164	0.0	73.8	0.0	33.2	2.9	14.9	2.6	6.71	3.0	D[v,0.9] 42.16µm
344	0.0	153	0.0	68.6	0.0	30.8	3.0	13.9	2.5	6.24	2.9	
319	0.0	142	0.0	63.8	0.0	28.7	3.2	12.9	2.3	5.80	2.6	
297	0.0	132	0.0	59.3	0.0	26.7	3.3	12.0	2.2			D[v,0.1] 5.22µm
273	0.0	123	0.0	55.2	0.5	24.9	3.3	11.2	2.0			

Source = :Sample	Beam length = 2.0 mm	Model indp	D[v,0.5] 17.26µm
	Log. Diff. = 4.208		
Focal length = 300 mm	Obscuration = 0.1889	Volume Conc. = 0.0342%	
Presentation = pil	Volume distribution	Sp.S.A 0.6128 m²/cc.	Shape OFF

UCT Physics Department

Sample: Lethabo fly ash as supplied.

Focal Length: 300mm

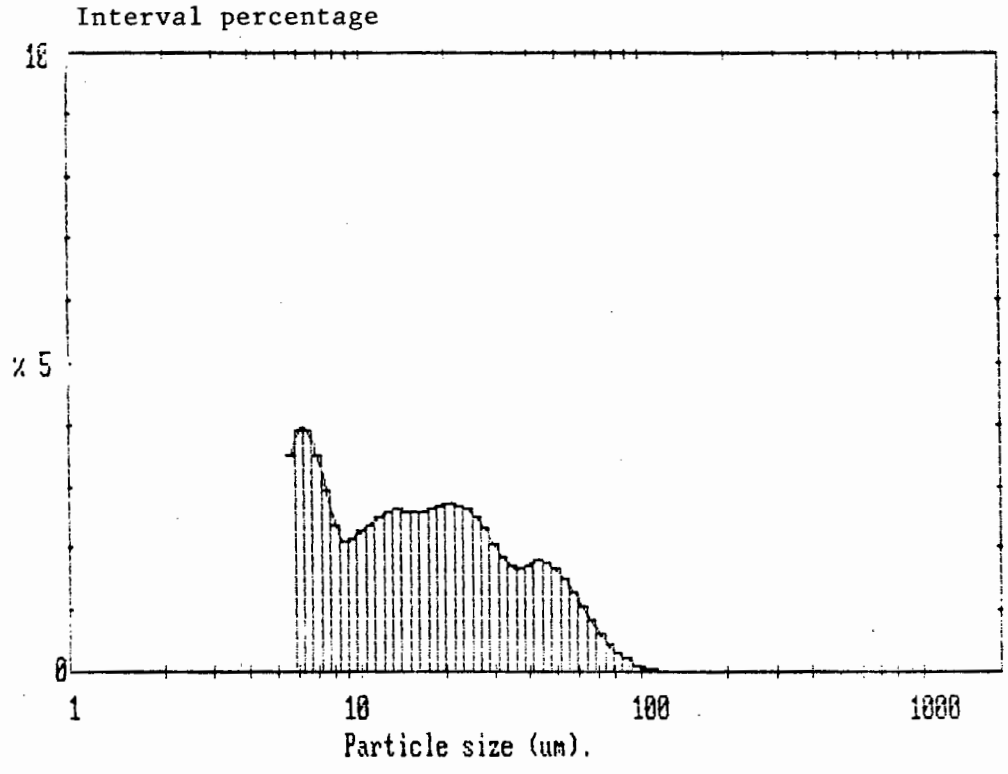

High Size	In %	High Size	In %	High Size	In %	High Size	In %	High Size	In %	High Size	In %	Span 3.09
564	0.0	254	0.0	114	0.0	51.3	1.7	23.1	2.7	10.4	2.3	D(4,3) 18.57µm
554	0.0	236	0.0	106	0.1	47.7	1.8	21.4	2.8	9.64	2.2	
488	0.0	219	0.0	98.6	0.1	44.4	1.8	19.9	2.7	8.97	2.1	
454	0.0	204	0.0	91.7	0.2	41.2	1.7	18.5	2.7	8.34	2.4	D(3,2) 8.06µm
422	0.0	190	0.0	85.3	0.3	38.4	1.7	17.2	2.6	7.76	3.0	
392	0.0	176	0.0	79.3	0.4	35.7	1.7	16.0	2.4	7.21	3.5	
366	0.0	164	0.0	73.8	0.6	33.2	1.9	14.9	2.5	6.71	3.7	D(v,0.9) 44.11µm
339	0.0	153	0.0	68.6	0.8	30.8	2.1	13.9	2.6	6.24	3.9	
315	0.0	142	0.0	63.8	1.1	28.7	2.3	12.9	2.6	5.80	3.6	
293	0.0	132	0.0	59.3	1.3	26.7	2.5	12.0	2.5			D(v,0.1) 4.65µm
273	0.0	123	0.0	55.2	1.5	24.8	2.6	11.2	2.4			

Source = :Sample	Beam length = 2.0 mm	Model indp	D(v,0.5) 12.76µm
	Log. Diff. = 2.668		
Focal length = 300 mm	Obscuration = 0.1924	Volume Conc. = 0.0286%	
Presentation = pll	Volume distribution	Sp.S.A 0.7472 m²/cc.	Shape OFF

UCT Physics Department

Sample: Lethabo(-63) fly ash.

Focal Length: 300mm

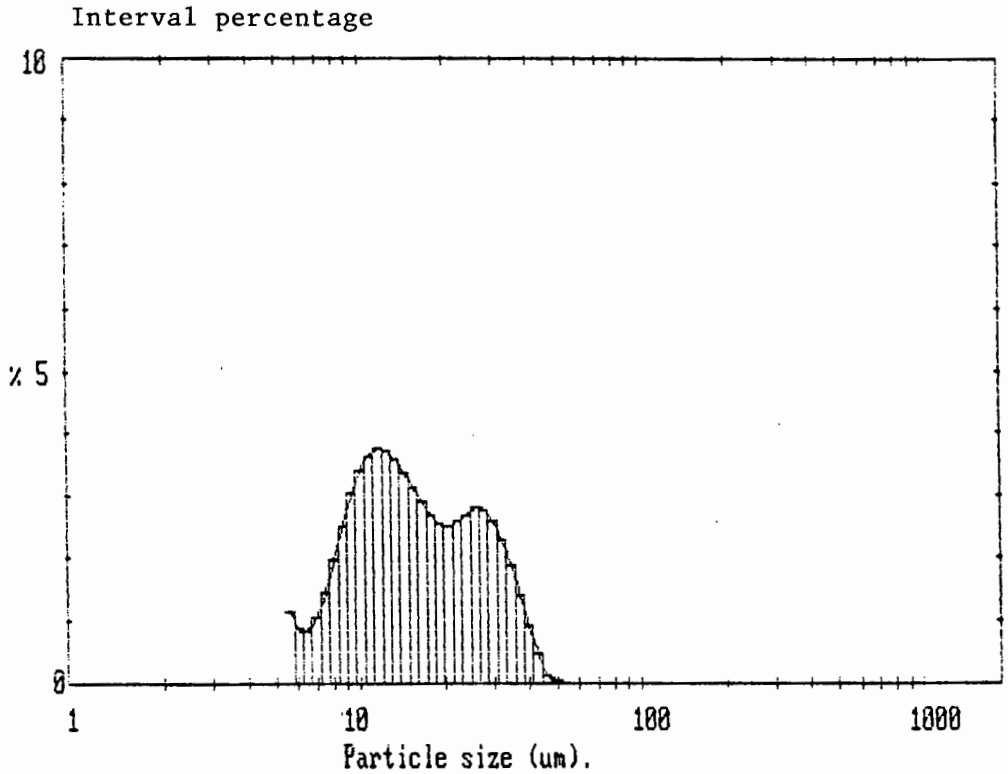

High Size	In %	High Size	In %	High Size	In %	High Size	In %	High Size	In %	High Size	In %	Span 2.37
564	0.0	254	0.0	114	0.0	51.3	0.1	23.1	2.6	10.4	3.4	D(4,3) 13.08µm
524	0.0	236	0.0	106	0.0	47.7	0.2	21.4	2.5	9.64	3.0	
488	0.0	219	0.0	98.6	0.0	44.4	0.5	19.9	2.6	8.97	2.5	
454	0.0	204	0.0	91.7	0.0	41.2	0.9	18.5	2.7	8.34	2.0	D(3,2) 6.39µm
422	0.0	190	0.0	85.3	0.0	38.4	1.4	17.2	2.9	7.76	1.5	
392	0.0	176	0.0	79.3	0.0	35.7	1.9	16.0	3.2	7.21	1.1	
365	0.0	164	0.0	73.8	0.0	33.2	2.3	14.9	3.4	6.71	0.9	D(v,0.9) 25.59µm
339	0.0	153	0.0	68.6	0.0	30.8	2.6	13.9	3.5	6.24	0.9	
315	0.0	142	0.0	63.8	0.0	28.7	2.6	12.9	3.7	5.80	1.2	
293	0.0	132	0.0	59.3	0.0	26.7	2.8	12.0	3.7			D(v,0.1) 2.63µm
273	0.0	123	0.0	55.2	0.0	24.8	2.7	11.2	3.6			

Source = :Sample	Beam length = 2.0 mm	Model indp	D(v,0.5) 10.98µm
Focal length = 300 mm	Log. Diff. = 3.500		
Presentation = pil	Obscuration = 0.1992	Volume Conc. = 0.0237%	Shape OFF
	Volume distribution	Sp.S.A 0.9393 m²/cc.	

UCT Physics Department

Sample: Duvha fly ash as supplied.

Focal Length: 300mm

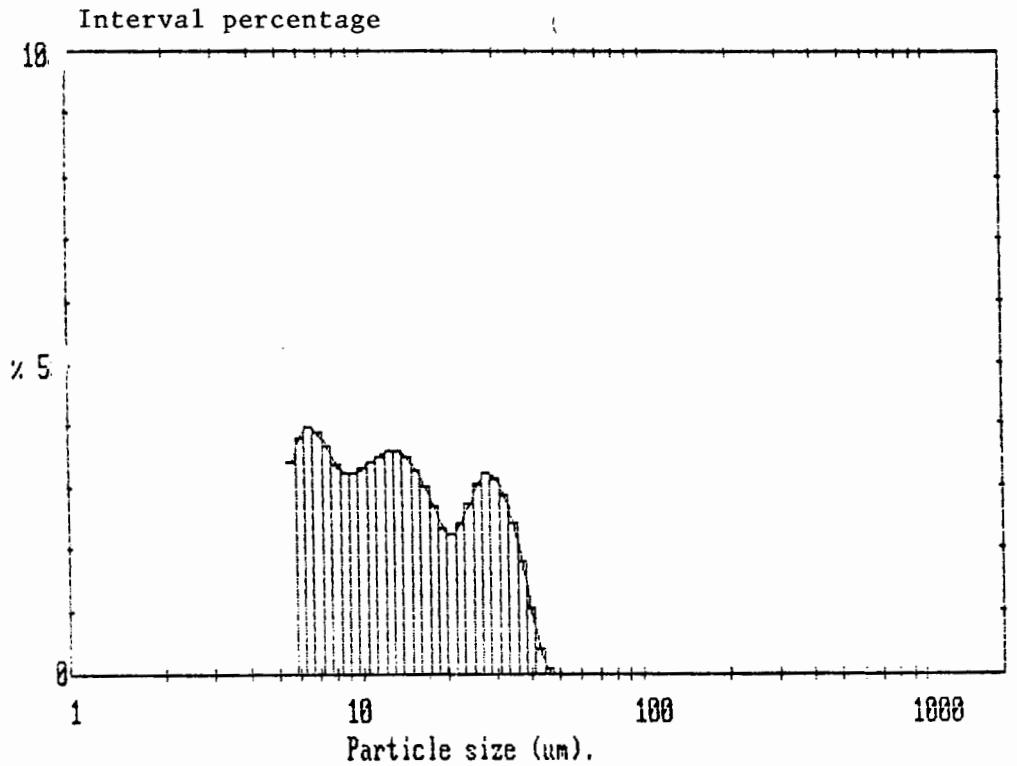

High Size	In %	High Size	In %	High Size	In %	High Size	In %	High Size	In %	High Size	In %	Span 2.19
564	0.0	254	0.0	114	0.0	51.3	0.0	23.1	2.4	10.4	3.3	D[4,3] 14.21µm
524	0.0	236	0.0	106	0.0	47.7	0.1	21.4	2.2	9.64	3.2	
488	0.0	219	0.0	98.6	0.0	44.4	0.4	19.9	2.4	8.97	3.2	
454	0.0	204	0.0	91.7	0.0	41.2	1.1	18.5	2.7	8.34	3.4	D[3,2] 7.97µm
422	0.0	190	0.0	85.3	0.0	38.4	1.8	17.2	3.0	7.76	3.7	
393	0.0	176	0.0	79.3	0.0	35.7	2.4	16.0	3.3	7.21	3.9	
365	0.0	164	0.0	73.8	0.0	33.2	2.9	14.9	3.5	6.71	4.0	D[v,0.9] 29.89µm
340	0.0	153	0.0	68.6	0.0	30.8	3.2	13.9	3.6	6.24	3.9	
316	0.0	142	0.0	63.8	0.0	28.7	3.2	12.9	3.6	5.80	3.4	
293	0.0	132	0.0	59.3	0.0	26.7	3.0	12.0	3.5			D[v,0.1] 2.92µm
273	0.0	123	0.0	55.2	0.0	24.8	2.7	11.2	3.4			

Source = :Sample	Beam length = 2.0 mm Log. Diff. = 4.327	Model indp	D[v,0.5] 11.40µm
Focal length = 300 mm	Obscuration = 0.1934	Volume Conc. = 0.0286%	
Presentation = pil	Volume distribution	Sp.S.A 0.7529 m²/cc.	Shape OFF

UCT Physics Department

Sample: Duvha(-63) fly ash.

Focal Length: 300mm

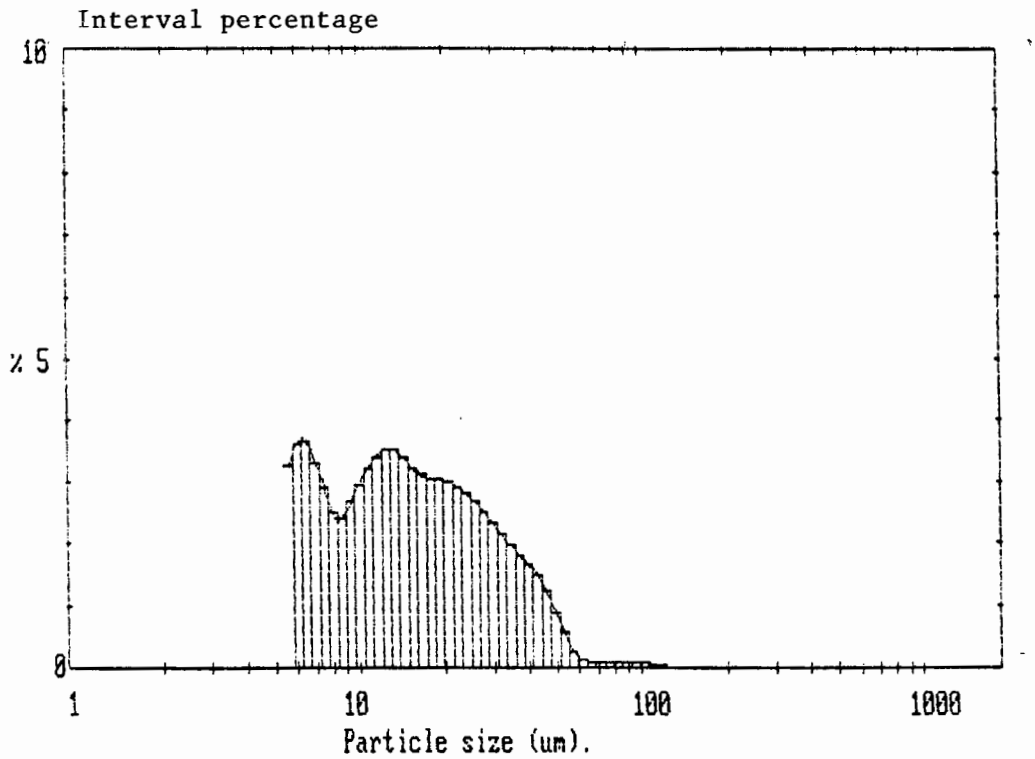

High Size	In %	High Size	In %	High Size	In %	High Size	In %	High Size	In %	High Size	In %	Span 2.33
554	0.0	254	0.0	114	0.0	51.3	0.9	23.1	2.9	10.4	3.0	D[4,3] 16.39µm
504	0.0	336	0.0	106	0.1	47.7	1.2	21.4	3.0	9.64	2.7	
488	0.0	219	0.0	98.6	0.1	44.4	1.3	19.9	3.0	8.97	2.4	D[3,2] 8.33µm
454	0.0	204	0.0	91.7	0.1	41.2	1.7	18.5	3.1	8.34	2.5	
422	0.0	190	0.0	85.3	0.1	38.4	1.8	17.2	3.1	7.76	2.9	
392	0.0	176	0.0	79.3	0.1	35.7	2.0	16.0	3.2	7.21	3.3	D[v,0.9] 34.32µm
365	0.0	164	0.0	73.8	0.1	33.2	2.2	14.9	3.4	6.71	3.7	
339	0.0	153	0.0	68.6	0.1	30.9	2.3	13.9	3.5	6.24	3.6	
315	0.0	142	0.0	63.8	0.2	28.7	2.6	12.9	3.5	5.80	3.3	
293	0.0	132	0.0	59.3	0.3	26.7	2.7	12.0	3.4			D[v,0.1] 4.92µm
273	0.0	123	0.0	55.2	0.6	24.8	2.8	11.2	3.2			

Source = :Sample	Beam length = 2.0 mm	Model indp	D[v,0.5] 12.60um
	Log. Diff. = 1.910		
Focal length = 300 mm	Obscuration = 0.1969	Volume Conc. = 0.0309%	
Presentation = pil	Volume distribution	Sp.S.A 0.7201 m²/cc.	Space OFF

UCT Physics Department

Sample: Van Eck clinker ash as collected.

Focal Length: 300mm

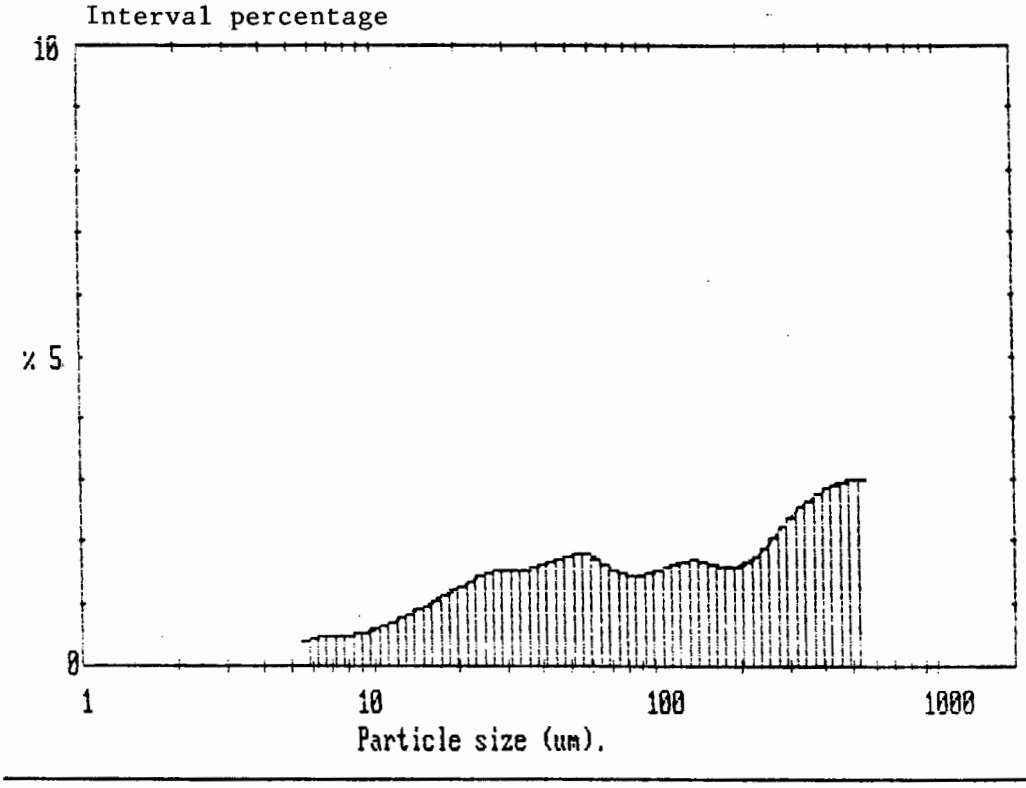

High Size	In %	High Size	In %	High Size	In %	High Size	In %	High Size	In %	Span 4.08
564	3.0	254	1.9	114	1.6	51.3	1.8	23.1	1.4	10.4	0.6	D[4,3] 172.14µm
524	3.0	236	1.8	106	1.5	47.7	1.7	21.4	1.3	9.64	0.6	
488	3.0	219	1.7	98.9	1.6	44.4	1.7	19.9	1.2	8.97	0.5	
454	2.9	204	1.6	91.7	1.5	41.2	1.6	18.5	1.1	8.34	0.5	D[3,2] 38.87µm
422	2.8	190	1.6	85.3	1.5	38.4	1.6	17.2	1.1	7.76	0.5	
392	2.8	176	1.6	79.3	1.5	35.7	1.6	16.0	1.0	7.21	0.5	
365	2.7	164	1.6	73.8	1.6	33.2	1.5	14.9	0.9	6.71	0.5	D[v,0.9] 442.83µm
339	2.6	153	1.7	68.6	1.7	30.8	1.5	13.9	0.8	6.24	0.4	
315	2.5	142	1.7	63.8	1.7	28.7	1.5	12.9	0.8	5.80	0.4	
293	2.4	132	1.7	59.3	1.8	26.7	1.5	12.0	0.7			D[v,0.1] 16.20µm
273	2.3	123	1.7	55.2	1.8	24.8	1.4	11.2	0.7			

Source = :Sample	Beam length = 2.0 mm Log. Diff. = 3.542	Model ind:	D[v,0.5] 104.70µm
Focal length = 300 mm Presentation = pil	Obscuration = 0.2199 Volume distribution	Volume Conc. = 0.1525% Sp.S.A 0.1627 m²/cc.	Shape OFF

UCT Physics Department

Sample: Van Eck milled clinker ash.

Focal Length: 300mm

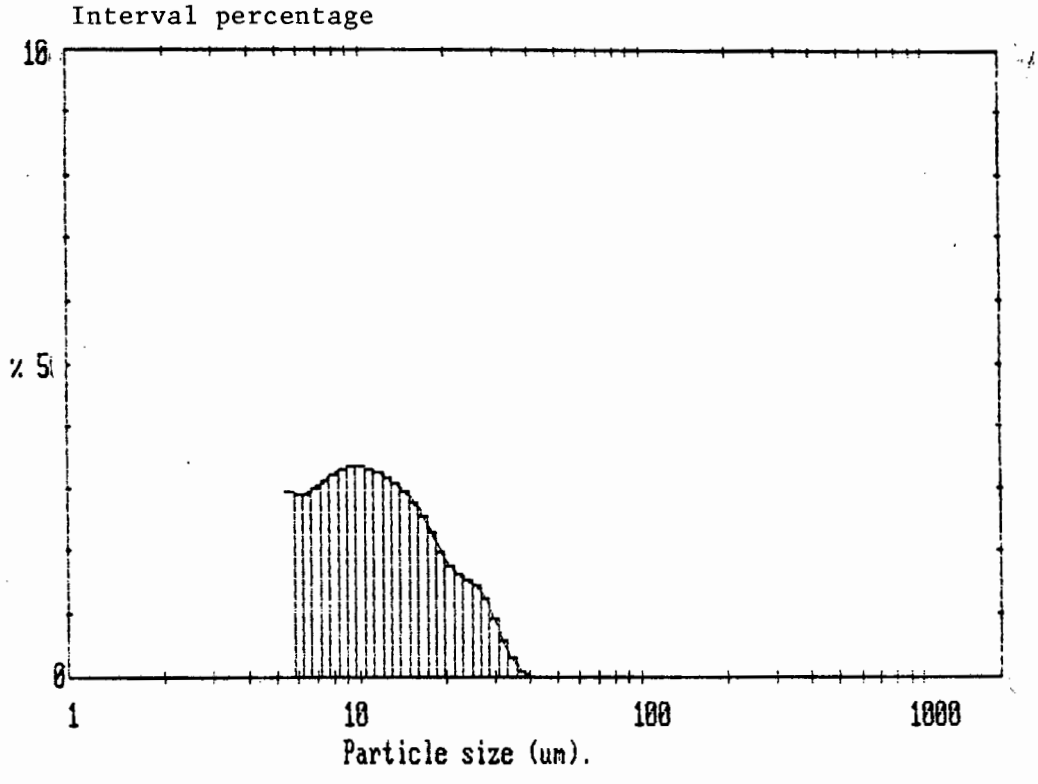

High Size	In %	High Size	In %	High Size	In %	High Size	In %	High Size	In %	High Size	In %	Span 2.26
564	0.0	254	0.0	114	0.0	51.3	0.0	23.1	1.6	10.4	3.4	D[4,3] 9.25µm
524	0.0	236	0.0	106	0.0	47.7	0.0	21.4	1.8	9.64	3.4	
488	0.0	219	0.0	98.6	0.0	44.4	0.0	19.9	2.0	8.97	3.3	
454	0.0	204	0.0	91.7	0.0	41.2	0.0	18.5	2.3	8.34	3.2	D[3,2] 5.28µm
422	0.0	190	0.0	85.3	0.0	38.4	0.1	17.2	2.6	7.76	3.1	
392	0.0	176	0.0	79.3	0.0	35.7	0.3	16.0	2.8	7.21	3.0	
365	0.0	164	0.0	73.8	0.0	33.2	0.6	14.9	3.0	6.71	2.9	D[v,0.9] 19.83µm
339	0.0	153	0.0	68.6	0.0	30.8	0.9	13.9	3.1	6.24	2.9	
315	0.0	142	0.0	63.8	0.0	28.7	1.2	12.9	3.2	5.80	3.0	
293	0.0	132	0.0	59.3	0.0	26.7	1.4	12.0	3.3			D[v,0.1] 2.69µm
273	0.0	123	0.0	55.2	0.0	24.8	1.6	11.2	3.3			

Source = :Sample	Beam length = 2.0 mm	Model indp	D[v,0.5] 7.48µm
	Log. Diff. = 4.416		
Focal length = 300 mm	Obscuration = 0.1986	Volume Conc. = 0.0195%	
Presentation = 3ll	Volume distribution	Sp.S.A 1.1354 m²/cc.	Shape OFF

UCT Physics Department

Sample: Van Eck(-63) milled clinker ash.

Focal Length: 300mm

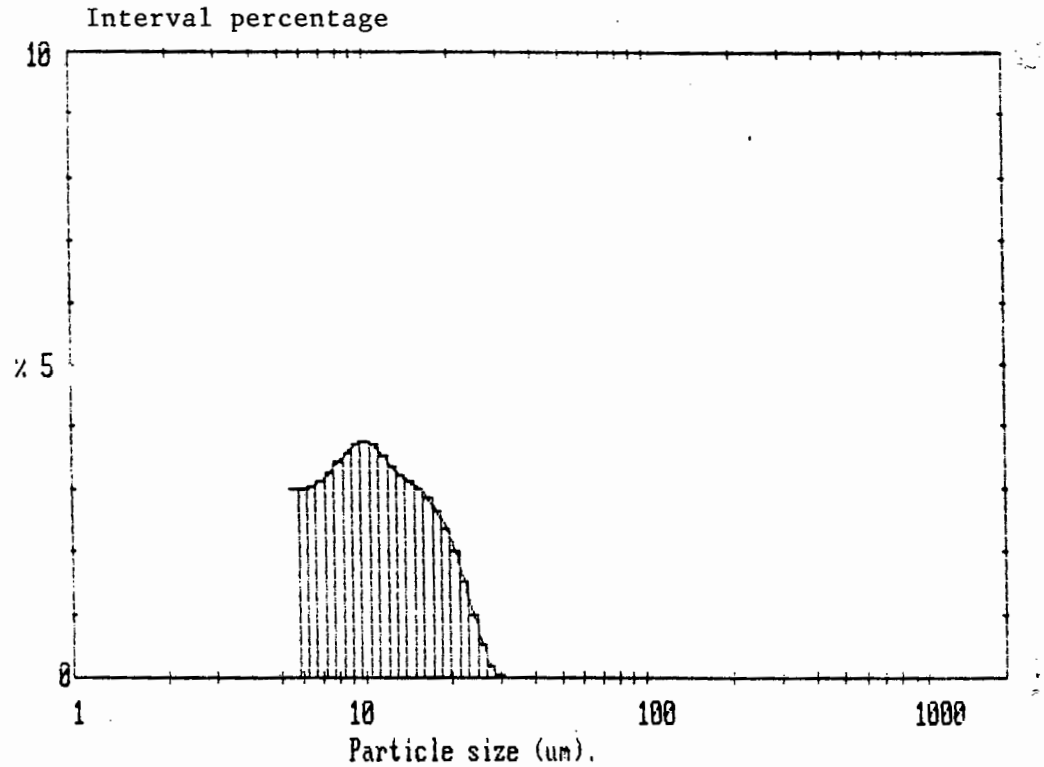

High Size	In %	High Size	In %	High Size	In %	High Size	In %	High Size	In %	High Size	In %	Span 1.99
564	0.0	284	0.0	114	0.0	51.3	0.0	23.1	1.5	10.4	3.8	D[4,3] 3.54µm
554	0.0	279	0.0	106	0.0	47.7	0.0	21.4	2.0	9.64	3.7	
488	0.0	246	0.0	98.6	0.0	44.4	0.0	19.9	2.4	8.97	3.6	D[3,2] 5.21µm
422	0.0	214	0.0	91.7	0.0	41.2	0.0	18.5	2.7	8.34	3.4	
411	0.0	207	0.0	85.3	0.0	38.4	0.0	17.2	2.9	7.76	3.3	D[v,0.9] 17.44µm
366	0.0	185	0.0	79.3	0.0	35.7	0.0	16.0	3.0	7.21	3.1	
366	0.0	184	0.0	73.8	0.0	33.3	0.0	14.9	3.1	6.71	3.0	
339	0.0	171	0.0	68.6	0.0	30.8	0.0	13.9	3.2	6.24	3.0	D[v,0.1] 2.70µm
315	0.0	159	0.0	63.8	0.0	28.7	0.2	12.9	3.4	5.80	3.0	
294	0.0	148	0.0	59.3	0.0	26.7	0.5	12.0	3.6			
273	0.0	138	0.0	55.2	0.0	24.8	1.0	11.2	3.7			

Source = :Sample	Beam length = 2.0 mm	Model indp	D[v,0.5] 7.40µm
	Log. Diff. = 4.864		
Focal length = 300 mm	Obscuration = 0.2279	Volume Conc. = 0.0225%	Shape OFF
Presentation = 3il	Volume distribution	Sp.S.A 1.1510 m²/cc.	

UCT Physics Department

Sample: Matla fly ash as supplied.

Focal Length: 300mm

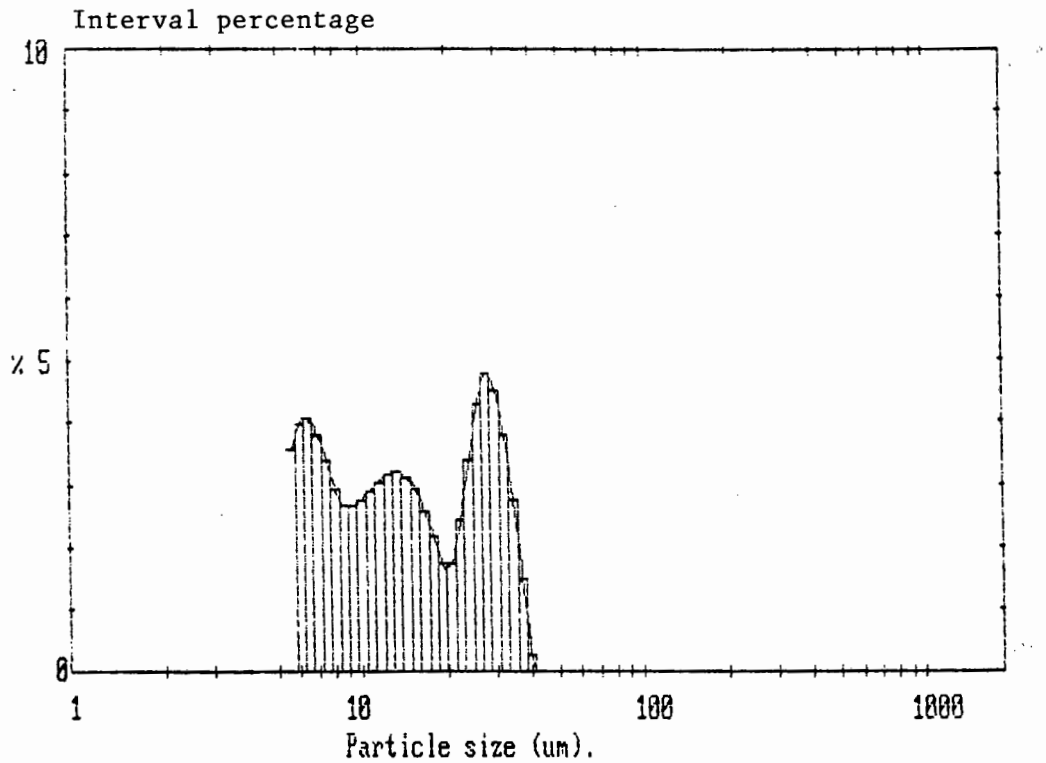

High Size	In %	High Size	In %	High Size	In %	High Size	In %	High Size	In %	High Size	In %	Span 2.17
564	0.0	254	0.0	114	0.0	51.3	0.0	23.1	2.5	10.4	2.9	D[4,3] 14.50µm
508	0.0	229	0.0	106	0.0	47.7	0.0	21.4	1.8	9.64	2.7	
488	0.0	219	0.0	98.6	0.0	44.4	0.0	19.9	1.8	8.97	2.7	
454	0.0	204	0.0	91.7	0.0	41.3	0.2	18.5	2.2	8.34	3.0	D[3,2] 7.80µm
402	0.0	180	0.0	85.3	0.0	38.4	1.5	17.2	2.6	7.76	3.4	
392	0.0	176	0.0	79.3	0.0	35.7	2.8	16.0	2.9	7.21	3.8	
365	0.0	164	0.0	73.8	0.0	33.2	3.8	14.9	3.2	6.71	4.1	D[v,0.9] 29.99µm
339	0.0	153	0.0	68.6	0.0	30.8	4.5	13.9	3.2	6.24	4.0	
315	0.0	142	0.0	63.8	0.0	28.7	4.6	12.9	3.2	5.80	3.6	
293	0.0	132	0.0	59.3	0.0	26.7	4.3	12.0	3.1			D[v,0.1] 4.74µm
273	0.0	123	0.0	55.2	0.0	24.8	3.4	11.2	2.9			

Source = Sample	Beam length = 2.0 mm	Model: udo	D[v,0.5] 11.84µm
	Loc. Diff. = 4.851		
Focal length = 300 mm	Obscuration = 0.1941	Volume Conc. = 0.023%	
Presentation = pil	Volume distribution	Sp.S.A 0.7694 m²/cc.	Erase OFF

UCT Physics Department

Sample: Matla(-63) fly ash.

Focal Length: 300mm

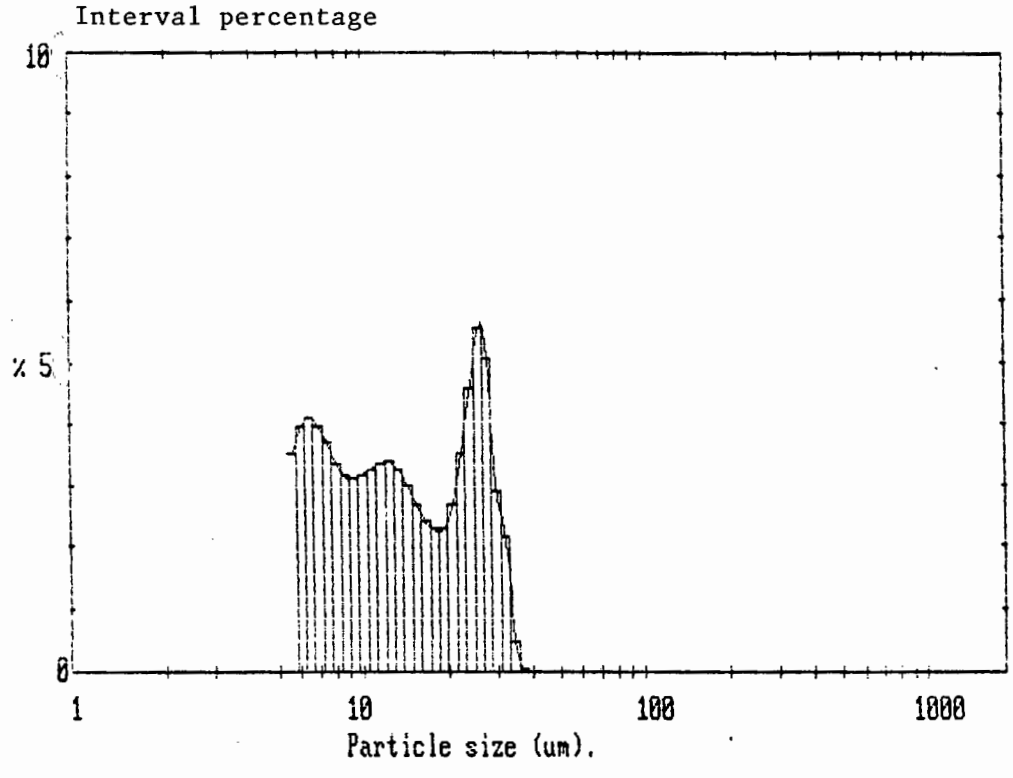

High Size	In %	High Size	In %	High Size	In %	High Size	In %	High Size	In %	High Size	In %	Span 1.98
564	0.0	254	0.0	114	0.0	51.3	0.0	23.1	3.6	10.4	3.2	D(4,3) 13.52µm
524	0.0	236	0.0	106	0.0	47.7	0.0	21.4	2.7	9.64	3.2	
488	0.0	219	0.0	98.6	0.0	44.4	0.0	19.9	2.3	8.97	3.2	
454	0.0	204	0.0	91.7	0.0	41.2	0.0	18.5	2.3	8.34	3.4	D(3,2) 7.76µm
422	0.0	190	0.0	85.3	0.0	38.4	0.0	17.2	2.4	7.76	3.7	
393	0.0	176	0.0	79.3	0.0	35.7	0.5	16.0	2.7	7.21	4.0	
366	0.0	164	0.0	73.8	0.0	33.2	2.2	14.9	3.0	6.71	4.1	D(v,0.9) 26.91µm
340	0.0	153	0.0	68.6	0.0	30.8	2.9	13.9	3.3	6.24	4.0	
316	0.0	142	0.0	63.8	0.0	28.7	3.1	12.9	3.4	5.80	3.8	
294	0.0	132	0.0	59.3	0.0	26.7	3.6	12.0	3.4			D(v,0.1) 4.85µm
273	0.0	123	0.0	55.2	0.0	24.8	4.6	11.2	3.3			

Source = :Sample	Beam length = 2.0 mm	Model indp	D(v,0.5) 11.14µm
	Log. Diff. = 4.858		
Focal length = 300 mm	Obscuration = 0.1962	Volume Conc. = 0.0283%	
Presentation = pil	Volume distribution	Sp.S.A 0.7732 m²/cc.	Shape OFF

UCT Physics Department

X-ray diffractogram for the Lethabo fly ash

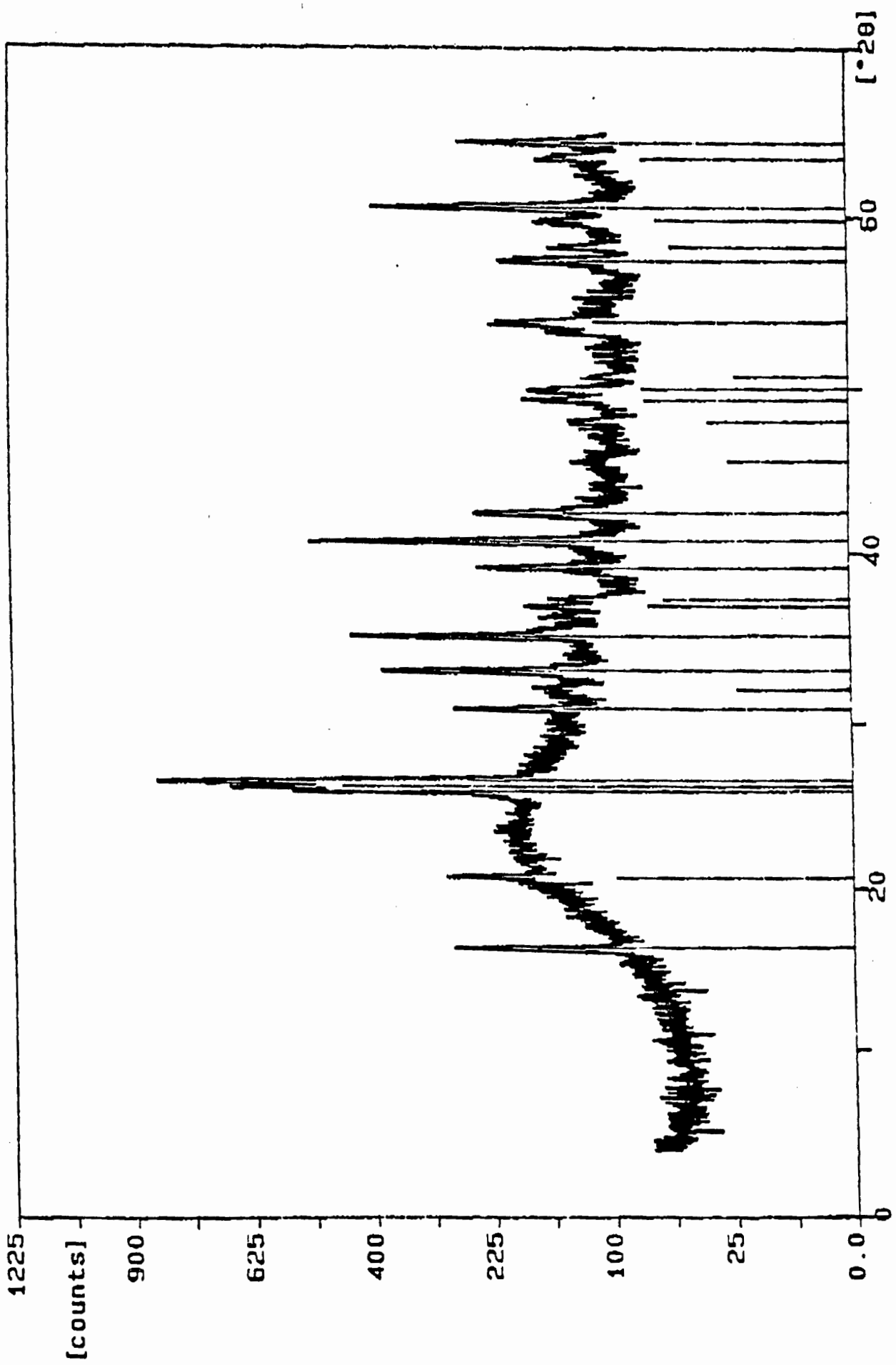

X-ray diffractogram for the Duvha fly ash

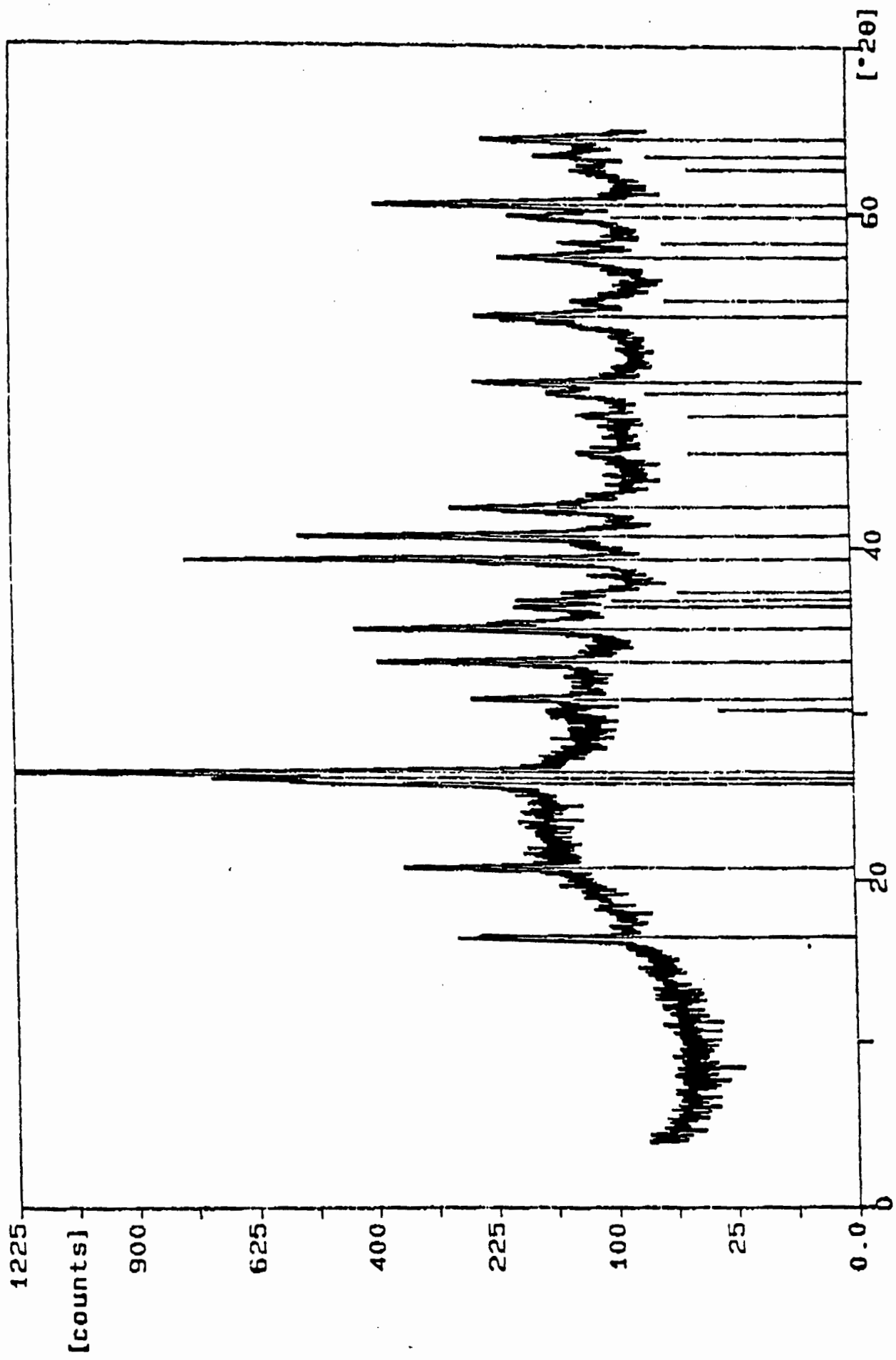

X-ray diffractogram for the Van Eck clinker ash

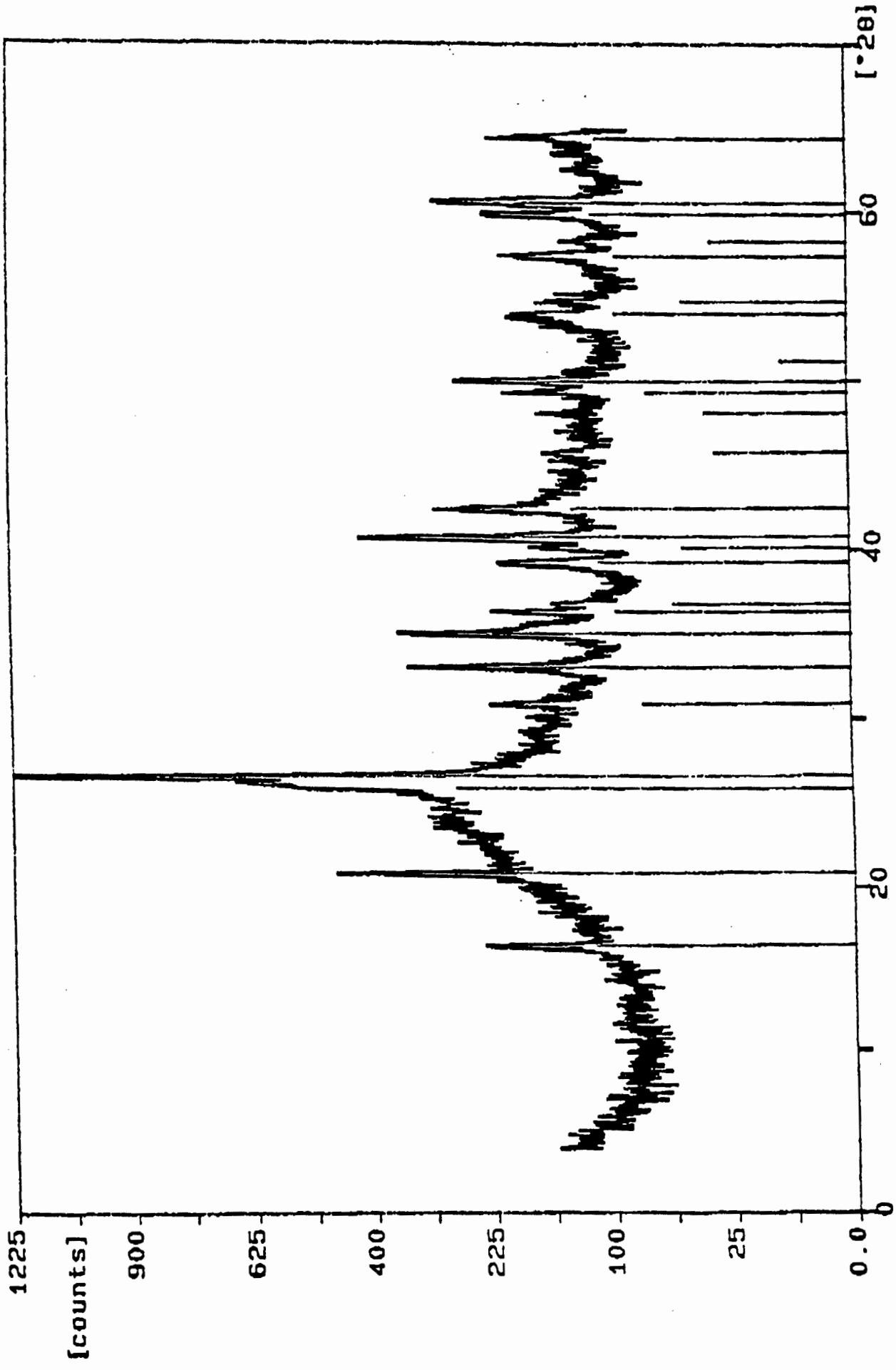

X-ray diffractogram for the Matla fly ash

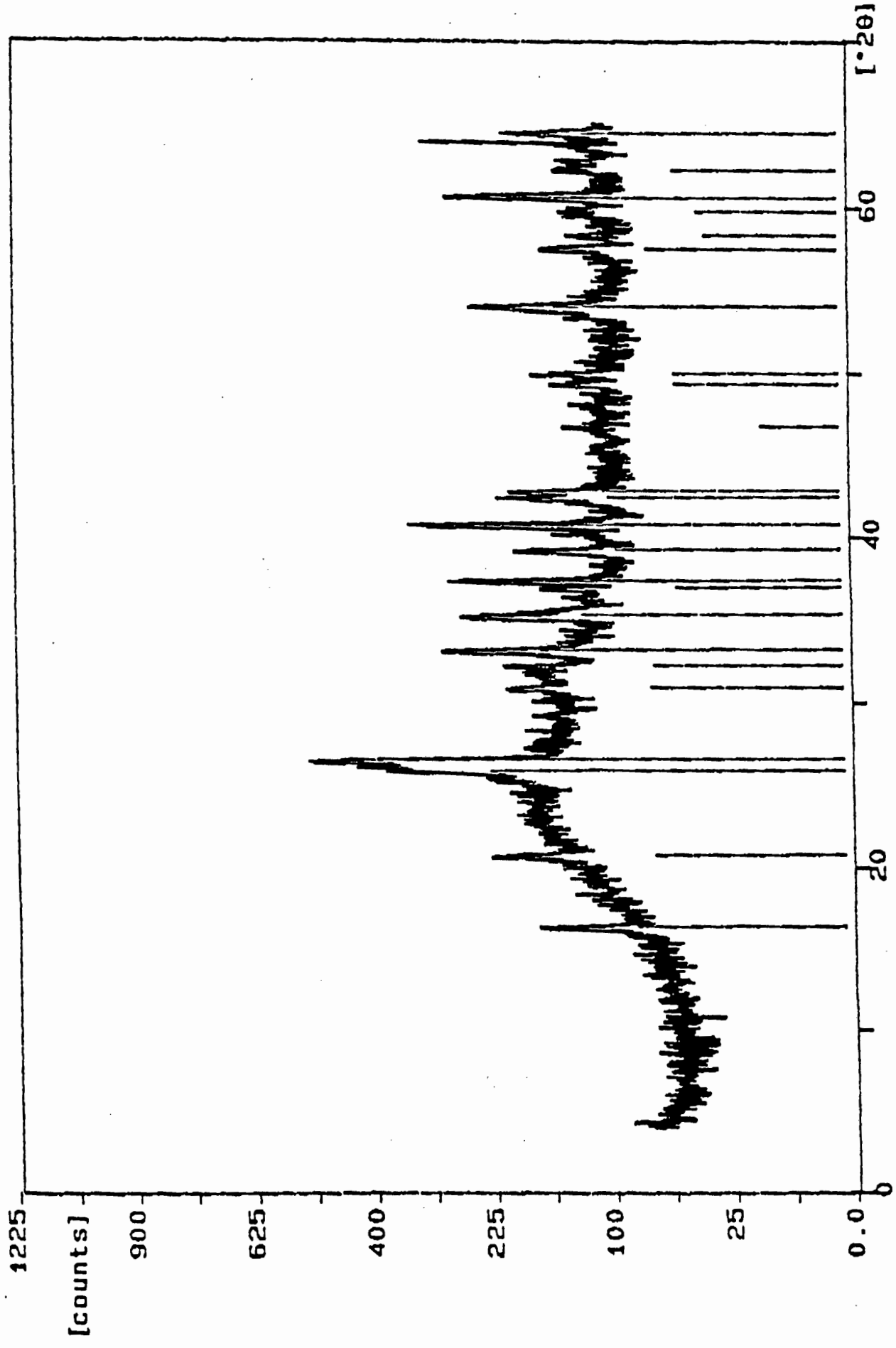

APPENDIX B

Concrete Cube Results for Control Mix

Cube	Sat. Vol. (ml)	Sat. Mass (g)	Density ((kg/m^3)	Compr.Str (MPa)
	3 Days : 17/09/1993			
A	1016.8	2473.7	2.433	18.3
B	1012.3	2462.8	2.433	16.4
C	1020.1	2484.3	2.435	18.1
D	1004.3	2444.4	2.434	18.3
Average	1013.4	2466.3	2.434	17.8
Std. Dev.	5.926	14.753	0.001	0.798
	7 Days : 21/09/1993			
A	1014.9	2466.5	2.430	24.5
B	1016.1	2494.3	2.455	27.6
C	1005.2	2459.9	2.447	26.1
D	1016.3	2470.9	2.431	26.1
Average	1013.1	2472.9	2.441	26.1
Std. Dev.	4.607	12.961	0.010	1.096
	14 Days : 28/09/1993			
A	1019.6	2488.2	2.440	32.4
B	1020.3	2490.1	2.441	33.4
C	1014.0	2476.8	2.443	32.4
D	1012.9	2469.1	2.438	34.5
Average	1016.7	2481.1	2.440	33.2
Std. Dev.	3.283	8.572	0.002	0.867
	21 Days : 05/10/1993			
A	1017.6	2491.2	2.448	36.6
B	1020.7	2491.3	2.441	36.1
C	1013.0	2475.5	2.444	37.1
D	1012.0	2464.7	2.435	37.4
Average	1015.8	2480.7	2.442	36.8
Std. Dev.	3.519	11.243	0.005	0.495
	28 Days : 12/10/1993			
A	1019.6	2483.8	2.436	38.4
B	1005.2	2448.2	2.436	39.8
C	1008.3	2460.8	2.441	38.7
D	1001.3	2438.4	2.435	39.1
Average	1008.6	2457.8	2.437	39.0
Std. Dev.	6.818	16.982	0.002	0.524

Concrete Cube Results for Lethabo (-63) Mix

Cube	Sat. Vol.	Sat. Mass	Density	Compr.Str
	(ml)	(g)	((kg/m^3)	(MPa)
		3 Days : 17/09/1993		
A	1018.1	2491.8	2.448	12.5
B	1007.8	2455.3	2.436	11.4
C	1009.0	2453.6	2.432	10.5
D	1019.0	2478.6	2.432	10.8
Average	1013.5	2469.8	2.437	11.3
Std. Dev.	5.103	16.079	0.006	0.765
		7 Days : 21/09/1993		
A	1013.6	2461.0	2.428	16.9
B	1017.5	2477.8	2.435	18.8
C	1015.5	2471.9	2.434	19.0
D	1000.3	2427.0	2.426	16.9
Average	1011.7	2459.4	2.431	17.9
Std. Dev.	6.739	19.667	0.004	1.002
		14 Days : 28/09/1993		
A	1007.2	2454.8	2.437	22.2
B	1009.6	2447.6	2.424	21.6
C	1013.7	2473.2	2.440	22.4
D	1015.7	2475.9	2.438	20.9
Average	1011.6	2462.9	2.435	21.8
Std. Dev.	3.338	11.987	0.006	0.585
		21 Days : 05/10/1993		
A	1014.1	2469.8	2.435	26.6
B	1007.3	2457.6	2.440	26.0
C	1013.6	2472.9	2.440	26.3
D	1009.3	2458.5	2.436	26.4
Average	1011.1	2464.7	2.438	26.3
Std. Dev.	2.869	6.747	0.002	0.217
		28 Days : 12/10/1993		
A	1020.1	2489.2	2.440	28.5
B	1017.8	2496.5	2.453	27.5
C	1008.3	2460.8	2.441	28.4
D	1001.3	2438.4	2.435	28.6
Average	1011.9	2471.2	2.442	28.3
Std. Dev.	7.539	23.174	0.006	0.439

Concrete Cube Results for Lethabo Mix

Cube	Sat. Vol. (ml)	Sat. Mass (g)	Density ((kg/m^3)	Compr.Str (MPa)
	3 Days : 18/09/1993			
A	1012.5	2445.7	2.416	10.3
B	1004.9	2446.7	2.435	10.4
C	1005.9	2446.7	2.432	10.0
D	1011.2	2451.8	2.425	9.4
Average	1008.6	2447.7	2.427	10.0
Std. Dev.	3.277	2.388	0.008	0.390
	7 Days : 22/09/1993			
A	1000.9	2431.6	2.429	15.5
B	1005.8	2449.7	2.436	16.1
C	1007.0	2460.2	2.443	15.3
D	1002.5	2439.0	2.433	16.4
Average	1004.1	2445.1	2.435	15.8
Std. Dev.	2.454	10.824	0.005	0.444
	14 Days : 29/09/1993			
A	1013.7	2466.6	2.433	21.9
B	1005.3	2437.4	2.425	20.4
C	1007.1	2457.2	2.440	21.4
D	1011.6	2454.9	2.427	20.1
Average	1009.4	2454.0	2.431	21.0
Std. Dev.	3.370	10.552	0.006	0.730
	21 Days : 06/10/1993			
A	999.3	2424.3	2.426	25.5
B	1013.3	2467.3	2.435	25.0
C	1014.8	2477.2	2.441	24.9
D	1008.0	2459.9	2.440	25.1
Average	1008.9	2457.2	2.436	25.1
Std. Dev.	6.065	19.948	0.006	0.228
	28 Days : 13/10/1993			
A	1010.4	2461.5	2.436	27.3
B	1006.4	2450.4	2.435	27.2
C	1013.8	2468.0	2.434	25.2
D	1008.8	2459.5	2.438	27.5
Average	1009.9	2459.9	2.436	26.8
Std. Dev.	2.688	6.296	0.001	0.930

Concrete Cube Results for Duvha (-63) Mix

Cube	Sat. Vol. (ml)	Sat. Mass (g)	Density ((kg/m^3)	Compr.Str (MPa)
	3 Days : 18/09/1993			
A	1003.1	2412.6	2.405	9.9
B	1011.1	2444.0	2.417	12.5
C	1011.6	2428.0	2.400	10.5
D	1011.0	2443.0	2.416	10.9
Average	1009.2	2431.9	2.410	11.0
Std. Dev.	3.529	12.819	0.007	0.963
	7 Days : 22/09/1993			
A	1010.2	2436.4	2.412	16.2
B	1002.5	2419.1	2.413	16.9
C	1007.3	2434.8	2.417	16.7
D	1020.8	2462.8	2.413	16.9
Average	1010.2	2438.3	2.414	16.7
Std. Dev.	6.709	15.690	0.002	0.286
	14 Days : 29/09/1993			
A	1012.9	2446.1	2.415	22.0
B	1017.1	2455.3	2.414	22.4
C	1019.3	2464.9	2.418	22.4
D	1014.2	2460.4	2.426	21.7
Average	1015.9	2456.7	2.418	22.1
Std. Dev.	2.494	6.987	0.005	0.295
	21 Days : 06/10/1993			
A	1026.1	2498.7	2.435	27.7
B	1008.0	2441.1	2.422	26.7
C	1022.7	2474.2	2.419	23.4
D	1008.8	2444.4	2.423	25.0
Average	1016.4	2464.6	2.425	25.7
Std. Dev.	8.095	23.533	0.006	1.642
	28 Days : 13/10/1993			
A	1014.8	2459.9	2.424	29.7
B	1022.4	2470.9	2.417	27.2
C	1022.2	2478.3	2.424	27.2
D	1000.8	2428.7	2.427	29.3
Average	1015.1	2459.5	2.423	28.4
Std. Dev.	8.779	18.922	0.004	1.159

Concrete Cube Results for Van Eck (-63) Mix

Cube	Sat. Vol.	Sat. Mass	Density	Compr.Str
	(ml)	(g)	((kg/m^3)	(MPa)
	3 Days : 19/09/1993			
A	1022.0	2473.6	2.420	12.5
B	1004.5	2423.7	2.413	12.4
C	1012.1	2446.4	2.417	12.8
D	1020.1	2466.3	2.418	13.5
Average	1014.7	2452.5	2.417	12.8
Std. Dev.	6.951	19.380	0.003	0.430
	7 Days : 23/09/1993			
A	1013.0	2446.1	2.415	19.2
B	1022.9	2467.9	2.413	20.8
C	1004.5	2414.7	2.404	19.9
D	1026.6	2472.4	2.408	20.5
Average	1016.8	2450.3	2.410	20.1
Std. Dev.	8.645	22.821	0.004	0.612
	14 Days : 30/09/1993			
A	1011.8	2446.3	2.418	23.7
B	1013.6	2451.6	2.419	24.7
C	1013.6	2449.0	2.416	25.6
D	999.5	2424.1	2.425	26.0
Average	1009.6	2442.8	2.419	25.0
Std. Dev.	5.892	10.929	0.003	0.886
	21 Days : 07/10/1993			
A	1009.6	2433.2	2.410	29.3
B	1014.6	2447.3	2.412	25.9
C	1012.3	2439.0	2.409	30.3
D	1010.4	2413.9	2.389	27.8
Average	1011.7	2433.4	2.405	28.3
Std. Dev.	1.928	12.297	0.009	1.659
	28 Days : 14/10/1993			
A	1014.6	2461.1	2.426	30.7
B	1020.3	2453.0	2.404	31.1
C	1014.3	2439.9	2.406	30.1
D	1024.0	2484.5	2.426	30.9
Average	1018.3	2459.6	2.415	30.7
Std. Dev.	4.068	16.232	0.011	0.374

Concrete Cube Results for Matla (-63) Mix

Cube	Sat. Vol. (ml)	Sat. Mass (g)	Density ((kg/m^3)	Compr.Str (MPa)
		3 Days : 19/09/1993		
A	1003.9	2459.3	2.450	11.0
B	1007.0	2458.3	2.441	10.0
C	1005.2	2457.6	2.445	10.4
D	999.4	2450.7	2.452	11.2
Average	1003.9	2456.5	2.447	10.7
Std. Dev.	2.808	3.388	0.004	0.477
		7 Days : 23/09/1993		
A	1007.7	2461.1	2.442	18.6
B	996.4	2424.2	2.433	16.4
C	1002.3	2453.1	2.447	19.1
D	1003.6	2450.9	2.442	17.7
Average	1002.5	2447.3	2.441	18.0
Std. Dev.	4.047	13.880	0.005	1.026
		14 Days : 30/09/1993		
A	1006.3	2463.4	2.448	23.7
B	1004.2	2456.7	2.446	22.2
C	998.2	2438.4	2.443	22.3
D	1010.0	2469.0	2.445	22.0
Average	1004.7	2456.9	2.445	22.6
Std. Dev.	4.276	11.521	0.002	0.673
		21 Days : 07/10/1993		
A	1004.0	2457.1	2.447	26.3
B	1013.8	2475.8	2.442	25.7
C	1005.3	2457.3	2.444	24.4
D	1002.9	2453.4	2.446	25.7
Average	1006.5	2460.9	2.445	25.5
Std. Dev.	4.299	8.742	0.002	0.694
		28 Days : 14/10/1993		
A	1003.3	2461.7	2.454	29.2
B	1009.2	2465.8	2.443	26.4
C	1008.5	2465.7	2.445	27.4
D	1002.1	2449.5	2.444	29.2
Average	1005.8	2460.7	2.447	28.1
Std. Dev.	3.114	6.660	0.004	1.203

Concrete Cube Results at 3 Days

	Sat. Vol. (ml)	Sat. Mass (g)	Density ((kg/m^3)	Compr.Str (MPa)
	Date of Testing: 17/09/1993			
M1A	1016.8	2473.7	2.433	18.3
M1B	1012.3	2462.8	2.433	16.4
M1C	1020.1	2484.3	2.435	18.1
M1D	1004.3	2444.4	2.434	18.3
Average	1013.4	2466.3	2.434	17.8
Std. Dev.	5.926	14.753	0.001	0.798
	Date of Testing: 17/09/1993			
M2A	1018.1	2491.8	2.448	12.5
M2B	1007.8	2455.3	2.436	11.4
M2C	1009.0	2453.6	2.432	10.5
M2D	1019.0	2478.6	2.432	10.8
Average	1013.5	2469.8	2.437	11.3
Std. Dev.	5.103	16.079	0.006	0.765
	Date of Testing: 18/09/1993			
M3A	1012.5	2445.7	2.416	10.3
M3B	1004.9	2446.7	2.435	10.4
M3C	1005.9	2446.7	2.432	10.0
M3D	1011.2	2451.8	2.425	9.4
Average	1008.6	2447.7	2.427	10.0
Std. Dev.	3.277	2.388	0.008	0.390

	Sat. Vol. (ml)	Sat. Mass (g)	Density ((kg/m^3)	Compr.Str (MPa)
	Date of Testing: 18/09/1993			
M4A	1003.1	2412.6	2.405	9.9
M4B	1011.1	2444.0	2.417	12.5
M4C	1011.6	2428.0	2.400	10.5
M4D	1011.0	2443.0	2.416	10.9
Average	1009.2	2431.9	2.410	11.0
Std. Dev.	3.529	12.819	0.007	0.963
	Date of Testing: 19/09/1993			
M5A	1022.0	2473.6	2.420	12.5
M5B	1004.5	2423.7	2.413	12.4
M5C	1012.1	2446.4	2.417	12.8
M5D	1020.1	2466.3	2.418	13.5
Average	1014.7	2452.5	2.417	12.8
Std. Dev.	6.951	19.380	0.003	0.430
	Date of Testing: 19/09/1993			
M6A	1003.9	2459.3	2.450	11.0
M6B	1007.0	2458.3	2.441	10.0
M6C	1005.2	2457.6	2.445	10.4
M6D	999.4	2450.7	2.452	11.2
Average	1003.9	2456.5	2.447	10.7
Std. Dev.	2.808	3.388	0.004	0.477

Mix	Compr.Str (MPa)
M1	17.8
M2	11.3
M3	10.0
M4	11.0
M5	12.8
M6	10.7

Concrete Cube Results at 7 Days

	Sat. Vol. (ml)	Sat. Mass (g)	Density ((kg/m^3)	Compr.Str (MPa)
Date of Testing: 21/09/1993				
M1A	1014.9	2466.5	2.430	24.5
M1B	1016.1	2494.3	2.455	27.6
M1C	1005.2	2459.9	2.447	26.1
M1D	1016.3	2470.9	2.431	26.1
Average	1013.1	2472.9	2.441	26.1
Std. Dev.	4.607	12.961	0.010	1.096
Date of Testing: 21/09/1993				
M2A	1013.6	2461.0	2.428	16.9
M2B	1017.5	2477.8	2.435	18.8
M2C	1015.5	2471.9	2.434	19.0
M2D	1000.3	2427.0	2.426	16.9
Average	1011.7	2459.4	2.431	17.9
Std. Dev.	6.739	19.667	0.004	1.002
Date of Testing: 22/09/1993				
M3A	1000.9	2431.6	2.429	15.5
M3B	1005.8	2449.7	2.436	16.1
M3C	1007.0	2460.2	2.443	15.3
M3D	1002.5	2439.0	2.433	16.4
Average	1004.1	2445.1	2.435	15.8
Std. Dev.	2.454	10.824	0.005	0.444

	Sat. Vol. (ml)	Sat. Mass (g)	Density ((kg/m^3)	Compr.Str (MPa)
Date of Testing: 22/09/1993				
M4A	1010.2	2436.4	2.412	16.2
M4B	1002.5	2419.1	2.413	16.9
M4C	1007.3	2434.8	2.417	16.7
M4D	1020.8	2462.8	2.413	16.9
Average	1010.2	2438.3	2.414	16.7
Std. Dev.	6.709	15.690	0.002	0.286
Date of Testing: 23/09/1993				
M5A	1013.0	2446.1	2.415	19.2
M5B	1022.9	2467.9	2.413	20.8
M5C	1004.5	2414.7	2.404	19.9
M5D	1026.6	2472.4	2.408	20.5
Average	1016.8	2450.3	2.410	20.1
Std. Dev.	8.645	22.821	0.004	0.612
Date of Testing: 23/09/1993				
M6A	1007.7	2461.1	2.442	18.6
M6B	996.4	2424.2	2.433	16.4
M6C	1002.3	2453.1	2.447	19.1
M6D	1003.6	2450.9	2.442	17.7
Average	1002.5	2447.3	2.441	18.0
Std. Dev.	4.047	13.880	0.005	1.026

Mix	Compr.Str (MPa)
M1	26.1
M2	17.9
M3	15.8
M4	16.7
M5	20.1
M6	18.0

Concrete Cube Results at 14 Days

	Sat. Vol. (ml)	Sat. Mass (g)	Density ((kg/m^3)	Compr.Str (MPa)
Date of Testing: 28/09/1993				
M1A	1019.6	2488.2	2.440	32.4
M1B	1020.3	2490.1	2.441	33.4
M1C	1014.0	2476.8	2.443	32.4
M1D	1012.9	2469.1	2.438	34.5
Average	1016.7	2481.1	2.440	33.2
Std. Dev.	3.283	8.572	0.002	0.867
Date of Testing: 28/09/1993				
M2A	1007.2	2454.8	2.437	22.2
M2B	1009.6	2447.6	2.424	21.6
M2C	1013.7	2473.2	2.440	22.4
M2D	1015.7	2475.9	2.438	20.9
Average	1011.6	2462.9	2.435	21.8
Std. Dev.	3.338	11.987	0.006	0.585
Date of Testing: 29/09/1993				
M3A	1013.7	2466.6	2.433	21.9
M3B	1005.3	2437.4	2.425	20.4
M3C	1007.1	2457.2	2.440	21.4
M3D	1011.6	2454.9	2.427	20.1
Average	1009.4	2454.0	2.431	21.0
Std. Dev.	3.370	10.552	0.006	0.730

	Sat. Vol. (ml)	Sat. Mass (g)	Density ((kg/m^3)	Compr.Str (MPa)
Date of Testing: 29/09/1993				
M4A	1012.9	2446.1	2.415	22.0
M4B	1017.1	2455.3	2.414	22.4
M4C	1019.3	2464.9	2.418	22.4
M4D	1014.2	2460.4	2.426	21.7
Average	1015.9	2456.7	2.418	22.1
Std. Dev.	2.494	6.987	0.005	0.295
Date of Testing: 30/09/1993				
M5A	1011.8	2446.3	2.418	23.7
M5B	1013.6	2451.6	2.419	24.7
M5C	1013.6	2449.0	2.416	25.6
M5D	999.5	2424.1	2.425	26.0
Average	1009.6	2442.8	2.419	25.0
Std. Dev.	5.892	10.929	0.003	0.886
Date of Testing: 30/09/1993				
M6A	1006.3	2463.4	2.448	23.7
M6B	1004.2	2456.7	2.446	22.2
M6C	998.2	2438.4	2.443	22.3
M6D	1010.0	2469.0	2.445	22.0
Average	1004.7	2456.9	2.445	22.6
Std. Dev.	4.276	11.521	0.002	0.673

Mix	Compr.Str (MPa)
M1	33.2
M2	21.8
M3	21.0
M4	22.1
M5	25.0
M6	22.6

Concrete Cube Results at 21 Days

	Sat. Vol. (ml)	Sat. Mass (g)	Density ((kg/m^3)	Compr.Str (MPa)
Date of Testing: 05/10/1993				
M1A	1017.6	2491.2	2.448	36.6
M1B	1020.7	2491.3	2.441	36.1
M1C	1013.0	2475.5	2.444	37.1
M1D	1012.0	2464.7	2.435	37.4
Average	1015.8	2480.7	2.442	36.8
Std. Dev.	3.519	11.243	0.005	0.495
Date of Testing: 05/10/1993				
M2A	1014.1	2469.8	2.435	26.6
M2B	1007.3	2457.6	2.440	26.0
M2C	1013.6	2472.9	2.440	26.3
M2D	1009.3	2458.5	2.436	26.4
Average	1011.1	2464.7	2.438	26.3
Std. Dev.	2.869	6.747	0.002	0.217
Date of Testing: 06/10/1993				
M3A	999.3	2424.3	2.426	25.5
M3B	1013.3	2467.3	2.435	25.0
M3C	1014.8	2477.2	2.441	24.9
M3D	1008.0	2459.9	2.440	25.1
Average	1008.9	2457.2	2.436	25.1
Std. Dev.	6.065	19.948	0.006	0.228

	Sat. Vol. (ml)	Sat. Mass (g)	Density ((kg/m^3)	Compr.Str (MPa)
Date of Testing: 06/10/1993				
M4A	1026.1	2498.7	2.435	27.7
M4B	1008.0	2441.1	2.422	26.7
M4C	1022.7	2474.2	2.419	23.4
M4D	1008.8	2444.4	2.423	25.0
Average	1016.4	2464.6	2.425	25.7
Std. Dev.	8.095	23.533	0.006	1.642
Date of Testing: 07/10/1993				
M5A	1009.6	2433.2	2.410	29.3
M5B	1014.6	2447.3	2.412	25.9
M5C	1012.3	2439.0	2.409	30.3
M5D	1010.4	2413.9	2.389	27.8
Average	1011.7	2433.4	2.405	28.3
Std. Dev.	1.928	12.297	0.009	1.659
Date of Testing: 07/10/1993				
M6A	1004.0	2457.1	2.447	26.3
M6B	1013.8	2475.8	2.442	25.7
M6C	1005.3	2457.3	2.444	24.4
M6D	1002.9	2453.4	2.446	25.7
Average	1006.5	2460.9	2.445	25.5
Std. Dev.	4.299	8.742	0.002	0.694

Mix	Compr.Str (MPa)
M1	36.8
M2	26.3
M3	25.1
M4	25.7
M5	28.3
M6	25.5

Concrete Cube Results at 28 Days

	Sat. Vol. (ml)	Sat. Mass (g)	Density ((kg/m^3)	Compr.Str (MPa)
Date of Testing: 12/10/1993				
M1A	1019.6	2483.8	2.436	38.4
M1B	1005.2	2448.2	2.436	39.8
M1C	1008.3	2460.8	2.441	38.7
M1D	1001.3	2438.4	2.435	39.1
Average	1008.6	2457.8	2.437	39.0
Std. Dev.	6.818	16.982	0.002	0.524
Date of Testing: 12/10/1993				
M2A	1020.1	2489.2	2.440	28.5
M2B	1017.8	2496.5	2.453	27.5
M2C	1008.3	2460.8	2.441	28.4
M2D	1001.3	2438.4	2.435	28.6
Average	1011.9	2471.2	2.442	28.3
Std. Dev.	7.539	23.174	0.006	0.439
Date of Testing: 13/10/1993				
M3A	1010.4	2461.5	2.436	27.3
M3B	1006.4	2450.4	2.435	27.2
M3C	1013.8	2468.0	2.434	25.2
M3D	1008.8	2459.5	2.438	27.5
Average	1009.9	2459.9	2.436	26.8
Std. Dev.	2.688	6.296	0.001	0.930

	Sat. Vol. (ml)	Sat. Mass (g)	Density ((kg/m^3)	Compr.Str (MPa)
Date of Testing: 13/10/1993				
M4A	1014.8	2459.9	2.424	29.7
M4B	1022.4	2470.9	2.417	27.2
M4C	1022.2	2478.3	2.424	27.2
M4D	1000.8	2428.7	2.427	29.3
Average	1015.1	2459.5	2.423	28.4
Std. Dev.	8.779	18.922	0.004	1.159
Date of Testing: 14/10/1993				
M5A	1014.6	2461.1	2.426	30.7
M5B	1020.3	2453.0	2.404	31.1
M5C	1014.3	2439.9	2.406	30.1
M5D	1024.0	2484.5	2.426	30.9
Average	1018.3	2459.6	2.415	30.7
Std. Dev.	4.068	16.232	0.011	0.374
Date of Testing: 14/10/1993				
M6A	1003.3	2461.7	2.454	29.2
M6B	1009.2	2465.8	2.443	26.4
M6C	1008.5	2465.7	2.445	27.4
M6D	1002.1	2449.5	2.444	29.2
Average	1005.8	2460.7	2.447	28.1
Std. Dev.	3.114	6.660	0.004	1.203

Mix	Compr.Str (MPa)
M1	39.0
M2	28.3
M3	26.8
M4	28.4
M5	30.7
M6	28.1

APPENDIX C

- DTG plots for the Van Eck(-63) paste over the complete curing period, analyzed in a normal air atmosphere. C41

DTA Thermogram after 3 Days

Dry Nitrogen Atmosphere

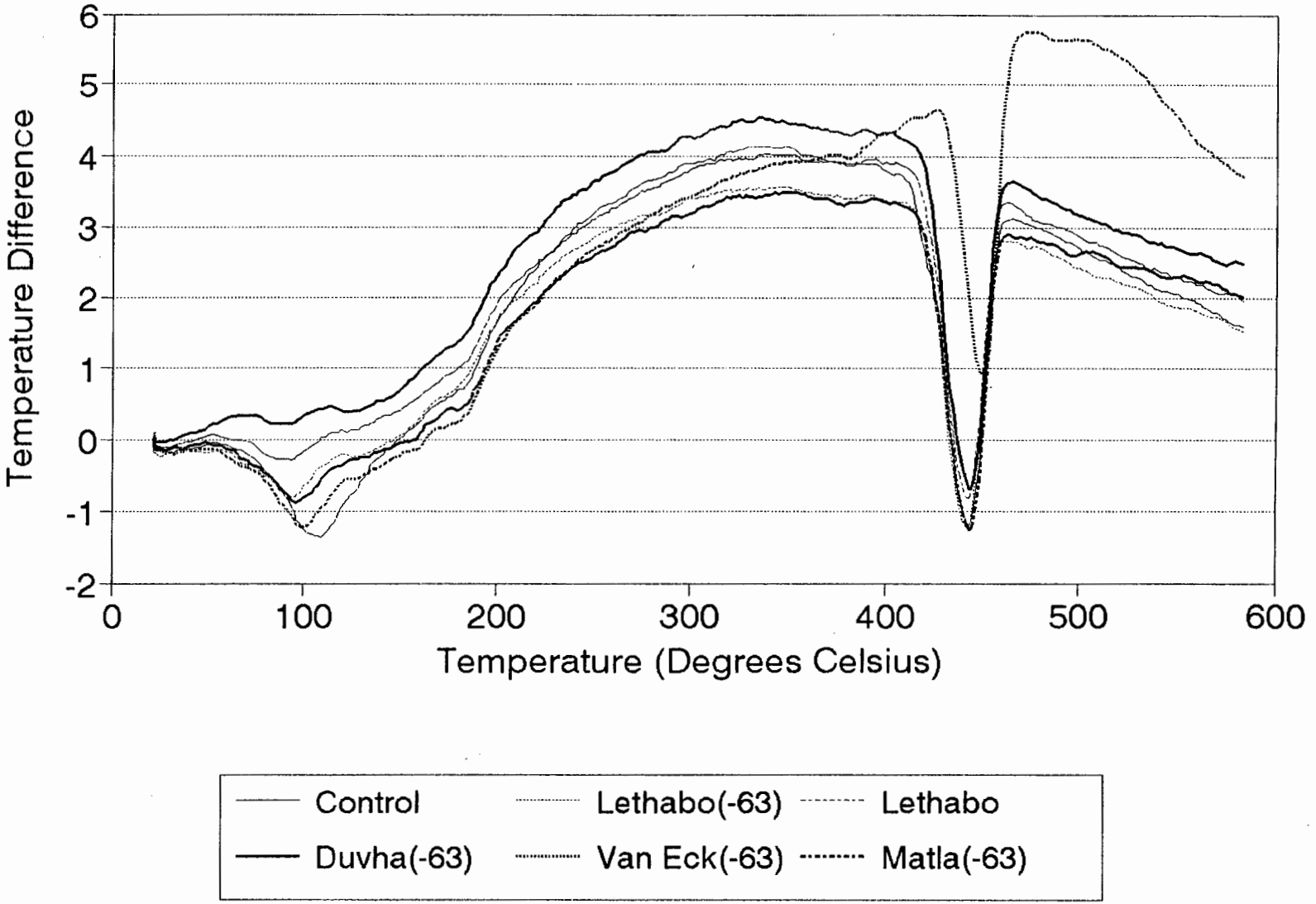

DTA Thermogram after 7 Days

Dry Nitrogen Atmosphere

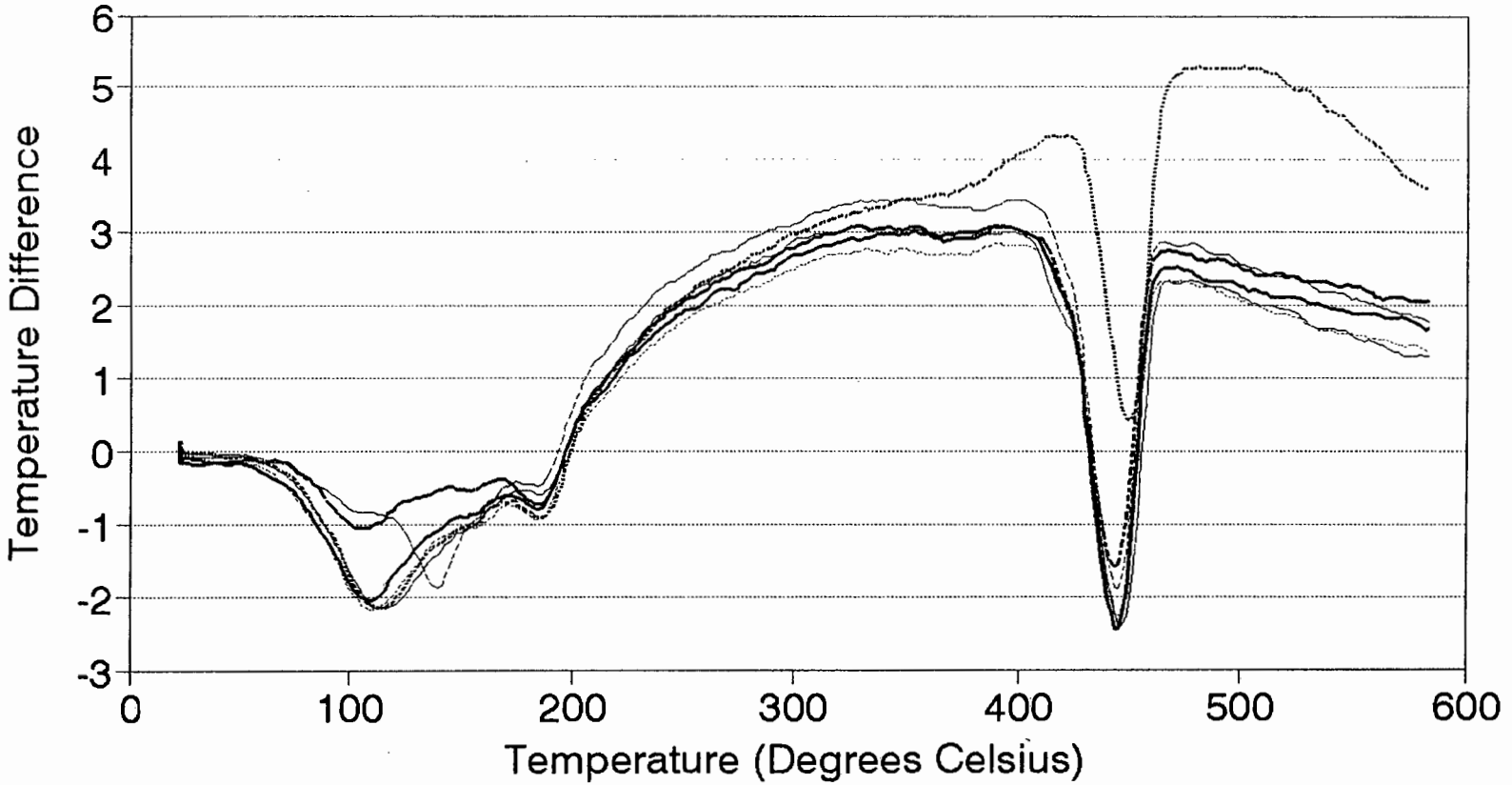

DTA Themogram after 14 Days

Dry Nitrogen Atmosphere

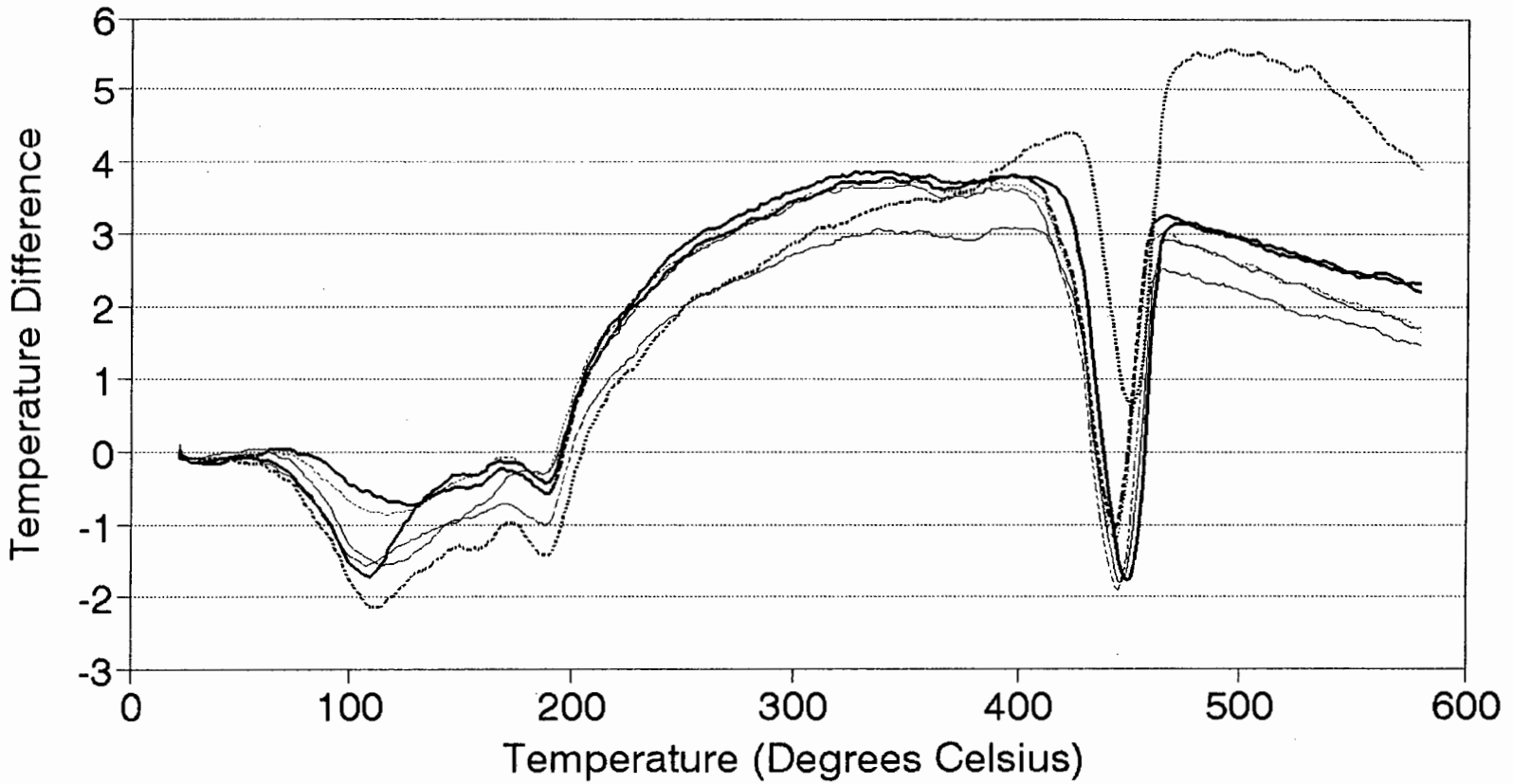

DTA Thermogram after 21 Days

Dry Nitrogen Atmosphere

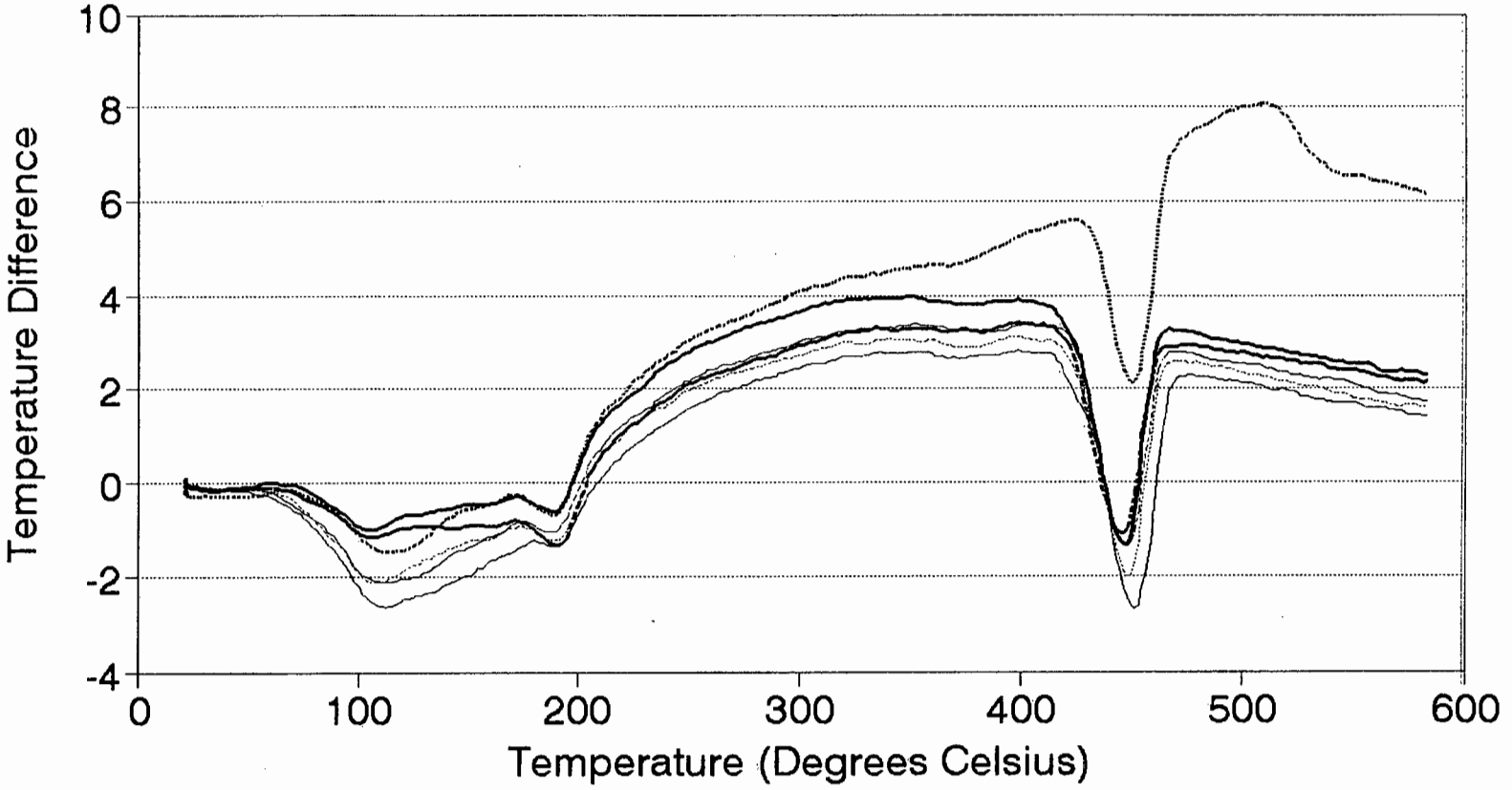

DTA Thermogram after 28 Days

Dry Nitrogen Atmosphere

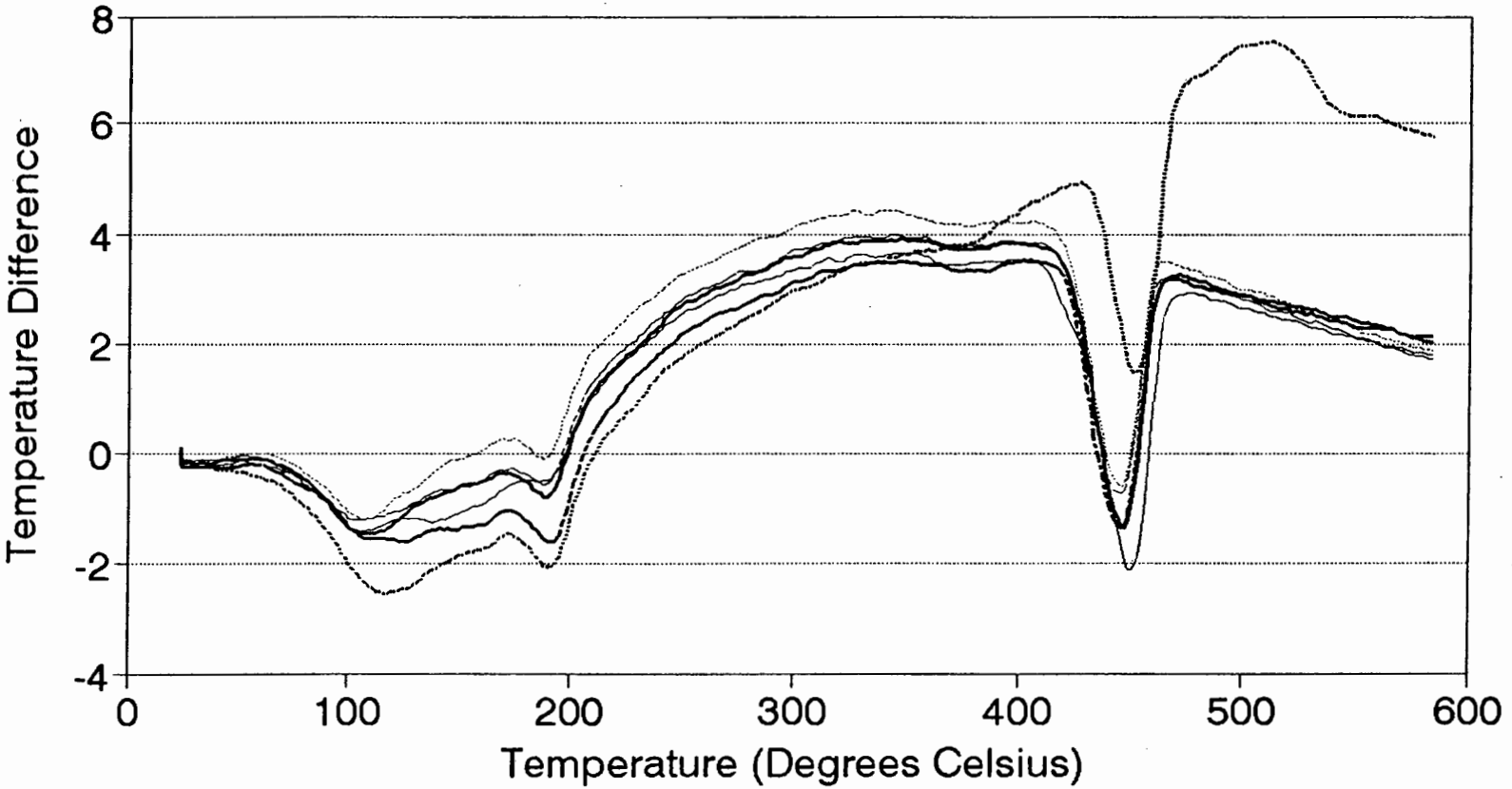

DTA Thermogram after 3 Days

Van Eck(-63) Paste in Normal Air

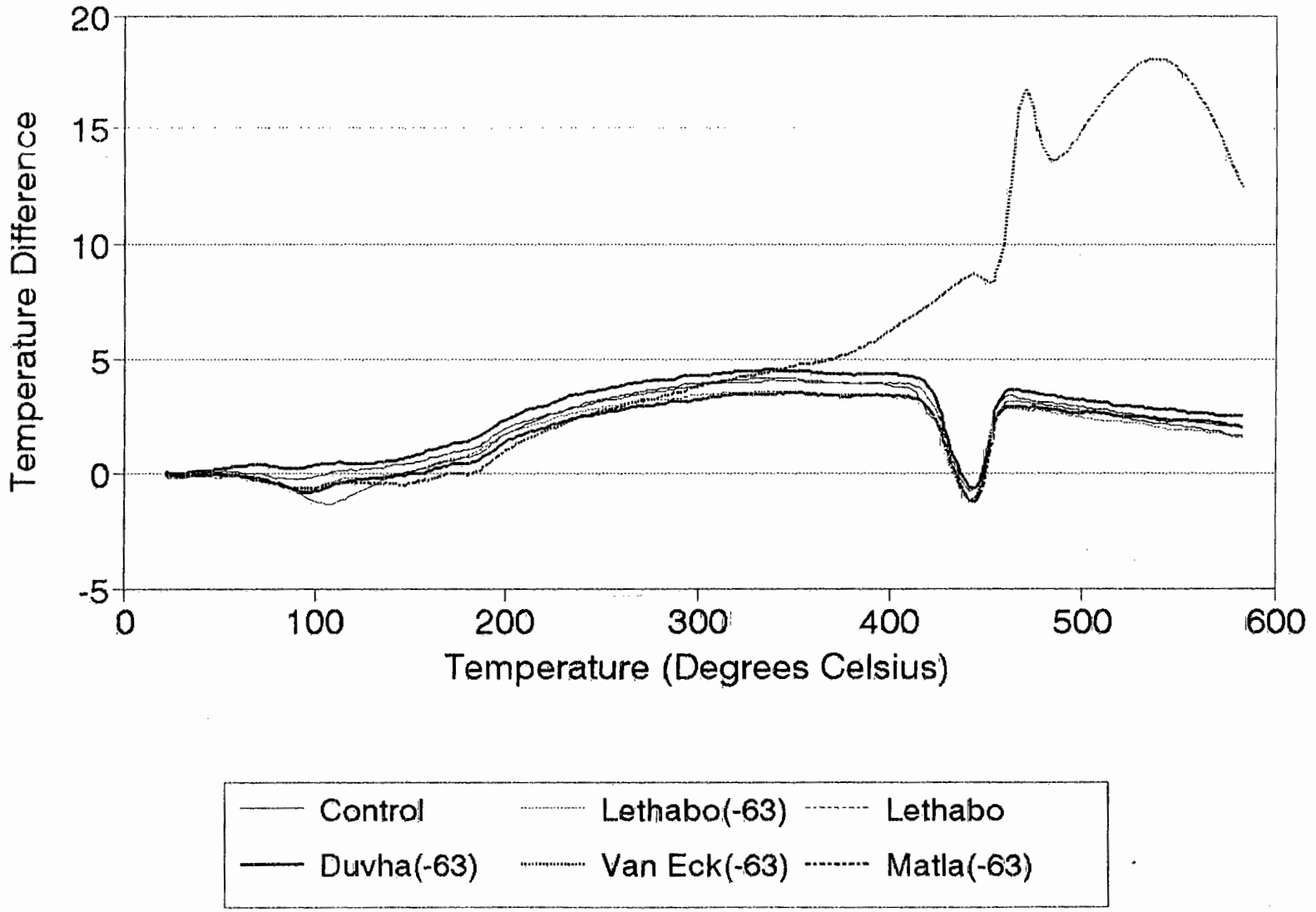

DTA Thermogram after 7 Days

Van Eck(-63) Paste in Normal Air

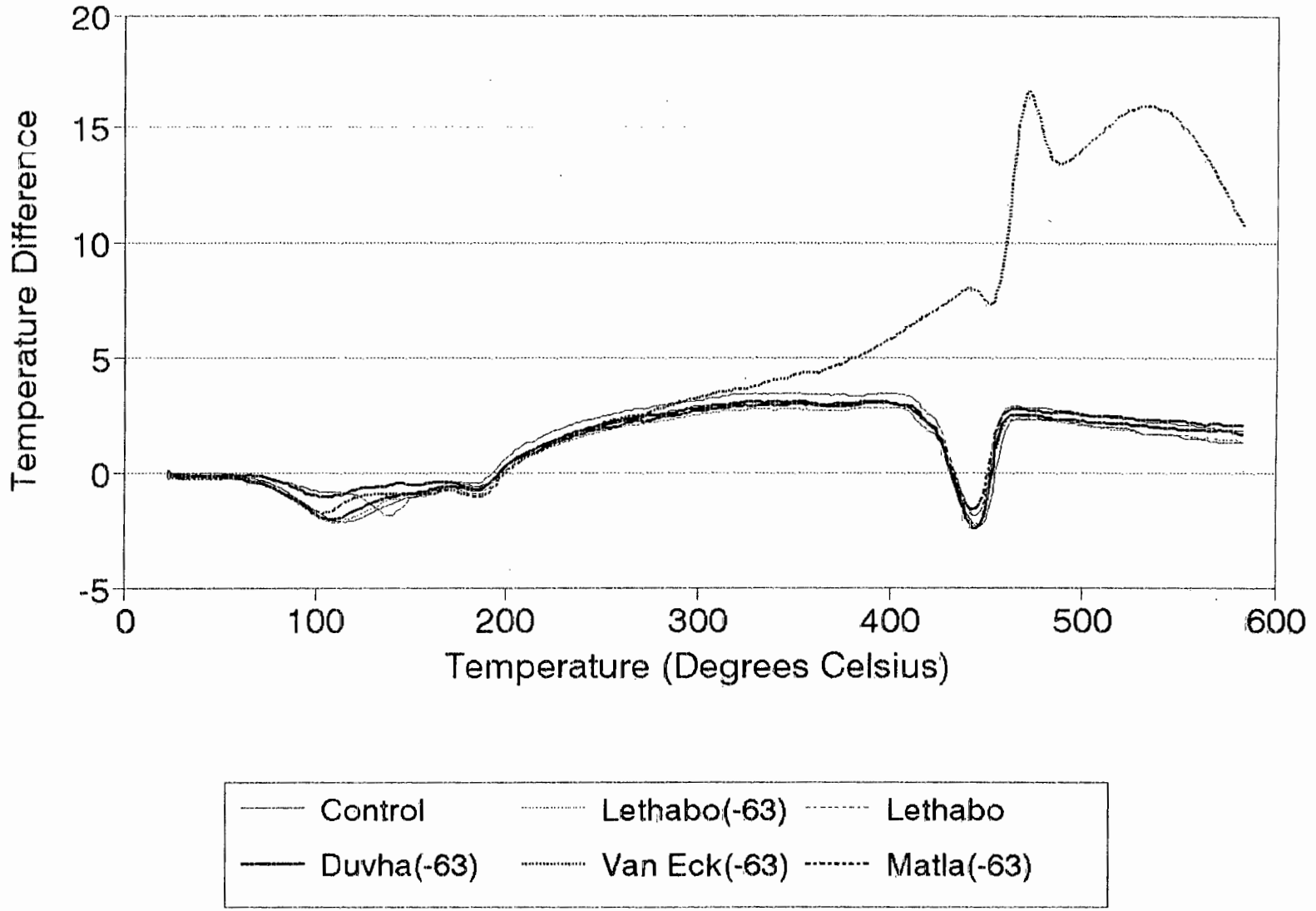

DTA Thermogram after 14 Days

Van Eck(-63) Paste in Normal Air

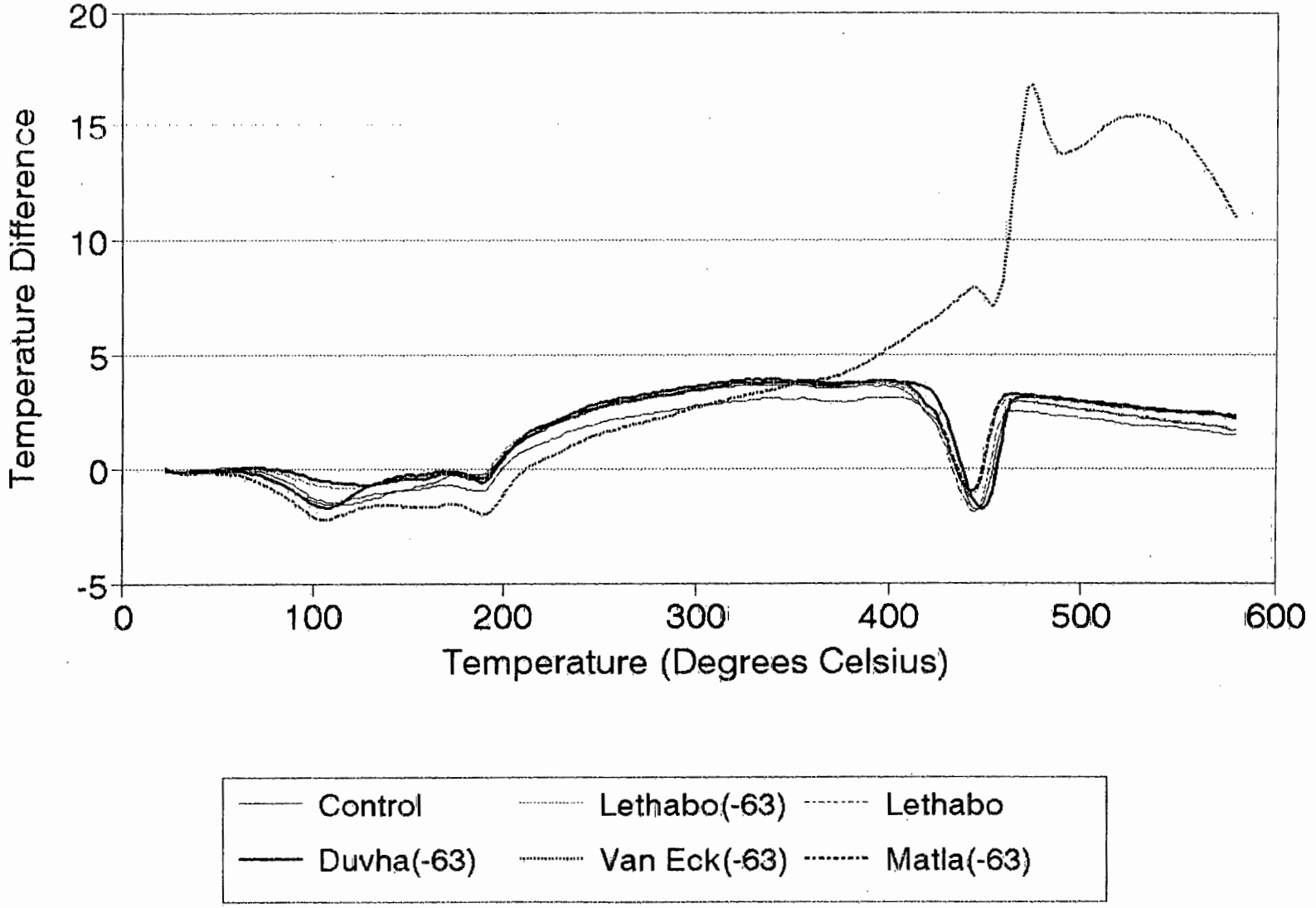

DTA Thermogram after 21 Days

Van Eck(-63) Paste in Normal Air

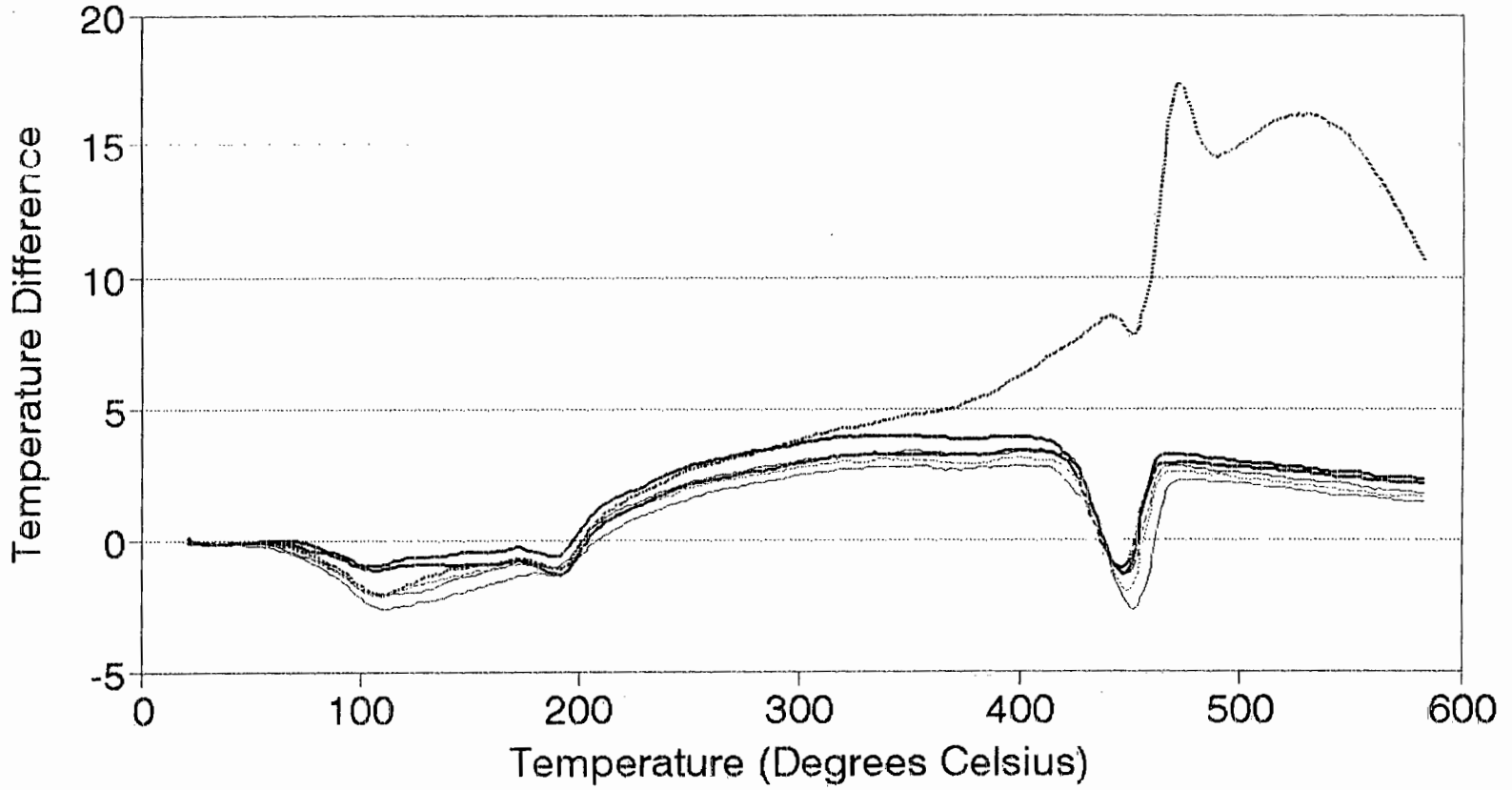

Control
Lethabo(-63)
Lethabo
Duvha(-63)
Van Eck(-630
Matla(-63)

DTA Thermogram after 28 Days

Van Eck(-63) Paste in Normal Air

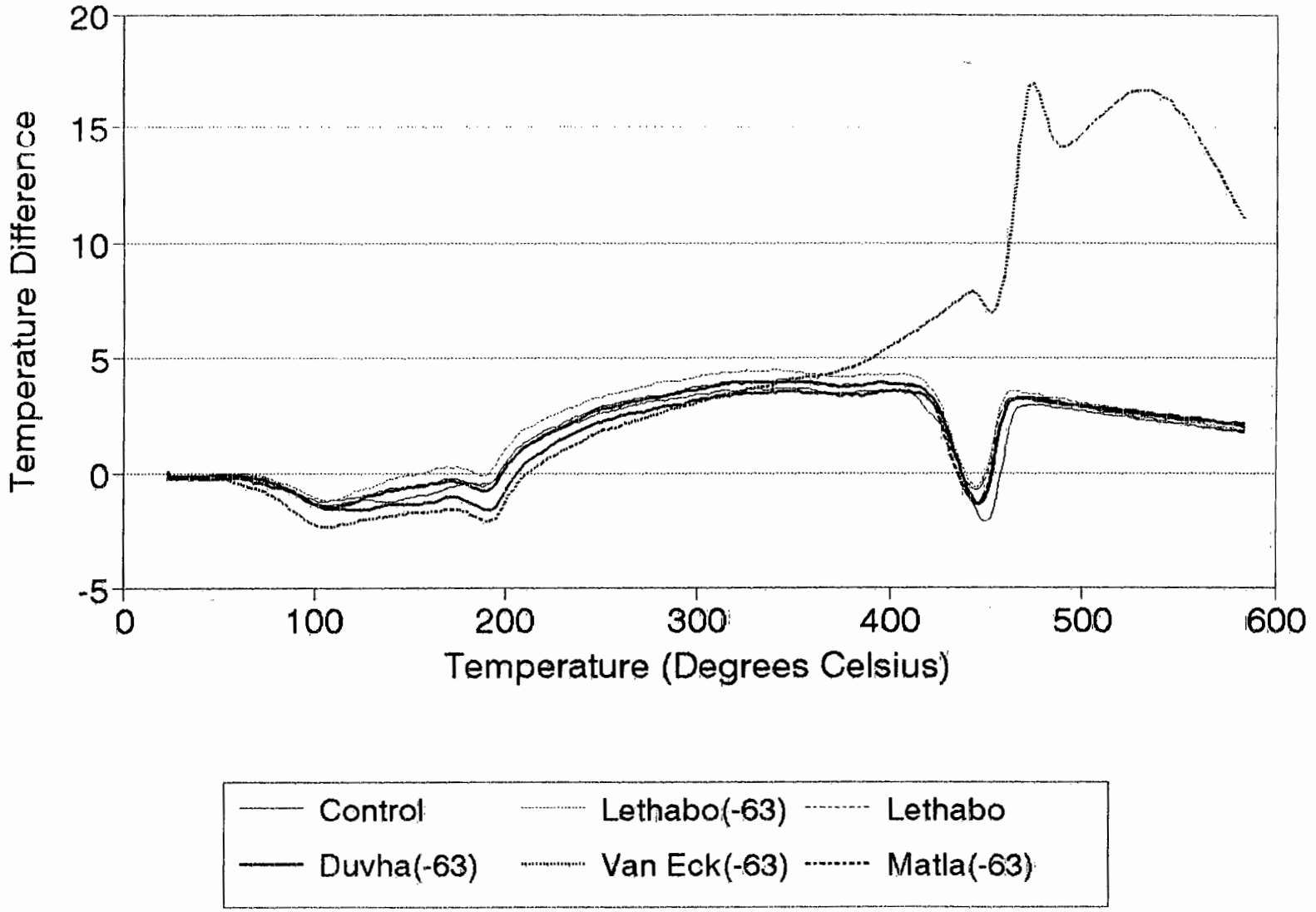

DTA Thermogram for the Control Paste

Dry Nitrogen Atmosphere

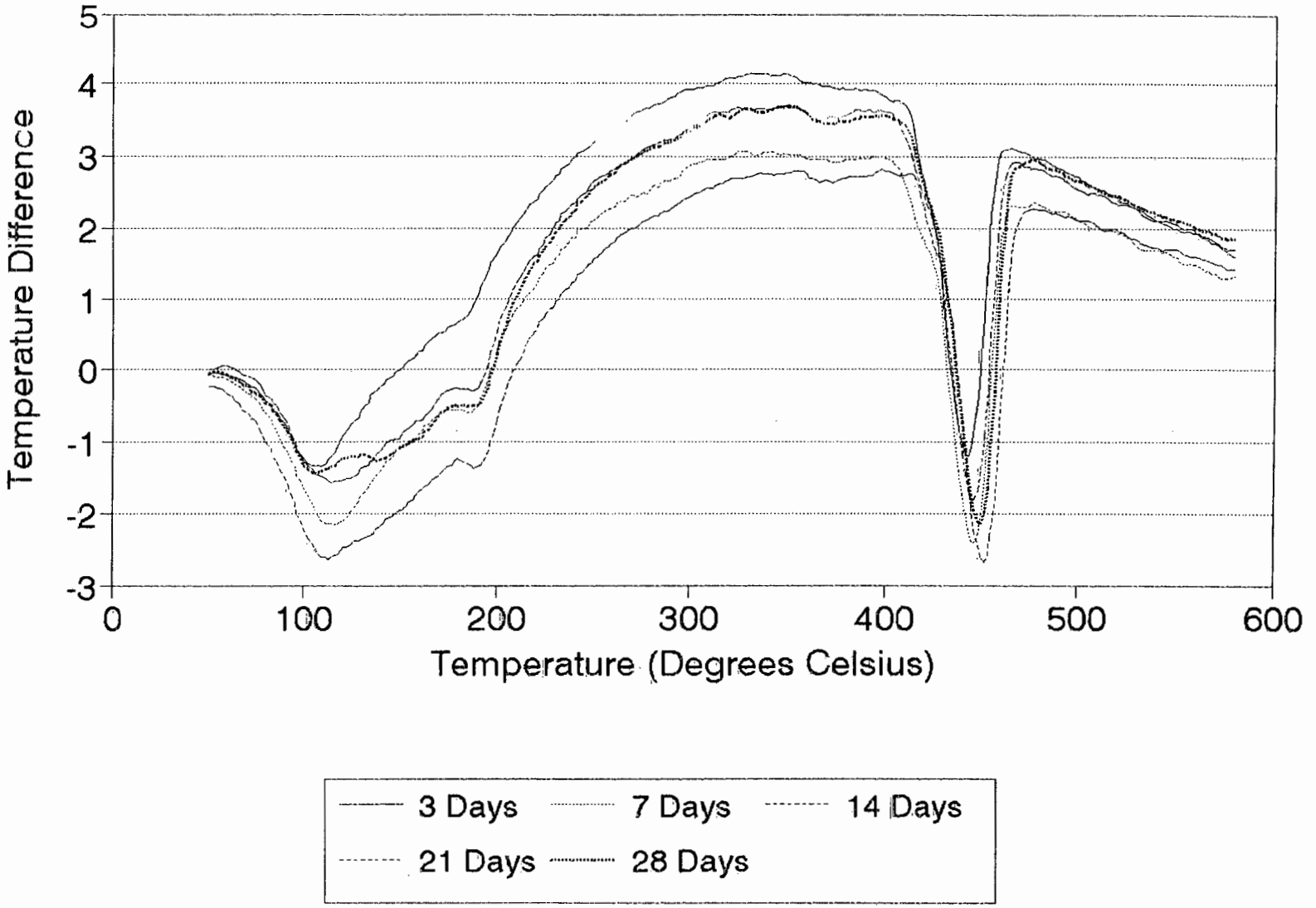

DTA Thermogram - Lethabo(-63) Paste

Dry Nitrogen Atmosphere

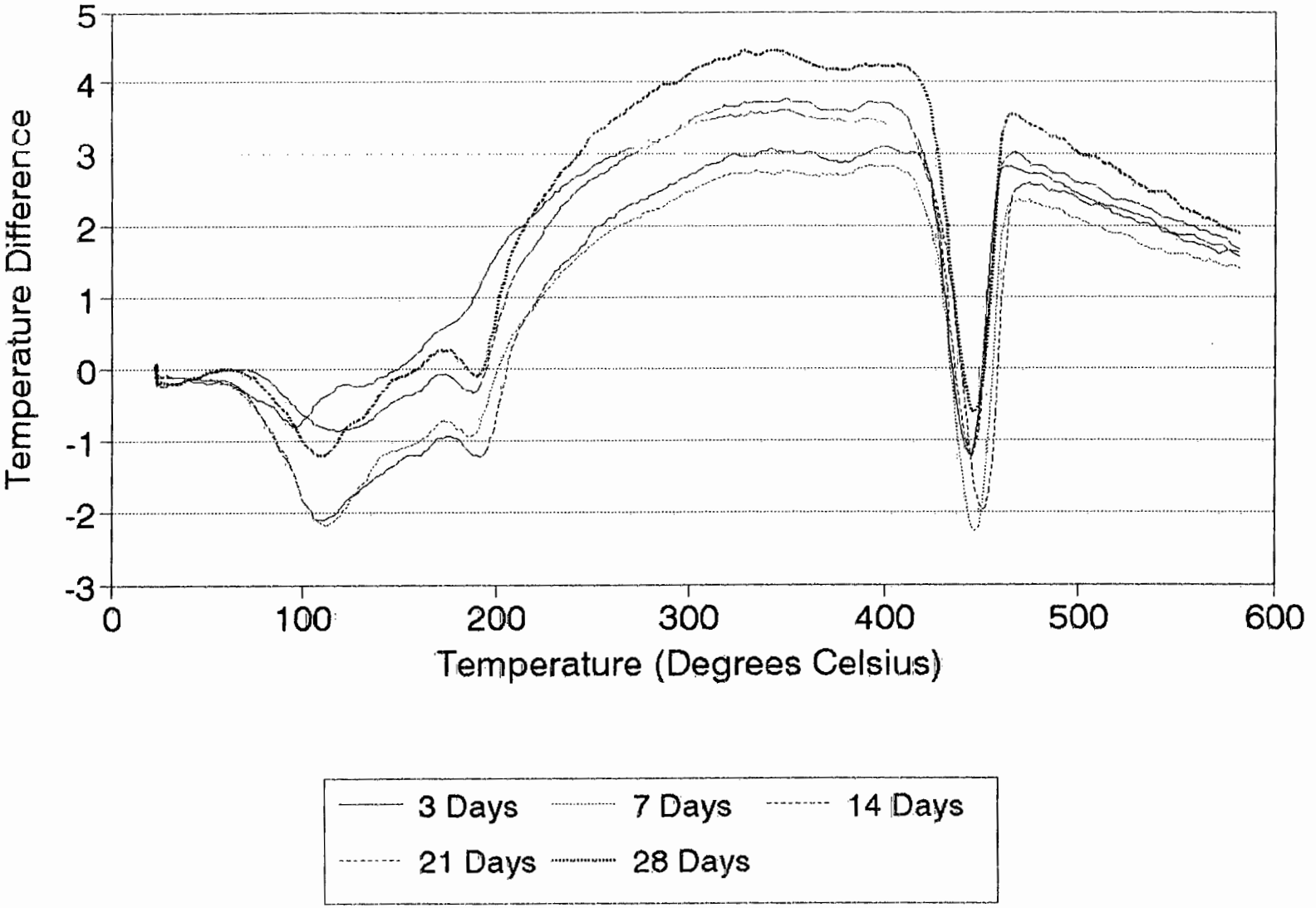

DTA Thermogram - Lethabo Paste

Dry Nitrogen Atmosphere

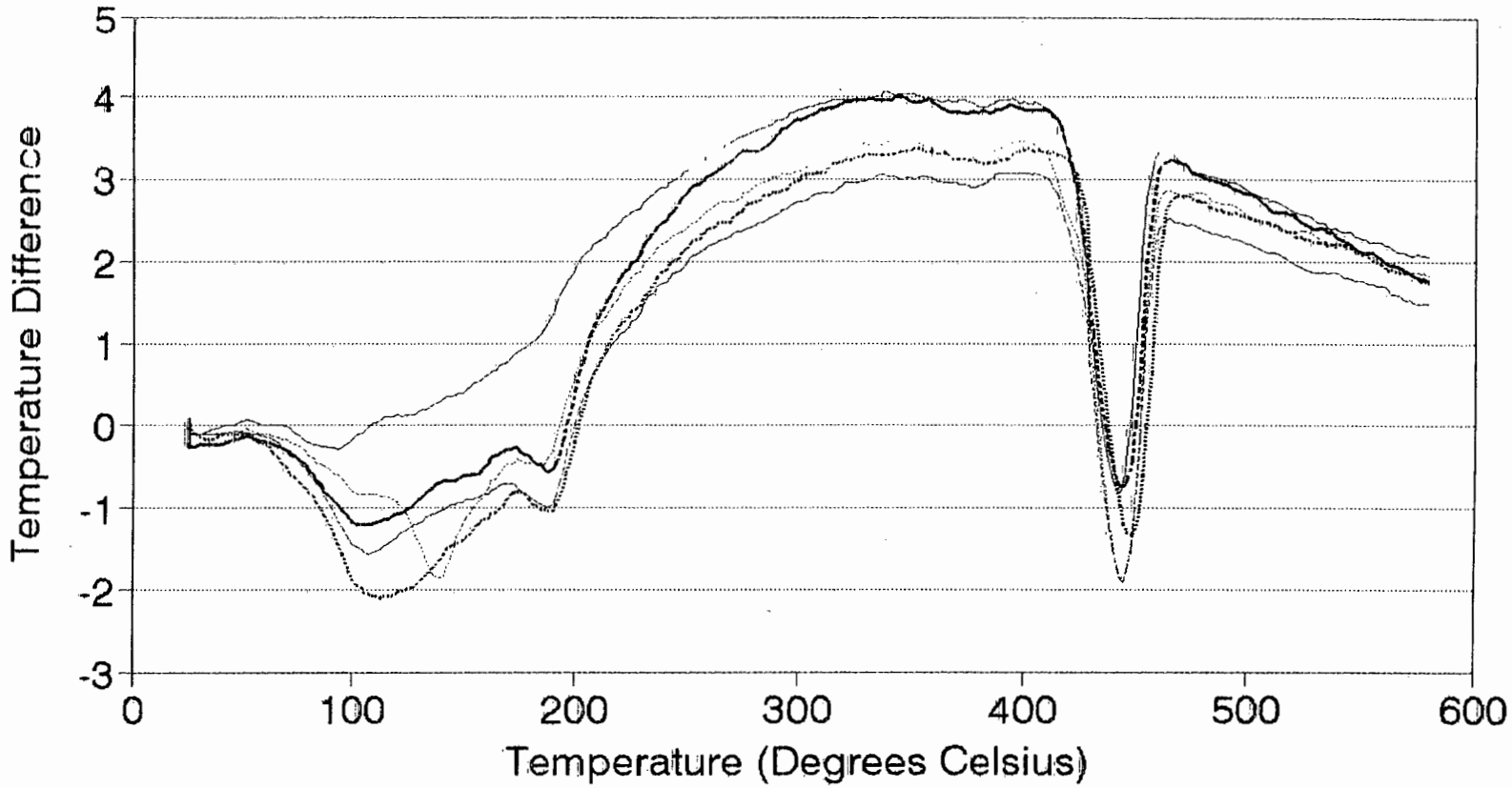

DTA Thermogram - Duvha(-63) Paste

Dry Nitrogen Atmosphere

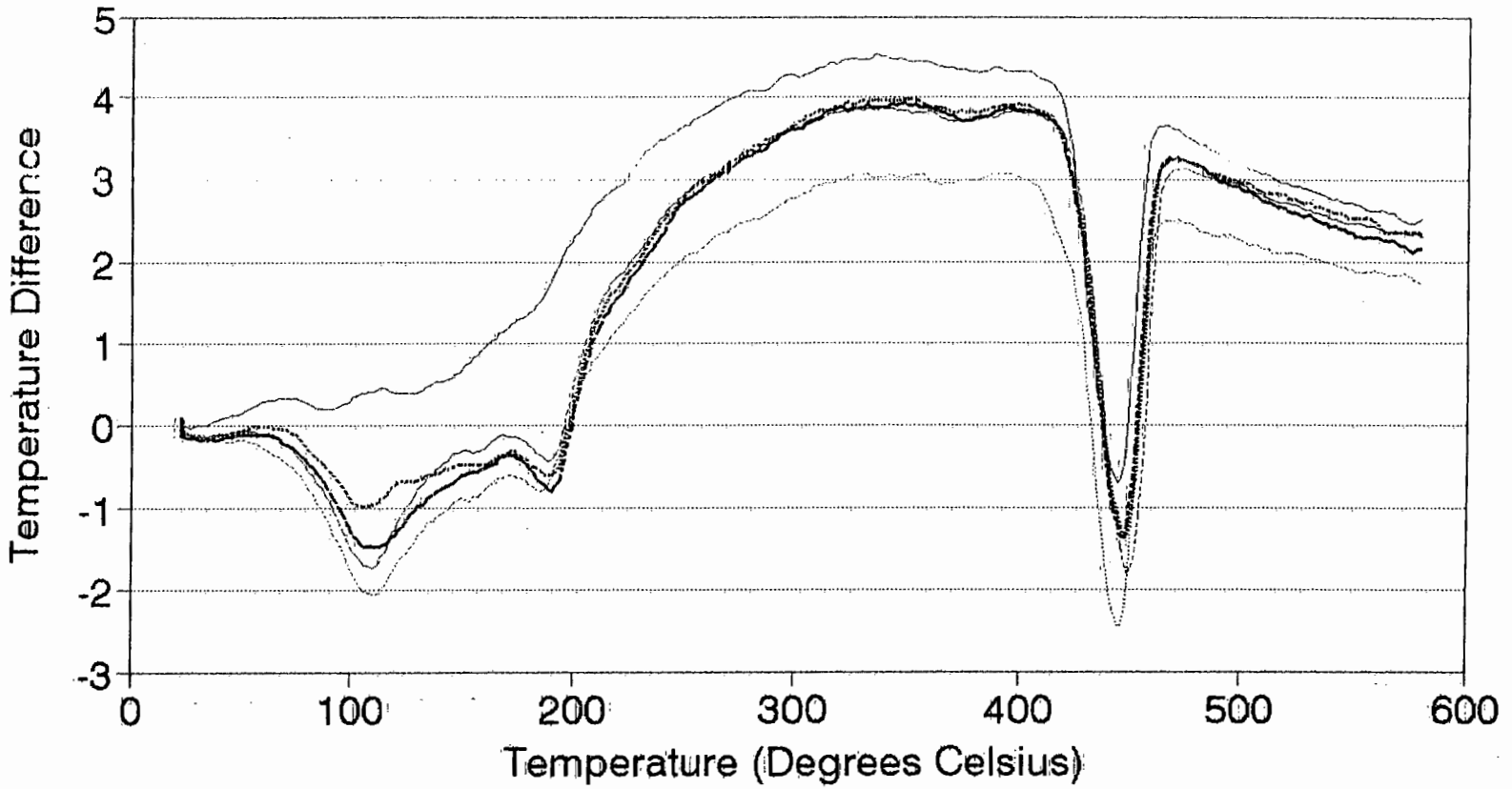

3 DAYS 7 DAYS 14 DAYS
21 DAYS 28 DAYS

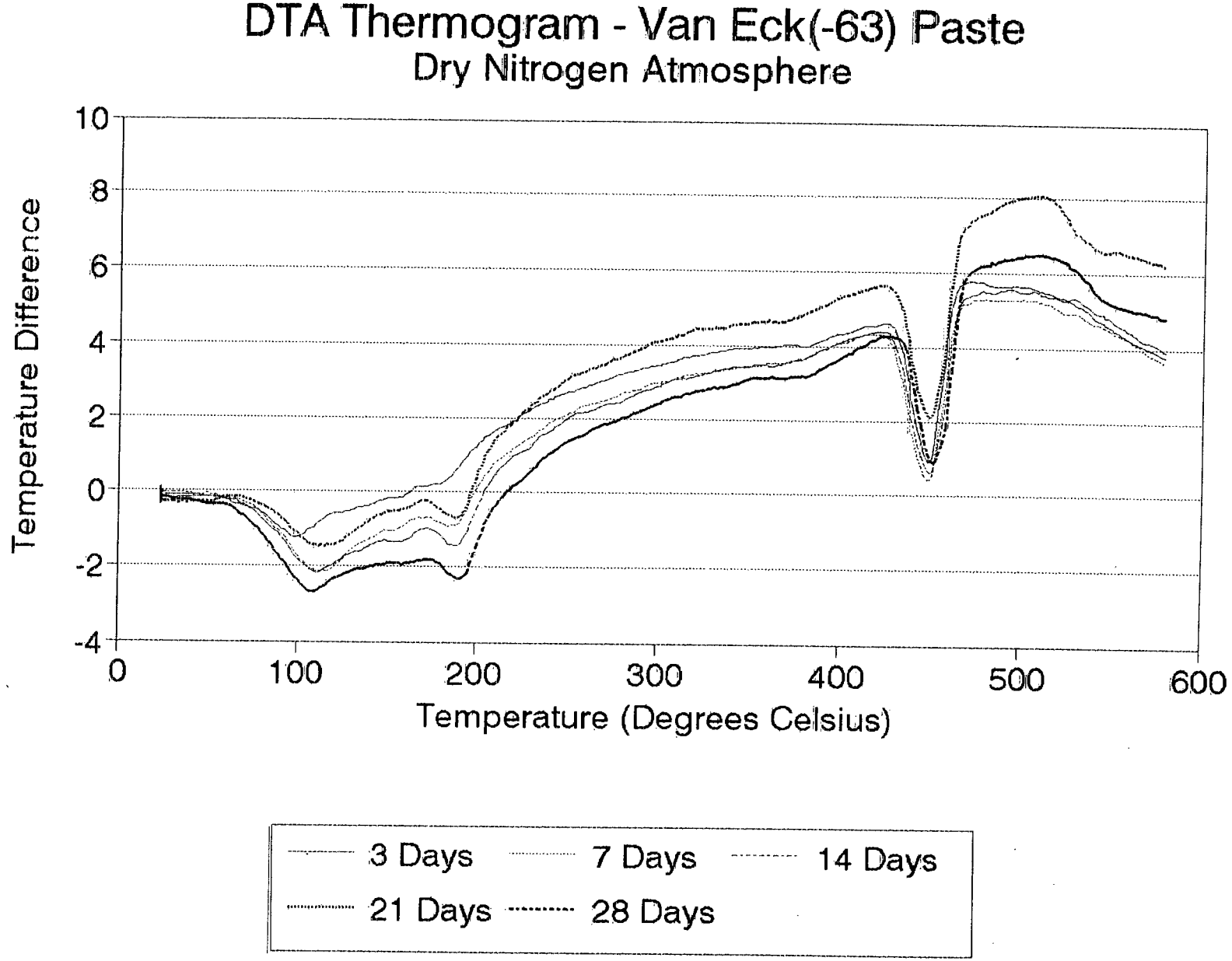
DTA Thermogram - Van Eck(-63) Paste
Dry Nitrogen Atmosphere
Temperature Difference
10
8
6
4
2
0
-2
-4
0
100
200
300
400
500
600
Temperature (Degrees Celsius)
3 Days
7 Days
14 Days
21 Days
28 Days

DTA Thermogram - Matla(-63) Paste

Dry Nitrogen Atmosphere

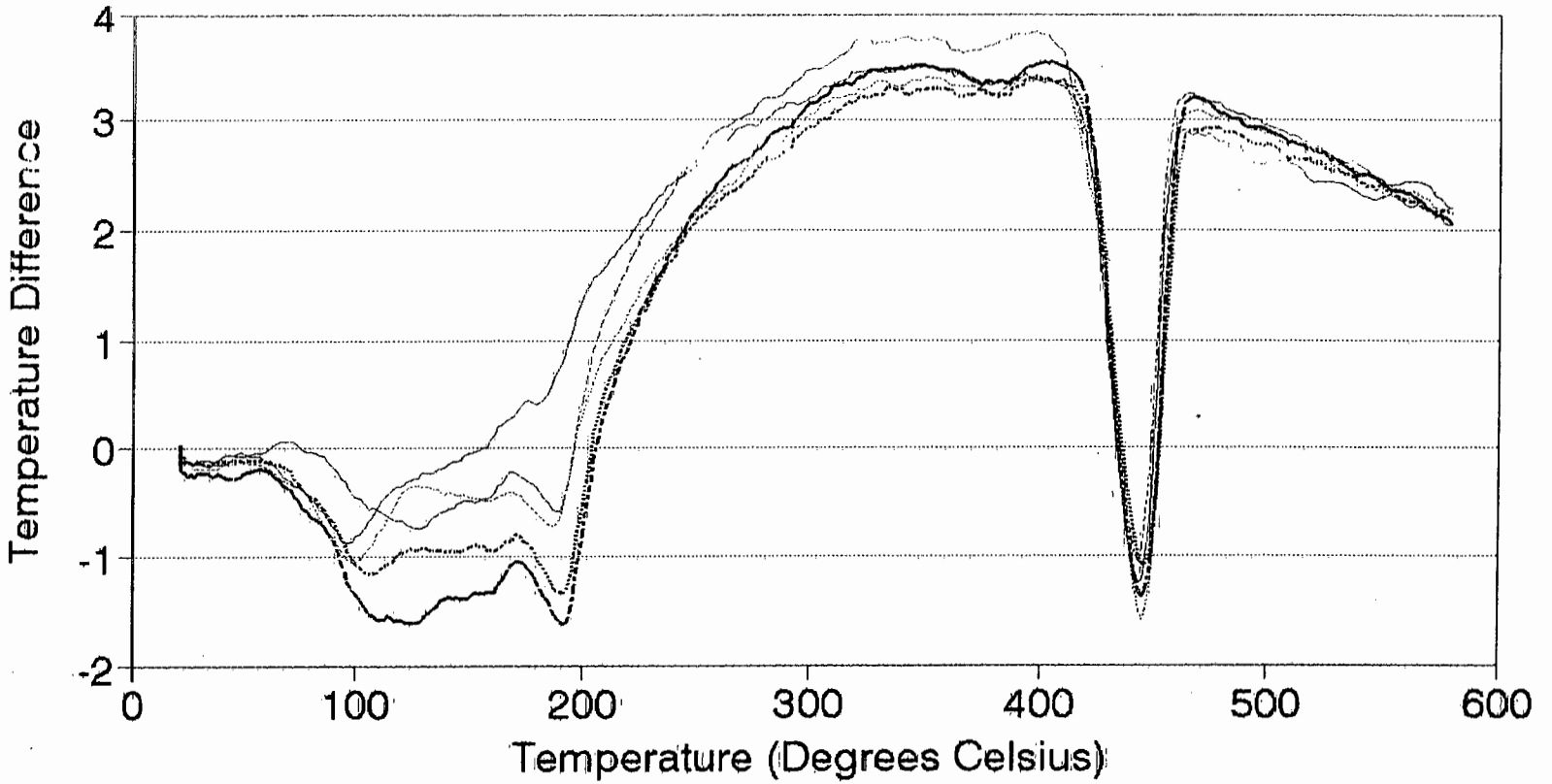

DTA Thermogram - Van Eck(-63) Paste

Normal Air Atmosphere

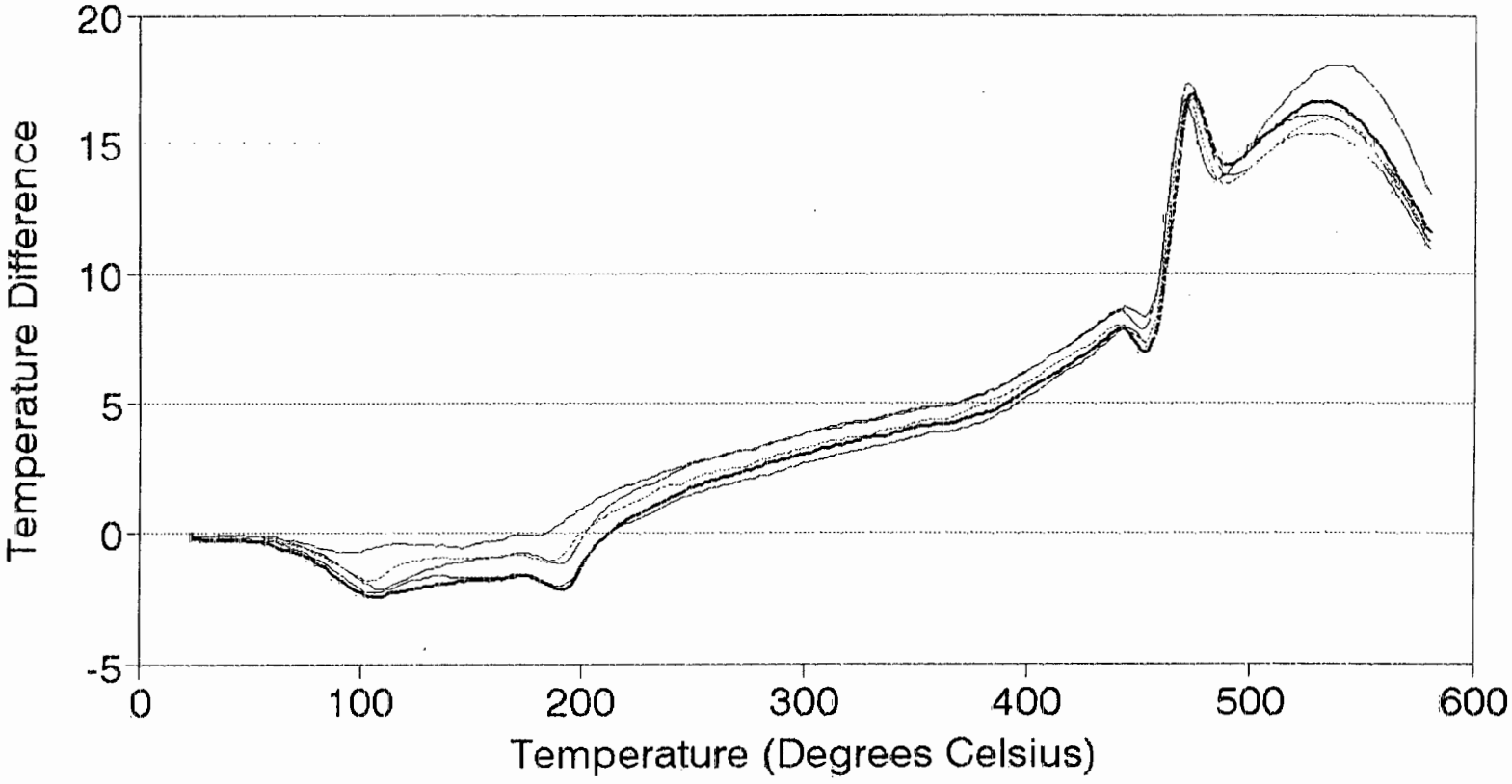

3 Days 7 Days 14 Days
21 Days 28 Days

TGA Plot after 3 Days
Dry Nitrogen Atmosphere

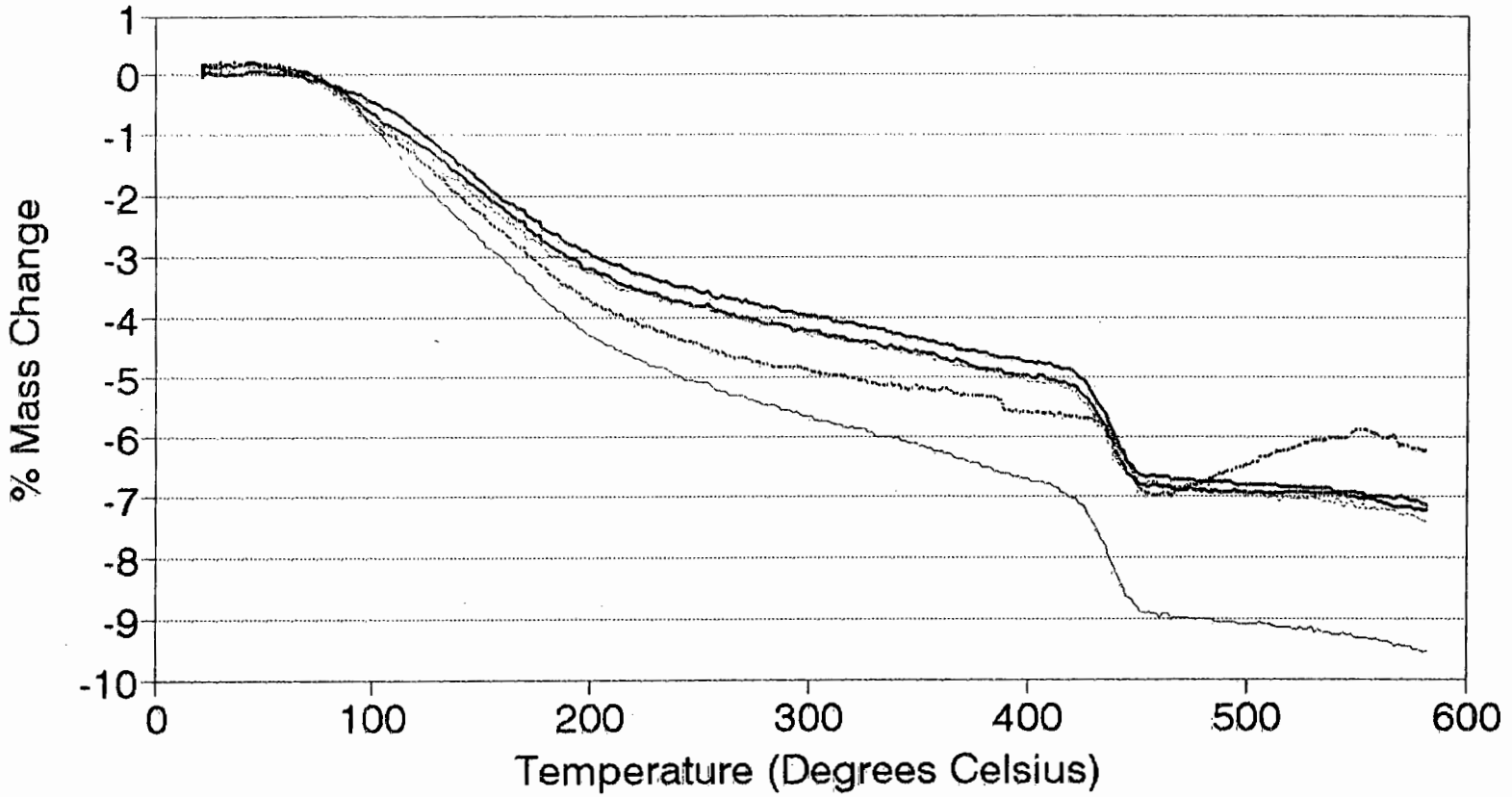

TGA Plot after 7 Days
Dry Nitrogen Atmosphere

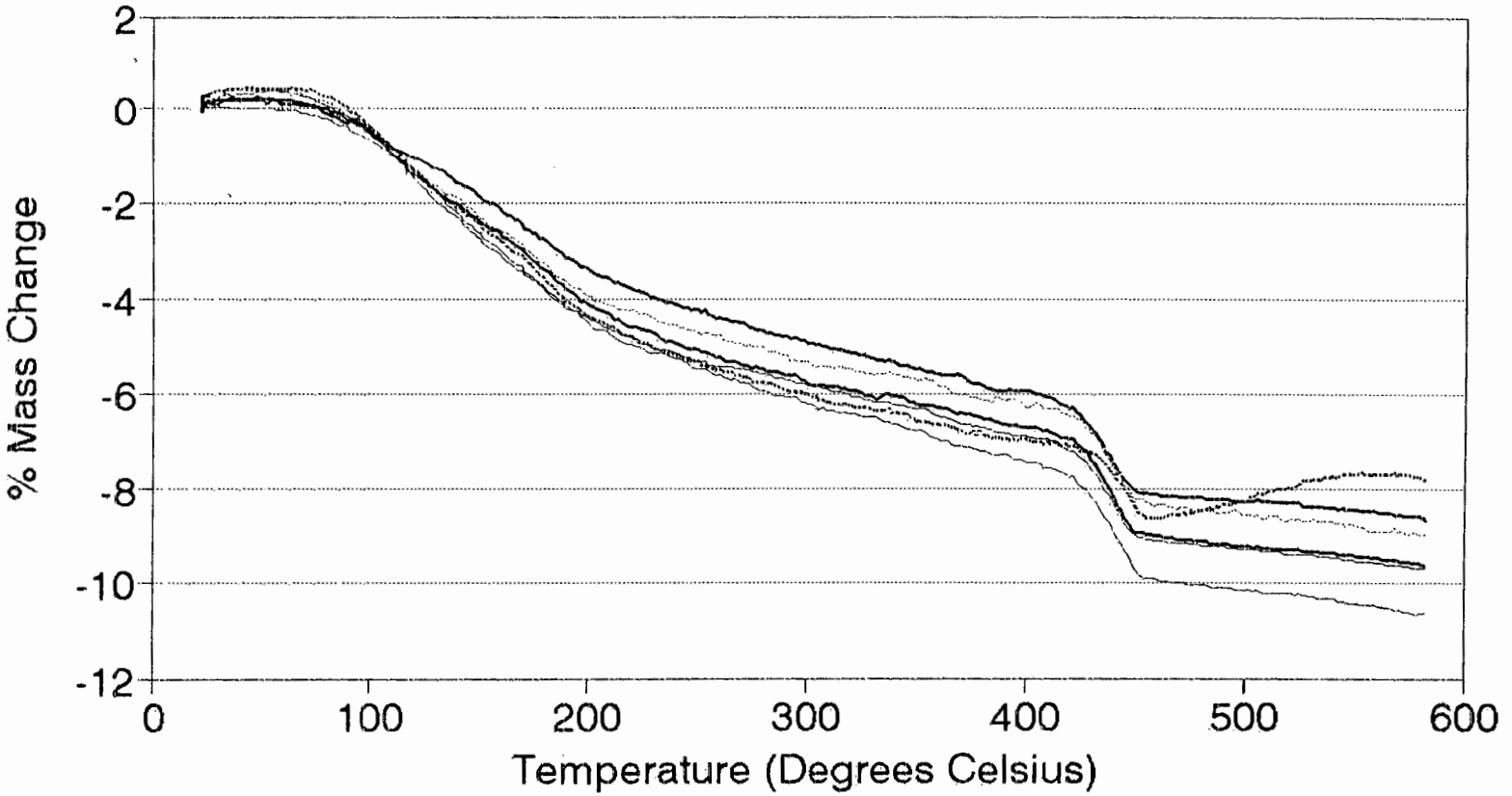

TGA Plot after 14 Days
Dry Nitrogen Atmosphere

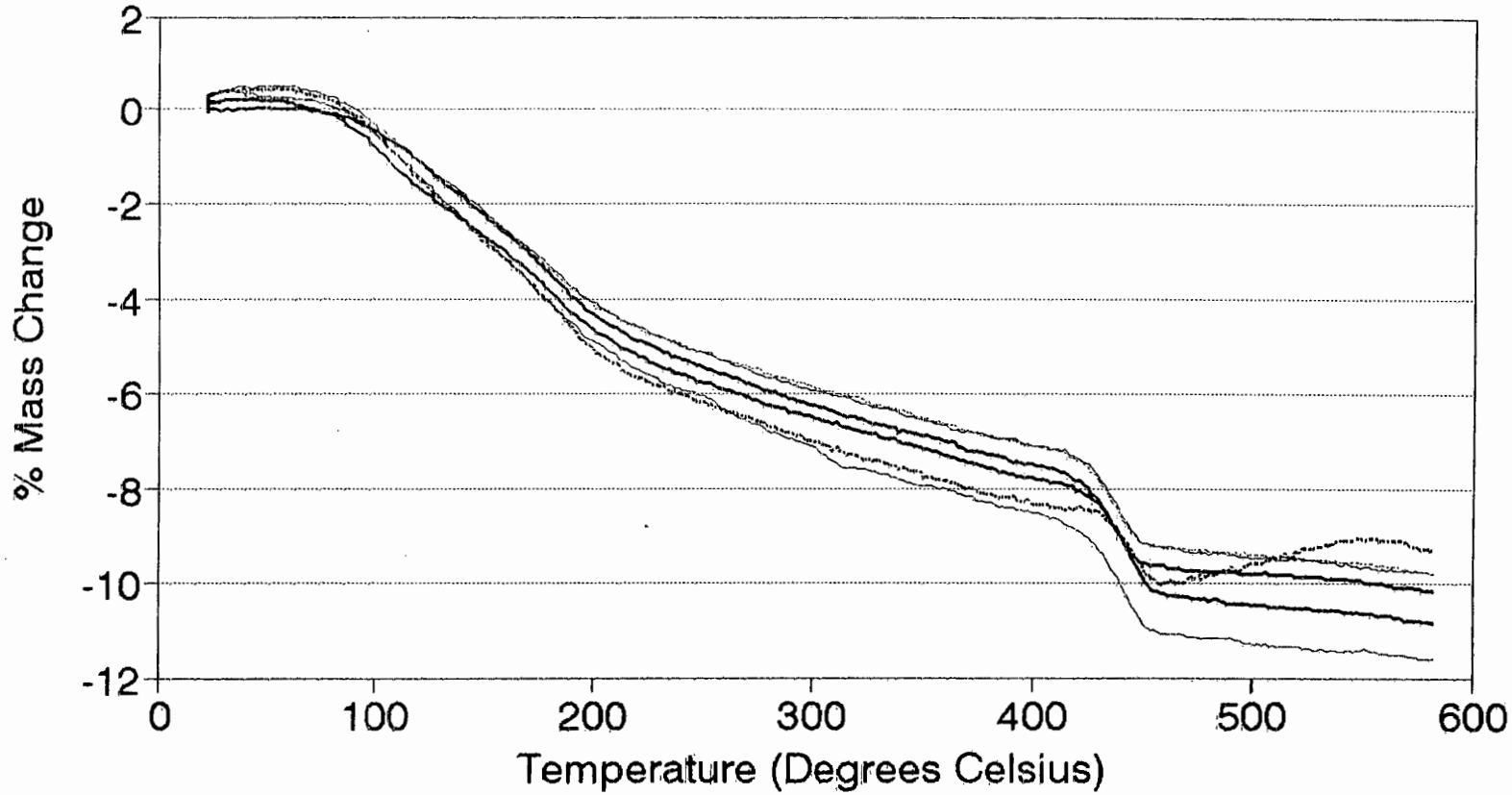

TGA Plot after 21 Days
Dry Nitrogen Atmosphere

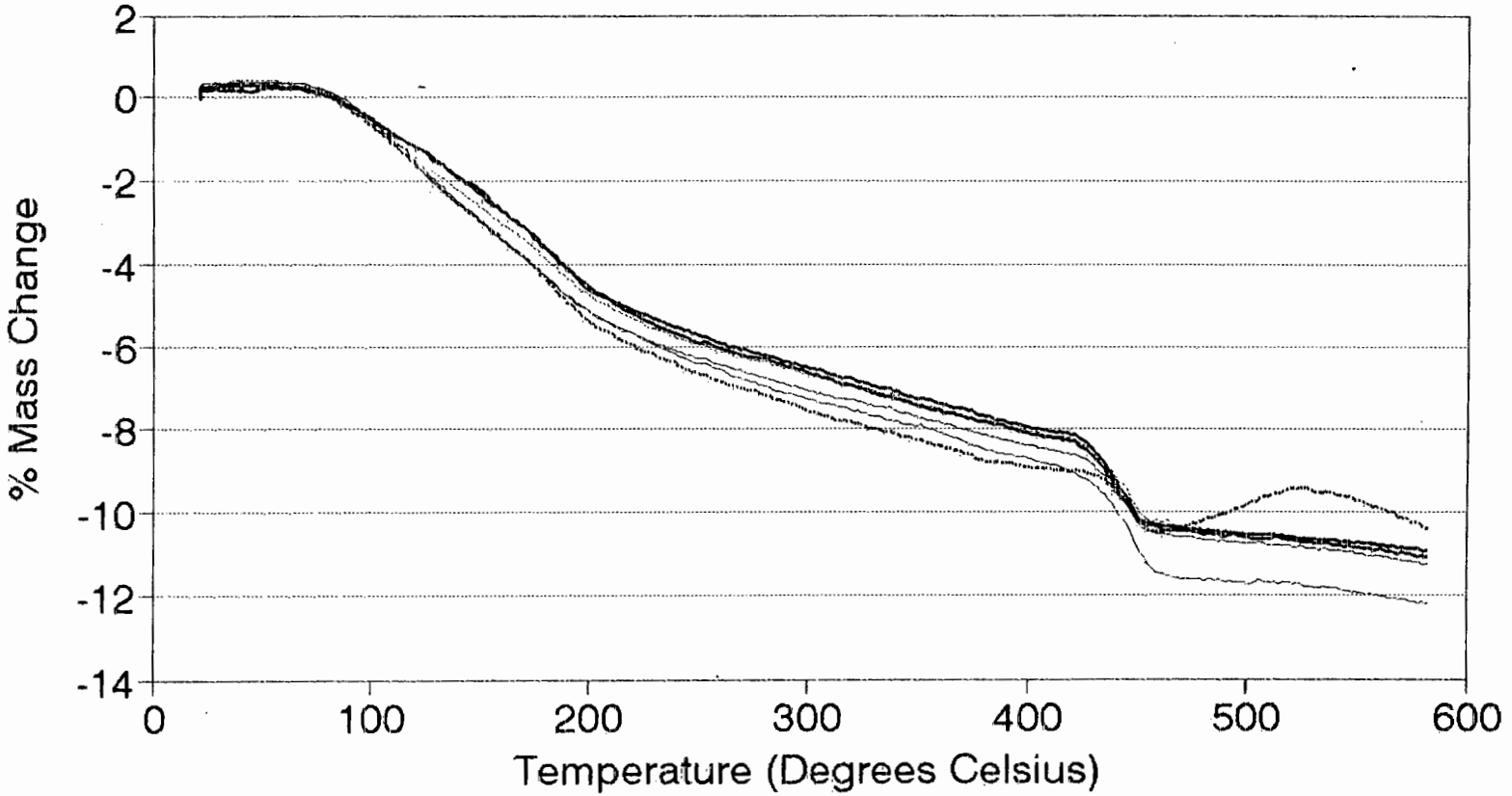

TGA Plot after 28 Days
Dry Nitrogen Atmosphere

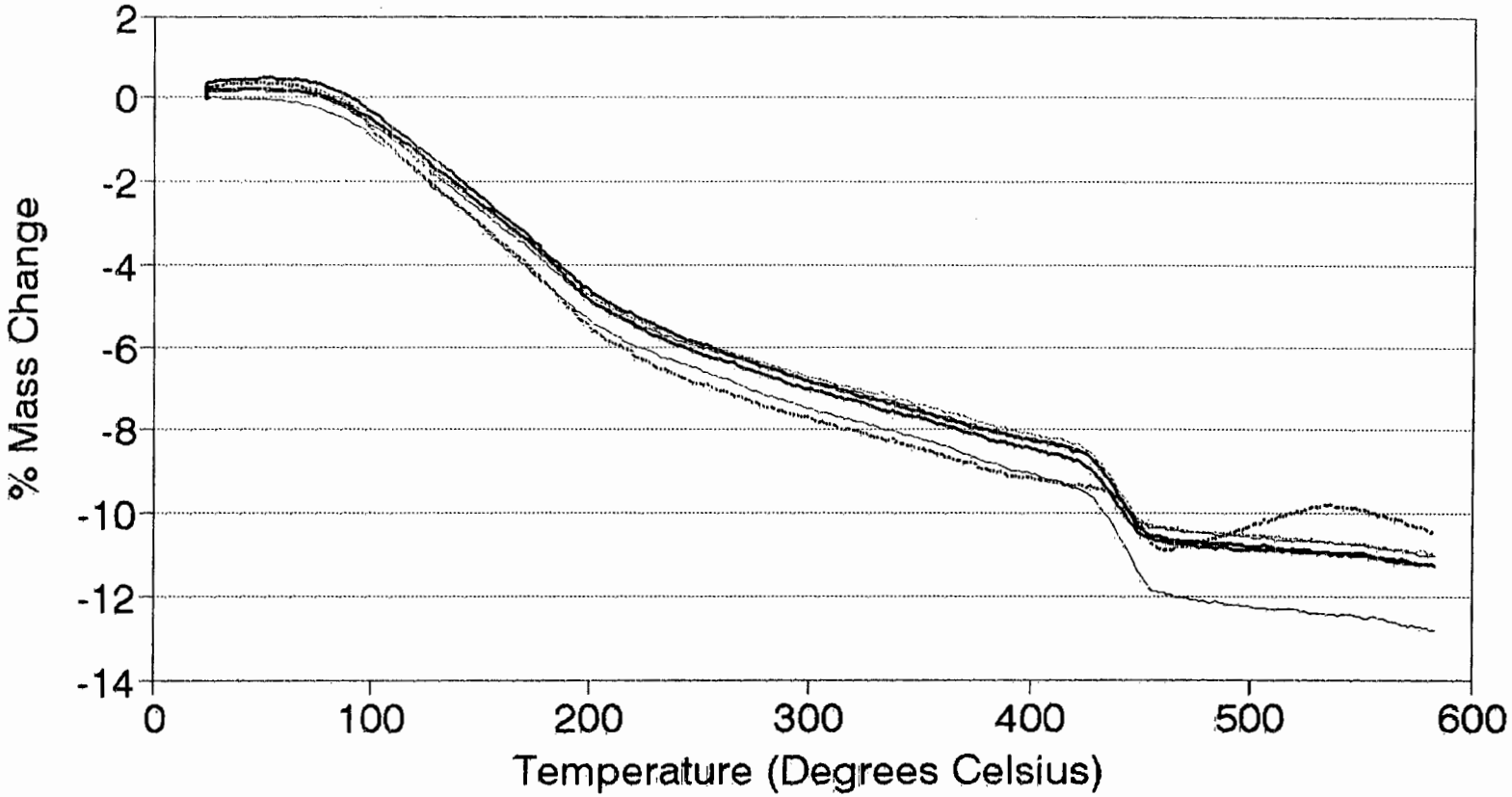

TGA Plot after 3 Days

Van Eck(-63) Paste in Normal Air

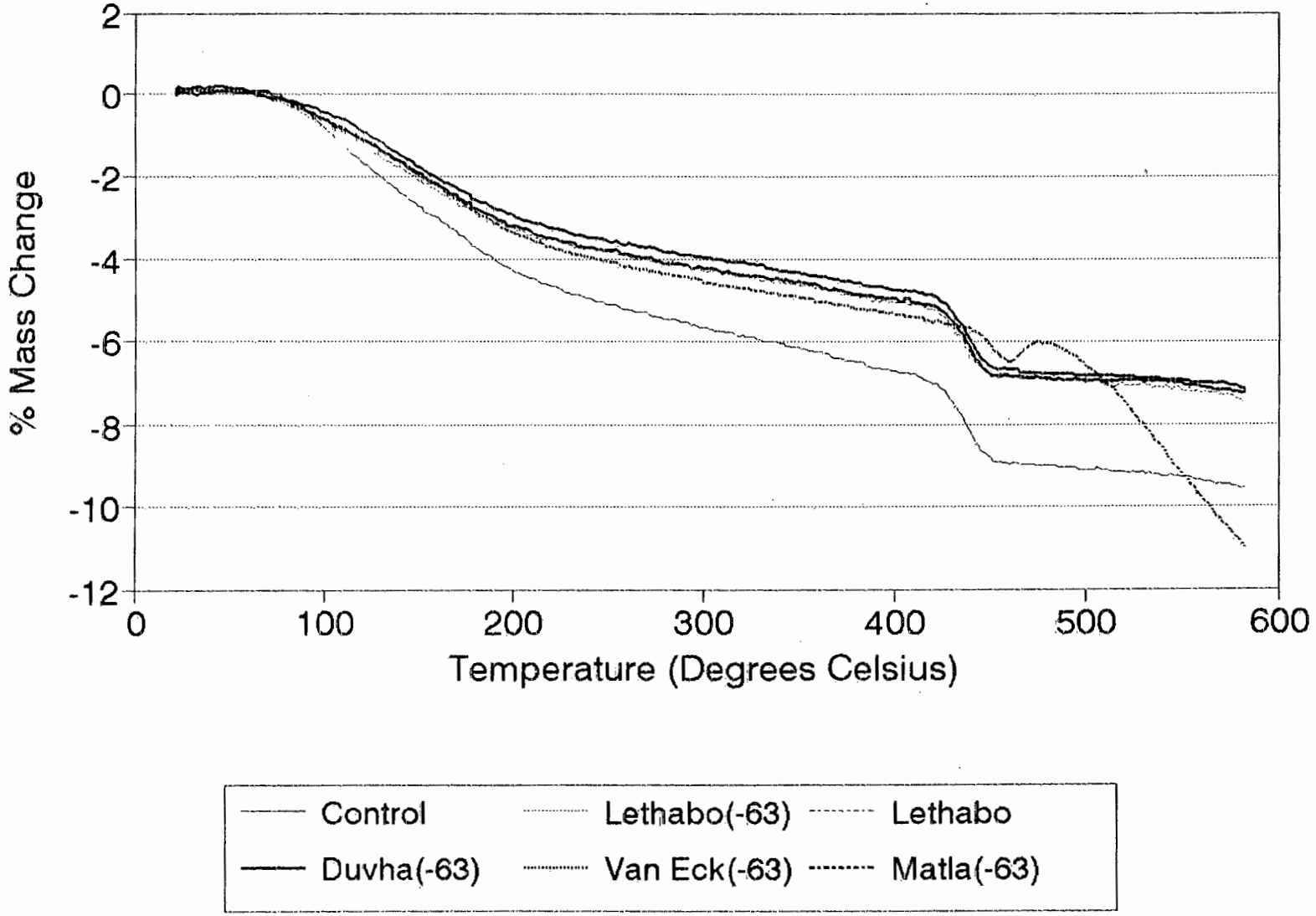

TGA Plot after 7 Days

Van Eck(-63)Paste in Normal Air

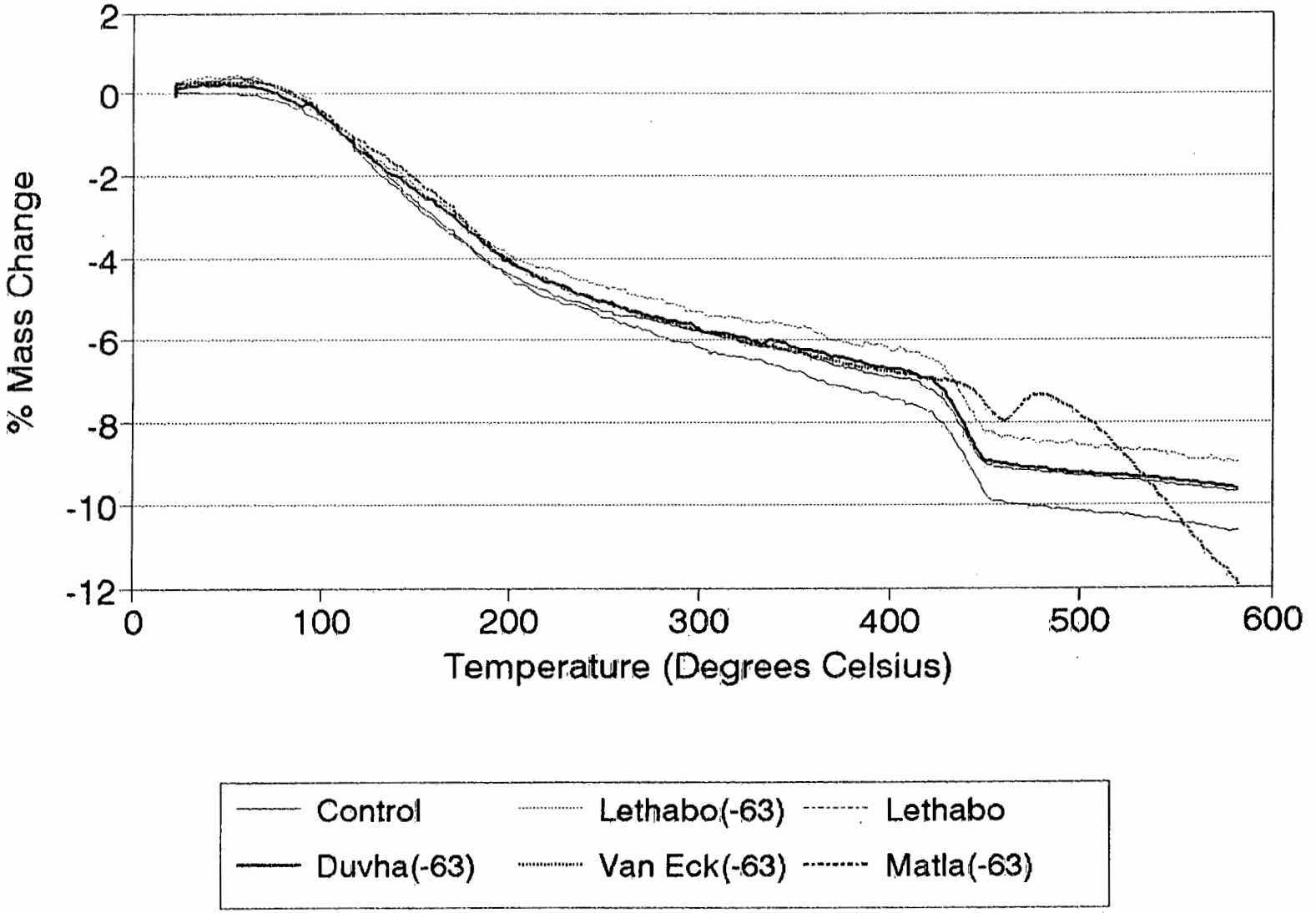

TGA Plot after 14 Days

Van Eck(-63) Paste in Normal Air

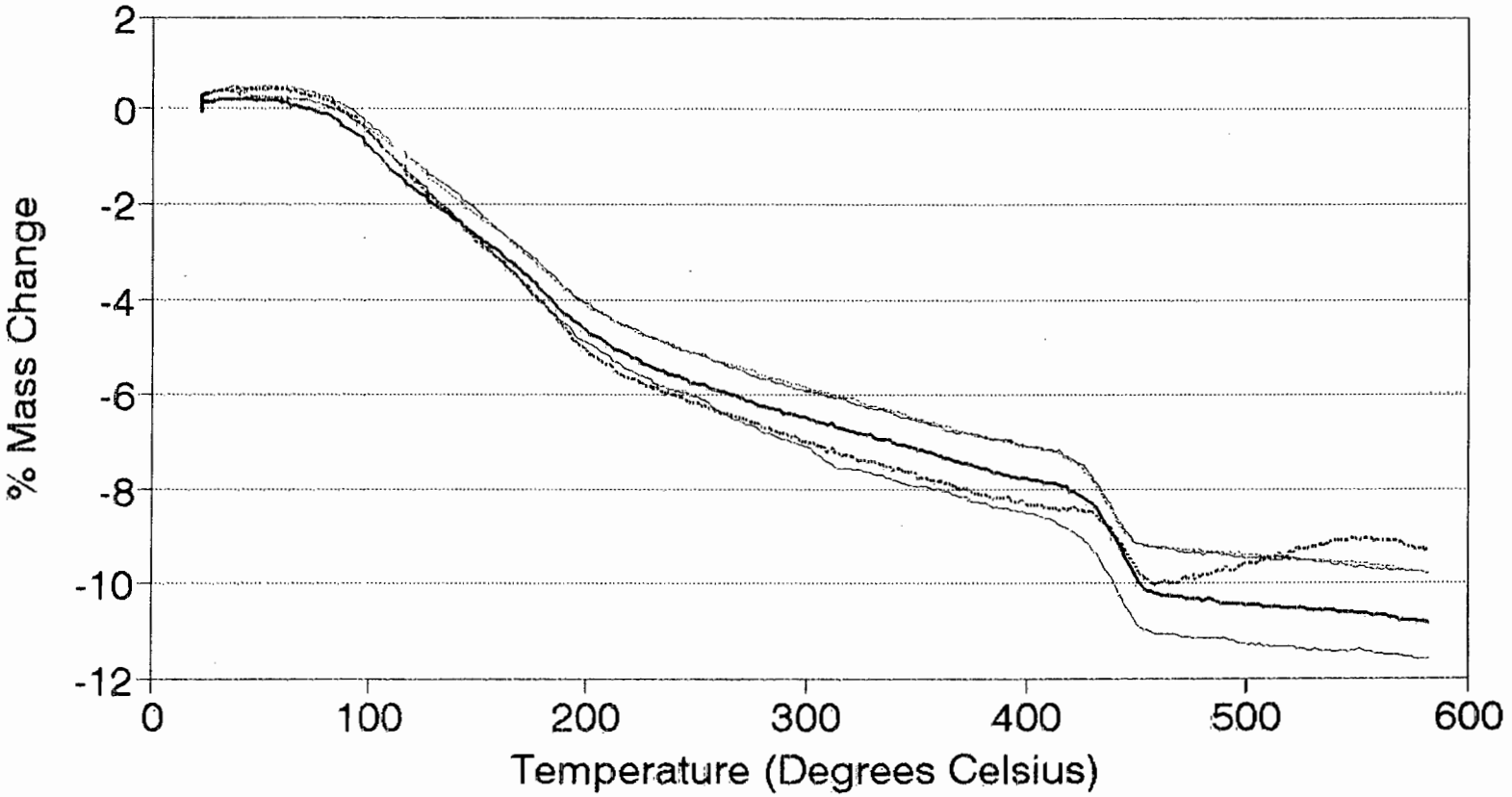

TGA Plot after 21 Days

Van Eck(-63) Paste in Normal Air

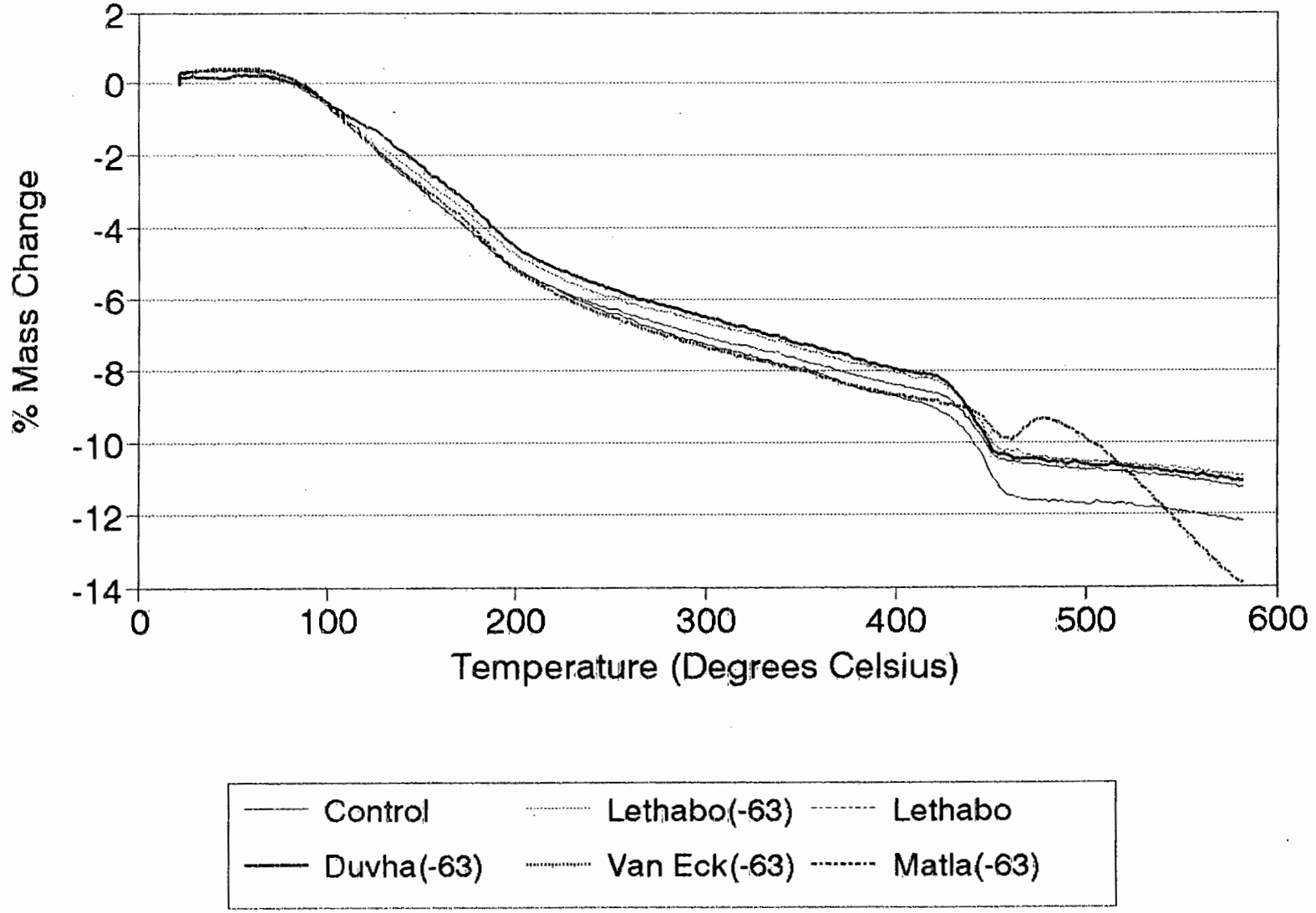

TGA Plot after 28 Days

Van Eck(-63) Paste in Normal Air

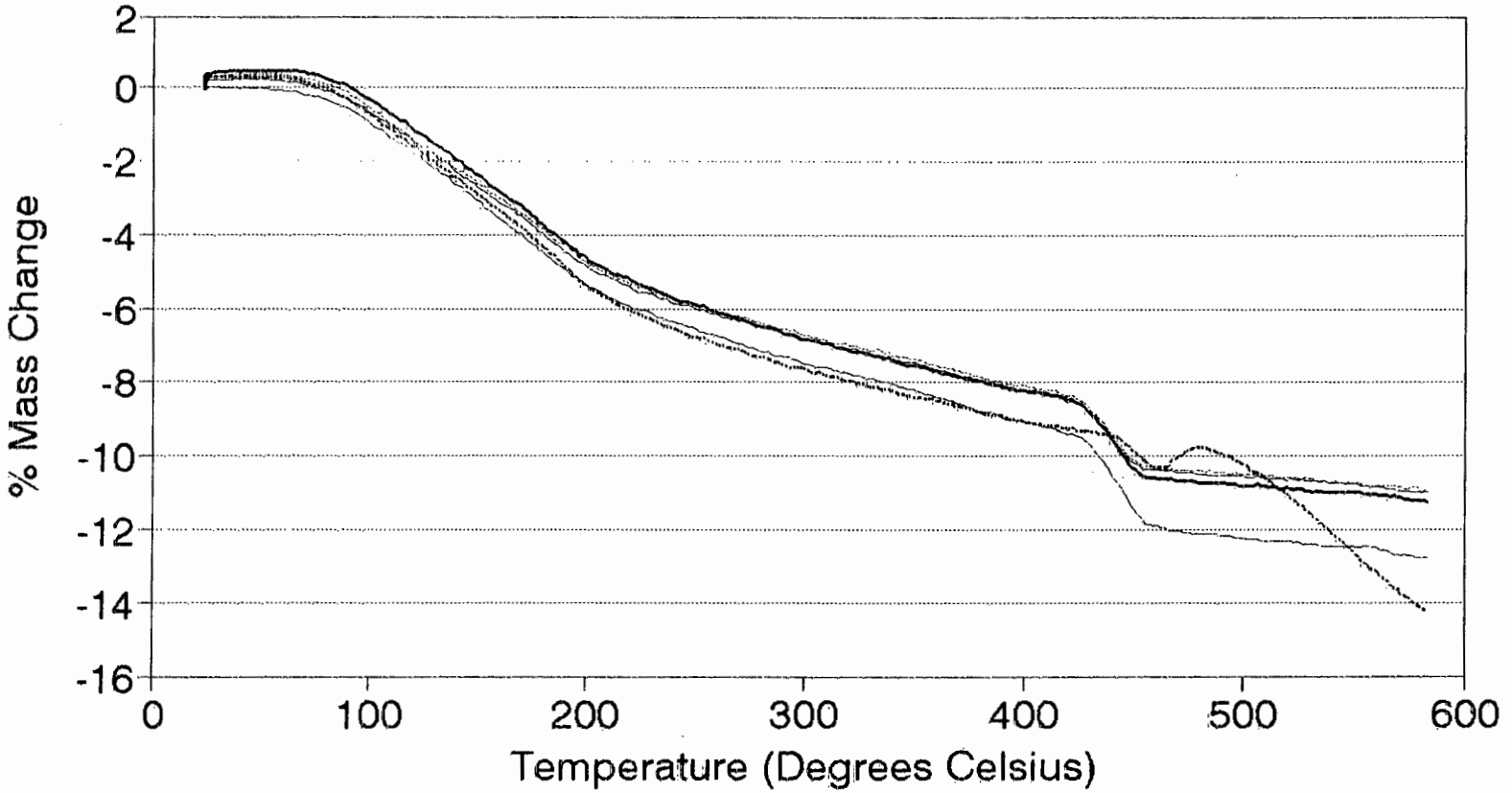

TGA Plot for the Control Paste

Dry Nitrogen Atmosphere

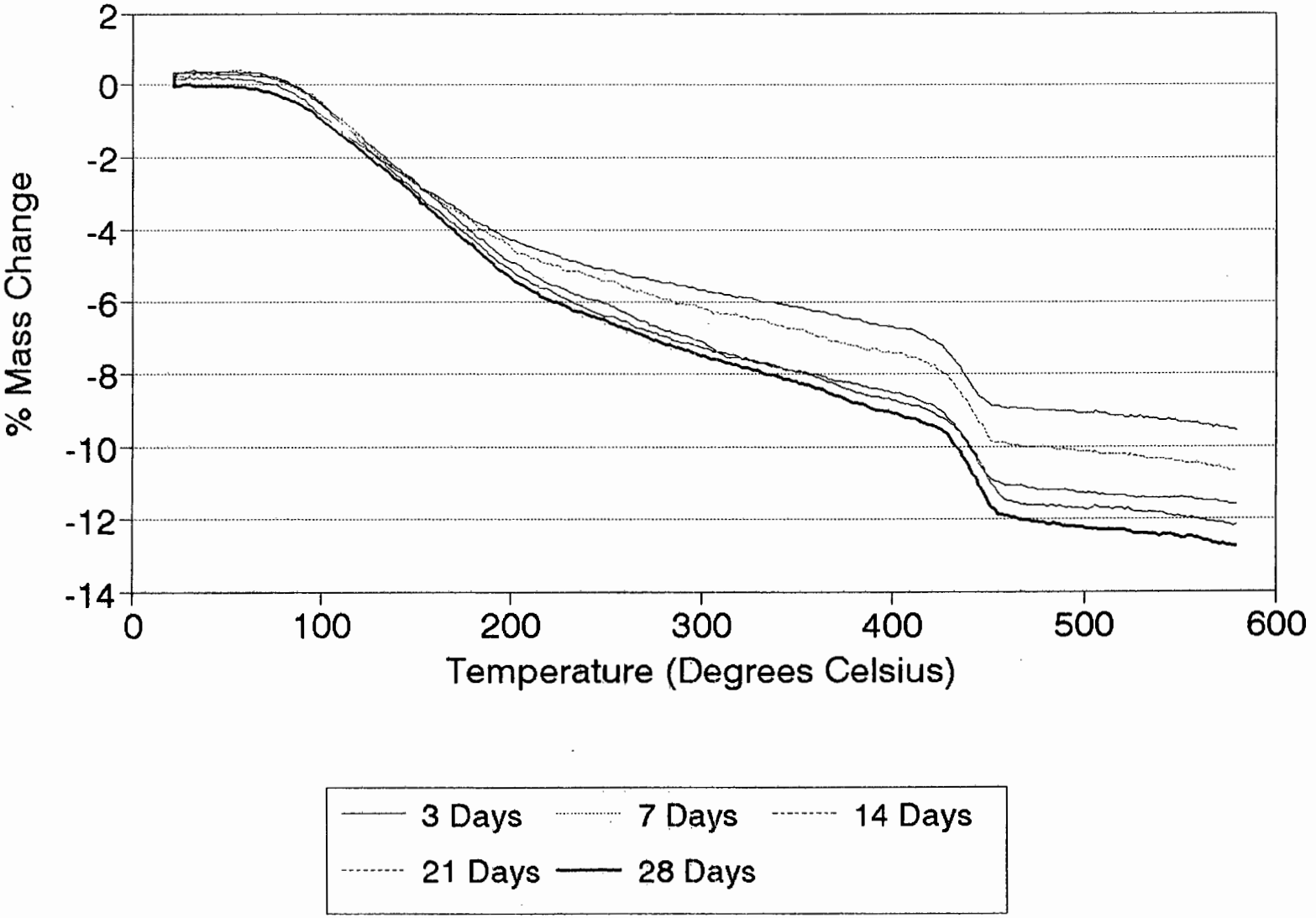

TGA Plot for the Lethabo(-63) Paste

Dry Nitrogen Atmosphere

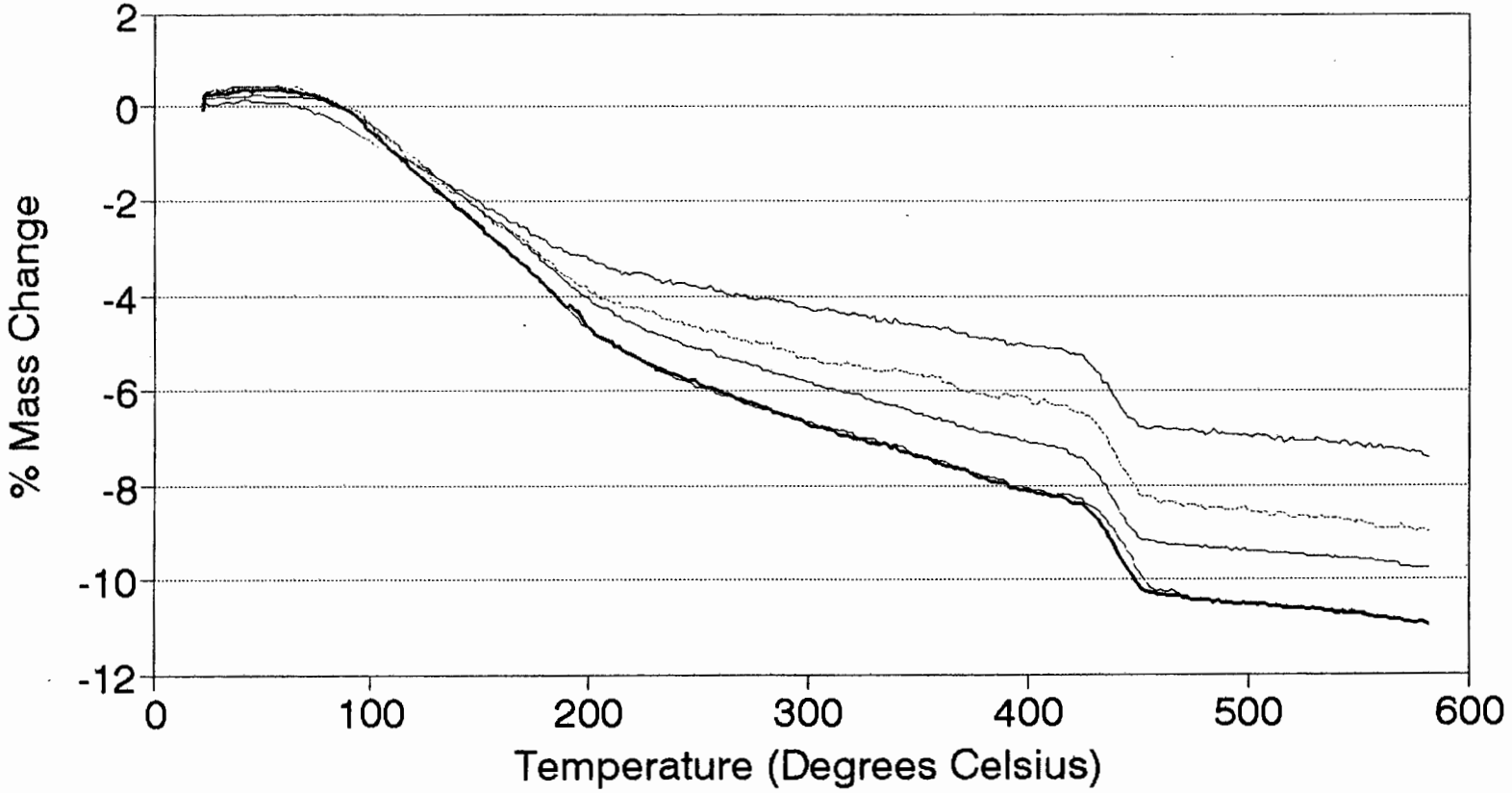

TGA Plot for the Lethabo Paste

Dry Nitrogen Atmosphere

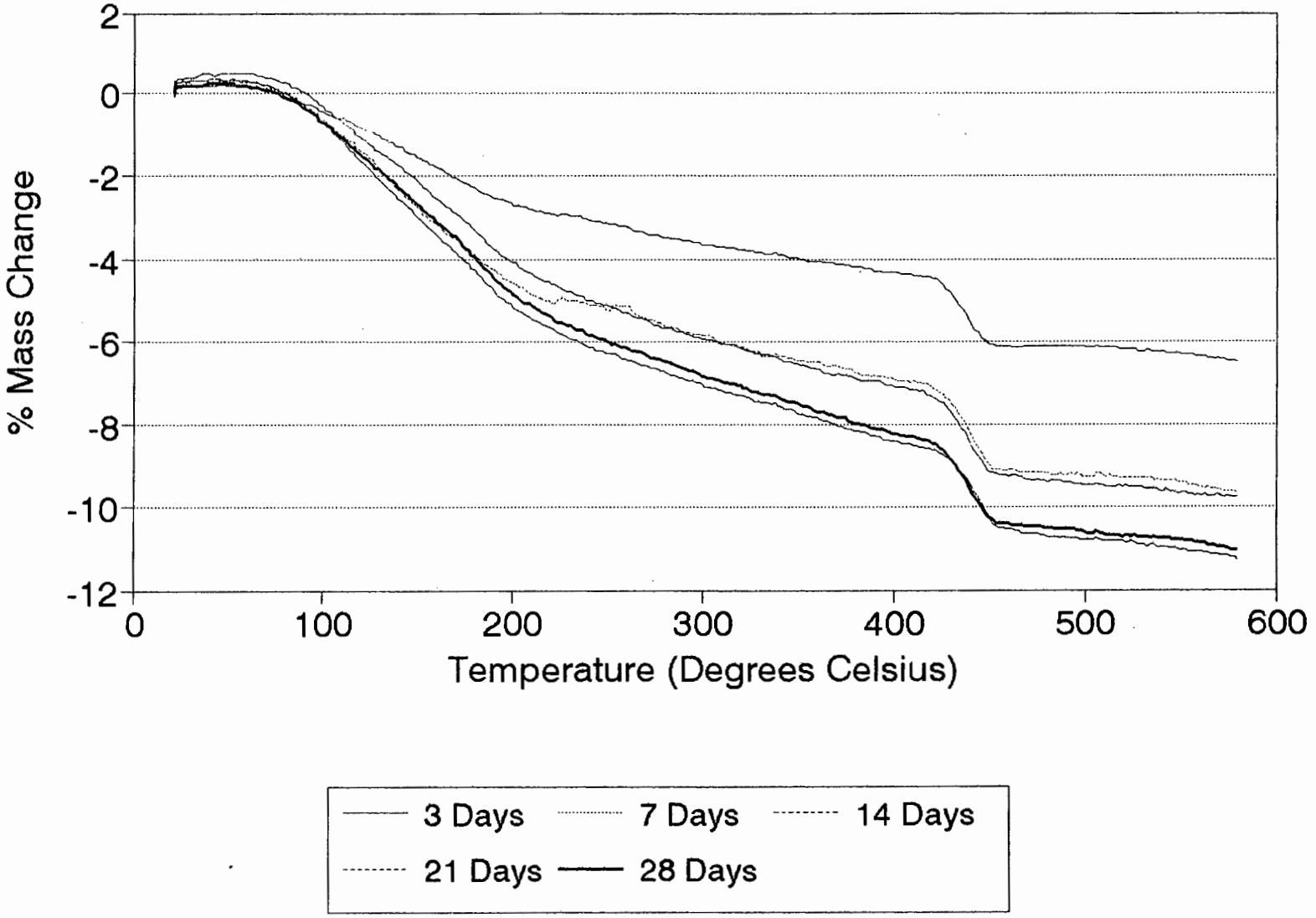

TGA Plot for the Duvha(-63) Paste

Dry Nitrogen Atmosphere

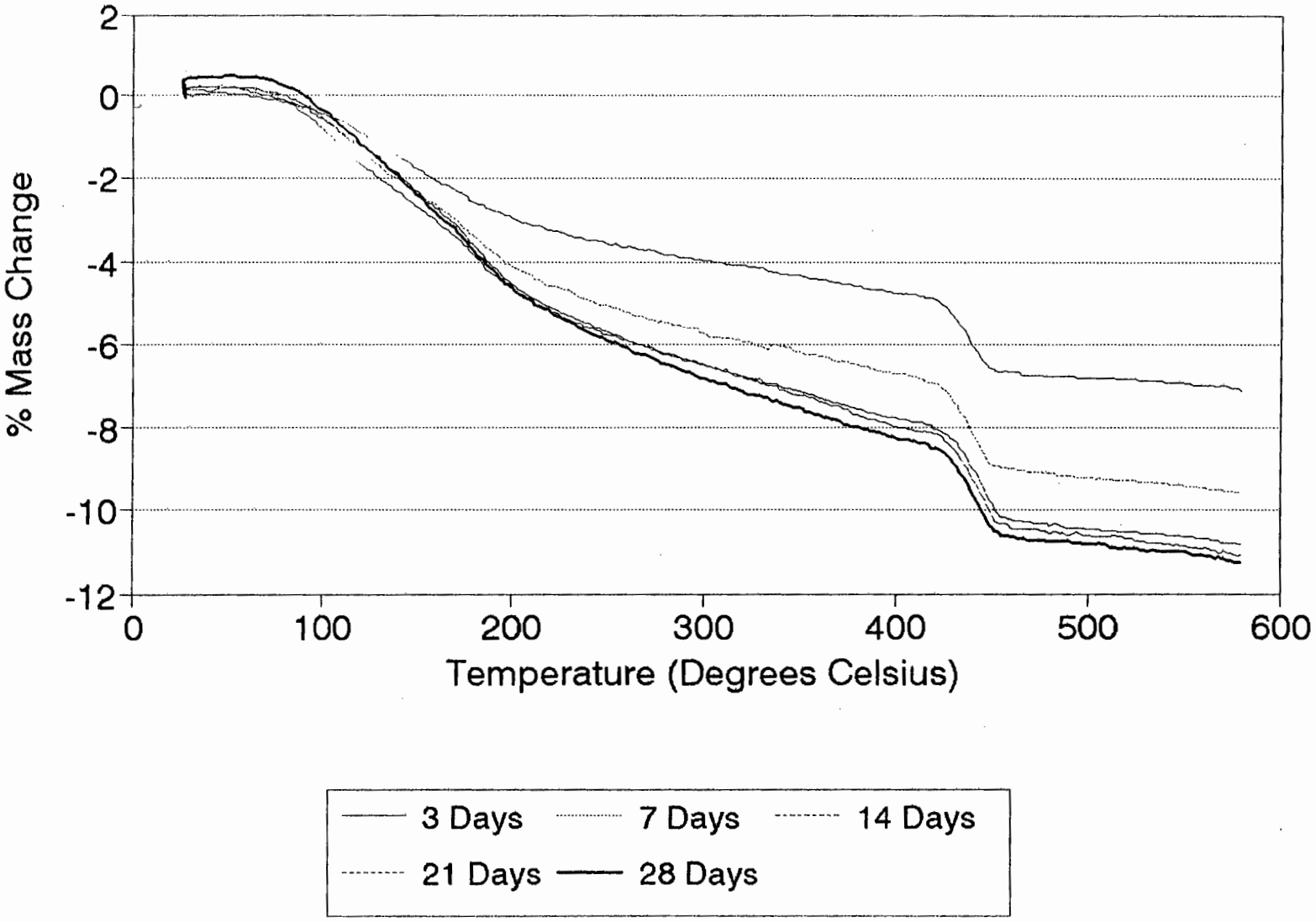

TGA Plot for the Van Eck(-63)Paste

Dry Nitrogen Atmosphere

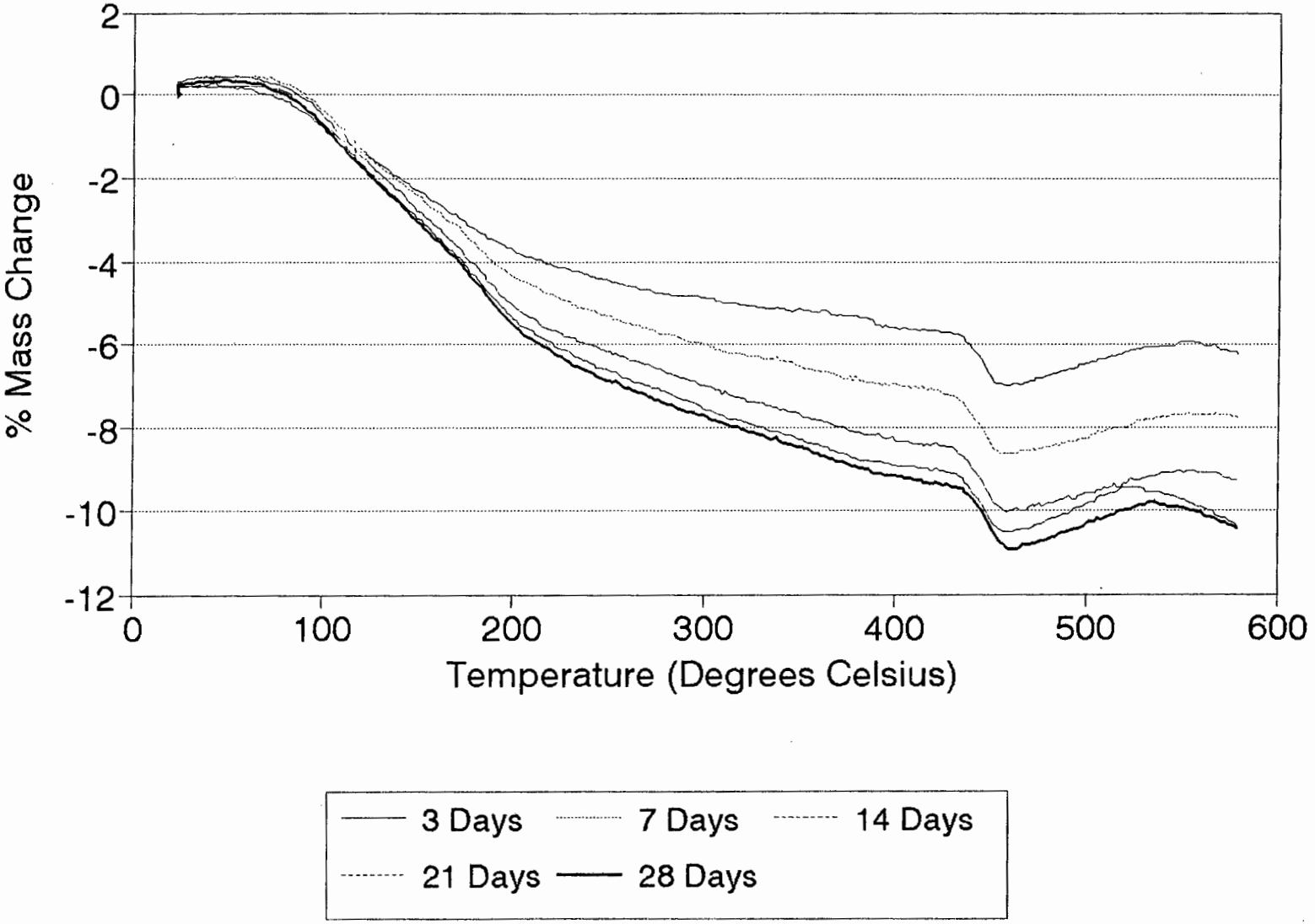

TGA Plot for the Matla(-63)Paste
Dry Nitrogen Atmosphere

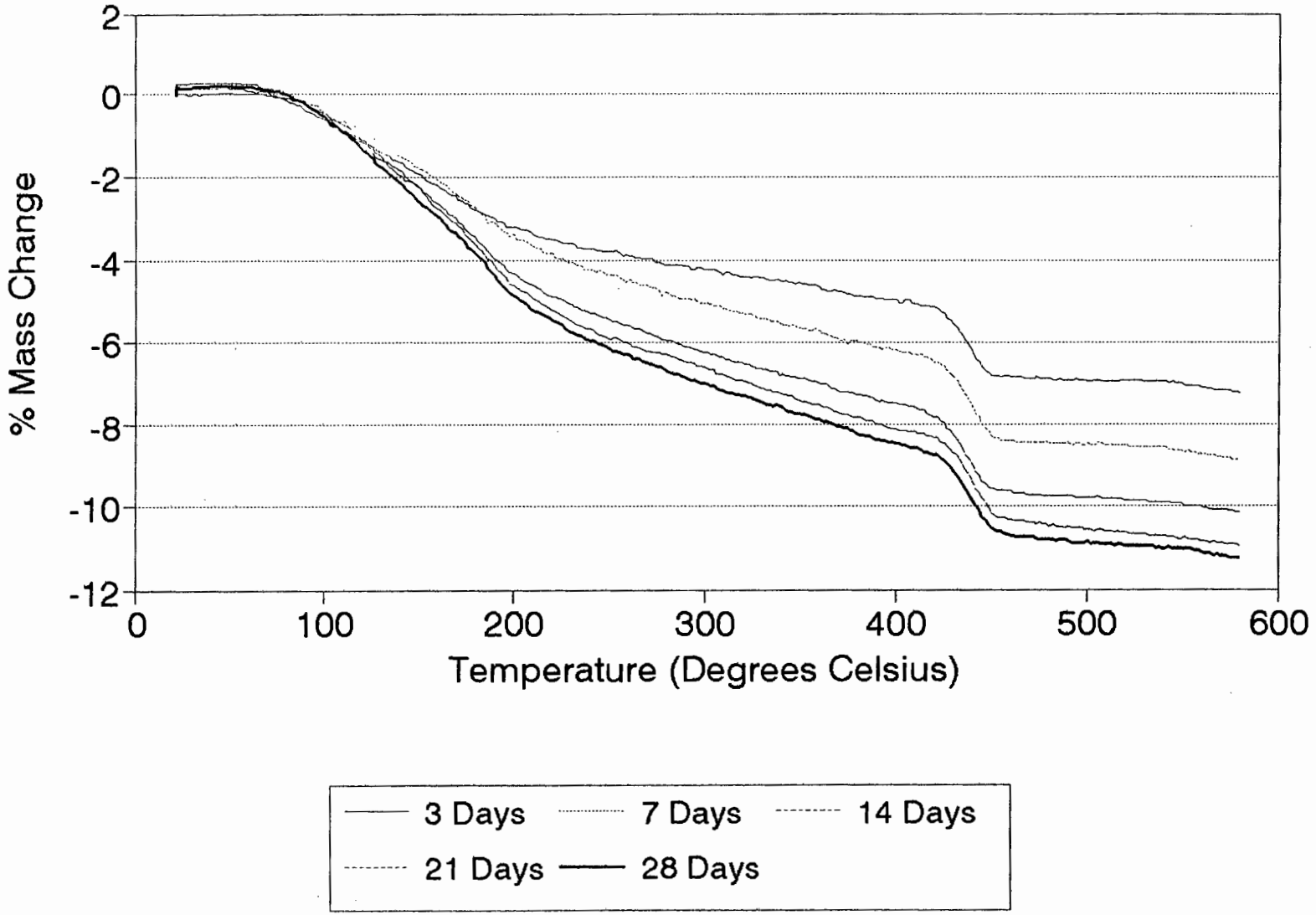

TGA Plot for the Van Eck(-63)Paste

Normal Air Atmosphere

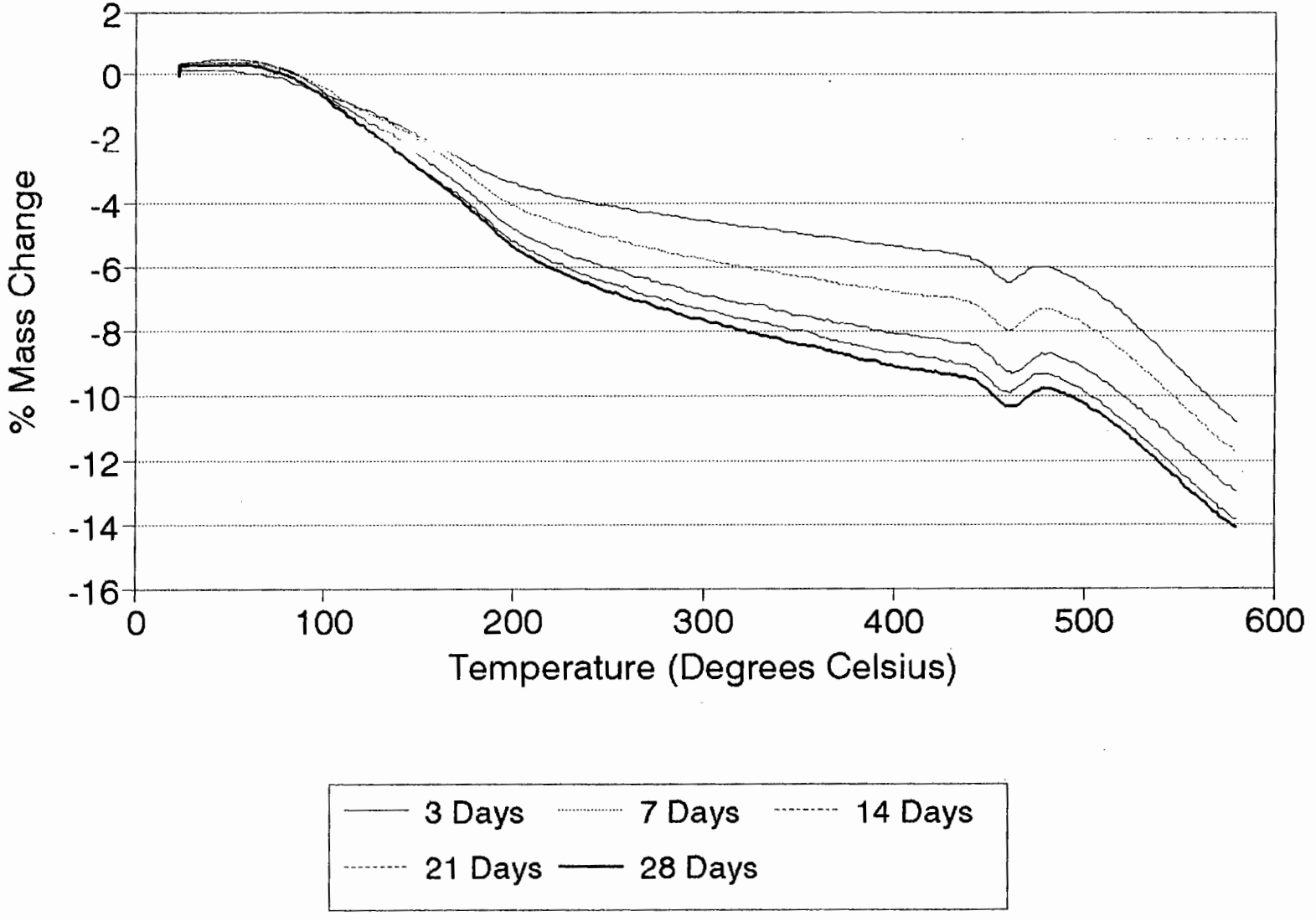

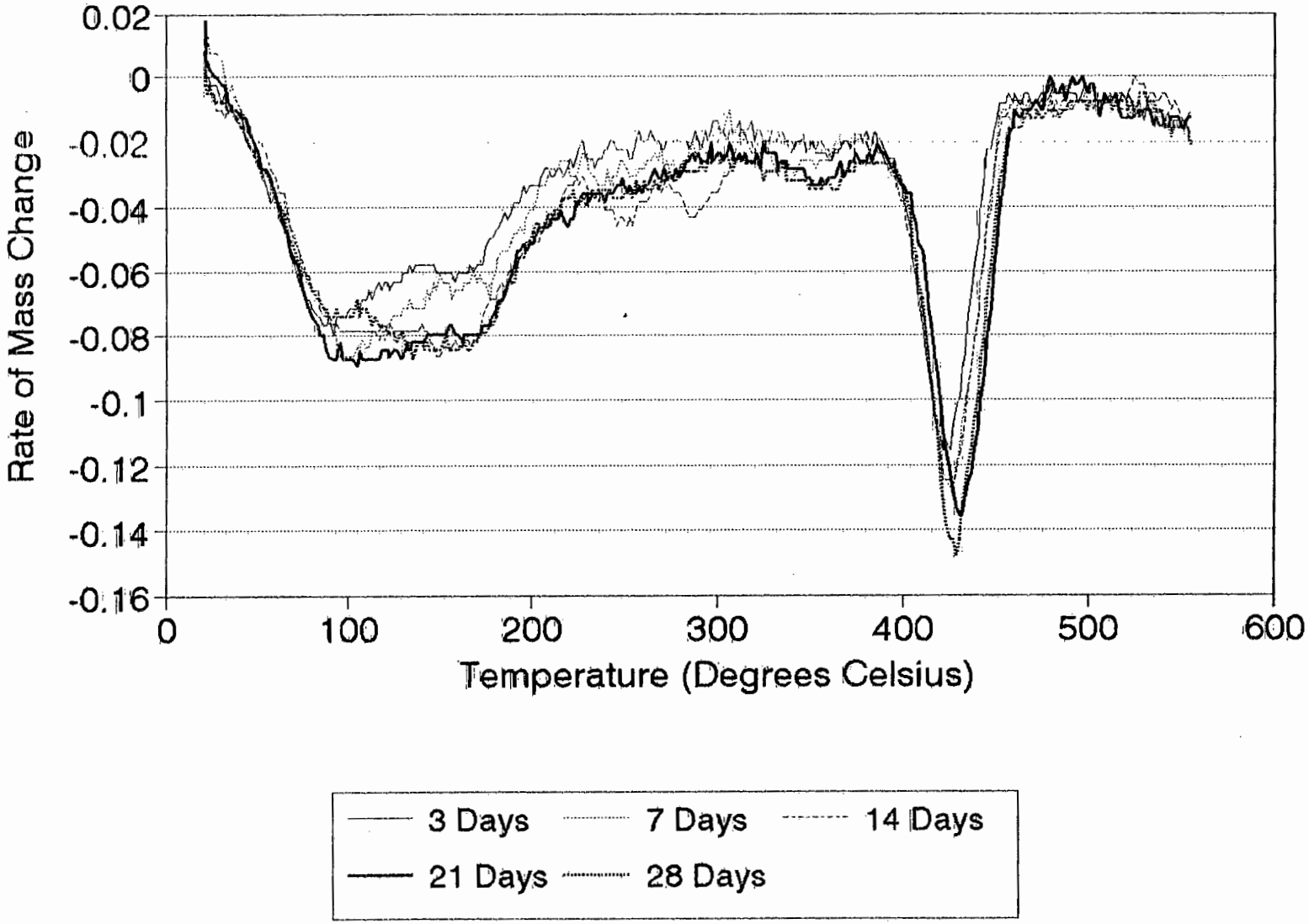
DTG Plot for the Control Paste
Dry Nitrogen Atmosphere
Rate of Mass Change
0.02
0
-0.02
-0.04
-0.06
-0.08
-0.1
-0.12
-0.14
-0.16
0
100
200
300
400
500
600
Temperature (Degrees Celsius)
3 Days
7 Days
14 Days
21 Days
28 Days

DTG Plot for the Lethabo(-63) Paste

Dry Nitrogen Atmosphere

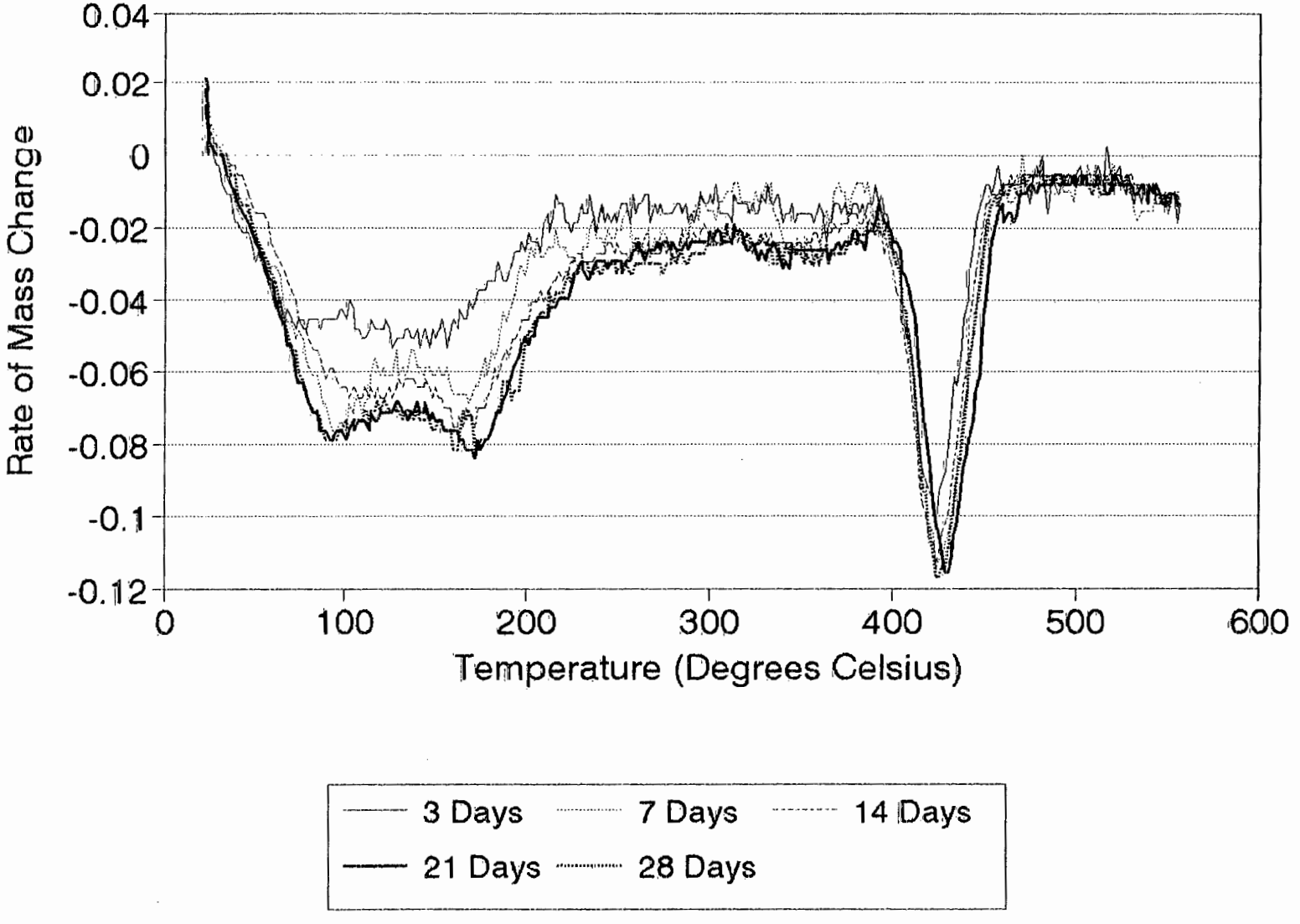

DTG Plot for the Lethabo Paste

Dry Nitrogen Atmosphere

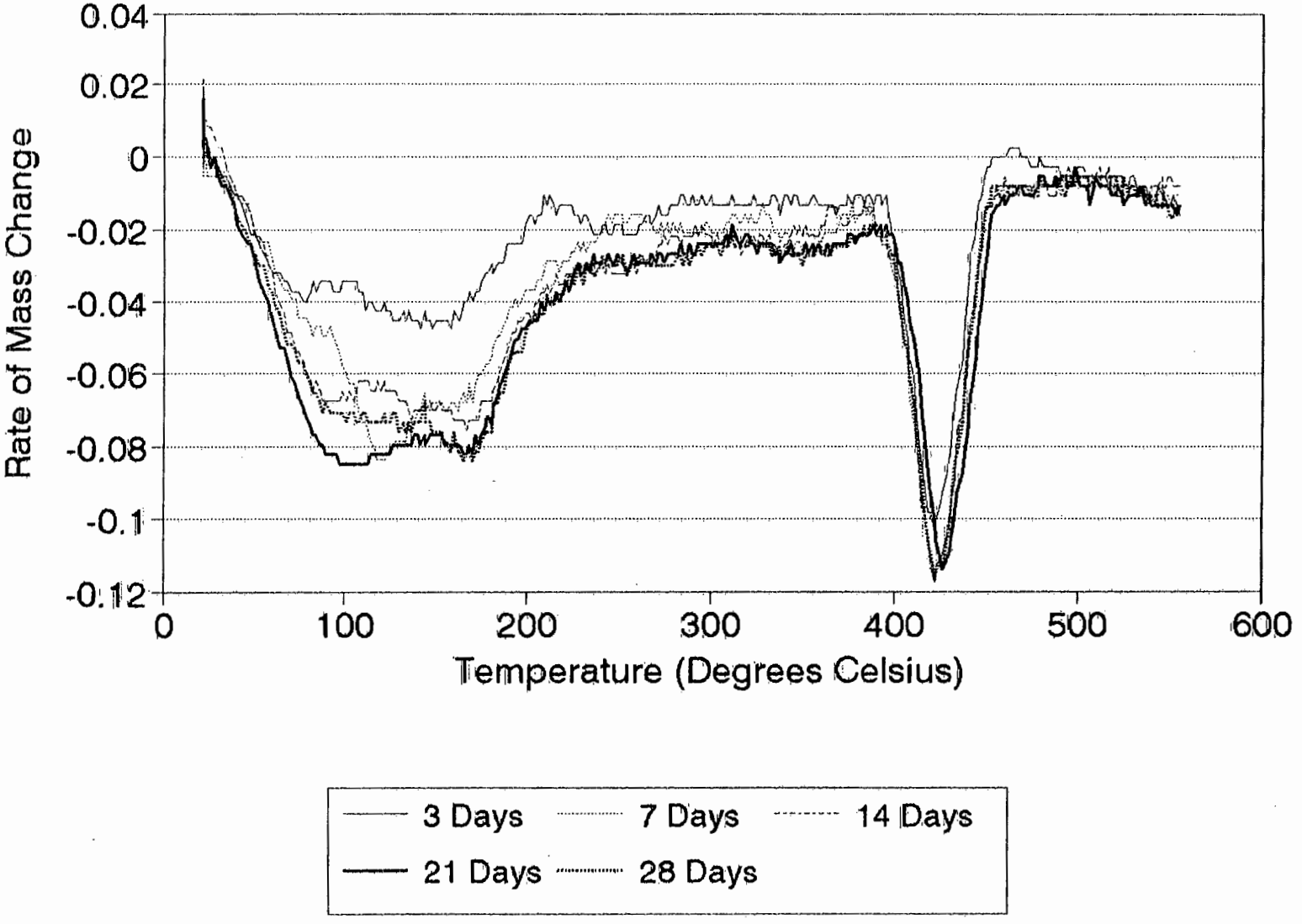

DTG Plot for the Duvha(-63) Paste

Dry Nitrogen Atmosphere

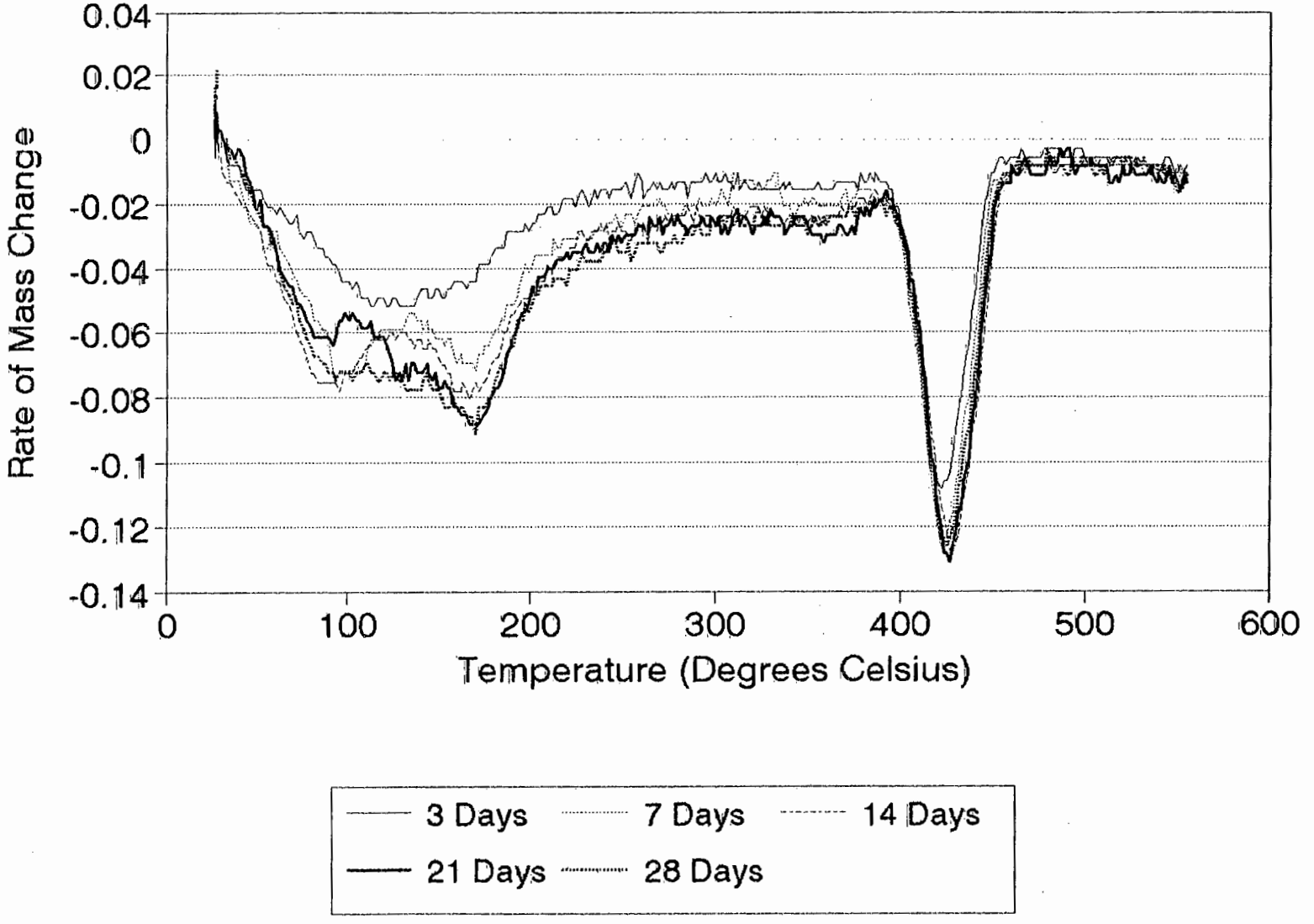

DTG Plot for the Van Eck(-63) Paste

Dry Nitrogen Atmosphere

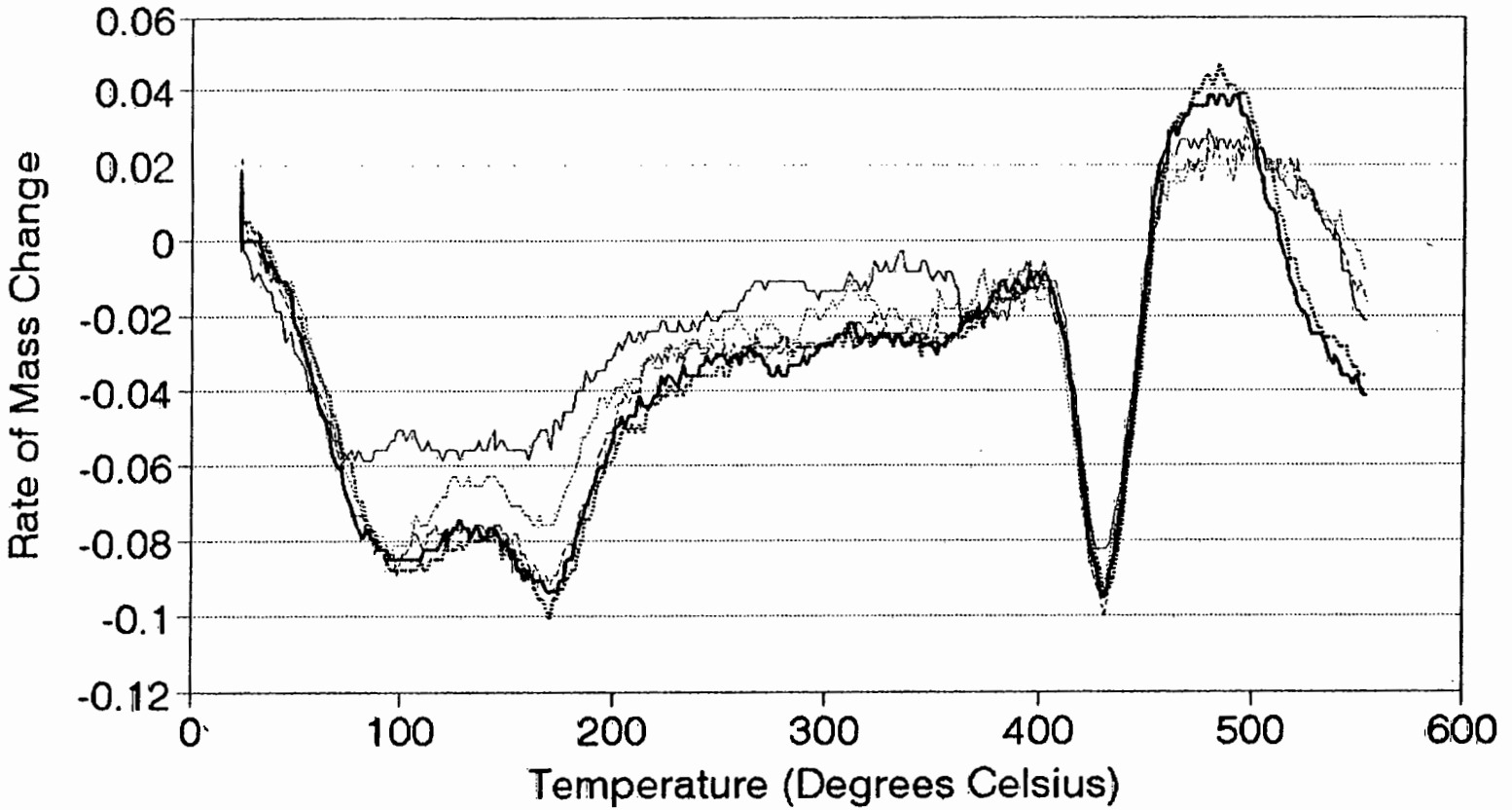

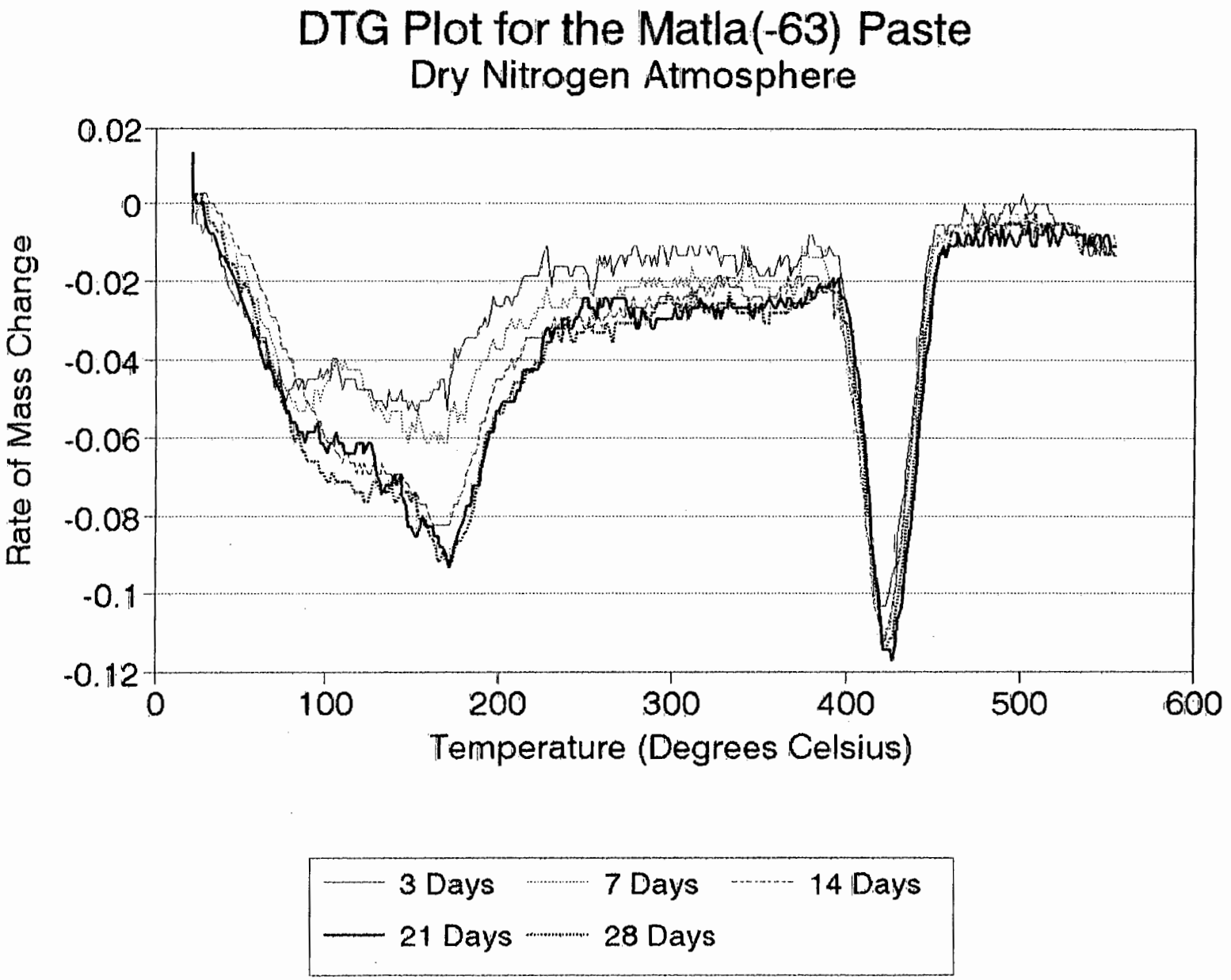
DTG Plot for the Matla(-63) Paste
Dry Nitrogen Atmosphere
Rate of Mass Change
0.02
0
-0.02
-0.04
-0.06
-0.08
-0.1
-0.12
0
100
200
300
400
500
600
Temperature (Degrees Celsius)
3 Days
7 Days
14 Days
21 Days
28 Days

DTG Plot for the Van Eck(-63) Paste

Normal Air Atmosphere

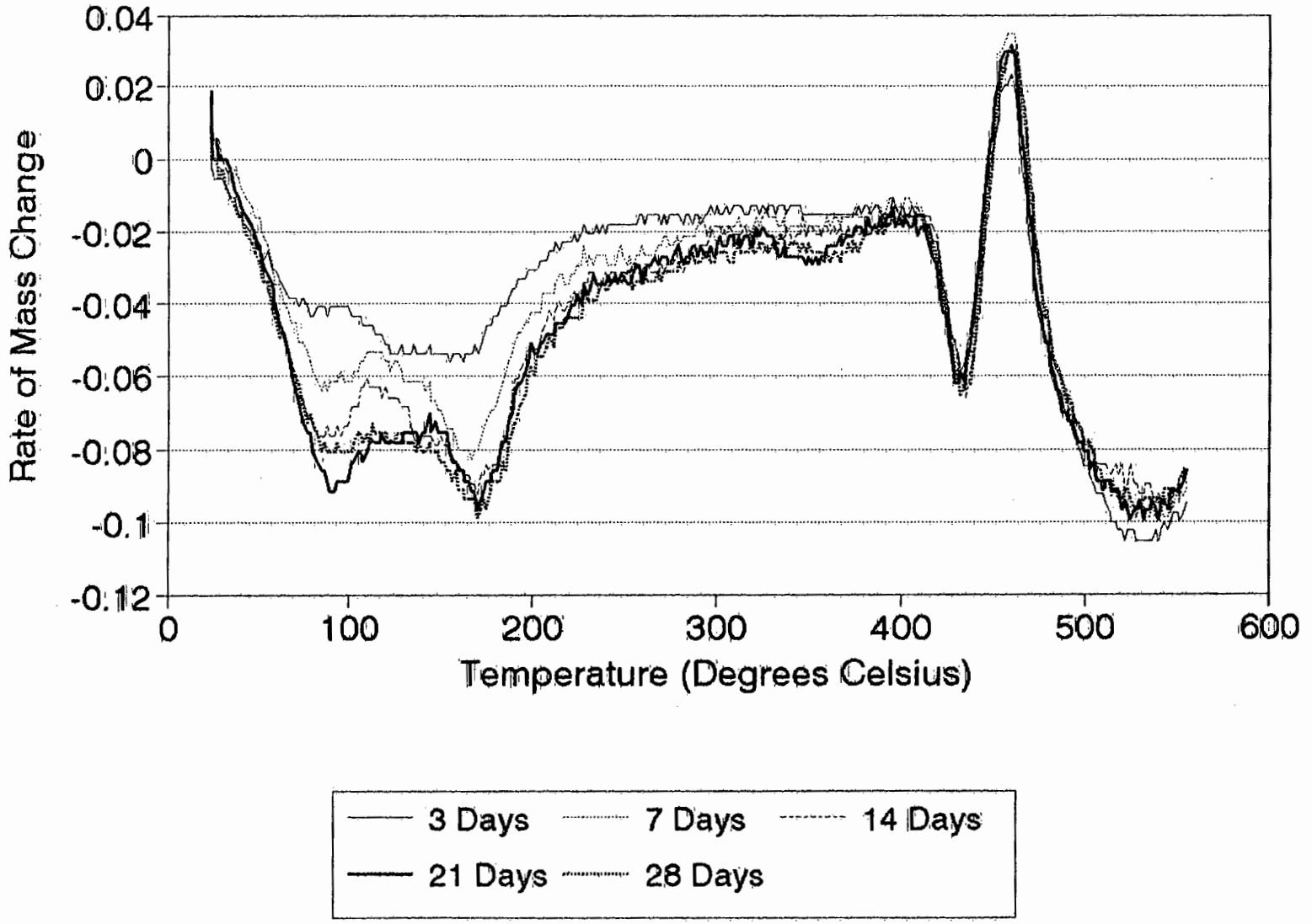

APPENDIX D

APPENDIX D

METHOD 1: CONCRETE MIX DESIGN INCORPORATING FLY ASH

Dhir (1986) gives the main steps to mix design of fly ash concrete as follows :

1. *Determination of free water/portland cement ratio (W/C)*

For a given target strength (28 days), Figure D.1 is used to find the relevant (W/C) ratio.

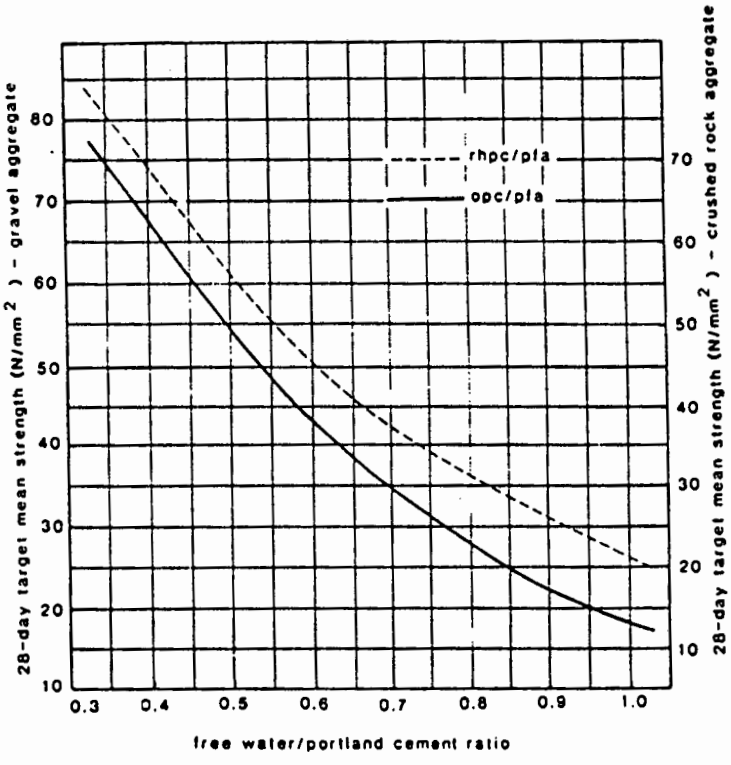

Figure D.1 : Relationship between 28-day strength and free water to portland cement ratio.

2. *Determination of fly ash/composite cement ratio (F/F+C)*

Figure D.2 is used to obtain the value for (F/F+C) in relation to the free water/portland cement ratio. The value from the graph is a first approximation and might be changed due to additional design requirements.

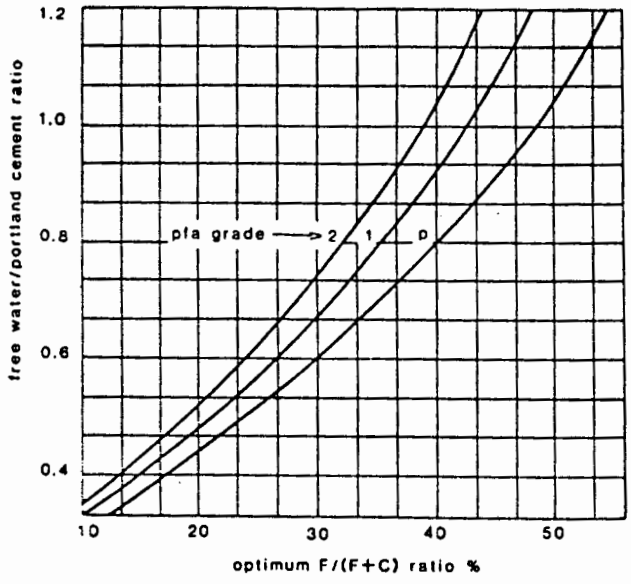

Figure D.2 : Relationship between free water/portland cement ratio and fly ash/total composite cement content.

3. *Determination of free water content (W)*

The free water content is chosen in terms of the coarse aggregate used and the required workability (measured as the slump). Table D.1 lists values for the water content for concrete containing 30% fly ash. For different percentages of fly ash, adjust as follows :

For fly ash >30%, subtract 1 litre/m^3 per 2% deviation.

For fly ash <30%, add 1litre/m^3 per 2% deviation.

Maximum aggregate size (mm)	Aggregate type	Grade* of pfa	Free water content, l/m³ Slump (mm) 10–30	30–60	60–120
10	Gravel	Premium	160	175	190
		1	170	185	200
		2	180	195	210
	Crushed	Premium	180	195	210
		1	190	205	220
		2	200	215	230
20	Gravel	Premium	140	155	170
		1	150	165	180
		2	160	175	190
	Crushed	Premium	160	175	190
		1	170	185	200
		2	180	195	210

Table D.1 : Approximate values for the free water content for fly ash concretes containing 30% fly ash.

4. *Determination of portland cement (C) and fly ash (F) contents*

The following equations are used with $X = 100\left(\frac{F}{F+C}\right)$

$$C = \left(\frac{W}{W/C}\right) \quad \text{and} \quad F = \left(\frac{C\left(X/100\right)}{1-\left(X/100\right)}\right)$$

5. *Determination of the total aggregate content (A)*

The first step is to estimate the plastic density of the concrete, α, from Figure D.3.

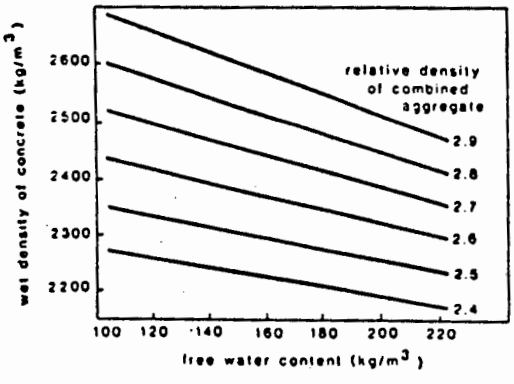

Figure D.3 : Relationship between the plastic density and free water content of compacted fly ash concrete.

The second step involves the calculation of the total aggregate content, A from the formula given by : $A = \alpha - (C + F + W)$

From the value obtained for the total aggregate, find the fine aggregate content, A_f, using figure D.4 or D.5.

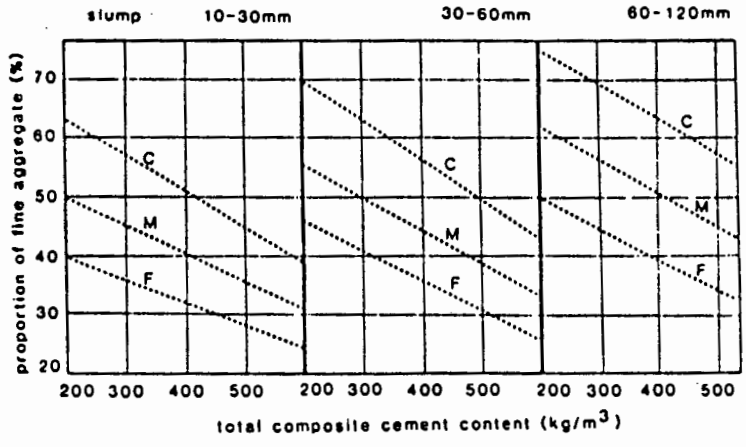

Figure D.4 : Determination of A_f for 10mm maximum aggregate size.

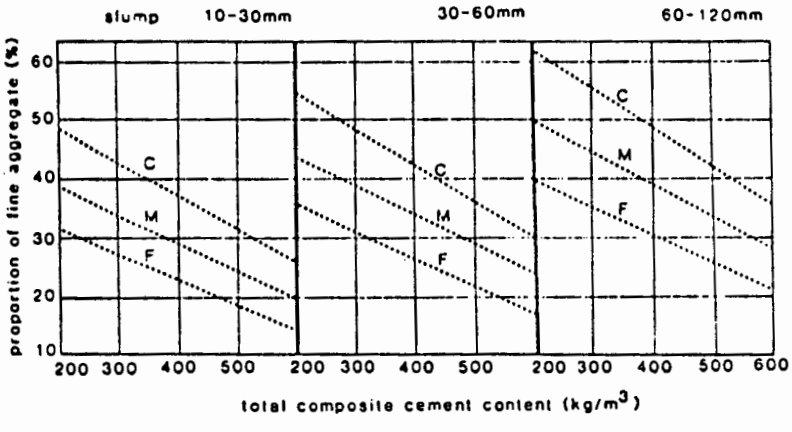

Figure D.5 : Determination of A_f for 20mm maximum aggregate size.

6. *Conduct a trial mix*

From the mix proportions determined so far, a trial mix is prepared and then characterized in terms of properties. If the workability (from slump test) differs from the design value, W, the free water content, has to be adjusted. If the strength (e.g. compressive cube strength) does not meet the set requirement, (W/C) has to be modified.

METHOD 2 : PCI METHOD OF CONCRETE MIX DESIGN INCORPORATING FLY ASH

A widely accepted method of concrete mix design has been developed by the Portland Cement Institute of South Africa. In the context of the presented topic of fly ash addition to concrete, the following report summarizes the important steps of the PCI method as given in Fulton's Concrete Technology (Addis, 1986).

1. *Selection of the fly ash content*

The normal practice is to use between 15% and 30% of fly ash by mass of total cementitious material. However mixes with up to 50% fly ash have proved successful in special applications. If the fineness of the ash is known, Figure D.6 gives information about fly ash content as a function of free water content.

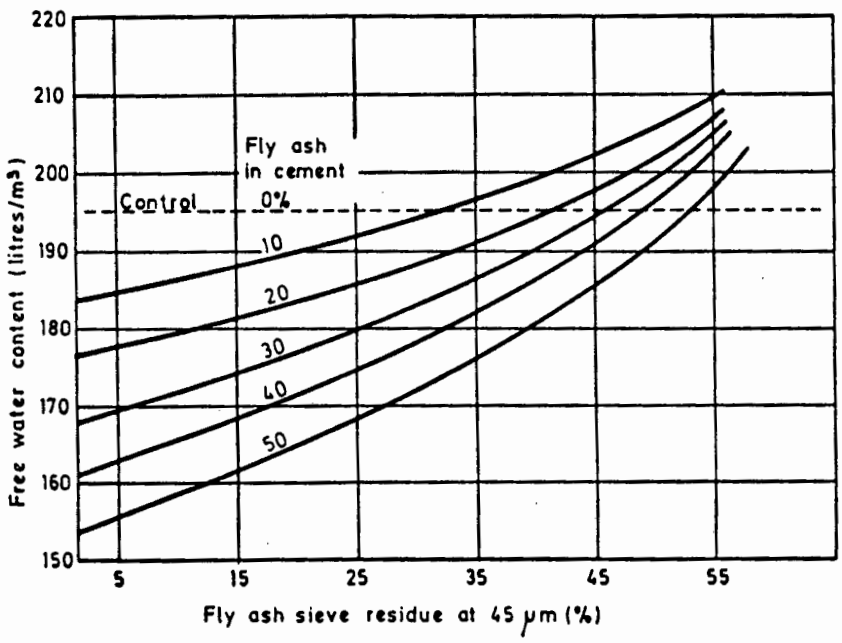

Figure D.6 : Relationship between fly ash fineness and free water content of concrete with 50-75mm slump as a function of different fly ash percentages; nominal cement content 300kg/m^3.

2. *Determination of (CT/W) ratio for a given target strength, where CT represents the total cementitious material content and W refers to the quantity of free water*

Figure D.7 gives some combinations of fly ash and concrete. In the case where different ratios are to be used, the presented curves may be extrapolated to find the value for (CT/W).

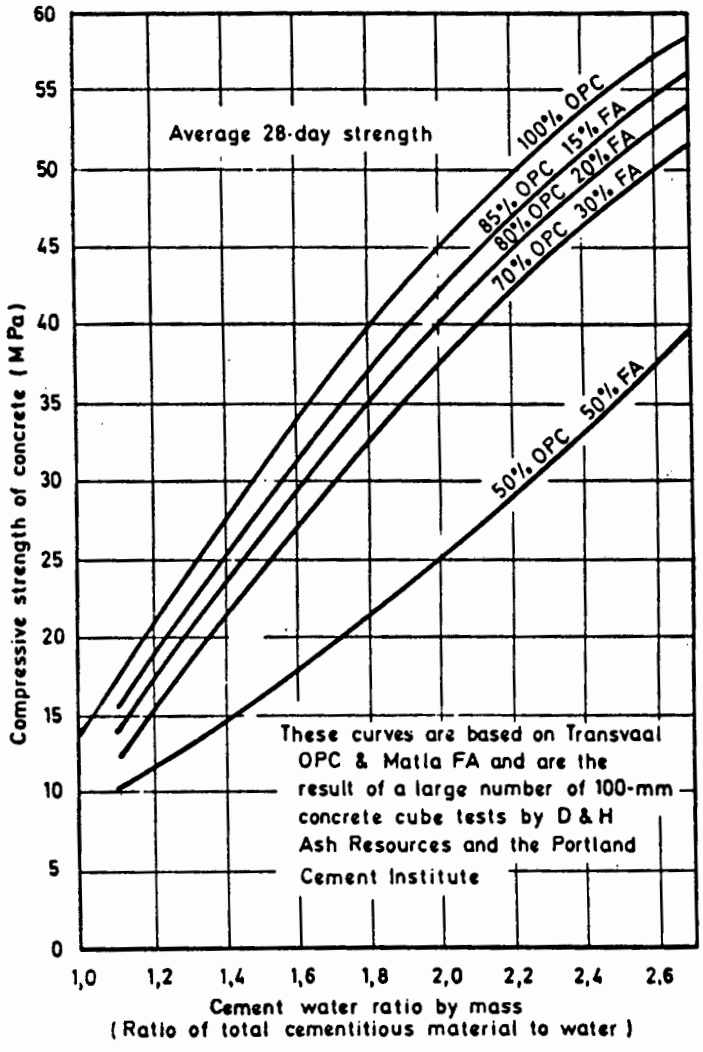

Figure D.7 : Relationship between the 28-day target strength and total cementitious material to water ratio for different proportions of fly ash additions.

Figure D.7 may also be used as starting point in the design of the mix. Then, if the target strength is known as well as the ratio of (CT/W), the relevant proportion of fly ash is chosen from the graph.

3. *Determination of the water content*

Fulton (Addis, 1986)indicates the approximate water contents for concrete with optimum 19mm stone quantity and slump of 75mm to be as given in Table D.2.

Table D.2 : Water content as a function of sand quality.

Sand Quality	Water Content (l/m^3)	
	Natural Sand	Crusher Sand
Very Poor	240	235
Poor	225	225
Average	210	215
Good	195	205
Excellent	180	195

An important step at this stage is to incorporate the reduced water requirement of a fly ash mix. A 10% reduction in water content relative to the straight cement mix is a commonly used figure.

Figure D.8 below relates the change in slump to a change in the water content. This presentation often becomes very useful once the first trial mix has been prepared.

Now that the figures for cement -, fly ash - and water content are known, the proportions of coarse and fine aggregate to be used are calculated.

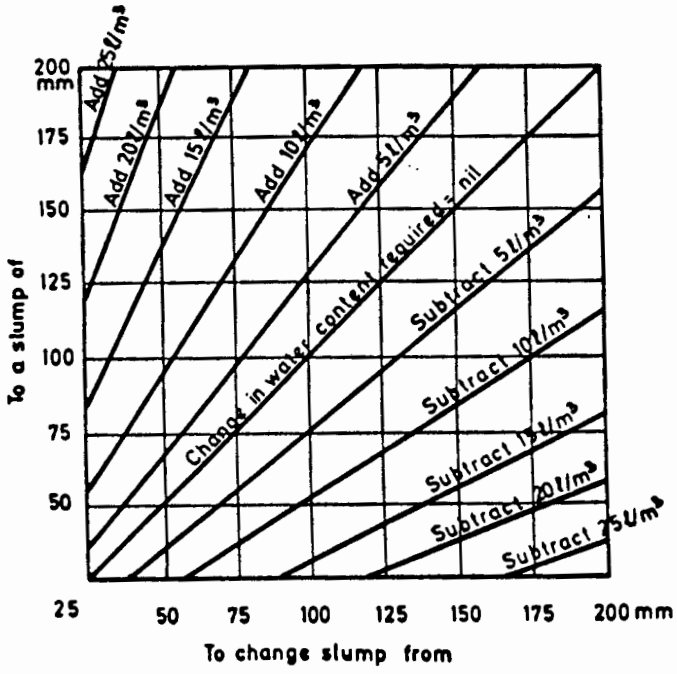

Figure D.8 : Change in water content required to bring about the desired change in slump.

4. *Determination of stone content*

The stone content is given by the formula :

$$S = CBD(K - 0.1FM)$$

where CBD = dry compacted bulk density of the stone

K = a factor which depends on the maximum stone size as well as the workability of the concrete

Fulton (Addis, 1986) lists the following values for the factor K as in Table D.3.

Table D.3 : Values for the factor K.

Slump range (mm)	Placing Method	K-Values Maximum Stone Size (mm)				
		9.5	13.2	19.0	26.5	37.5
75-150	Hand Compaction	0.75	0.84	0.94	0.99	1.05
25-100	Moderate Vibration	0.80	0.90	1.00	1.02	1.10

If the compacted bulk density of the stone equals the value of 1529kg/m^3, then the above table expressed graphically is presented in Figure D.9.

In the case where the CBD value of the stone to be used differs from 1520kg/m^3, Figure D.9 may still be used; the only alteration being that the value obtained from the graph for the stone content is to be multiplied by a factor of (actual CBD/1520) to compensate for the difference.

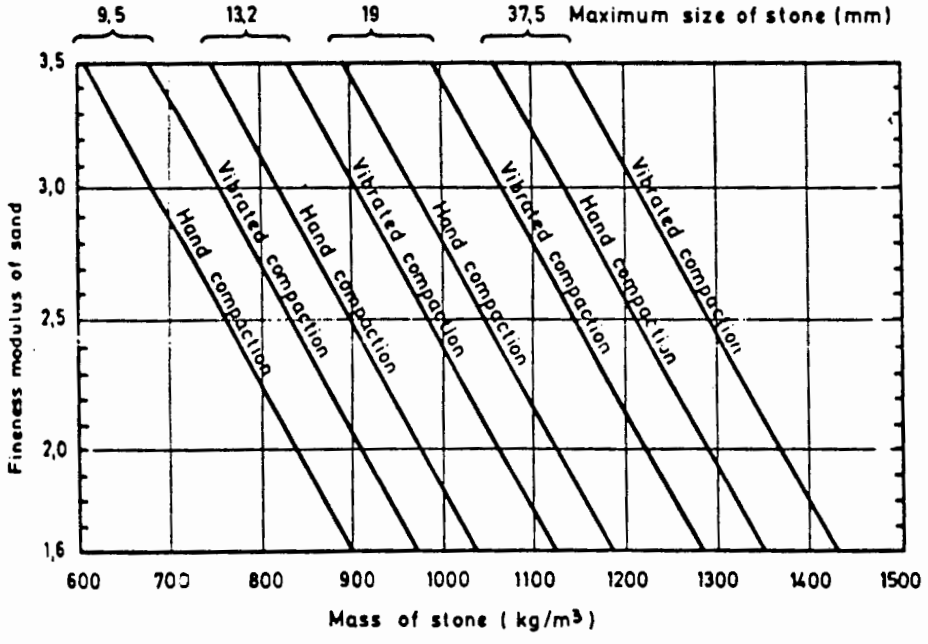

Figure D.9 : Stone content as a function of the fineness modulus of the sand as well as the method of placing.

The stone content calculated has to be adjusted to account for the increase in the volume of fines due to the fly ash addition. Use is made of Figure D.10 to find the percentage adjustment.

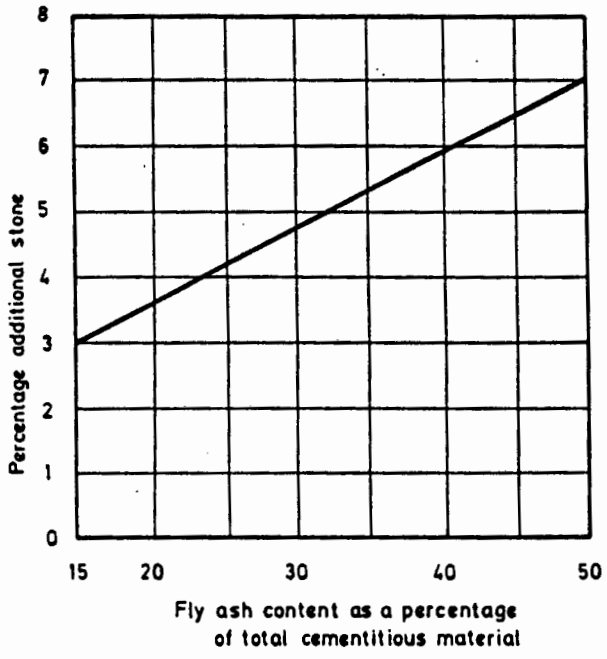

Figure D.10 : Chart for increasing the stone content.

5. *Calculation of the sand content*

The following formula applies in this case :

$$Sand = RDsand*1000\left[1-\left(\frac{Cement}{RD*1000}\right)-\left(\frac{Stone}{RD*1000}\right)-\left(\frac{FlyAsh}{RD*1000}\right)-\left(\frac{Water}{RD*1000}\right)\right]w$$

here RD refers to the relative density of the material.

(If not specified, use RD=2.30 for fly ash.)

6. *Conduction of a trial mix*

A trial mix is prepared and its properties examined, leaving room for possible adjustment of the parameters used in the design.

METHOD 3 : MODIFIED PCI METHOD FOR FLY ASH CONCRETE MIX DESIGN (National Building Research Institute, 1985)

The method which was developed by the National Building Research Institute and is based on the PCI method of concrete mix design for ordinary OPC mixes not containing mineral admixtures. The principle is to design a concrete which will have the same workability and 28-day compressive strength as the corresponding OPC concrete.

1. *Given the specified 28-day cube compressive strength, the target strength is chosen.*

According to SABS 0100-2(1992), the characteristic strength is the value of the compressive strength of the concrete, below which not more than 5% of the valid test results obtained from cubes of concrete of the same grade fall. The target strength is an average value of concrete strength which is higher that the specified strength, and that is aimed for to ensure that the characteristic strength is attained. Based on statistical analyses, a formula was derived to calculate the target strength:

$$f_t = f_c + (1.7 * \delta)$$

where f_t = target strength in MPa

f_c = characteristic strength in MPa

δ = standard deviation in MPa

The standard deviation is a characteristic of the materials, the mix proportioning, mixing methodology employed, as well as the curing conditions prevailing.

2. *Choice of water/cement ratio to give required target strength.*

The (W/C) ratio is obtained from Figure D.11 which is based on ordinary Portland cement concrete mixes.

Use $\alpha = 1.0$ for average 28-day strength

Use $\alpha = 1.85$ for minimum 28-day strength for ordinary portland cement.

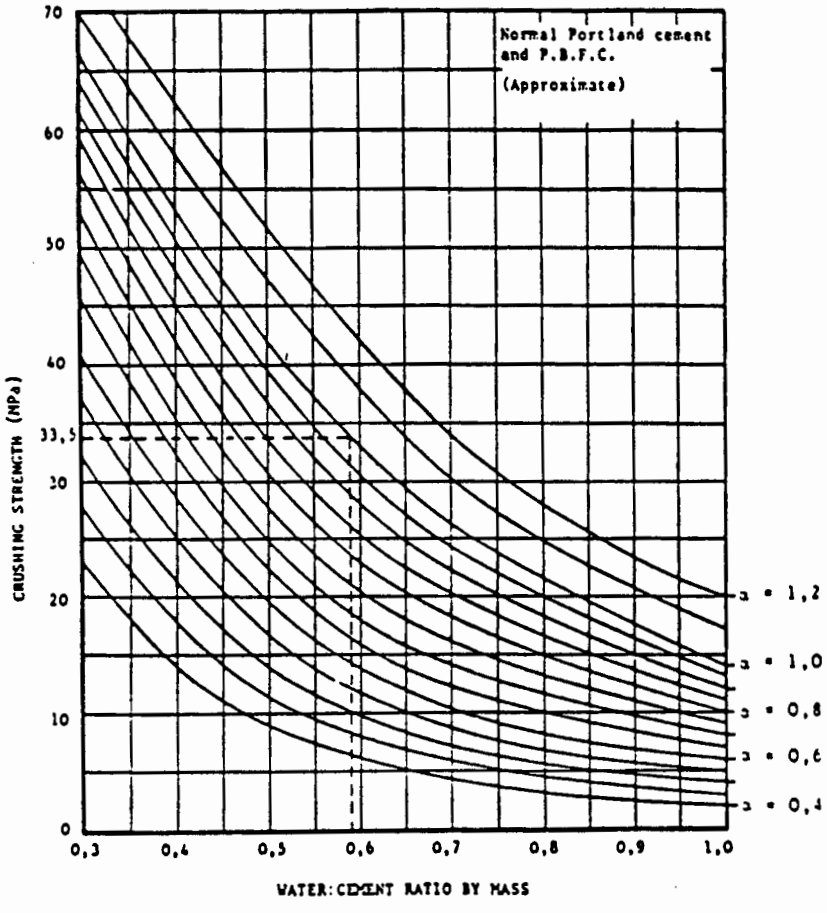

Figure D.11 : Relationship between the compressive strength and water to cement ratio.

3. *Determination of the water content.*

The water content is greatly influenced by the (fine) aggregate used. Table D.2 presented earlier, gives guidelines in choosing the water content as a function of the quality of the sand used. The water content for fly ash concretes is about 10% less than that of portland cement concretes (for the same workability and 28-day strength). This 10% deduction has to be incorporated for.

4. *Calculation of the cement content.*

Based on a cementing efficiency equal to 0.4, the following formula has been derived:

$$C = \left(\frac{W}{W/C}\right) * \left[\frac{(1-P)}{1-0.6P}\right]$$

where C = portland cement content in kg per m^3

W = water content in liters per m^3

P = fly ash fraction of total cementitious binder content.

5. *Determination of the fly ash content*

The following formula is used:

$$F = \frac{P * C}{1-P}$$

where F = fly ash content in kg per m^3

6. *Determination of the stone content*

Figure D.9 given previously is used to obtain the stone content. This figure is based on a consolidated bulk density for the stone of 1520kg/m^3 and the stone content has to be adjusted if the CBD value differs.

$$\text{Adjusted SC} = \text{SC}*\left(\frac{\text{Bulk Density}}{1520}\right)$$

where SC = stone content in kg per m^3

The fineness of the fly ash, the reduced portland cement content as well as the reduced water content all influence the quantity of aggregate. This is why a further modification to the stone content is prescribed:

$$SC_f = SC + \left(F\left(\frac{W}{C}\right)\right)$$

where SC_f = final stone content for the particular mix

7. *Calculation of the sand content.*

The following formula applies:

$$Sand = \left[1000 - \left(\frac{C}{RD}\right) - \left(\frac{F}{RD}\right) - \left(\frac{SC_f}{RD}\right) - W\right] * RD_{Sand}$$

where Sand = sand content in kg per m^3

RD = respective relative densities

8. *Trial mix*

When the quantities for all the concrete components have been calculated, a trial mix is made. If the required slump has not been achieved, Figure D.8 given earlier is used to find the relevant adjustment.

CONCLUSIONS

Three methods of fly ash concrete mix design have been presented. The common aim is to calculate the quantities of concrete constituents on the basis of certain criteria. Each method approaches the topic from a different angle which is determined by the knowledge of material properties and relative material interactions. Apart from these more theoretical considerations, the practical experience of concreting has greatly aided the development of such design methods.

The first method approaches the free water to cementitious material ratio in two steps. Firstly, for a specified target strength (28-day compressive), a free water to portland cement ratio is chosen. Secondly, an optimum ratio of fly ash to fly ash plus portland cement is determined which is a function of the grade of fly ash used. The different grades are summarized in Table D.4.

Table D.4 : Classification of fly ash for the use in concrete (Dhir, 1986).

Grade of Fly Ash	% Fineness*	Characteristic
Premium	< 5	Excellent Properties
1	5-20	Good Properties
2	20-35	Good to Adequate Properties
3	> 35	Doubtful economic viability

* Percentage fly ash sieve residue at 45μm

The second method, developed by the Portland Cement Institute of South Africa, requires the prior knowledge of the percentage fly ash to be used. With this in mind, the ratio of total cementitious material to water is chosen as a function of the

28-day target strength. The free water content is related to the quality of the fine aggregate to be used. (In the case where a detailed sieve analysis of the ash is available, the percentage ash retained on the 45μm sieve may be used as a further guideline to determine the water content of the mix.)

The third method relies on the principle that the fly ash concrete designed according to it, will have the same 28-day wet-cured compressive strength and workability as a comparable OPC mix designed according to the PCI method for OPC mixes. The selection of water to cement ratio is based on a straight OPC mix and is influenced by alpha, a factor indicating the cementing efficiency. The water content is determined in relation to the quality of the (fine) aggregate.

The relevance of a particular method can not be predicted with absolute confidence and the concrete technologist has thus to rely on trial mixes to show whether the required specifications have indeed been met. The adjustment of a concrete mix after unsatisfactory performance of the trial mix is often influenced by experience more than by finite numbers.

In general, the availability of a wide range of admixtures for concrete, opens up the overall scope of mix design. However the application of admixtures should always be given careful consideration in terms of type and quantity, as the effect(s) derived from using these might have unforeseen consequences. These might be short-term, for example the incompatibility with other concrete constituents, or long-term, for example reduced durability performance.